VISIT…

DRUGS AND THE PHARMACEUTICAL SCIENCES VOLUME 106

Oral Drug Absorption

Prediction and Assessment

edited by
Jennifer B. Dressman
Hans Lennernäs

Oral Drug Absorption

Prediction and Assessment

edited by

Jennifer B. Dressman

Institute of Pharmaceutical Technology
Johann Wolfgang Goethe University
Frankfurt on Main, Germany

Hans Lennernäs

Biopharmaceutics Group
Department of Pharmacy
Uppsala University
Uppsala, Sweden

MARCEL DEKKER, INC. NEW YORK • BASEL

Copyright © 2000 by Marcel Dekker, Inc. All Rights Reserved.

ISBN: 0-8247-0272-7

This book is printed on acid-free paper.

Headquarters
Marcel Dekker, Inc.
270 Madison Avenue, New York, NY 10016
tel: 212-696-9000; fax: 212-685-4540

Eastern Hemisphere Distribution
Marcel Dekker AG
Hutgasse 4, Postfach 812, CH-4001 Basel, Switzerland
tel: 41-61-261-8482; fax: 41-61-261-8896

World Wide Web
http://www.dekker.com

The publisher offers discounts on this book when ordered in bulk quantities. For more information, write to Special Sales/Professional Marketing at the headquarters address above.

Copyright © 2000 by Marcel Dekker, Inc. All Rights Reserved.

Neither this book nor any part may be reproduced or transmitted in any form or by any means, electronic or mechanical, including photocopying, microfilming, and recording, or by any information storage and retrieval system, without permission in writing from the publisher.

Current printing (last digit):
10 9 8 7 6 5 4 3 2 1

PRINTED IN THE UNITED STATES OF AMERICA

DRUGS AND THE PHARMACEUTICAL SCIENCES

Executive Editor

James Swarbrick
PharmaceuTech, Inc.
Pinehurst, North Carolina

Advisory Board

Larry L. Augsburger
University of Maryland
Baltimore, Maryland

Douwe D. Breimer
Gorlaeus Laboratories
Leiden, The Netherlands

Trevor M. Jones
The Association of the
British Pharmaceutical Industry
London, United Kingdom

Hans E. Junginger
Leiden/Amsterdam Center
for Drug Research
Leiden, The Netherlands

Vincent H. L. Lee
University of Southern California
Los Angeles, California

David E. Nichols
Purdue University
West Lafayette, Indiana

Stephen G. Schulman
University of Florida
Gainesville, Florida

Jerome P. Skelly
Alexandria, Virginia

Felix Theeuwes
Alza Corporation
Palo Alto, California

Geoffrey T. Tucker
University of Sheffield
Royal Hallamshire Hospital
Sheffield, United Kingdom

Peter G. Welling
Institut de Recherche Jouveinal
Fresnes, France

DRUGS AND THE PHARMACEUTICAL SCIENCES

A Series of Textbooks and Monographs

1. Pharmacokinetics, *Milo Gibaldi and Donald Perrier*
2. Good Manufacturing Practices for Pharmaceuticals: A Plan for Total Quality Control, *Sidney H. Willig, Murray M. Tuckerman, and William S. Hitchings IV*
3. Microencapsulation, *edited by J. R. Nixon*
4. Drug Metabolism: Chemical and Biochemical Aspects, *Bernard Testa and Peter Jenner*
5. New Drugs: Discovery and Development, *edited by Alan A. Rubin*
6. Sustained and Controlled Release Drug Delivery Systems, *edited by Joseph R. Robinson*
7. Modern Pharmaceutics, *edited by Gilbert S. Banker and Christopher T. Rhodes*
8. Prescription Drugs in Short Supply: Case Histories, *Michael A. Schwartz*
9. Activated Charcoal: Antidotal and Other Medical Uses, *David O. Cooney*
10. Concepts in Drug Metabolism (in two parts), *edited by Peter Jenner and Bernard Testa*
11. Pharmaceutical Analysis: Modern Methods (in two parts), *edited by James W. Munson*
12. Techniques of Solubilization of Drugs, *edited by Samuel H. Yalkowsky*
13. Orphan Drugs, *edited by Fred E. Karch*
14. Novel Drug Delivery Systems: Fundamentals, Developmental Concepts, Biomedical Assessments, *Yie W. Chien*
15. Pharmacokinetics: Second Edition, Revised and Expanded, *Milo Gibaldi and Donald Perrier*
16. Good Manufacturing Practices for Pharmaceuticals: A Plan for Total Quality Control, Second Edition, Revised and Expanded, *Sidney H. Willig, Murray M. Tuckerman, and William S. Hitchings IV*
17. Formulation of Veterinary Dosage Forms, *edited by Jack Blodinger*
18. Dermatological Formulations: Percutaneous Absorption, *Brian W. Barry*
19. The Clinical Research Process in the Pharmaceutical Industry, *edited by Gary M. Matoren*
20. Microencapsulation and Related Drug Processes, *Patrick B. Deasy*
21. Drugs and Nutrients: The Interactive Effects, *edited by Daphne A. Roe and T. Colin Campbell*
22. Biotechnology of Industrial Antibiotics, *Erick J. Vandamme*
23. Pharmaceutical Process Validation, *edited by Bernard T. Loftus and Robert A. Nash*

24. Anticancer and Interferon Agents: Synthesis and Properties, *edited by Raphael M. Ottenbrite and George B. Butler*
25. Pharmaceutical Statistics: Practical and Clinical Applications, *Sanford Bolton*
26. Drug Dynamics for Analytical, Clinical, and Biological Chemists, *Benjamin J. Gudzinowicz, Burrows T. Younkin, Jr., and Michael J. Gudzinowicz*
27. Modern Analysis of Antibiotics, *edited by Adjoran Aszalos*
28. Solubility and Related Properties, *Kenneth C. James*
29. Controlled Drug Delivery: Fundamentals and Applications, Second Edition, Revised and Expanded, *edited by Joseph R. Robinson and Vincent H. Lee*
30. New Drug Approval Process: Clinical and Regulatory Management, *edited by Richard A. Guarino*
31. Transdermal Controlled Systemic Medications, *edited by Yie W. Chien*
32. Drug Delivery Devices: Fundamentals and Applications, *edited by Praveen Tyle*
33. Pharmacokinetics: Regulatory • Industrial • Academic Perspectives, *edited by Peter G. Welling and Francis L. S. Tse*
34. Clinical Drug Trials and Tribulations, *edited by Allen E. Cato*
35. Transdermal Drug Delivery: Developmental Issues and Research Initiatives, *edited by Jonathan Hadgraft and Richard H. Guy*
36. Aqueous Polymeric Coatings for Pharmaceutical Dosage Forms, *edited by James W. McGinity*
37. Pharmaceutical Pelletization Technology, *edited by Isaac Ghebre-Sellassie*
38. Good Laboratory Practice Regulations, *edited by Allen F. Hirsch*
39. Nasal Systemic Drug Delivery, *Yie W. Chien, Kenneth S. E. Su, and Shyi-Feu Chang*
40. Modern Pharmaceutics: Second Edition, Revised and Expanded, *edited by Gilbert S. Banker and Christopher T. Rhodes*
41. Specialized Drug Delivery Systems: Manufacturing and Production Technology, *edited by Praveen Tyle*
42. Topical Drug Delivery Formulations, *edited by David W. Osborne and Anton H. Amann*
43. Drug Stability: Principles and Practices, *Jens T. Carstensen*
44. Pharmaceutical Statistics: Practical and Clinical Applications, Second Edition, Revised and Expanded, *Sanford Bolton*
45. Biodegradable Polymers as Drug Delivery Systems, *edited by Mark Chasin and Robert Langer*
46. Preclinical Drug Disposition: A Laboratory Handbook, *Francis L. S. Tse and James J. Jaffe*
47. HPLC in the Pharmaceutical Industry, *edited by Godwin W. Fong and Stanley K. Lam*
48. Pharmaceutical Bioequivalence, *edited by Peter G. Welling, Francis L. S. Tse, and Shrikant V. Dinghe*
49. Pharmaceutical Dissolution Testing, *Umesh V. Banakar*

50. Novel Drug Delivery Systems: Second Edition, Revised and Expanded, *Yie W. Chien*
51. Managing the Clinical Drug Development Process, *David M. Cocchetto and Ronald V. Nardi*
52. Good Manufacturing Practices for Pharmaceuticals: A Plan for Total Quality Control, Third Edition, *edited by Sidney H. Willig and James R. Stoker*
53. Prodrugs: Topical and Ocular Drug Delivery, *edited by Kenneth B. Sloan*
54. Pharmaceutical Inhalation Aerosol Technology, *edited by Anthony J. Hickey*
55. Radiopharmaceuticals: Chemistry and Pharmacology, *edited by Adrian D. Nunn*
56. New Drug Approval Process: Second Edition, Revised and Expanded, *edited by Richard A. Guarino*
57. Pharmaceutical Process Validation: Second Edition, Revised and Expanded, *edited by Ira R. Berry and Robert A. Nash*
58. Ophthalmic Drug Delivery Systems, *edited by Ashim K. Mitra*
59. Pharmaceutical Skin Penetration Enhancement, *edited by Kenneth A. Walters and Jonathan Hadgraft*
60. Colonic Drug Absorption and Metabolism, *edited by Peter R. Bieck*
61. Pharmaceutical Particulate Carriers: Therapeutic Applications, *edited by Alain Rolland*
62. Drug Permeation Enhancement: Theory and Applications, *edited by Dean S. Hsieh*
63. Glycopeptide Antibiotics, *edited by Ramakrishnan Nagarajan*
64. Achieving Sterility in Medical and Pharmaceutical Products, *Nigel A. Halls*
65. Multiparticulate Oral Drug Delivery, *edited by Isaac Ghebre-Sellassie*
66. Colloidal Drug Delivery Systems, *edited by Jörg Kreuter*
67. Pharmacokinetics: Regulatory • Industrial • Academic Perspectives, Second Edition, *edited by Peter G. Welling and Francis L. S. Tse*
68. Drug Stability: Principles and Practices, Second Edition, Revised and Expanded, *Jens T. Carstensen*
69. Good Laboratory Practice Regulations: Second Edition, Revised and Expanded, *edited by Sandy Weinberg*
70. Physical Characterization of Pharmaceutical Solids, *edited by Harry G. Brittain*
71. Pharmaceutical Powder Compaction Technology, *edited by Göran Alderborn and Christer Nyström*
72. Modern Pharmaceutics: Third Edition, Revised and Expanded, *edited by Gilbert S. Banker and Christopher T. Rhodes*
73. Microencapsulation: Methods and Industrial Applications, *edited by Simon Benita*
74. Oral Mucosal Drug Delivery, *edited by Michael J. Rathbone*
75. Clinical Research in Pharmaceutical Development, *edited by Barry Bleidt and Michael Montagne*

76. The Drug Development Process: Increasing Efficiency and Cost Effectiveness, *edited by Peter G. Welling, Louis Lasagna, and Umesh V. Banakar*
77. Microparticulate Systems for the Delivery of Proteins and Vaccines, *edited by Smadar Cohen and Howard Bernstein*
78. Good Manufacturing Practices for Pharmaceuticals: A Plan for Total Quality Control, Fourth Edition, Revised and Expanded, *Sidney H. Willig and James R. Stoker*
79. Aqueous Polymeric Coatings for Pharmaceutical Dosage Forms: Second Edition, Revised and Expanded, *edited by James W. McGinity*
80. Pharmaceutical Statistics: Practical and Clinical Applications, Third Edition, *Sanford Bolton*
81. Handbook of Pharmaceutical Granulation Technology, *edited by Dilip M. Parikh*
82. Biotechnology of Antibiotics: Second Edition, Revised and Expanded, *edited by William R. Strohl*
83. Mechanisms of Transdermal Drug Delivery, *edited by Russell O. Potts and Richard H. Guy*
84. Pharmaceutical Enzymes, *edited by Albert Lauwers and Simon Scharpé*
85. Development of Biopharmaceutical Parenteral Dosage Forms, *edited by John A. Bontempo*
86. Pharmaceutical Project Management, *edited by Tony Kennedy*
87. Drug Products for Clinical Trials: An International Guide to Formulation • Production • Quality Control, *edited by Donald C. Monkhouse and Christopher T. Rhodes*
88. Development and Formulation of Veterinary Dosage Forms: Second Edition, Revised and Expanded, *edited by Gregory E. Hardee and J. Desmond Baggot*
89. Receptor-Based Drug Design, *edited by Paul Leff*
90. Automation and Validation of Information in Pharmaceutical Processing, *edited by Joseph F. deSpautz*
91. Dermal Absorption and Toxicity Assessment, *edited by Michael S. Roberts and Kenneth A. Walters*
92. Pharmaceutical Experimental Design, *Gareth A. Lewis, Didier Mathieu, and Roger Phan-Tan-Luu*
93. Preparing for FDA Pre-Approval Inspections, *edited by Martin D. Hynes III*
94. Pharmaceutical Excipients: Characterization by IR, Raman, and NMR Spectroscopy, *David E. Bugay and W. Paul Findlay*
95. Polymorphism in Pharmaceutical Solids, *edited by Harry G. Brittain*
96. Freeze-Drying/Lyophilization of Pharmaceutical and Biological Products, *edited by Louis Rey and Joan C. May*
97. Percutaneous Absorption: Drugs–Cosmetics–Mechanisms–Methodology, Third Edition, Revised and Expanded, *edited by Robert L. Bronaugh and Howard I. Maibach*

98. Bioadhesive Drug Delivery Systems: Fundamentals, Novel Approaches, and Development, *edited by Edith Mathiowitz, Donald E. Chickering III, and Claus-Michael Lehr*
99. Protein Formulation and Delivery, *edited by Eugene J. McNally*
100. New Drug Approval Process: Third Edition, The Global Challenge, *edited by Richard A. Guarino*
101. Peptide and Protein Drug Analysis, *edited by Ronald E. Reid*
102. Transport Processes in Pharmaceutical Systems, *edited by Gordon L. Amidon, Ping I. Lee, and Elizabeth M. Topp*
103. Excipient Toxicity and Safety, *edited by Myra L. Weiner and Lois A. Kotkoskie*
104. The Clinical Audit in Pharmaceutical Development, *edited by Michael R. Hamrell*
105. Pharmaceutical Emulsions and Suspensions, *edited by Francoise Nielloud and Gilberte Marti-Mestres*
106. Oral Drug Absorption: Prediction and Assessment, *edited by Jennifer B. Dressman and Hans Lennernäs*
107. Drug Stability: Principles and Practices, Third Edition, Revised and Expanded, *edited by Jens T. Carstensen and C. T. Rhodes*
108. Containment in the Pharmaceutical Industry, *edited by James P. Wood*
109. Good Manufacturing Practices for Pharmaceuticals: A Plan for Total Quality Control from Manufacturer to Consumer, Fifth Edition, Revised and Expanded, *Sidney H. Willig*
110. Advanced Pharmaceutical Solids, *Jens T. Carstensen*
111. Endotoxins: Pyrogens, LAL Testing, and Depyrogenation, Second Edition, Revised and Expanded, *Kevin L. Williams*
112. Pharmaceutical Process Engineering, *Anthony J. Hickey and David Ganderton*
113. Pharmacogenomics, *edited by Werner Kalow, Urs A. Meyer, and Rachel F. Tyndale*
114. Handbook of Drug Screening, *edited by Ramakrishna Seethala and Prabhavathi B. Fernandes*
115. Drug Targeting Technology: Physical • Chemical • Biological Methods, *edited by Hans Schreier*
116. Drug–Drug Interactions, *edited by A. David Rodrigues*
117. Handbook of Pharmaceutical Analysis, *edited by Lena Ohannesian and Anthony J. Streeter*
118. Pharmaceutical Process Scale-Up, *edited by Michael Levin*
119. Dermatological and Transdermal Formulations, *edited by Kenneth A. Walters*
120. Clinical Drug Trials and Tribulations: Second Edition, Revised and Expanded, *edited by Allen Cato, Lynda Sutton, and Allen Cato III*
121. Modern Pharmaceutics: Fourth Edition, Revised and Expanded, *edited by Gilbert S. Banker and Christopher T. Rhodes*
122. Surfactants and Polymers in Drug Delivery, *Martin Malmsten*
123. Transdermal Drug Delivery: Second Edition, Revised and Expanded, *edited by Richard H. Guy and Jonathan Hadgraft*

124. Good Laboratory Practice Regulations: Second Edition, Revised and Expanded, *edited by Sandy Weinberg*
125. Parenteral Quality Control: Sterility, Pyrogen, Particulate, and Package Integrity Testing: Third Edition, Revised and Expanded, *Michael J. Akers, Daniel S. Larrimore, and Dana Morton Guazzo*
126. Modified-Release Drug Delivery Technology, *edited by Michael J. Rathbone, Jonathan Hadgraft, and Michael S. Roberts*
127. Simulation for Designing Clinical Trials: A Pharmacokinetic-Pharmacodynamic Modeling Perspective, *edited by Hui C. Kimko and Stephen B. Duffull*
128. Affinity Capillary Electrophoresis in Pharmaceutics and Biopharmaceutics, *edited by Reinhard H. H. Neubert and Hans-Hermann Rüttinger*
129. Pharmaceutical Process Validation: An International Third Edition, Revised and Expanded, *edited by Robert A. Nash and Alfred H. Wachter*
130. Ophthalmic Drug Delivery Systems: Second Edition, Revised and Expanded, *edited by Ashim K. Mitra*
131. Pharmaceutical Gene Delivery Systems, *edited by Alain Rolland and Sean M. Sullivan*

ADDITIONAL VOLUMES IN PREPARATION

Biomarkers in Clinical Drug Development, *edited by John Bloom*

Pharmaceutical Inhalation Aerosol Technology: Second Edition, Revised and Expanded, *edited by Anthony J. Hickey*

Pharmaceutical Extrusion Technology, *edited by Isaac Ghebre-Sellassie and Charles Martin*

Pharmaceutical Compliance, *edited by Carmen Medina*

To the memory of Graham Garratt,
publisher, scholar, and gentleman.
Without his encouragement
this book would not have been published.

Preface

A crucial question in the development of any new drug is whether it will be bioavailable after oral administration. Good oral availability opens up a variety of formulation possibilities, makes it easier to provide dose-to-dose and batch-to-batch reproducibility, and improves flexibility with respect to dosing conditions. In comparison with other routes of administration and drugs with restrictive dosing conditions, an oral dosage form that can be administered under a variety of dosing conditions often leads to better patient compliance.

Oral Drug Absorption: Prediction and Assessment focuses on the key factors involved in the release of drug from the dosage form and its subsequent passage across the gut wall. The book begins with three chapters devoted to aspects of physiology and pathophysiology that can play a role in drug absorption, including motility issues and how diseases of the gastrointestinal tract can change the integrity of the mucosa as well as affect the composition of lumenal fluids. Chapters 4 through 8 are concerned with the assessment of permeability of the absorbing mucosa to the drug. All currently used methods are considered, ranging from *in silico* calculations to cell culture and animal tissue methods to perfusions in whole animals and humans. Chapter 8 provides a particularly interesting perspective on how the pharmaceutical industry currently combines the various methodologies to evaluate the permeability of new chemical entities and what is needed to bring these studies to high-throughput efficiencies.

Chapters 9 through 13 focus on solubility and dissolution limitations of oral bioavailability. Guidance is given on appropriate dissolution testing

conditions for both immediate (Chap. 10) and extended-release (Chap. 11) dosage forms. As in the permeability chapters, there is also a chapter specifically addressing practical concerns in the pharmaceutical industry with respect to assessment of release rate, illuminated by numerous examples. Chapter 13 provides guidelines on how to set up dissolution tests so that meaningful data can be obtained and discusses critically the various options for evaluating data and comparing results among various formulations.

The last section of the book is devoted to in vitro–in vivo correlations, including both deconvolution and convolution methods. The different types and levels of correlation are clearly described and their advantages and disadvantages critically discussed. It is hoped that this combination of topics will enable the reader to obtain a broad overview of the range of studies on predicting and assessing oral drug absorption of new chemical entities and that sufficient detail is given to enable selection of the appropriate tests for a given compound and stage of development. Of course, it is recognized that factors such as instability of the drug in the lumenal fluids and potential metabolism in the gut wall and/or liver may also place major restrictions on bioavailability after oral administration. Although some attention is given in this book to gut-wall metabolism, the reader is referred to other texts that specifically address liver metabolism (e.g., Woolf T, ed., *Handbook of Drug Metabolism*, Marcel Dekker, 1999) to integrate this possibility into an evaluation of new drug substances.

We would like to thank the authors for their cooperation in the timely preparation of manuscripts, which allowed us to produce a book that reflects state-of-the-art thinking in oral drug absorption. Further, we would like to thank the editors at Marcel Dekker, Inc., in particular Sandra Beberman and Jane Roh, for their accessibility and helpfulness in all aspects of the book's production.

Jennifer B. Dressman
Hans Lennernäs

Contents

Preface *v*
Contributors *ix*

I. Gastrointestinal Variables

1. Gastrointestinal Transit and Drug Absorption 1
Clive G. Wilson

2. Permeability in the Gastrointestinal Tract 11
Lars Knutson, F. Knutson, and T. Knutson

3. Gastrointestinal Disease and Dosage Form Performance 17
Vladan Milovic and Jürgen Stein

II. Membrane Permeability

4. Intestinal Permeability: Prediction from Theory 31
Han van de Waterbeemd

5. In Vitro Methods for the Assessment of Permeability 51
Josef J. Tukker

6. Animal Perfusion Studies 73
Hans Lennernäs

7. Human Perfusion Studies 99
Hans Lennernäs

8. The Role of Permeability Studies in Preclinical Evaluation 119
Philip L. Smith

III. Solubility and Drug Dissolution

9. Solubility as a Limiting Factor to Drug Absorption 137
Raimar Löbenberg, Michael Vieira, and Gordon L. Amidon

10. Dissolution Testing of Immediate-Release Products and Its Application to Forecasting In Vivo Performance 155
Jennifer B. Dressman

11. Dissolution Tests for Extended-Release Products 183
Barbara Sievert and Martin Siewert

12. Dissolution Testing in the Development of Oral Drug Products 197
Bertil Abrahamsson

13. Analysis of Drug Dissolution Data 229
Christos Reppas and Eleftheria Nicolaides

IV. In Vivo–In Vitro Correlations

14. Convolution and Deconvolution Methods 255
Richard Süverkrüp

15. The Correlation of In Vitro and In Vivo Drug Dissolution 281
Dierk Brockmeier

16. IVIVC: A Perspective from the Workbench 307
Johannes Krämer

Index *323*

Contributors

Bertil Abrahamsson, Ph.D. Department of Biopharmaceutics, AstraZeneca R&D, Mölndal, Sweden

Gordon L. Amidon, Ph.D. College of Pharmacy, The University of Michigan, Ann Arbor, Michigan

Dierk Brockmeier, Ph.D. Clinical Pharmacology, Justus Liebig University, Giessen, Germany

Jennifer B. Dressman, Ph.D. Institute of Pharmaceutical Technology, Johann Wolfgang Goethe University, Frankfurt on Main, Germany

F. Knutson, M.D., Ph.D. Departments of Clinical Immunology and Transfusion Medicine, Enköping Hospital, Uppsala University, Uppsala, Sweden

Lars Knutson, Ph.D. Department of Surgery, Enköping Hospital, Uppsala University, Uppsala, Sweden

T. Knutson Department of Anesthesiology, Enköping Hospital, Uppsala University, Uppsala, Sweden

Johannes Krämer, Ph.D. LQS, Eschborn, Germany

Hans Lennernäs, Ph.D. Biopharmaceutics Group, Department of Pharmacy, Uppsala University, Uppsala, Sweden

Raimar Löbenberg, Ph.D.* College of Pharmacy, The University of Michigan, Ann Arbor, Michigan

Vladan Milovic, M.D., M.Sc. Second Department of Medicine, Johann Wolfgang Goethe University, Frankfurt on Main, Germany

Eleftheria Nicolaides Laboratory of Biopharmaceutics and Pharmacokinetics, Department of Pharmacy, University of Athens, Athens, Greece

Christos Reppas, Ph.D. Laboratory of Biopharmaceutics and Pharmacokinetics, Department of Pharmacy, University of Athens, Athens, Greece

Barbara Sievert Aventis Pharma, Frankfurt on Main, Germany

Martin Siewert, Ph.D. Quality Operations, Environment, Health, and Safety, Aventis Pharma, Frankfurt on Main, Germany

Philip L. Smith, Ph.D. Pharmaceutical Technologies, SmithKline Beecham Pharmaceuticals, Collegeville, Pennsylvania

Jürgen Stein, M.D., Ph.D. Second Department of Medicine, Johann Wolfgang Goethe University, Frankfurt on Main, Germany

Richard Süverkrüp, Ph.D. Department of Pharmaceutics, Pharmaceutical Institute, University of Bonn, Bonn, Germany

Josef J. Tukker, Ph.D. University of Utrecht, Utrecht, the Netherlands

Han van de Waterbeemd, Ph.D. Department of Drug Metabolism, Pfizer Central Research, Sandwich, Kent, United Kingdom

Michael Vieira, Ph.D. Port Systems LLC, Ann Arbor, Michigan

Clive G. Wilson, Ph.D. Department of Pharmaceutical Sciences, Strathclyde Institute for Biomedical Sciences, University of Strathclyde, Glasgow, Scotland, United Kingdom

---

* *Present Affiliation*: The University of Alberta, Edmonton, Alberta, Canada.

1
Gastrointestinal Transit and Drug Absorption

Clive G. Wilson
Strathclyde Institute for Biomedical Sciences, University of Strathclyde, Glasgow, Scotland, United Kingdom

I. INTRODUCTION

The human gut has evolved over many thousands of years to provide an efficient system for the extraction of nutrients from a varied diet. Functionally, the gut is divided into a preparative and primary storage region (mouth and stomach), a secretory and absorptive region (the midgut), a water reclamation system (ascending colon), and finally, a waste-product storage system (the descending and sigmoid colon regions and the rectum). The organization of the upper gut facilitates the controlled presentation of calories to the systemic circulation allowing the replete person to perform physical work, to undergo social activities, and to go to sleep. In spite of this wondrous organization it is still necessary, or at least desirable, in a modern lifestyle to take three meals a day. On the other hand, most of us wish to take our medications only once a day.

Although the human race has relied on medicines for an indeterminate number of years, the physiology of the digestive process is less than convenient for the efficient absorption of many of the modern therapeutic entities we wish to administer. The influence of feeding and temporal patterns on gastrointestinal transit, therefore, is of great relevance in attempting to optimize drug absorption. In this chapter, we will consider how data from recent experiments might have an influence on how we think about dosing issues.

We will start with swallowing a medicine and finish with transit through the large intestine.

II. ESOPHAGEAL TRANSIT

After the dosage form leaves the buccal cavity, which is a relatively benign environment, transit through the esophagus is normally complete within 5–15 s, depending on posture. It has been known for many years that disorders of normal motility (dysphagia), left-sided heart enlargement, or stricture of the esophagus can result in impaired clearance of formulations. In some cases this can lead to damage of the esophageal wall. The elderly have a decreased ability to swallow large dosage forms, a phenomenon that may be related to the loss of secondary peristaltic mechanisms. Impairment of the ability to swallow with advancing age has been identified as a major health care problem in an aging population. Radiological studies of an asymptomatic group of 56 patients, mean age 83 years, showed that a normal pattern of deglutition was present in only 16% of individuals (1). Oral abnormalities, which included difficulty in controlling and delivering a bolus to the esophagus following ingestion were noted in 63% of cases. Structural abnormalities capable of causing esophageal dysphagia include neoplasms, strictures, and diverticula, although several workers have commented that only minor changes of structure and function are associated with aging. The difficulty, therefore, appears to relate to neurological mechanisms associated with the coordination of tongue, oropharynx, and upper esophagus during a swallow.

In scintigraphic studies of transit rates of hard gelatin capsules and tablets, elderly subjects were frequently unable to clear the capsules (2,3). This appears to be due to the separation of the bolus of water and capsule in the oropharynx, resulting in a ''dry'' swallow. As a result, capsule adherence occurred in the lower third of the esophagus. In this region, adherence is not sensorially detected: subjects were unaware of sticking. The importance of buoyancy in capsule formulation has hitherto been ignored and may be an additional risk factor in dosing the elderly.

III. GASTRIC RETENTION

Our understanding of the behavior of dosage forms in the stomach has been gained largely from scintigraphic studies in which phases of a meal and formulations are labeled with different radionuclides, particularly technetium-99m

and indium-111 (4,5). Such studies have demonstrated that retention times of formulations in the stomach are dependent on the size of the formulation (6) and whether or not the formulation is taken with a meal (5). Enteric-coated or enteric matrix tablets may be retained for a considerable time if dosed with a heavy breakfast (7).

Multiparticulate dosage forms will empty more slowly in the presence of food and, because the dosage forms mix evenly with the food, the entry into the small intestine will be strongly influenced by the calorific density and bulk of the ingested meal (8). The rate of gastric emptying, therefore, predicts the absorption behavior and is reasonably reproducible. In contrast, the absorption of drugs from small, soft gelatin capsules is sometimes less predictable, and other nonradionuclide measurements may aid in the understanding of dosage form behavior in this case. In recent studies in our laboratory, we noted erratic performance of a soft gel formulation containing a poorly soluble drug. Reduction of dose size increased the variability, and we were at some difficulty in explaining these results. Therefore, we had to look for other imaging possibilities, including magnetic resonance imaging (MRI). The differences in proton shift of gut contents and tissues can be used to explore the behavior of formulations in the GI tract, provided that movement artifacts can be minimized.

It is well established that, after eating a meal, the shape of the stomach changes and the upper part (the fundus) relaxes to accommodate the extra volume. There is a short lag phase before the mixing movements in the lower part of the stomach, the pyloric antrum, increase. There is, therefore, a sharp contrast between the activity in the top and bottom halves of the stomach. This difference disappears when the subject lies prone in the MRI magnet: the pressure of the viscera causes mixing to abruptly cease and the liquid and solid phases separate in the stomach. This enabled us to perform studies to show previously unexplored mechanisms contributing to variability. Figure 1 shows the semisolid fraction of a sandwich-based meal lying in the stomach. Because the solid phase is not fully hydrated, it shows up as a bright doughnut-shaped solid against the liquid phase above it. Over a period of about 30 min to an hour, the solids gradually hydrate and the two phases are no longer distinct. During the early phase of digestion, the center of the lumen is relatively immobile, and the secreted gastric juice flows around the food mass. The poor homogeneity of the lumenal contents prevents efficient mixing. A small capsule given soon after the meal floats on the liquid above the solid mass, becoming stuck in the gastric rugae in the body of the stomach, or floats off ahead of the bulk of the gastric contents. The process is illustrated in Fig. 2.

FIG. 1 MRI image showing a cross section through the upper abdomen: The semi-solid fraction of a sandwich-based meal can be seen as a consolidated mass in the stomach. The stomach has squeezed the carbohydrate to an oblong mass. Image was taken within 10 min of consumption.

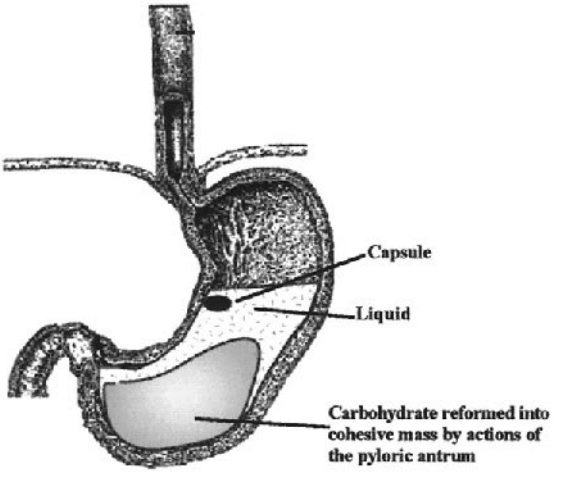

FIG. 2 Diagram showing how a small capsule given soon after the sandwich floats on the liquid above the solid mass.

IV. SMALL INTESTINE

In the small intestine, contact time with the absorptive epithelium is limited, and a small-intestinal transit time of 3.5–4.5 h is typical in healthy volunteers. The Holy Grail of drug delivery would be to discover a mechanism that extended the period of contact with this area of the gastrointestinal tract. Various approaches have been suggested, although a universal solution is not evident, and data demonstrating phenomena which extend GI residence are often a subject of controversy. Florence (9) has argued that nanoparticulates show intercellular transport and increased residence in the GI tract, but other workers have questioned the importance of this observation. Microparticulates are retained by the stomach, which may contribute to a prolongation of the absorptive phase—their capacity is, however, limited (Thair and colleagues, unpublished data). Prolonged stasis of pellets and tablets has been reported to occur at the ileocecal junction, but in our experience gastric emptying of subsequent meals causes movement of the material from terminal small bowel to cecum. Fat causes an extension of the small intestinal transit time, but the effect is modest (30–60 min), and it does not appear that this mechanism is exploitable in drug delivery.

V. COLONIC ABSORPTION

For most formulations, colonic absorption represents the only real opportunity to increase the interval between doses. Transit through the lower part of the gut is quoted at about 24 h, but in reality only the ascending colonic environment has sufficient fluid to facilitate dissolution. In the cecum, the fermentation of soluble fiber will produce fatty acid and gas (largely carbon dioxide, but with small amounts of hydrogen and methane if the redox conditions are appropriate). The gas rises into the transverse colon and can form temporary pockets, restricting access of water to the formulation. Consequently, distal release of drug is associated with poor spreading, reduced surface area, and restricted absorption. In the colon, water availability is low past the hepatic flexure, as the ascending colon is extremely efficient at water absorption. Changing the water content of the human colon by coadministering 20 g lactulose for 3 days markedly increases dispersion and dissolution in the transverse colon (Fig. 3). In the study shown in subjects were dosed with quinine sulfate in a colon-targeted device (Pulsincap) after receiving either lactulose for 3 days or codeine 30 mg t.d.s. Fiber dosing, 20 g/day, was used as a control.

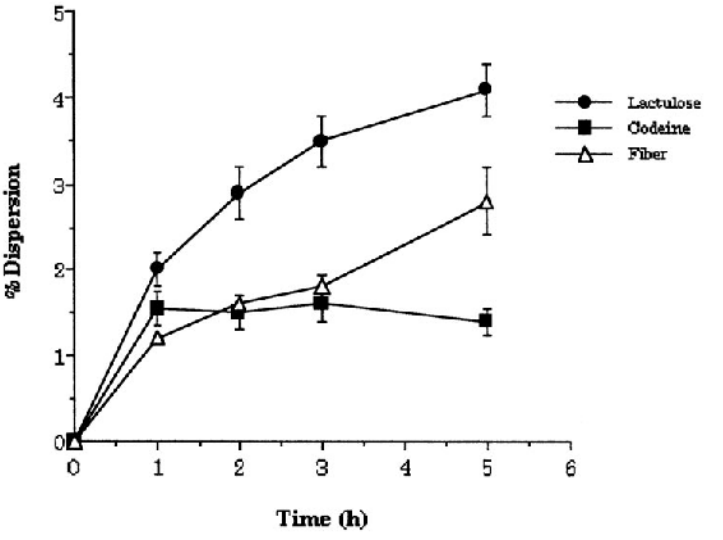

FIG. 3 Graph illustrating the dispersion of colonic contents of a Pulsincap released in the ascending bowel.

In comparison with either codeine or fiber control, lactulose treatment caused a marked increase in dispersion of the released contents (Hebden JM, et al., unpublished data).

VI. ROLE OF THE DISTAL COLON

The anatomy of the distal colon, with its thick muscular walls, suggests a predominantly propulsive activity in this region. Studies with single administrations of pellets or Pulsincap devices suggested that this area is difficult to treat because the second half of the transverse colon and the descending colon function as a conduit. Steady-state measurements confirm this assertion (10). Subjects were dosed daily with indium-111-labeled Amberlite resin and imaged throughout the day. On the fourth day, the division of activity in the colon was 67% in the proximal half and 33% in the distal half. Subsequent experiments in patients with left-sided colitis have suggested that the division is even more exaggerated in colitis, which may provide an explanation for

poor therapeutic results often seen with orally administered medications in patients with active disease.

Release at the ileocecal junction (i.e., before significant absorption of lumenal water has occurred) appears to provide satisfactory dispersion in the right colon. It has been suggested that there is a degree of stirring in the cecum, facilitated by the relatively liquid nature of the lumenal contents at this point. The cecum receives volumes of fluid sporadically, amounting to about 1L/day, from meals and associated intestinal secretions.

VII. THE IMPORTANCE OF TIME OF DOSING

The time of dosing appears to be an important factor in maximizing colonic contact, particularly in the ascending colon. Morning dosing without fasting is a common regimen in clinical trials, and patterns of motility, at least in healthy volunteers, have been well-established using scintigraphy. Following early-morning dosing, a nondisintegrating unit clears the stomach in 1–2 h and has a small-intestinal transit time of 3–4 h. Thus, at about 1 PM, the unit will be expected to be at the ileocecal junction or will have just entered the colon. Colonic transit through the proximal colon of intact objects such as capsules is usually 5–7 h. For a nondisintegrating object, dosed in the morning, the unit will have arrived at the hepatic flexure by 7–8 PM. Thus, assuming the drug is absorbed in the colon, the maximum time window for absorption is 6–8 h following morning dosing with a monolith. Because the transit of a dispersed particulate phase through the proximal colon is longer, about 12 h (11,12) the maximum time window for absorption in this case is somewhat longer, 12–15 h. Further studies using the Pulsincap system (13) were carried out in our laboratories with the objective of targeting the distal colon using a pulsed delivery of a transcellular probe (quinine) and ^{51}Cr-EDTA, a paracellular probe (14). In these studies, subjects were dosed at 10 PM to ensure delivery to the descending colon by lunchtime the following day. The site of release was identified by incorporating ^{111}In-labeled resin into the unit and the subjects were imaged with a gamma camera. A total of 39 subjects were investigated. Fifteen hours after nocturnal administration, the majority of the delivery systems were situated in the proximal colon at their predicted release time and had not advanced further than a similar set of systems viewed only 6 h after dosing. This relative stagnation appears to reflect the lack of propulsive activity in response to by the intake of food and the effect of sleep in reducing colonic electrical and contractile activity (15–19). Delayed nocturnal gastric emptying (20) and reduced propagation velocity of the intestinal migrating

motor complex (21) may also have been contributory, as supported by the finding that in two individuals the delivery system did not enter the colon until 12.5 and 13.5 h after ingestion.

If a delayed release formulation is taken close to 5 PM in the afternoon, it will have progressed through to the ascending colon by the time the patient goes to bed. Quiescence of propulsive movements in the large bowel during the night causes a relative stagnation, and units remain in the ascending colon. Potentially, this can increase the time of contact to 11–13 h even for a slowly dissolving matrix. On rising, the change in posture stimulates mass movements, experienced by the subject as an urge to defecate, and contents move from the right to the left side of the colon.

From the studies conducted using gamma scintigraphy and MRI, it appears that both temporal and dietary factors are important codeterminants of transit. For poorly soluble substances, the reserve time is an important determinant of bioavailability. Moving away from the current practice of dosing sustained-release formulations in the mornings might allow a reduction in the dosing frequency and increased efficacy of colon-targeted drugs, and would be especially suitable for formulations used to prevent acute disease episodes at night and in the early morning.

ACKNOWLEDGMENTS

Most of the work decribed in this chapter was carried out under the aegis of a MRC LINK award to the author and R. C. Spiller. I gratefully acknowledge the support of colleagues in the conduct of this work.

REFERENCES

1. Ekeberg O, Feinberg MJ. Altered swallowing function in elderly patients without dysphagia: radiological findings in 56 cases. Am J Roentgenol 1991; 156:1181–1184.
2. Perkins AC, Wilson CG, Blackshaw PE, Vincent RM, Dansereau RJ, Juhlin KD, Bekker PJ, Spiller RC. Impaired oesophageal transit of capsule versus tablet formulation in the elderly. Gut 1994; 35:1363–1367.
3. Perkins AC, Wilson CG, Frier M, Vincent RM, Blackshaw PE, Dansereau RJ, Juhlin KD, Bekker PJ, Spiller RC. Esophageal transit of risedronate cellulose-coated tablet and gelatin capsule formulations. Int J Pharm 1999; 186:169–175.

4. Hardy JG, Wilson CG. Radionuclide imaging in pharmaceutical, physiological and pharmacological research. Clin Phys Physiol Meas 1981; 2:71–121.
5. Wilson CG, Washington N. Assessment of disintegration and dissolution of dosage forms in vivo using gamma scintigraphy. Drug Dev Ind Pharm 1988; 14: 211–218.
6. Davis SS, Hardy JG, Taylor MJ, Whalley DR, Wilson CG. A comparative study of the gastrointestinal transit of a pellet and tablet formulation. Int J Pharm 1984; 21:167–177.
7. Wilson CG, Washington N, Greaves JL, Kamali F, Rees JA, Sempik AK, Lampard JF. Bimodal release of ibuprofen in a sustained-release formulation: a scintigraphic and pharmacokinetic open study in healthy volunteers under different conditions of food intake. Int J Pharm 1989; 50:155–161.
8. O'Reilly S, Wilson CG, Hardy JG. The influence of food on the gastric emptying of multiparticulate dosage forms. 1987; 34:213–216.
9. Florence AT. The oral uptake of micro- and nanoparticulates; neither exceptional nor unusual. Pharm Res 1997; 14:259–266.
10. Hebden JM, Perkins AC, Frier M, Wilson CG, Spiller RC. Limited exposure of left colon to daily dosed oral formulations in active distal ulcerative colitis: exploration of poor response to treatment? Gut 1997; 40:112.
11. Hardy JG, Wilson CG, Wood EE. Drug delivery to the proximal colon. Pharm Pharmacol 1985; 37:874–77.
12. Barrow L, Spiller RC, Wilson CG. Pathological influences on colonic motility: implications for drug delivery. Adv Drug Deliv Rev 1991; 7:201–218.
13. Rashid A. Dispensing Device. British Patent Application 2230441A; 15 February 1990.
14. Hebden JM, Wilson CG, Spiller RC, Gilchrist PJ, Blackshaw E, Frier ME, Perkins AC. Regional differences in quinine absorption from the undisturbed human colon assessed using a timed release delivery system. Pharm Res 1999; 16:1087–1092.
15. Frexinos J, Bueno L, Fioramonti J. Diurnal changes in myoelectric spiking activity of the human colon. Gastroenterology 1985; 88:1104–1110.
16. Narducci FG, Bassotti G, Gaburri M, Morrelli A. Twenty four hour manometric recording of colonic motor activity in healthy man. Gut 1987; 28:17–25.
17. Bassotti G, Betti C, Imbimbo BP, Pelli MA, Morelli A. Colonic motor response to eating: a manometric investigation in the proximal and distal portions of the viscus in man. Am J Gastroenterol 1989; 84:118–122.
18. Bassotti G, Betti C, Imbimbo BP, Pelli MA, Morelli A. Colonic high-amplitude propagated contractions (mass movements): repeated 24-h manometric studies in healthy volunteers. J Gastrointest Motil 1992; 4:187–191.
19. Soffer EE, Scalabrini P, Wingate D. Prolonged ambulant monitoring of human colonic motility. Am J Physiol 1989; 257:G601–G606.
20. Ghoo RH, Moore JG, Greenberg E, Alazraki NP. Circadian variation in gastric emptying of meals in humans. Gastroenterology 1987; 93:515–518.
21. Kumar D, Wingate D, Ruckebusch Y. Circadian variation in the propagation velocity of the migrating motor complex. Gastroenterology 1986; 91:926–930.

2
Permeability in the Gastrointestinal Tract

Lars Knutson, F. Knutson, and T. Knutson
Enköping Hospital, Uppsala University, Uppsala, Sweden

I. INTRODUCTION

The specificity of most drug actions suggests a bond formation between the drug and some cellular constituent, generally referred to as a receptor. Drug–receptor interactions may initiate responses by altering the permeability of membranes, by interfering with carrier mechanisms, by modifying templates, or by acting on enzymes.

Current trends in fundamental research on drug effects focus on transport of ions and the binding and release of endogenous mediators, with much work being done in isolated systems.

Agonistic or antagonistic effects demonstrated in the test tube can, however, be completely different when we start to evaluate the action of the drug in the human body. Claude Bernard stated, in 1865, that the study of drug effects and permeability implied ''. . . dealing with the elementary parts of organisms where the elementary properties of vital phenomena have their seat.'' Being a surgeon whose main interest is focused on intestinal physiology and abdominal diseases, my own personal opinion is that the seat for the vital phenomena stated by Bernard is the gastrointestinal tract, or putting it more generally: ''The road to a man's heart goes through his intestine.''

Various physiological factors must be considered to achieve beneficial and therapeutic effects from a drug. The goal is not only to have an effect on ''a man's heart'' but on the entire organism or special organ systems. This

demands certain qualities in the preparation and characteristics of a drug which will enable it to be absorbed into the body. Here the oral route of administration can be more demanding than any other method of administration.

II. INTESTINAL PERMEABILITY

Two major functions of the small intestine are, at first glance, contradictory. These are the efficient absorption of nutrients, fluids, electrolytes, and drugs, and the simultaneous exclusion of potentially antigenic or toxic inflammatory substances (1). The selective ability of the intestinal epithelium to provide a barrier to the absorption of these potentially harmful compounds is often referred to as permeability. Abnormal permeability may be important in the pathogenesis and pathophysiology of various diseases, such as celiac disease, rheumatoid arthritis, nonsteroidal anti-inflammatory drug (NSAID)-associated enteritis, and Crohn's disease (2). To achieve more dependable methods to study permeability and permeability changes, the degree of penetration through the intestinal wall by water-soluble molecules has been investigated. A variety of different probes have been used and described in studies of permeability of the small intestine (3,4). Usually these probes are administered orally, and their excretion rate in the urine is used to measure their penetration through the intestinal barrier.

A. Dissenting Permeability Data

Since the 1970s, there have been more than 20 studies assessing the intestinal permeability of patients with Crohn's disease. Some of these studies show that the results of permeability studies vary according to the type of probe used. However, studies using the same probe in seemingly identical patient groups also diverge; the reasons why are unclear. Evidently, permeability studies using different orally ingested smaller and larger probes only address some of the pathological changes taking place in patients with gastrointestinal diarrheal disease. Altered gastric-emptying rate, shortened intestinal transit time, absorption of permeability probes in different parts of the small intestine, or differences in degree of mucosal inflammation or area available for absorption are factors that are not fully controlled when the probes are administered by mouth. Different and new techniques are needed to obtain a purer measure of intestinal permeability before a clear understanding of the importance of the barrier can be reached, not only for drug absorption, but also for the gene-

sis and perpetuation of intestinal disorders such as Crohn's disease, celiac disease, and other forms of food intolerance.

Loc-I-Gut Techniques

Through intestinal perfusion using the Loc-I-Gut instrument—a multichanneled tube with two or more balloons for insulation of different intestinal segments—it is possible to control and also determine permeability and release of inflammatory mediators as well as to perform controlled and accurate studies of absorption of different pharmacological compounds (Fig. 1). A more

FIG. 1 The Loc-I-Gut technique enables precise determination of drug permeability in defined segments of the small intestine.

detailed description of the technique is given elsewhere (5) and some permeability data obtained with the Loc-I-Gut are presented in Chapter 7.

III. MUCOSAL INTEGRITY

Studies of gastrointestinal physiology reveal an intricate interaction between central and peripheral nerves, hormones, and peptides inside and outside the intestinal cell. This is exemplified by the different phases of vagal stimulation, made known to the rest of the world by Pavlov's classic studies in dogs in the 19th century. To use a slight understatement: Our knowledge has expanded since the work of Pavlov. We know now that physiological intestinal homeostasis is mediated through several mechanisms, whereby the way in which cellular mucosal defense is achieved is of utmost importance for maintaining mucosal integrity and thus also very relevant to drug absorption.

Bicarbonate secretion in the stomach and proximal duodenum is capable of maintaining a neutral pH on the mucosal surface despite pH values as low as 2 in the lumen. This is achieved through the effect of bicarbonate secretion and the unstirred mucous gel layer (6). The formation of bicarbonate and acid is in equilibrium with carbon dioxide and water through the Hendersson–Hasselbalch equation and mediated through the effect of the enzyme carbonic anhydrase. Carbonic anhydrase is, in fact, very important in maintaining acid–base balance throughout the body (7,8).

Although the incidence of peptic ulcers had already declined previous to the introduction of H_2-blockers, pharmacological treatment of peptic ulcer disease has transformed peptic ulcer surgeons into an endangered species. The effect on the parietal cell by H_2-blockers and hydrogen pump inhibitors is economically worldwide truly impressive. Furthermore, if it had been suggested in earlier decades that the bleeding ulcer the surgeon was treating with the knife was, in fact, an infectious disease caused by an organism called *Helicobacter pylori* and should be treated with antibiotics, the world would probably have scoffed at the idea.

IV. INCREASED MUCOSAL INFLAMMATION

Different intestinal diseases also have an influence on drug absorption through mucosal activation of different inflammatory reactions. Basically, an antigen is presented to a macrophage in the intestinal wall. This causes release of different cytokines and inflammatory mediators and induces activation of T

cells, with concomitant increase in immunoglobulins. Further inflammatory cascades include complement pathway activation as well as induction of synthesis of eicosanoids (i.e., leukotrienes, prostaglandins, or prostacyclins).

V. AN INTRIGUING PANENTERITIS

An immunologically very interesting intestinal disease is Crohn's disease. The pathophysiology of this disease, as well as ulcerative colitis, involves a sequence of immunological steps, with an intense activation of different effector cells. The precise nature of the antigens that initiate inflammatory bowel disease is unknown, but it is likely that Crohn's disease represents the final expression of a variety of genetic and environmental factors. These initiating factors may well differ from those factors that cause relapse of the disease.

Crohn's disease is a diffuse lesion of the entire gastrointestinal (GI) tract. This is exemplified by studies of intestinal histamine release and complement activation, which have shown that disease activity in the distal part of the small intestine has a significant influence on cells in the wall of the intestine as far as 3-m proximal to the site of macroscopic as well as microscopic inflammation (9,10). Increased prostaglandin activation can even be detected in clinically completely healthy first-degree relatives (11).

VI. CONCLUSION

Human perfusion studies add to our knowledge of intestinal variables relative to pathophysiology, physiology, and immunology, especially in certain diseases for which we lack satisfactory animal models. The oral administration of many drugs and drug candidates is prevented by their poor penetration through the intestinal barrier. Several highly potent polypeptides and protein drugs belong to this group of compounds, and it is of considerable interest to improve the understanding of this barrier to enable and optimize oral administration of such substances. Thorough research studies in our own species are needed for the final evaluation of any new or generic drug.

REFERENCES

1. Ma TY, Hollander D, Krugliak P, Katz K. PEG 400, a hydrophilic molecular probe for measuring intestinal permeability. Gastroenterology 1990; 98:39–46.

2. Hollander D, Vadheim CM, Brettholz E, Petersen GM, Delahunty T, Rotter JI. Increased permeability in patients with Crohn's disease and their relatives—a possible etiological factor. Ann Intern Med 1986; 105:883–885.
3. Editorial. Intestinal permeability. Lancet 1985; 1:256–258.
4. Hollander D, Koyama S, Dadufalza V, Tran DQ, Krugliak P, Ma T, Ling K-Y. Polyethylene glycol 900 permeability of rat intestinal and colonic segments in vivo and brush border membrane in vitro. J Lab Clin Med 1989; 113:505–515.
5. Knutson L, Odlind B, Hällgren R. A new technique for segmental jejunal perfusion in man. Am J Gastroenterol 1989; 84:1278–1284.
6. Knutson L, Flemström G, Gustavsson S, Jedstedt G, Lönnerholm G. HCO^-_3 secretion in rat duodenum after treatment with omeprazole and ranitidine. Scand J Gastroenterol 1987; 22:87–90.
7. Lönnerholm G, Knutson L, Wistrand PJ, Flemström G. Carbonic anhydrase in the normal rat stomach and duodenum and after treatment with omeprazole and ranitidine. Acta Physiol Scand 1989; 136:253–262.
8. Knutson TW, Koss MA, Hogan DL, Isenberg J, Knutson L. Acetazolamide inhibits its basal and stimulated HCO^-_3 secretion in the human proximal duodenum. Gastroenterology 1995; 108:102–107.
9. Knutson L, Ahrenstedt Ö, Odlind B, Hällgren R. The jejunal secretion of histamine is increased in active Crohn's disease. Gastroenterology 1990; 98:849–854.
10. Ahrenstedt Ö, Knutson L, Nilsson B, Nilsson–Ekdahl K, Krogh M, Odling B, Hällgren R. Evidence of enhanced local production of the complement components C4, C3 and factor B in the small intestine in Crohn's disease. N Engl J Med 1990; 322:1345–1349.
11. Ahrenstedt Ö, Hällgren R, Knutson L. Jejunal release of prostaglandin E_2 in Crohn's disease. Relation to disease activity and first-degree relatives. J Gastroenterol Hepatol 1994; 9:539–543.

3
Gastrointestinal Disease and Dosage Form Performance

Vladan Milovic and Jürgen Stein
Johann Wolfgang Goethe University, Frankfurt on Main, Germany

I. INTRODUCTION

Most of the data about bioavailability of orally administered drugs are obtained from healthy control individuals. However, many drugs are actually administered to patients in whom the underlying disease might affect either their absorption or overall bioavailability. This is particularly true for patients suffering from diseases of intestinal absorption and digestion. In spite of a great potential importance for both clinicians and pharmacists, there are only a few reviews on this topic published to date (1,2). Therefore, the aim of this chapter is to point out some gastrointestinal and systemic diseases that may affect drug absorption in humans.

Drug absorption from the gastrointestinal tract is influenced by the following factors:

1. Gastric and intestinal motility
2. Physicochemical properties of the environment in the small intestine
3. Surface area available for absorption

Although the motility might influence the completeness of intestinal absorption, the intestinal environment can, in addition, dictate the physicochemical behavior of orally administered drugs. Gastrointestinal diseases, systemic diseases with intestinal involvement, and the consequences of gastrointestinal surgery may modify any or all of the foregoing factors. Subsequently, changes

in the therapeutic effects of drugs administered by the oral route may occur. Bioavailability of orally administered drugs in patients with gastrointestinal disease can deviate greatly from that in healthy subjects, depending on the type and severity of the disease and complexities of the pathology involved. Consequently, both clinicians and pharmacists should be aware that in patients with gastrointestinal diseases the possibility of altered bioavailability exists, and anticipate any monitoring of, or alterations in, therapy that may have to be made.

Because gastrointestinal transit is discussed in detail elsewhere (see Chapter 1), this review will be restricted to diseases of intestinal absorption and digestion, and a review of recent literature related to their influence on drug absorption and bioavailability in humans.

II. INTESTINAL MALABSORPTION AND MALDIGESTION

In the last decades there has been an increase in our knowledge on the mechanisms and underlying diseases leading to intestinal malabsorption (3). A better understanding of the pathophysiology of fat digestion and absorption, definition of isolated defects of transport systems located at the apical membrane of the small intestinal epithelial cells, mechanisms of bile acid absorption in health and disease, and access to the intestinal lumen by means of specific laboratory tests, are among the milestones that have been achieved in the investigation of pathophysiological mechanisms and consequences of intestinal malabsorption and maldigestion.

A. Malabsorption

Malabsorption is defined as impaired absorption of nutrients, occurring either when there is

1. A defect in membrane transport systems of the small intestinal epithelium, without morphological changes (primary malabsorption)
2. Defects in the epithelial absorptive surface, with concomitant morphological changes of the mucosa (secondary malabsorption)

In addition, there is a difference between global and partial (isolated) malabsorption syndrome (Table 1).

The major pathophysiological mechanisms in malabsorption are as follows:

Defects of the luminal phase of digestion
Defects of the mucosal phase of terminal digestion and absorption
Defects of the transport phase (Table 2).

Table 1 Global and Partial or Isolated Malabsorption Syndrome

Global malabsorption syndromes
Small intestinal disease with diffuse mucosal involvement
Celiac disease
Autoimmune enteropathy
Tropical sprue
Reduced absorptive surface
Short-bowel syndrome
Partial or isolated malabsorption syndromes
Carbohydrate intolerance
Bile acid malabsorption
Bacterial overgrowth
Protein-losing enteropathy
Maldigestion in
Exocrine pancreatic insufficiency
Cholestasis
Bacterial overgrowth
Bile acid malabsorption
Gastrinoma
Small-bowel resection
Radiation enteritis
Intestinal lymphatic obstruction

1. Fat Malabsorption

Fat malabsorption may affect absorption of lipophilic drug formulations and, as such, deserves particular attention. The basic mechanisms of fat digestion and absorption are now well understood. By the action of pancreatic lipase, dietary triglycerides are degraded to monoglycerides and fatty acids. Bile salts in the jejunal lumen are responsible for micelle formation and subsequent solubilization of monoglycerides and fatty acids, allowing them to penetrate the intestinal mucosa. Triglycerides are resynthesized in the mucosa and, in the form of chylomicrons, are transported first to the intestinal lymphatics and subsequently into the general circulation.

Disturbances of each particular phase of dietary fat degradation, solubilization, and delivery into the systemic circulation may lead to fat malabsorption and steatorrhea. Impaired production or activity of pancreatic lipase (exocrine pancreatic insufficiency), disorders of bile acid metabolism (obstructive jaundice, bile acid malabsorption, and bacterial overgrowth), decreased absorptive

Table 2 Pathophysiology of Maldigestion and Malabsorption

Luminal phase
Reduced nutrient availability
Cofactor deficiency (pernicious anemia, gastric resection)
Increased nutrient consumption (bacterial overgrowth)
Impaired fat solubilization
Reduced bile salt synthesis (hepatocellular disease)
Impaired bile salt secretion (cholestasis)
Bile salt inactivation (bacterial overgrowth)
Impaired CCK release (mucosal disease such as celiac disease)
Increased bile salt loss (terminal ileal disease or resection)
Defective nutrient hydrolysis
Lipase inactivation (Zollinger–Ellison syndrome)
Enzyme insufficiency (pancreatic insufficiency)
Improper mixing or intestinal hurry (resection, bypass, hyperthyroidism)
Mucosal phase
Extensive mucosal loss (resection, infarction)
Diffuse mucosal disease (celiac disease, autoimmune enteropathy, tropical sprue, Crohn's disease, infections, drugs)
Enterocyte defects
Microvillus inclusion disease
Tufting enteropathy
Brush border hydrolase deficiency (lactase deficiency)
Transport defects (glucose–galactose malabsorption, Hartnup's disease)
Epithelial processing (abetalipoproteinemia)
Transport phase
Vascular (vasculitis)
Lymphatic (Whipple's disease, intestinal lymphangiectasia, radiation enteritis, tumor invasion)

surface area (resection, inflammation, atrophy), or abnormalities in lymphatic flow in the gut (see Table 2) are among the potential causes of fat malabsorption. *Steatorrhea* (defined as stool fat > 7 g/day) leads to enteral loss of dietary fat, lipid-soluble vitamins, and calcium, as well as to an increased oxalate absorption with resultant ''enteric'' hyperoxaluria. Disturbances of bile acid metabolism may also cause steatorrhea and malabsorption, by the impairment of the micellar phase of fat digestion in the small-intestinal lumen. An excess enteral loss of bile acids can be compensated by an increase of bile acid synthesis in the liver. This, however, often results in watery diarrhea owing to the impairment of water reabsorption in the colon by bile acids. If intestinal bile

acid loss is higher than the synthetic capacity of the liver (for example, in ileal resection, or short-bowel syndrome), bile acid concentration in the intestinal lumen will be insufficient to induce micelle formation, resulting in decompensated bile acid malabsorption and associated diarrhea and steatorrhea. Small-intestinal bacterial overgrowth is a consequence of morphological changes of the intestine (diverticula, fistulas, strictures, or stenosis) as well as motility disorders (diabetic gastroenteropathy and scleroderma). When deconjugated and dehydroxylated by the intestinal bacteria, bile acids exert a toxic effect on the colonic mucosa, again leading to a watery diarrhea. Because of the bacterial activity, the concentration of conjugated bile acids will be increased, resulting in malabsorption of fat and fat-soluble vitamins (A, D, E, and K). Bacterial overgrowth in the gut also leads to fermentation of carbohydrates in the intestinal lumen.

2. *Carbohydrate Malabsorption*

Starch, sucrose, and lactose are the most abundant digestible carbohydrates in the intestinal lumen. On the other hand, many of the polysaccharides originating from plants cannot be digested in the lumen. Impaired absorption of normally digestible carbohydrates may occur because of a lack in pancreatic α-amylase defects in disaccharidase activity in the small intestinal epithelium, or reduced absorptive intestinal surface. In primary carbohydrate malabsorption, single functional elements of carbohydrate digestion or absorption are missing (lactase, sucrase, glucose carrier) without apparent morphological changes. A generalized reduction of the intestinal absorptive surface can also lead to an impaired digestive and absorptive capacity in the gut (e.g., villus atrophy in celiac disease), resulting in secondary carbohydrate malabsorption (4).

Carbohydrates that are not digested and absorbed in the small intestine undergo bacterial degradation in the colon. The terminal phase of bacterial carbohydrate degradation is fermentation, resulting in formation of short-chain fatty acids (butyrate, propionate, acetate, lactate), as well as CO_2, H_2, and CH_4. Short-chain fatty acids can be further utilized by the body through efficient reabsorption in the colon. Bacterial fermentation of carbohydrates secondary to malabsorption results in acidic stools, abdominal distension, meteorism, and flatulence. Similarly, dietary fibers can be degraded by bacterial enzyme activity in the colon; the extent of their degradation determines their effect on stool volume. Thus, poorly degradable fibers increase stool volume and regulate bowel movements, and are, therefore, useful in the treatment of constipation.

3. Protein Malabsorption

Impaired digestion and absorption of dietary protein occurs when pancreatic protease secretion or activity is impaired (exocrine pancreatic insufficiency), in rare isolated absorption defects (e.g., Hartnup disease), and in generalized reduction of the intestinal absorptive surface (e.g., celiac disease). Of particular clinical importance is protein-losing enteropathy, in which plasma protein is excreted into the intestinal lumen, resulting in development of hypoalbuminemia and edema.

B. Maldigestion

Maldigestion is a consequence of impaired digestion of nutrients within the intestinal lumen, or at the terminal digestive site of the brush-border membrane of mucosal epithelial cells. It can occur because of congenital or acquired disease in which pancreatic enzyme activity, bile acid concentration, or small-intestinal mucosal enzymes are decreased or absent.

The pathophysiological possibilities leading to malabsorption–maldigestion syndrome are listed in Table 3. If there is impaired digestion, pancreatic insufficiency is the most frequent cause. The insufficiency may be due to chronic pancreatitis, pancreatic surgery, cystic fibrosis, pancreatic carcinoma,

Table 3 Diseases Resulting in Malabsorption and Maldigestion

Maldigestion caused by deficiency or inactivation of pancreatic enzymes
Chronic pancreatitis
Surgical resection of the pancreas
Pancreatic cancer
Cystic fibrosis
Zollinger–Ellison syndrome
Maldigestion caused by impaired luminal bile acid concentration
Obstructive jaundice
Intrahepatic cholestasis
Primary biliary cirrhosis
Primary sclerosing cholangitis
Small intestinal bacterial overgrowth (blind loop syndrome, fistulas, strictures, diverticula, afferent loop syndrome, motility disorders in scleroderma, and diabetic gastroenteropathy)
Ileal resection (decompensated bile acid loss)
Crohn's disease of the ileum
Maldigestion/malabsorption caused by small-intestinal diseases

Table 3 *Continued*

- Primary malabsorption: congenital diseases with selective defect of single functions of epithelial cells (disorders of the brush border membrane)
  - Lactose intolerance
  - Sucrose–isomaltose intolerance
  - Trehalose intolerance
  - Enterokinase deficiency
  - Glucose–galactose intolerance
  - Cystinuria
- Secondary malabsorption: acquired small-intestinal diseases
  - Celiac disease
  - Tropical sprue
  - Whipple's disease
  - Primary intestinal lymphoma
  - Hypogammaglobulinemia
  - Selective IgA deficiency
  - Eosinophilic gastroenteritis
  - Amyloidosis
  - Parasitoses (giardiasis, strongyloidosis, ascaridosis, ancylostomiasis)
  - HIV enteropathy with wasting syndrome
  - Tuberculosis
  - Lymphogranulomatosis
  - Kwashiorkor
  - Short bowel syndrome
  - Intestinal ischemia
  - Radiation enteritis
- Various disorders of digestion and absorption
  - Postgastrectomy syndrome
  - Postvagotomy syndrome
  - Diabetic gastroenteropathy
  - Endocrinopathies (hyper- and hypothyroidism, hyper- and hypoparathyroidism, Addison's disease, medullary carcinoma of the thyroid)
  - Glucagonoma, gastrinoma, VIPoma
  - Scleroderma
- Drug-induced malabsorption
  - Cholestyramine
  - Laxatives
  - Colchicin
  - Antineoplastic drugs
  - Neomycin
  - *p*-Aminosalicylic acid (PAS)
  - Biguanides
  - Lactulose, sorbitol, fructose
  - Nonsteroidal anti-inflammatory drugs (NSAID)
  - Alcohol

Zollinger–Ellison syndrome, (rare) congenital lipase deficiency, or postoperative postprandial pancreaticobiliary asynchrony (5). Cystic fibrosis, usually diagnosed in childhood, leads to exocrine pancreatic insufficiency in adults. Chronic diarrhea with accompanying steatorrhea can also occur in gastrinoma (Zollinger–Ellison syndrome). In this case, the high volumes of gastric juice entering the small intestine prevent the critical bile acid concentration necessary for the formation of micelles during fat digestion from being reached and also inactivate pancreatic lipase owing to the low pH.

Postoperative syndromes (gastric resection by Billroth II operation, vagotomy, Whipple's operation) not only lead to motility disorders, but can also, in spite of preserved function of the exocrine pancreas, lead to a disturbed digestion. The mechanism responsible for this disorder is the rapid gastric emptying that induces impaired or decreased hormonal stimulation of the exocrine pancreas (postprandial pancreaticobiliary asynchrony) (6).

Maldigestion can also develop when critical micellar concentration of bile acids is insufficient to contribute to fat digestion (intraluminal impairment of bile acids) under the following conditions:

1. If there is an impaired secretion of bile acids into the lumen (obstructive jaundice, intrahepatic cholestasis, primary biliary cirrhosis)
2. If there is an extensive bile acid loss from the lumen, higher than the synthetic capacity in the liver
3. If bile acids are deconjugated in the intestinal lumen owing to bacterial overgrowth syndrome

An increased enteral bile acid loss occurs most frequently in Crohn's disease with ileal involvement, and after surgical resection of the ileum. If less than 1 m of ileum is removed or functionally impaired, a compensated chologenic diarrhea occurs, and it can be efficiently treated with ion-exchangers (cholestyramine, cholestipol). Diarrhea is watery and occurs because of the laxative effect of bile acids on the large bowel mucosa. If enteral bile acid loss exceeds the maximal synthetic capacity of the liver (e.g., ileal resection of more than 1 m), an impairment of the ability to reach the critical bile acid micellar concentration occurs, with consequent fat maldigestion and steatorrhea. This decompensated chologenic diarrhea will become even worse if treated with anion-exchange resins.

Ingestion of a nonabsorbable artificial sweetener, sorbitol, can lead to an osmotic diarrhea (''chewing gum diarrhea''). As little as 5 g sorbitol can induce intestinal symptoms, and 10 g leads to meteorisms, flatulence, and

diarrhea. The symptoms can be worsened by the addition of fructose, which is also poorly absorbed in the gut.

III. GASTROINTESTINAL DISEASES THAT CAN INFLUENCE DRUG ABSORPTION

Drug absorption in patients with gastrointestinal disorders is influenced by changes in gastric and intestinal motility, changes in the surface area available for drug absorption, and altered physical and chemical properties of the intestinal luminal content. These properties are usually changed in combination, the degree of each being dependent on the duration and severity of the disease.

A. Crohn's disease

The incidence of Crohn's disease has been increasing in recent years; in the United States, the total population with this disease is estimated to be 200,000–400,000, with 15,000–30,000 new cases occurring each year. The etiology of Crohn's disease remains unknown, although various infectious agents, immunological causes, and familial clustering are thought to contribute to its development. Although Crohn's disease may be distributed along the entire intestine, it most commonly involves the ileocolic region. More than one area of the gut can be affected, while the bowel in between appears normal, giving rise to so-called skip areas. Typical manifestations are a thickening of the intestinal wall, mucosal fissures, fistulas, inflammatory masses, and benign strictures. The resulting clinical findings include diarrhea, abdominal pain, fever, and weight loss.

Because of its highly variable clinical presentation, Crohn's disease may lead to impaired drug absorption by any of the three mechanisms of malabsorption: the thickened bowel wall and strictures may significantly alter the bowel motility; mucosal lesions may lead to changes in intestinal permeability; and involvement of specific intestinal areas (e.g., terminal ileum) may cause bile acid malabsorption and subsequent fat maldigestion. Although nowadays this disorder can be treated efficiently with anti-inflammatory agents (e.g., acetylsalicylic acid and its derivatives, and corticosteroids), anatomical changes of the intestine may well result in altered drug absorption, even in patients in remission. For this reason, particular emphasis should be given to drug dosage and formulation in patients with Crohn's disease.

B. Celiac Disease

Celiac disease is characterized by atrophy of the small intestinal mucosa, with subsequent impairment of absorption of all nutrients, including fat. It is caused by hypersensitivity to a protein present in wheat: gluten. Elimination of wheat (gluten-free diet) results in the normalization of small-intestinal morphology and restored absorptive function.

C. AIDS Enteropathy

As a part of acquired immunodeficiency syndrome (AIDS), diarrhea and a general wasting syndrome frequently occur (7). This is not always due to accompanying infections; the AIDS virus itself can damage the intestinal mucosa. Patients with AIDS enteropathy have an abnormal carbohydrate malabsorption, bacterial overgrowth of the intestine, often also some disaccharidase deficiency, bile acid malabsorption, and steatorrhea (8). Reduced total drug exposure is related to malabsorption in persons with human immunodeficiency virus (HIV) infection or AIDS (9).

Furthermore, intestinal permeability in patients with AIDS enteropathy is increased, in a way similar to celiac disease. The duodenum of HIV-infected patients with diarrhea showed an impaired epithelial barrier function, which was thought to contribute to diarrhea by a leak–flux mechanism (10). Despite the increase in permeability, some protease inhibitors used in the treatment of patients with HIV infection (e.g., saquinavir) have kinetic profiles characterized by reduced absorption and a high first-pass effect, resulting in poor bioavailability. Administration with food led to an improvement in absorption in the case of saquinavir. Further pathophysiological factors, such as achlorhydria, malabsorption, and hepatic dysfunction, may also influence the bioavailability of the protease inhibitors in patients with HIV disease (11).

D. Small-Intestinal Involvement in Systemic Diseases

Systemic diseases, as well as a number of disorders primarily involving an organ system other than the GI tract, may also result in impaired small-intestinal function and result in malabsorption. For example, patients with diabetes mellitus frequently develop diabetic neuropathy, which may involve the autonomous nervous system in the gut. This then results in delayed gastric emptying in patients with diabetes (diabetic gastroparesis) and in impaired small intestinal motility, which, in turn, may lead to bacterial overgrowth syndrome and steatorrhea.

Diarrhea and steatorrhea are frequent accompanying features of hyperthyroidism, and are caused by dysmotility. The small-intestinal mucosa remains morphologically normal. Treatment of the underlying disease improves the gastrointestinal symptoms. Hypothyroidism, on the other hand, is characterized by dysmotility-induced constipation. Malabsorption can also occur. Correction of the underlying hypothyroidism also leads to the improvement of malabsorption.

Amyloidosis, scleroderma, and dermatomyositis can be accompanied by malabsorption syndrome. The etiology is a motility disorder resulting in bacterial overgrowth in the small intestine.

Systemic vasculitis with small-intestinal involvement may influence drug absorption owing to either altered motility or mucosal damage. The decreased absorption of diazepam, phenytoin, and acetaminophen was attributed to inflammatory and vascular changes in the duodenum in Behcet's syndrome, even in the absence of clinical evidence for a malabsorption syndrome (12).

Pancreatic insufficiency is also often associated with malabsorption. The most frequent cause of exocrine pancreatic insufficiency is chronic pancreatitis, and in 75% of these patients the disease is due to chronic alcoholism of long duration. In chronic pancreatitis, the pancreas may be enlarged or atrophic, and dilated ducts are filled with thick protein-rich fluid. Protein plugs formed in the smaller ductules may calcify, and are thought to initiate a recurrent cycle of obstruction, inflammation, and fibrosis. The ultimate result of the disease is exhaustion of the reserve of exocrine pancreas, cessation of the secretion of the part of the pancreatic juice that is rich in proteolytic and lipolytic enzymes, and maldigestion. Patients with exocrine pancreatic insufficiency also exhibit decreased pancreatic bicarbonate secretion. As a result, duodenal pH is reduced after a meal, leading to inactivation of orally administered exogenous enzymes and decreased nuclear solubilization of bile salts. Treatment of pancreatic insufficiency consists of high-dose enzyme replacement therapy with or without gastric acid suppression; this may reduce clinical symptoms and improve malabsorption, but may cause additional problems for drug absorption and interactions if additional drug therapy is required (18).

E. Drug- and Irradiation-Induced Malabsorption

There are numerous reports on various chemically and pharmacologically different substances that can induce malabsorption syndrome. For example, cholestyramine is a drug of choice in the treatment of chologenic diarrhea, but it can, because of its high bile acid-binding capacity, reduce their content in the gut, with subsequent impairment of the micellar phase of fat digestion.

Neomycin and kanamycin also cause reduced absorption of fat, proteins, carotene, vitamin B_{12}, and glucose. Neomycin-induced lactase deficiency is typical.

Together with oral antidiabetic drugs, biguanides may cause malabsorption leading to an impaired absorption of carbohydrates, amino acids, bile acids, and vitamin B_{12} (13). The pseudotetrasaccharide acarbose, a competitive inhibitor of α-glucosidases in the intestinal mucosa, leads to malabsorption of carbohydrates (meteorism, flatulence, diarrhea). Para-aminosalicylic acid (PAS) may cause steatorrhea and impaired absorption of vitamin B_{12}, folic acid, and iron.

Irradiation enteritis occurs less frequently than colonic lesions after radiotherapy. Adhesions in the ileocecal area after irradiation therapy of gynecological malignancies may lead to watery diarrhea.

F. Aging

Although there is little clinical evidence that significant malnutrition occurs in any normal elderly person as a result of the aging process itself (14,15), almost all diseases that may cause malabsorption occur in the elderly. Malnutrition resulting from chronic congestive heart failure (cardiac cachexia) is relatively common. Impaired absorption of fat is related to the clinical severity of heart failure, but is apparently not associated with small-bowel bacterial overgrowth (16). Malabsorption in the elderly can be caused by gastric hypochlorhydria, with subsequent small-bowel bacterial overgrowth, or by gastrointestinal dysmotility caused by subclinical hypothyroidism. Moreover, a true defect in calcium absorption in the elderly has been described (17).

G. Small-Bowel Resection

Short bowel syndrome is defined as a series of metabolic and nutritional events developing after an extensive intestinal resection. Surgical removal of up to approximately 50% of the small intestine can be well tolerated, because the remaining intestine adapts to an increased demand to absorb nutrients. However, intestinal adaptation takes place only when enteral feeding is used to stimulate the intestinal epithelium to hyperproliferate either directly (owing to the effect of nutrients themselves), or indirectly by stimulating pancreaticobiliary secretions and by hormonal mechanisms. Resection of 70–80% of the small intestine results in severe malabsorption.

Malabsorption in small-intestinal resection is caused by a variety of factors:

1. Marked reduction of the absorptive surface
2. Gastric acid hypersecretion, resulting in pancreatic lipase inactivation and fat maldigestion
3. Reduction of bile acid pool below the amounts necessary for critical micellar concentration
4. Stimulation of colonic secretion by hydroxy fatty acids produced by bacterial hydroxylation of nonabsorbed fat

In the early postoperative phase, small-bowel resection results in a severe watery diarrhea with global malabsorption. During the intermediate phase after surgery, steatorrhea will occur, with subsequent weight loss, and malabsorption of fat-soluble vitamins, essential fatty acids, and trace metals. In the late postoperative phase, intestinal adaptation mechanisms are fully operative and, if enough small intestine is left, the symptoms may gradually normalize. However, intestinal adaptation may not be adequate to sustain overall nutrition without supplementary, intermittent, or continuous parenteral support. Because the mucosal absorptive area may be drastically reduced, absorption of perorally administered drugs can be seriously diminished in patients with a small-bowel resection.

Clinical sequellae of small-bowel resection depend on the extent of the resection, length of the residual small bowel, health of the remaining intestine, site of resection, presence or absence of colon, and time after resection. The intestinal adaptation will occur several weeks after surgery, and will involve changes in small-bowel structure, cytokinetics, and digestive–absorptive function.

In summary, many diseases with primary loci elsewhere in the body as well as local gastrointestinal problems can lead to maldigestion and malabsorption. This can result in changes in release of drug from the dosage form and transport of drug through the intestinal mucosa. Adjustment of drug dosage/formulation or route of administration may be warranted in some patients.

REFERENCES

1. Gubbins PO, Bertch KE. Drug absorption in gastrointestinal disease and surgery. Pharmacotherapy 1989; 9:285–295.
2. Lamka J, Rudisar L, Kvetina J. On the limiting factors affecting the distribution of model drugs from blood into the lymphatic system. Eur J Drug Metab Pharmacokinet 1991; 3:47–51.

3. Lembcke B, Caspary WF. Malabsorption syndromes. Baillière's Clin Gastroenterol 1988; 2:329–352.
4. Caspary WF. Diarrhoea associated with carbohydrate malabsorption. Clin Gastroenterol 1986; 15:631–655.
5. Caspary WF. Interruption of the enteropancreatic axis: effects of induced malabsorption. Eur J Clin Invest 1990; 20(suppl 1):58–64.
6. Becker HD, Caspary WF. Postvagotomy and Postgastrectomy Syndromes. Berlin: Springer Verlag, 1980.
7. Simon D, Brandt LJ. Diarrhea in patients with the acquired immunodeficiency syndrome. Gastroenterology 1993; 106:1238–1242.
8. Ehrenpreis ED, Carlson SJ, Boorstein HL, Craig RM. Malabsorption and deficiency of vitamin B_{12} in HIV-infected patients with chronic diarrhea. Dig Dis Sci 1994; 39:2159–2162.
9. Sahai J, Gallicano K, Swick L, Tailor S, Garber G, Seguin I, Oliveras L, Walker S, Rachlis A, Cameron DW. Reduced plasma concentrations of antituberculosis drugs in patients with HIV infection. Ann Intern Med 1997; 127:289–293.
10. Stockmann M, Fromm M, Schmitz H, Schmidt W, Riecken EO, Schulzke JD. Duodenal biopsies of HIV-infected patients with diarrhoea exhibit epithelial barrier defects but no active secretion. AIDS 1998; 12:43–51.
11. Barry M, Gibbons S, Back D, Mulcahy F. Protease inhibitors in patients with HIV disease: clinically important pharmacokinetic considerations. Clin Pharmacokinet 1997; 32:194–209, 1997.
12. Chaleby K, el-Yazigi A, Atiyeh M. Decreased drug absorption in a patient with Behcet's syndrome. Clin Chem 1987; 33:1679–1681.
13. Caspary WF. Biguanides and intestinal absorption. Acta Hepatogastroenterol 1977; 24:473–480.
14. Arora S, Kassarjian Z, Kraskinski SD, Croffey B, Kaplan MM, Russell RM. Effect of age on tests of intestinal and hepatic functions in healthy humans. Gastroenterology 1989; 96:1560–1564.
15. Lovat LB. Age related changes in gut physiology and nutritional status. Gut 1996; 38:306–309.
16. King D, Smith ML, Chapman TJ, Stockdale HR, Lye M. Fat malabsorption in elderly patients with cardiac cachexia. Age Ageing 1996; 25:144–149.
17. Armbrecht HJ, Zenser TV, Bruns MEH. Effect of age on intestinal calcium absorption and adaptation to dietary calcium. Am J Physiol 1979; 236:E769–E773.
18. Bruno MJ, Haverkort EB, Tytgat GN, van Leeuwen DJ. Maldigestion associated with exocrine pancreatic insufficiency: implications of gastrointestinal physiology and properties of enzyme preparations for a cause-related and patient-tailored treatment. Am J Gastroenterol 1995; 90:1383–1393.

4

Intestinal Permeability: Prediction from Theory

Han van de Waterbeemd
Pfizer Central Research, Sandwich, Kent, United Kingdom

I. BIOAVAILABILITY AND INTESTINAL ABSORPTION

The oral route of administration is preferred for many classes of drugs; ease and patient compliance are the main reasons. Making reliable estimates of oral bioavailability in humans for the selection of the best developmental candidates are a considerable challenge to the pharmaceutical industry. In recent years, several promising in vitro models became available for the study of the absorption potential of new compounds (1). Systemic bioavailability is influenced by a variety of factors (Table 1), with poor solubility, poor permeation, intestinal and liver metabolism, and P-glycoprotein (P-gp)-mediated efflux being among the most common detrimental influences on drug absorption. In this chapter we focus attention on the physicochemical properties of a drug and their influence on the overall bioavailability (2). These properties can have a particularly important effect on the absorption process (Fig. 1). The main uptake mechanism through mucosal membranes is by passive diffusion, using the transcellular pathway (A_1). However, several alternative processes (A_0, A_2–A_6), all of which may affect the final fraction absorbed, need to be considered. These processes may not be independent, and they partly take place in parallel. Often the relative weights (a_0–a_6) of the contributions of each of these potential processes is unknown. Membrane diffusion by the trans- and paracellular pathway is a physicochemical process; therefore, physicochemical properties are believed to have an important influence on these membrane transport

TABLE 1 Factors Influencing Bioavailability

Physiological factors	Pharmacokinetic factors
Membrane transport	GI and liver metabolism (first pass effect)
GI motility	Chemical instability
Stomach emptying	Absorption
Disease state	Distribution and elimination
Formulation	Physicochemical properties
Crystal form (polymorphism)	Lipophilicity
Particle size	Solubility
Absorption enhancers	Degree of ionization (pK_a)
Dissolution rate	Molecular size and shape
Solution, capsule, tablet, or other	Hydrogen-bonding potential

processes. Molecular properties (i.e., structural features and physicochemical properties) can be assessed by experimental and computational approaches. As will be demonstrated in this chapter, by combining these two, reliable estimates of intestinal permeability can be made. However, besides using computation and physicochemical methods, additional in vitro and in vivo studies should be performed to make confident estimates of absorption behavior in humans.

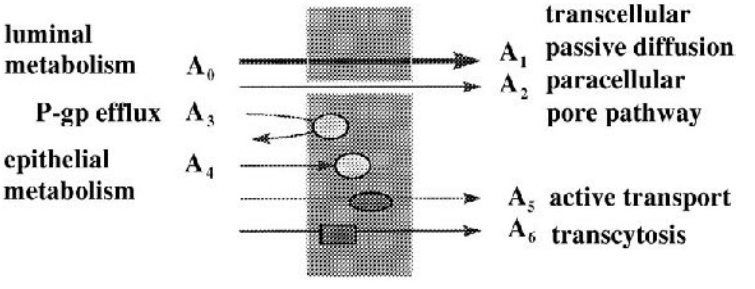

FIG. 1 Mechanisms of oral GI absorption: Many compounds may use several of these alternative routes, although the relative weight of each route is usually unknown.

II. CALCULATED AND EXPERIMENTAL MOLECULAR PROPERTIES

A. Colinearities

Molecular properties relevant to intestinal absorption include lipophilicity, molecular size, charge, hydrogen bonding, and solubility (3). Importantly, most of these properties are dependent on one another. In other words, changing one property of a molecule usually affects one or more of the other properties. Well-established relations include those between lipophilicity and solubility (4,5); lipophilicity and molecular size and hydrogen-bonding (6); and lipophilicity, ionization, and charge (7).

Of particular interest is the finding that log P or log D values are, in fact, a combination of two major contributions, one related to the size of the compound and one related to its capability to form hydrogen bonds (6,8–10).

B. Computational Alerts: The Rule of 5

A retrospective analysis of the World Drug Index (WDI) in terms of calculated physicochemical properties resulted in the definition of the ''rule of 5.'' This rule (11) states that poor absorption or permeation are more likely when

1. There are more than 5 H-bond donors (expressed as the sum of OHs and NHs).
2. There are more than 10 H-bond acceptors (expressed as the sum of Ns and Os).
3. The MW is over 500.
4. The log P is over 5.
5. Compound classes that are substrates for biological transporters are exceptions to the rule.

We have recently analyzed the NCEs introduced to the world market in the years 1993–1995 (n = 43 in 1993, n = 44 in 1994, and n = 36 in 1995; see *Annual Reports in Medicinal Chemistry*). In Fig. 2 the molecular weight (MW) and polar surface area as hydrogen bond descriptors (12,13)—both recognized as key parameters in the rule of 5—have been plotted for these compounds. It can been seen in Fig. 2 that the majority of the compounds that are given orally have a MW lower than 500 and a polar surface area smaller than 120 $Å^2$. The only exceptions are dirithromycin, tacrolimus, saquinavir, ceftidoren, efonidipine, cytarabine, sobuzoxane, valaciclovir, voglibose,

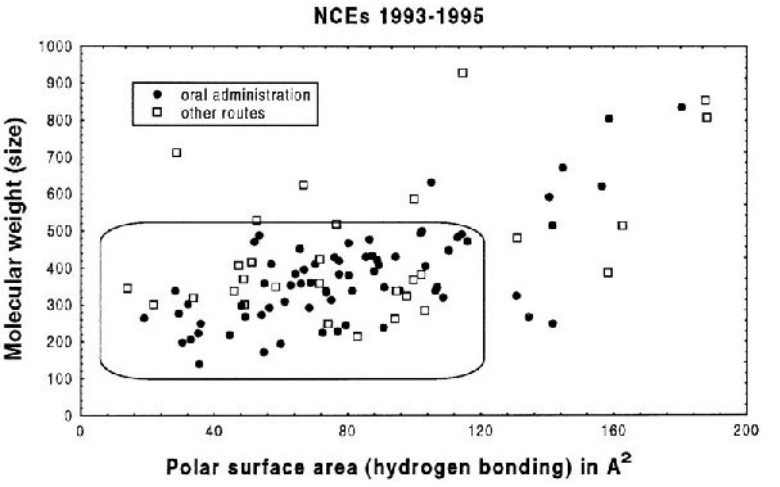

FIG. 2 Plot of the key properties of the NCEs introduced on the market between 1993 and 1995.

and alendronate. Most of these are prodrugs, which should probably be judged on their active principle.

The rule-of-5 is now widely recognized as fundamental for the design of orally absorbed compounds. It is based purely on a computational evaluation of compounds. However, it identifies the most prominent factors influencing oral drug absorption. Combining the findings of Lipinski and those presented in Fig. 2 leads to a description of good leads for orally absorbed compounds as visualized in Fig. 3. Molecular size and hydrogen-bonding capability should be kept below a certain limit, whereas lipophilicity in terms of log *P* or log *D* should fall within a certain range.

In the following sections we will first discuss some key issues around calculated and experimental physicochemical properties, including solubility, lipophilicity, molecular size, and hydrogen bonding. A number of examples of how these properties have been used in the prediction of absorption will then be presented.

C. Solubility

Dissolution rate and solubility are linearly related properties (4). Poorly soluble compounds, therefore, are expected to have dissolution-limited absorption.

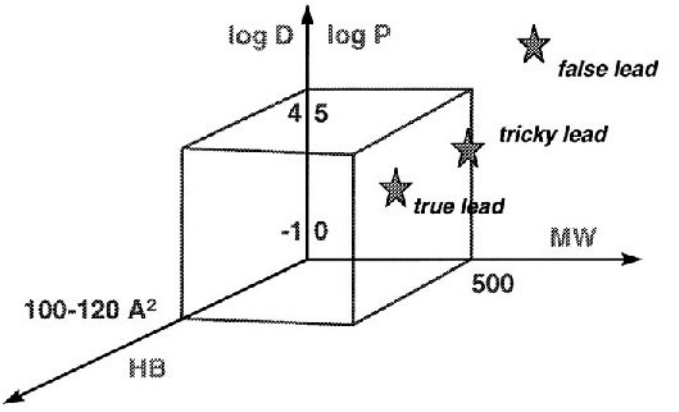

FIG. 3 Optimal properties for orally active compounds are found within the log*P*/log*D*-HB-MW box.

Aqueous solubility (log *S*) is approximately inversely related to lipophilicity (log *P*). Better correlations are obtained when the melting point (mp) of the investigated compounds is taken into account. Equation (1) is the simplified form of the relation between these three properties.

$$\log S = -\log P - 0.01 \text{ mp} + 1.2 \tag{1}$$

The obvious disadvantage of Eq. (1) is that the melting point of the compound is required. This approach cannot be used prospectively. Therefore, several attempts have been made to estimate solubility from molecular structure. The linear solvation energy relationship (LSER) approach of Kamlet and colleagues (14) clearly demonstrates that solubility is dependent on several factors. In their method molecular size, polarity, and hydrogen-donating and hydrogen-accepting factors are the major contributors to solubility. With this approach the solubilities of 105 liquid organic nonelectrolytes of various chemical classes could be correlated as

$$\begin{aligned} \log S = {} & -3.32(\pm 0.05)\, V/100 + 0.46(\pm 0.07)\, \pi^* \\ & + 5.17(\pm 0.06)\, \beta + 0.54\ (\pm 0.08) \\ & n = 105;\ r = 0.995 \end{aligned} \tag{2}$$

where V is the molar volume, π^* the dipolarity–polarizability, and β the H-bond acceptor basicity of the solute. Equations such as Eq. (2) demonstrate that aqueous solubility can be broken down into more fundamental properties, namely solute size and H-bonding potential. Before discussing these in more

detail, we first will demonstrate that these two fundamental properties are also the basis of lipophilicity (3,6,8–10).

D. Lipophilicity

1. Partition (log P) and Distribution (log D) Coefficients

For most biological processes in which biological membranes are involved the lipophilicity is a key descriptor. Particularly 1-octanol/water distribution coefficients at a selected pH (log *D*) and 1-octanol/water partition coefficients (log *P*) had considerable success in quantitative structure–activity relation (QSAR) approaches. However, alternative measures of lipophilicity have also been used (Fig. 4).

In the design phase of new compounds a priori estimates of log *P* and log *D* values can be made using computational approaches (15–20) (Table 2).

The major components of the property lipophilicity are molecular size and hydrogen bonding. A graphic representation of this relation is shown in Fig. 5. In this figure highly absorbed (over 80%) drugs are symbolized as

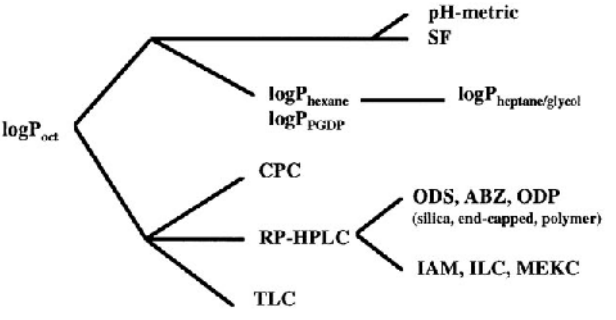

FIG. 4 "Evolutionary tree" of experimental methods for lipophilicity determination. Key of abbreviations: logP_{oct}, 1-octanol/water partition coefficient; logP_{hexane}, 1-hexane/water partition coefficient; logP_{PGDP}, propyleneglycol dipelargonate/water partition coefficient; log*P* heptane/glycol, a nonaqueous system; SF, shake-flask; pH–metric, log*P* determination based on potentiometric titration in water and octanol/water; CPC, centrifugal partition chromatography; RP–HPLC, reversed-phase high-performance liquid chromatography; TLC, thin-layer chromatography; ODS, octadecylsilane; ABZ, end-capped silica RP-18 column; ODP, octadecylpolyvinyl packing; IAM, immobilized artificial membrane; ILC, immobilized liposome chromatography; MEKC, micellar electrokinetic capillary chromatography.

TABLE 2 Programs for log *P* Calculation

Program name	Software package/vendor
ALOGP	Tsar 3.1/Oxford Molecular Group
ACD/logD	ACD/Labs/Advanced Chemistry Development Inc
ACD/logP	ACD/Labs/Advanced Chemistry Development Inc
CHEMICALC	/(18)
CLIP/logP	/University of Lausanne
CLOGP	Pcmodels/Daylight CIS, CLOGP/Biobyte
HINT/logP	/Edusoft
KLOGP	/Multicase Inc.
LISP	/O. Raevsky
LOGKOW	/Syracuse Research Corp.
MLOGP	/(17)
PrologD	PALLAS 2.0/Compudrug Chemistry Ltd.
PrologP	PALLAS 2.0/Compudrug Chemistry Ltd.
SCILOGP	SCILOGP/Scivision
TLOGP	/(19)
XLOGP	/(20)

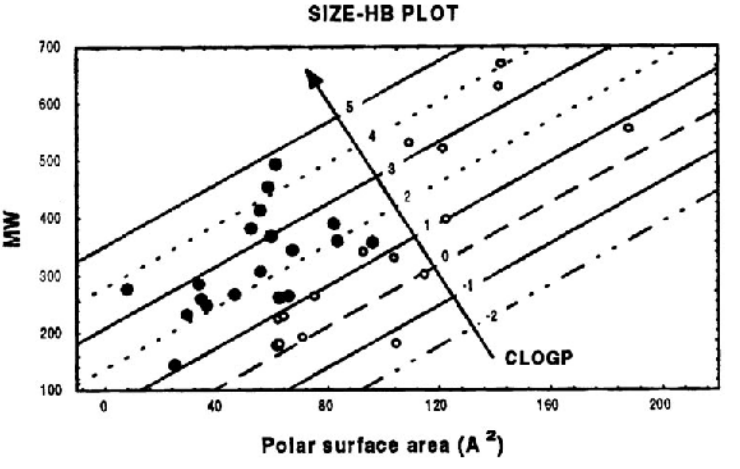

FIG. 5 Lipophilicity (CLOGP) deconstructed into its two main contributors: molecular size (molecular weight, MW) and hydrogen-bonding (polar surface area). The lines are obtained as linear contour plots, connecting points of identical CLOGP value. Filled circles are compounds with > 80% human intestinal absorption. (From Ref. 3.)

filled circles. It can be seen that these are found in a restricted physicochemical property space, as would be expected from the rule of 5.

2. Use of Immobilized Artificial Membranes

It has been suggested that immobilized artificial membranes (IAM) (21,22) or immobilized liposome chromatography (ILC) (23) be used instead of octanol/water distribution coefficients, because these should better mimic membrane partitioning. Typically, linear relations between measures of permeability and log k'_{IAM} have been evaluated and compared with other lipophilicity scales (21,22). However, as we will discuss later, it should be stressed that the relation between permeability and log k'_{IAM} is commonly considered to be sigmoidal (see references under Sec. III.A). Therefore, the claims for usefulness of IAM columns still remain questionable. Furthermore, in many studies, IAM or ILC log k' values appear to be well correlated to 1-octanol/water log D values. If this is true the potential advantages of the IAM technology over log D are limited.

E. Molecular Size

The most convenient way to define molecular size is the use of molecular weight (MW). However, this may not be sufficient, because MW, as such, contains no information about the actual three-dimentional (3D) shape of the molecules. In Table 3 several other metrics of molecular size are given.

F. Hydrogen Bonding

The use of hydrogen bonding as a factor affecting permeability goes back to early work of Collander (30), Stein (31), and Seiler (32). Table 4 lists various more recent proposals, including polar surface area (12,13) and dynamic polar surface area (35,36). We have demonstrated that most of these scales show considerable intercorrelation (13).

G. The Biopharmaceutics Classification System

On the basis of in vitro solubility and in vivo permeability drugs can be divided into four groups under the biopharmaceutics classification system (BCS): class 1 (high-permeability–high-solubility = HP:HS), class 2 (high-permeability–low-solubility = HP:LS), class 3 (low-permeability–high-solubility = LP:HS), and class 4 (low-permeability–low-solubility = LP:LS) (41). Both

Table 3 Molecular Size and Shape Descriptors

Calculated		
Molecular weight	MWT	
Molar refractivity	MR	
van der Waals volume	V	
Total surface area	S	
Water accessible volume	VW	
Water accessible surface	SW	
Ovality	O	(24)
Nonpolar part of the volume	VNP	
Nonpolar part of the surface area	SNP	
Principal axes	X, Y, Z	
Ratio length/width 1	X/Y	
Ratio length/width 2	X/Z	
Experimental		
Molecular radius (Stokes–Einstein radius)	r	(25)
Hydrodynamic radius/size	r	(26)
Hydrodynamic volume	K_d	(27)
Cross-sectional area	A_D	(28,29)

Source: Ref. 13.

Table 4 Selection of Potential H-Bond Descriptors

Calculated		
Number of donors and acceptors	HD, HA	(31)
Total number of heteroatoms	HT	(33)
Total number of possible H bonds	HBOND	(34)
Free-energy factors	Ca, Cd	(10)
Total of free-energy factors	Cad	(13)
Polar surface area	SP	(12,13)
Dynamic polar surface area	SPA	(35,36)
Experimental		
From partitioning in different solvent systems	$\Delta\log P$	(32,37–40)
Polarity contribution in log*P*	Λ	(6,8)

properties, solubility and permeability, are considered in the framework of the BCS as fundamental to define the rate and extent of absorption of the active ingredient of a drug product. However, because both of these properties are dependent on others; as shown in the foregoing, it may be questioned whether these are indeed sufficiently ''fundamental'' or should be further deconstructed (3). The more fundamental properties, on which both solubility and lipophilicity depend, are molecular size and hydrogen-bonding capability of the drug.

III. PREDICTION OF INTESTINAL PERMEABILITY

A. Theoretical Background

Reports aimed at describing membrane permeation in terms of physicochemical properties were already appearing in the literature in the 1970s. Important contributions came from the group of Higuchi (42). A recent review is available (43). It is now generally accepted that the relation between membrane permeability and lipophilicity has a sigmoidal shape. It has been suggested that, in fact, a set of molecular weight-dependent sigmoidal curves should be considered (44). We were recently able to confirm this view by adding an aqueous pore pathway to a previously proposed membrane permeability model (45,46).

B. Prediction of Caco-2 or Other Epithelial Cell Line Flux

A well-established in vitro model used for screening of absorbable compounds is the Caco-2 monolayer cell culture system (47,48). An alternative is the HT29-18-C1 intestinal epithelial cell line (49). These models simulate two types of barriers to drug absorption: biochemical and physicochemical. Because many drugs are absorbed by the passive diffusion transcellular pathway, physicochemical properties of the drugs are thought to have an important influence on this process. Therefore permeability data have frequently been plotted against log *P* or log *D*, molecular weight, or some descriptor for H-bonding (35,36,48–52).

In several studies, a linear correlation between hydrogen-bonding properties of the solute and permeability coefficients through Caco-2 layers have been found (36,51). Later it was suggested that this relation may be sigmoidal (13,35).

Relations between membrane permeability and lipophilicity have been studied by a number of groups. Therefore, it was logical to investigate a putative relation between Caco-2 flux and log *D* values. In some of the earlier

work it was suggested that there is only a coarse correlation (52). However, as described in the following, this conclusion was made on the assumption that this relation is a single linear one.

We would like to present here a reanalysis of two data sets in which permeability is described as a function of log *D* and molecular weight. With the HT29-18-C1 cell line, Wils et al. (49) demonstrated that there is an interval of octanol/buffer distribution coefficients corresponding to optimal transepithelial passage of drugs. At values higher than log *D* 3.5, low oral absorption was found. However, the reasons can be manifold. Highly lipophilic compounds tend to be poorly soluble, resulting in dissolution-limited absorption. In the cited study these compounds also had the highest molecular weight. Therefore we propose Fig. 6, in which we use a set of curves reflecting the simultaneous effect of log *D* and molecular weight, to account for this data set. Because this data set is obviously rather small, we more recently analyzed a larger set of compounds for which Caco-2 permeation was measured (46). This resulted in Fig. 7, showing the use of a set of sigmoidals to rationalize the permeability data.

The foregoing analyses demonstrate that H-bonding and molecular size have an important influence on permeation through Caco-2 monolayers. By

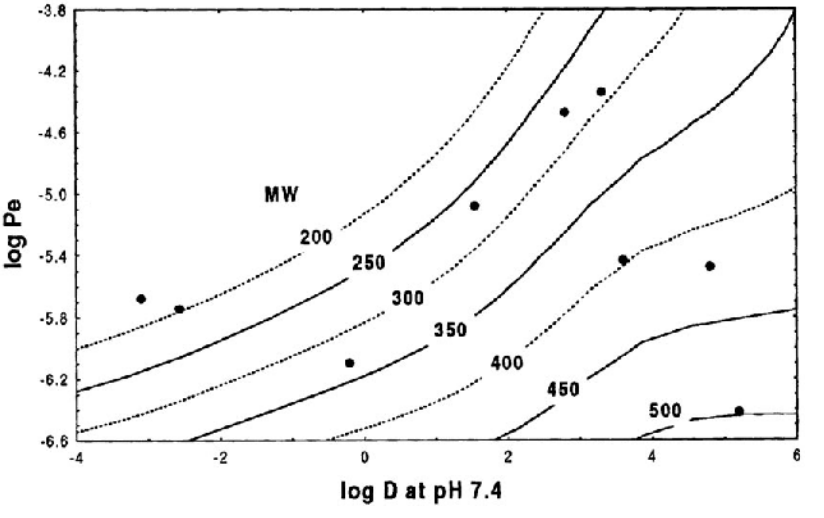

FIG. 6 Relation between log *D* and transepithelial permeability: Reanalysis of data presented by Wils et al. (49).

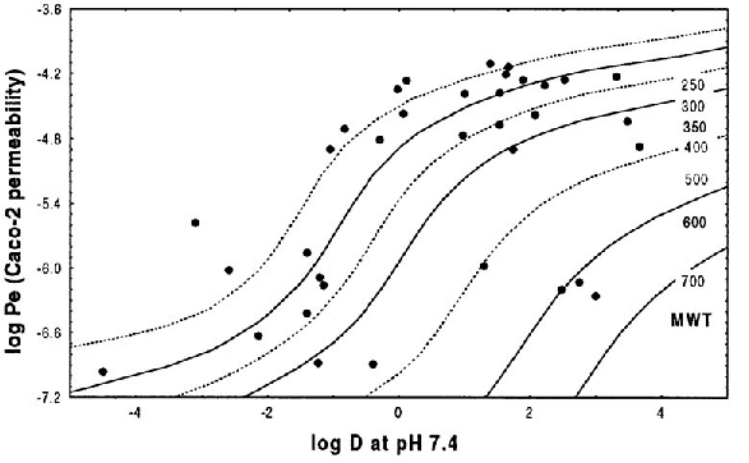

FIG. 7 Influence of MWT on permeability through Caco-2 monolayers. (From Ref. 46.)

combining these, a multiparameter equation was developed to relate experimental Caco-2 permeability data to calculated physicochemical properties of these molecules (53):

$$\log P_{app} = -0.0065\ \mathrm{SA} - 0.27\ \mathrm{HB} + 0.03\ \mathrm{SE} + 8.05 \tag{3}$$

where SA is surface area, HB the number of potential hydrogen bonds, and SE solvation energy.

We have used several of the descriptors mentioned in Tables 2 and 3 to predict Caco-2 permeation (log P_e) using multivariate techniques, such as principal component analysis (PCA) and cluster analysis (13). By using the principal components, Eq. 4 was derived. PC1 contains information on H-bonding capacity and PC2 reflects mainly molecular size. By selecting a representative of each class of descriptors (i.e., a molecular size and H-bonding descriptor), an almost equally significant correlation with Caco-2 permeability was found, as exemplified in Eq. 5 (54).

$$\log P_e = -0.18(\pm 0.04)\ \mathrm{PC1} - 0.24(\pm 0.04)\ \mathrm{PC2} - 5.34(\pm 0.13)\ n = 17;\ r = 0.884 \tag{4}$$

$$\log P_e = 0.008(\pm 0.002)\ \mathrm{MW} - 0.043(\pm 0.008)\ \mathrm{SP} - 5.17(\pm 0.61)\ n = 17;\ r = 0.833 \tag{5}$$

A similar multivariate approach using partial least-squares (PLS) regression was recently presented (55). Molecular descriptors were computed with the MolSurf program. An interesting finding was that the most important factors influencing Caco-2 transport are associated with hydrogen bonding. Furthermore it appears that the number of possible sites engaged in H-bond interactions seems more important than the actual strength of these interactions.

C. Animal Models

The single-pass rat perfusion model has been used successfully to predict human intestinal absorption (2,50,56). For a series of renin inhibitors there appears to be a moderate relation ($r^2 = 0.8$) between membrane permeability in this model and octanol/water log D values (50). However, by considering a nonlinear relation and including the effect of molecular weight, we have proposed a new approach to analyze such data. A set of hyperbolic curves was obtained when drawing a contour plot using the MW as third parameter (57).

D. Prediction of Human Intestinal Absorption

Only a limited amount of data are available in the literature on direct studies of human intestinal absorption (48,52,58); this is in contrast to more extensive compilations on bioavailability (59,60).

By using the reported human absorption data of Yee (48) and the corresponding log D values, Fig. 8 was obtained. The effect of MW on absorption is observed for small compounds (MW < 200) and for the larger ones (MW > 500). These two categories of compounds tend to be respectively above or below a theoretical sigmoidal curve that can be drawn through the absorption data for compounds having a MW in the range 200–500. Compounds with a MW less than 200 are expected to use the paracellular pathway (61). Larger compounds using the transcellular uptake route will diffuse with more difficulty through membranes, resulting in lower overall absorption. This effect of molecular size on drug permeation is approximately inverse

$$P_m = \frac{K_m}{MW} \tag{6}$$

where K_m is the membrane partitioning coefficient (21). If we assume that K_m can be estimated by log D in octanol/water, the MW-normalized log D values should be predictive for solute membrane permeability. However, this normal-

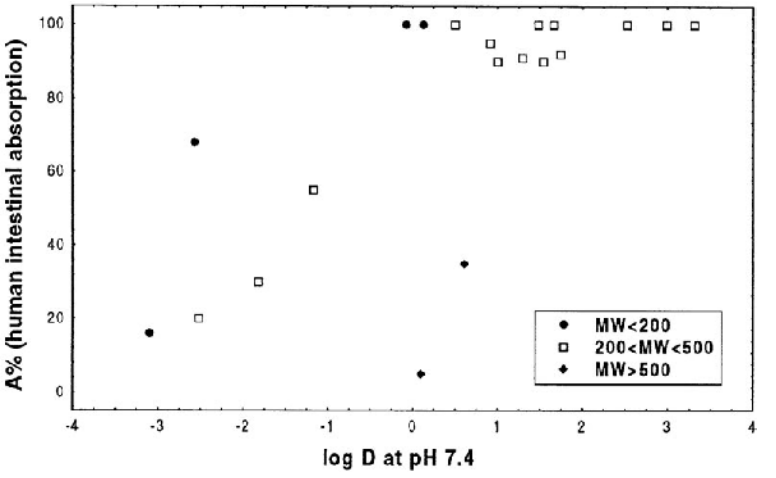

FIG. 8 Relation between oral absorption and log *D*: compounds in the range MW 200–500 fall on a theoretically expected sigmoidal curve. Smaller compounds (MW < 200 owing to paracellular or active transport), as well as larger ones (MW > 500 owing to size limitations) deviate from the theoretical curve. (Absorption data from Ref. 48.)

ization procedure offers little advantage over the information obtainable from Fig. 8.

Given previous work in Caco-2 cells, the correlation between human absorption and the hydrogen-bonding potential of drugs was investigated. It appears that a sigmoidal curve describes the relation between human absorption and dynamic polar surface area (PSA) (35). Drugs that are completely absorbed (> 90%) had a PSA of less than 60 $\AA^2$, whereas poorly absorbed compounds (<10%) had a PSA of more than 140 $\AA^2$. A much steeper and, therefore, less discriminative sigmoidal relation was obtained when the total number of hydrogen bonds or the number of hydrogen bond acceptors was used. A further advantage of PSA is that it accounts for intramolecular hydrogen bonding.

IV. FUTURE

This chapter has focused on the role of physicochemical properties in oral drug absorption. However, in recent years, the role of transporter proteins in

membrane transport processes has been further elucidated. The role of the multidrug resistance-related P-glycoprotein (P-gp), a 12TM 170-kDa protein, has received particular attention. Furthermore, a functional link between P-gp and the intestinal epithelial cytochrome P-450 isoenzyme, CYP3A4 has been suggested (62). P-gp is believed to be responsible for poor intestinal uptake of several classes of compounds. It will be important in the future to describe the structural features and physicochemical properties of drug candidates that make them susceptible to efflux pumps and gut wall metabolism. There have been suggestions that lipophilicity (63) and hydrogen bonding (29,64) are important properties for a drug to be efficiently effluxed by P-gp. Therefore, the question ''P-gp or log *P*?'' can, we hope, be better addressed in the near future.

V. CONCLUSION

Measurement and calculation of structural and physicochemical properties can be a helpful guide in the selection of compounds that will have sufficient oral absorption in humans. These *in computro (in silico)* methods need to be combined with other in vitro and in vivo approaches to be able to extrapolate to human absorption and bioavailability with confidence.

REFERENCES

1. Smith P. Special issue. Adv Drug Deliv Rev 1997; 23(1–3).
2. Chan OH, Stewart BH. Physicochemical and drug-delivery considerations for oral drug bioavailability. Drug Discov Today 1996; 1:461–473.
3. van de Waterbeemd H. The fundamental variables of the biopharmaceutics classification system (BCS)—a commentary. Eur J Pharm Sci 1998; 7:1–3.
4. Yalkowski SH, Banerjee S. Aqueous Solubility. Methods of Estimation for Organic Compounds. New York: Marcel Dekker, 1992.
5. Yalkowski SH, Valvani SC, Roseman TJ. Solubility and partitioning VI: octanol solubility and octanol–water partition coefficients. J Pharm Sci 1983; 72:866–870.
6. El Tayar N, Testa B, Carrupt PA. Polar intermolecular interactions encoded in partition coefficients: an indirect estimation of hydrogen-bond parameters of polyfunctional solutes. J Phys Chem 1992; 96:1455–1459.
7. Avdeef A. Assessment of distribution–pH profiles. In: Pliska V, Testa B, van de Waterbeemd H, eds. Lipophilicity in Drug Action and Toxicology. Weinheim: VCH, 1996:109–137.

8. Testa B, Seiler P. Steric and lipophilic components of the hydrophobic fragmental constant. Arzneim Helforschung 1981; 31:1053–1058.
9. van de Waterbeemd H, Testa B. The parameterization of lipophilicity and other structural properties in drug design. Adv Drug Des 1987; 16:85–225.
10. Raevsky OA, Schaper KJ, Seydel JK. H-bond contribution to octanol–water partition coefficients of polar compounds. Quant Struct Act Relat 1995; 14:433–436.
11. Lipinski CA, Lombardo F, Dominy BW, Feeney PJ. Experimental and computational approaches to estimate solubility and permeability in drug discovery and development settings. Adv Drug Deliv Rev 1997; 23:3–25.
12. van de Waterbeemd H, Kansy M. Hydrogen-bonding capacity and brain penetration. Chimia 1992; 46:299–303.
13. van de Waterbeemd H, Camenisch G, Folkers G, Raevsky OA. Estimation of Caco-2 permeability using calculated molecular descriptors. Quant Struct Act Relat 1996; 15:480–490.
14. Kamlet MJ, Doherty RM, Abboud JLM, Abraham MH, Taft RW. Linear solvation energy relationships: 36. Molecular properties governing solubilities of organic nonelectrolytes in water. J Pharm Sci 1986; 75:338–349.
15. Carrupt P, Testa B, Gaillard P. Computational approaches to lipophilicity: methods and applications. In: Lipkowitz KB, Boyd DB, eds. Reviews in Computational Chemistry. Vol. 11. New York: Wiley–VCH, 1997: p. 241–315.
16. van de Waterbeemd H, Mannhold R. Programs and methods for calculation of log P values. Quant Struct Act Relat 1996; 15:410–412.
17. Moriguchi I, Hirono S, Nakagome I, Hirano H. Comparison of reliability of log P values for drugs calculated by several methods. Chem Pharm Bull 1994; 42: 976–978.
18. Suzuki T, Kudo Y. Automatic log P estimation based on combined additive modeling methods. J Comput Aided Mol Des 1990; 4:155–198.
19. Junghans M, Pretsch E. Estimation of partition coefficients of organic compounds: local database modeling with uniform-length structure descriptors. Fresenius J Anal Chem 1997; 359:88–92.
20. Wang R, Fu Y, Lai L. A new atom-additive method for calculating partition coefficients. J Chem Inf Comput Sci 1997; 37:615–621.
21. Yang CY, Cai SJ, Liu H, Pidgeon C. Immobilized artificial membranes—screens for drug membrane interactions. Adv Drug Deliv Rev 1996; 23:229–256.
22. Ong S, Liu H, Pidgeon C. Immobilized-artificial-membrane chromatography: measurements of membrane partition coefficient and predicting drug membrane permeability. J Chromatogr A 1996; 728:113–128.
23. Lundahl P, Beigi F. Immobilized liposome chromatography of drugs for model analysis of drug–membrane interactions. Adv Drug Deliv Rev 1997; 23:221–227.
24. Bodor N, Huang MJ. An extended version of a novel method for estimation of partition coefficients. J Pharm Sci 1992; 81:272–281.
25. Paulett GM, Okumu FW, Borchardt RT. Effect of size and charge on the passive

diffusion of peptides across Caco-2 cell monolayers via the paracellular pathway. Pharm Res 1997; 14:164–168.
26. Adson A, Raub TJ, Burton PS, Barsuhn CL, Hilgers AR, Audus KL, Ho NFH. Quantitative approaches to delineate paracellular diffusion in cultured epithelial cell monolayers. J Pharm Sci 1994; 83:1529–1536.
27. Pauletti GM, Gangwar S, Okumu FW, Siahaqan TJ, Stella VJ, Borchardt RT. Esterase-sensitive cyclic prodrugs of peptides: evaluation of an acyloxyalkoxy promoiety in a model hexapeptide. Pharm Res 1996; 13:1615–1623.
28. Seelig A, Gottschlich R, Devant RM. A method to determine the ability of drugs to diffuse through the blood–brain barrier. Proc Natl Acad Sci USA 1994; 91: 68–72.
29. Fischer H. The Diffusion of Drugs Through Biological Membranes. Ph.D. dissertation, University of Basel, Switzerland, 1998.
30. Collander R, Bärlund H. Permeabilitätsstudien an *Chara ceratophylla*. Acta Bot Fenn 1932; 11:1–114.
31. Stein WD. In: The Movement of Molecules Across Cell Membranes. London: Academic Press, 1967:65–125.
32. Seiler P. Interconversion of lipophilicities from hydrocarbon/water systems into the octanol/water system. Eur J Med Chem 1974; 9:473–479.
33. Lien EJ, Lien LL, Gao H. Structure-system–activity relationship analysis of drug disposition. In: Sanz F, Giraldo J, Manaut F, eds. QSAR and Molecular Modelling. Barcelona: Prous, 1995:94–100.
34. Basak SC, Gute BD, Drewes LR. Predicting blood–brain transport of drugs: a computational approach. Pharm Res 1996; 13:775–778.
35. Palm K, Stenberg P, Luthman K, Artursson P. Polar molecular surface properties predict the intestinal absorption of drugs in humans. Pharm Res 1997; 14:568–571.
36. Palm K, Luthman K, Ungell AL, Strandlund G, Artursson P. Correlation of drug absorption with molecular surface properties. J Pharm Sci 1996; 85:32–39.
37. Young RC, Mitchell RC, Brown TH, Ganellin CR, Griffiths R, Jones M, Rana KK, Saunders D, Smith IR, Sore NE, Wilks TJ. Development of a new physicochemical model for brain penetration and its application to the design of centrally acting H_2 receptor histamine antagonists. J Med Chem 1988; 31:656–671.
38. ter Laak AM, Tsai RS, Donné-Op den Kelder GM, Carrupt PA, Testa B, Timmerman H. Lipophilicity and hydrogen-bonding capacity of H_1-antihistaminic agents in relation to their central sedative side-effects. Eur J Pharm Sci 1994; 2:373–384.
39. Buur A, Trier L, Magnusson C, Artursson P. Permeability of 5-fluorouracil and prodrugs in Caco-2 cell monolayers. Int J Pharm 1996; 129:223–231.
40. von Geldern TW, Hoffman DJ, Kester JA, Nellans HN, Dayton BD, Calzadilla SV, Marsch KC, Hernandez L, Chiou W, Dixon DB, Wu-Wong JR, Opgenorth TJ. Azole endothelin antagonists. 3. Using Δlog P as a tool to improve absorption. J Med Chem 1996; 39:982–991.
41. Amidon GL, Lennernäs H, Shah VP, Crison JR. A theoretical basis for a biophar-

maceutic drug classification: the correlation of in vitro drug product dissolution and in vivo bioavailability. Pharm Res 1995; 12:413–420.
42. Stehle RG, Higuchi WI. In vitro model for transport of solutes in three-phase system I: theoretical principles. J Pharm Sci 1972; 61:1922–1930.
43. Camenisch G, Folkers G, van de Waterbeemd H. Review of theoretical passive drug absorption models: historical background, recent developments and limitations. Pharm Acta Helv 1996; 71:309–327.
44. Leahy DE, Lynch J, Taylor DC. Mechanisms of absorption of small molecules. In: Prescott LF, Nimmo WS, eds. Novel Drug Delivery and Its Therapeutic Application. New York: Wiley, 1989:33–44.
45. Camenisch G, Folkers G, van de Waterbeemd H. Shapes of membrane permeability–lipophilicity curves: extension of theoretical models with an aqueous pore pathway. Eur J Pharm Sci 1998; 6:321–329.
46. Camenisch G, Alsenz J, van de Waterbeemd H, Folkers G. Estimation of permeability by passive diffusion through Caco-2 cell monolayers using the drug's lipophilicity and molecular weight. Eur J Pharm Sci 1998; 6:313–319.
47. Artursson P, Palm K, Luthman K. Caco-2 monolayers in experimental and theoretical predictions of drug transport. Adv Drug Deliv Rev 1996; 22:67–84.
48. Yee S. In vitro permeability across Caco-2 cells (colonic) can predict in vivo (small intestinal) absorption in man—fact or myth. Pharm Res 1997; 14:763–766.
49. Wils P, Warnery A, Phung-Ba V, Legrain S, Scherman D. High lipophilicity decreases drug transport across intestinal epithelial cells. J Pharmacol Exp Ther 1994; 2:654–658.
50. Hamilton HW, Steinbaugh BA, Stewart BH, Chan OH, Schmid HL, Schroeder R, Ryan MJ, Keiser J, Taylor MD, Blankley CJ, Kaltenbronn JS, Wright J, Hick J. Evaluation of physicochemical parameters important to the oral bioavailability of peptide-like compounds: implications for the synthesis of renin inhibitors. J Med Chem 1995; 38:1446–1455.
51. Conradi RA, Hilgers AR, Ho NFH, Burton PS. The influence of peptide structure on transport across Caco-2 cells. II. Peptide bond modification which results in improved permeability. Pharm Res 1992; 9:435–439.
52. Artursson P, Karlsson J. Correlation between oral drug absorption in humans and apparent drug permeability coefficients in human intestinal epithelial (Caco-2) cells. Biochem Biophys Res Commun 1991; 175:880–885.
53. Gan LSL, Thakker DR. Applications of the Caco-2 model in the design and development of orally active drugs: elucidation of biochemical and physical barriers posed by the intestinal epithelium. Adv Drug Deliv Revs 1997; 23:77–98.
54. Camenisch G. Drug Transport Across Membranes. Structure–Property Correlations in the Prediction of Passive Membrane Permeation. Ph.D. dissertation, ETH Zürich, Switzerland, 1996.
55. Norinder U, Österberg T, Artursson P. Theoretical calculation and prediction of Caco-2 cell permeability using MolSurf parameterization and PLS statistics. Pharm Res 1997; 14:1786–179.

56. Levet-Trafit B, Gruyer MS, Marjanovic M, Chou RC. Estimation of oral drug absorption in man based on intestine permeability in rats. Life Sci 1996; 58: 359–363.
57. van de Waterbeemd H. Application of physicochemical methods to oral drug absorption estimation. Eur J Pharm Sci 1997; 5(suppl 2):S26–S27.
58. Kansy M, Senner F, Gubernator K. Physicochemical high throughput screening: parallel artificial membrane permeation assay in the description of passive absorption processes. J Med Chem 1998; 41:1007–1010.
59. Sietsema WK. The absolute oral bioavailability of selected drugs. Int J Clin Pharmacol Ther Toxicol 1989; 27:179–211.
60. Benet LZ, Øie S, Schwartz JB. Design and optimization of dosage regimens; pharmacokinetic data. In: Hardman JG, Limbird LE, eds. Goodman and Gilman's the Pharmacological Basis of Therapeutics, 9th ed. New York: McGraw-Hill, 1996:1712–1792.
61. Lennernäs H. Does fluid flow across the intestinal mucosa affect quantitative oral drug absorption? Is it time for a reevaluation? Pharm Res 1995; 12:1573–1582.
62. Wacher VJ, Salphati L, Benet LZ. Active secretion and enterocytic drug metabolism barriers to drug absorption. Adv Drug Deliv Rev 1996; 20:99–112.
63. Lampidis TJ, Kolonias D, Podona T, Israel M, Safa AR, Lothstein L, Savaraj N, Tapiero H, Priebe W. Circumvention of P-gp MDR as a function of anthracycline lipophilicity and charge. Biochemistry 1997; 36:2679–2685.
64. Seelig A. A general pattern for substrate recognition by P-glycoprotein. Eur J Biochem 1998; 251:252–261.

5
In Vitro Methods for the Assessment of Permeability

Josef J. Tukker
University of Utrecht, Utrecht, the Netherlands

I. INTRODUCTION

Assessment of the absorption of a given compound from the gastrointestinal (GI) tract should, in fact, simply mean establishing the permeation of this compound across the wall of the gastrointestinal tract, but there are more factors involved in the net result. Apart from the permeation resulting in translocation, there are also factors that have a negative influence on the absorption of drugs from the gastrointestinal tract. These include the dissolution properties of the compound, which may be affected by physiological components such as gastric juice and bile, precipitation at the absorption site, adsorption to components in the gastrointestinal tract, chemical and/or bacterial degradation, and the metabolism of the compound in the lumen, at the brush border, or in the intestinal wall. No method can assess all these aspects simultaneously, with the exception of studies in intact animals or in humans. Whole animal or human studies suffer two drawbacks: first, they are unsuitable for screening large numbers of compounds at an experimental stage. Second, they pose ethical difficulties if the pharmacological effects and side effects are insufficiently well defined. As a result, a great variety of alternative methods have been developed to assess the permeation characteristics of new drugs. It should be kept in mind that each of these methods covers only some of the foregoing aspects, and does not take into account other factors that may be important

to the bioavailability of the compound. These techniques can be applied to assess or predict the availability after oral administration and are based on methods ranging from the purely calculational, through in vitro permeation/uptake studies to perfusions in humans (e.g., 1).

This chapter will focus on the biological in vitro methods, in which cultured cells of human origin or intestinal tissue sampled from animals or humans are utilized to assess permeability of the GI mucosa to a given drug.

The in vitro biological methods that will be discussed here are, in order of appearance, the brush border membrane vesicles (BBMV), isolated intestinal cells, intestinal rings, everted intestinal sacs, side-by-side diffusion chambers equipped with intestinal tissue from animal or human origin, and cultured cells in the uptake mode or in a two-compartment system.

Some advantages of the biological approaches compared with the calculational methods are that permeants can not only be compared on the basis of their physicochemical characteristics, but also on their ability to be absorbed by carrier-mediated translocation or transport involving a second (membrane-bound) protein. Biological methods can also be applied to investigate the influence of additives, such as solubilizers and wetting agents, on membrane transport. Moreover, depending on the method applied, steps that form a critical barrier in vivo in the overall transport of a specific solute, such as adsorption to mucus, metabolism, or efflux by P-glycoprotein, can be studied. This immediately implies that the particular method chosen might give a generally good impression of permeant transport, but may deviate in forecasting the absolute permeabilities. For example, for a permeant that predominantly diffuses through the tight junctions, this diffusional paracellular pathway should accurately reflect the in vivo situation in the chosen model; the use of vesicles or isolated cells, both of which lack tight junctions, would give a false impression of the transport characteristics in this particular case.

Transport can be looked at experimentally in two fundamentally different ways: uptake of the permeant into the system, or transport of the permeant through the system (Fig. 1). The choice of the system is important and will depend very much on the underlying question to be answered, but it also has consequences from an analytical point of view. After uptake of the permeant into one of the uptake approaches shown in Fig. 1, the concentration of the permeant inside the system must be quantified: cleanup procedures can be cumbersome and, at low levels of uptake, there may be problems with the detection limit. Although these problems can be circumvented by use of radiolabels, radiolabeled material is only seldom available in the early stages of drug development.

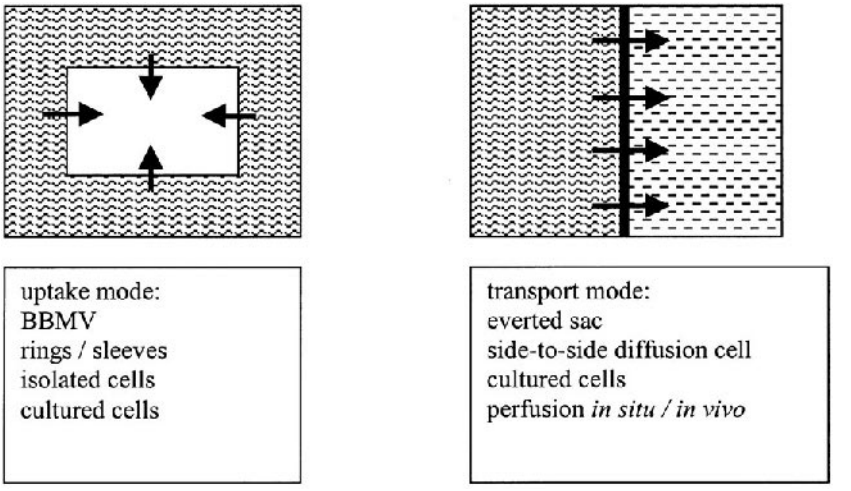

FIGURE 1 Subdivision of the methods discussed in this chapter based on the mode of assessment: uptake or transport systems.

II. METHODS

A. Brush Border Membrane Vesicles

In this approach, cell homogenates or intestinal scrapings are treated with the $CaCl_2$ precipitation method using centrifugation (2). The final pellet contains the luminal wall-bound proteins and phospholipids, which contain most of the brush border enzymatic and carrier activity. Resuspension of the pellet in buffer results in the formation of vesicles. These vesicles are mixed with the permeant in buffer and filtered after a fixed time; the amount of permeant taken up by the vesicles is then determined. Because the precipitation–centrifugation procedure results in isolation of only the brush border components, typically only the apical transcellular transport is measured by this system.

Despite drawbacks, such as the need for a radiolabeled compound and day-to-day variation in preparation, this method is useful for mechanistic studies of the drug absorption process.

An interesting modification of this procedure has been proposed by Pidgeon et al. (3), who isolated brush border components and immobilized the components on a chromatographic column, leading to immobilized artificial membranes (IAM). The drug(s) under investigation are eluted with an aqueous

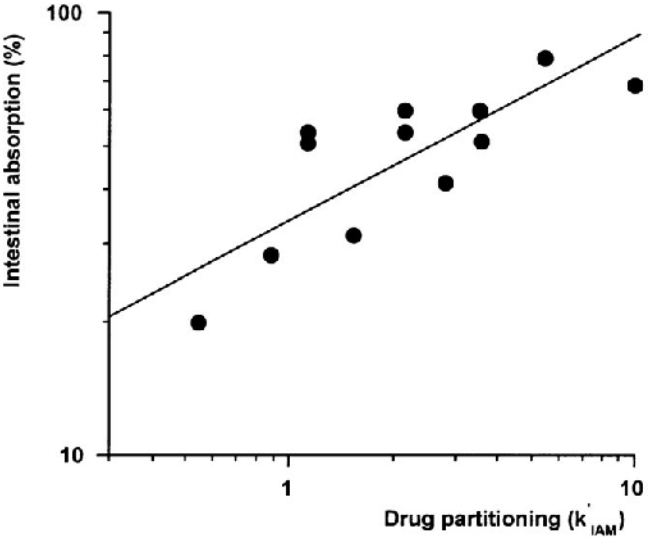

FIGURE 2 Correlation of rat intestinal absorption with drug partitioning to an IAM-column. (From Ref. 3.)

eluent, thus enabling the estimate of permeation capacity factors. Despite some of the limitations associated with this approach, the prediction of bioavailability for a series of compounds was comparable with the more-complicated permeability measurement procedure using Caco-2 cells. In Fig. 2, partitioning behavior of a series of 12 structurally unrelated drugs is compared with in vivo absorption in rats, indicating that the intestinal transport of the compounds is well predicted by IAM-chromatography; it should be emphasized, however, that all of the compounds shown in the correlation are transported passively. This approach may be especially suitable for high-throughput and large-volume screening of experimental compounds at an early developmental stage.

B. Isolated Intestinal Cells

Isolated cells from the intestine of animal or human origin can be used as uptake systems in the assessment of oral bioavailability and have been described in several papers. The procedures used to isolate mucosal cells can be divided fundamentally in two categories: an in situ procedure, in which

the intestine is perfused with enzyme solutions that release the cells; and an ex vivo approach, in which the cells are treated by chelating agents or by enzymatic means (2,4). The freshly isolated cells are immediately suspended in Krebs–Henseleit buffer with 10 mM glucose added and kept on ice for 15 min, during which they are bubbled with carbogen (95% O_2/5% CO_2). The exposure to glucose increases the viability of the cells, even after the media have been replaced by glucose-free media (2).

In a typical experiment, the cells are separated from the primary buffer by centrifugation, resuspended in buffer under O_2/CO_2 in the presence of the permeant, and shaken well. After a designated time, the cells are separated by gradient-centrifugation or rapid filtration, and extracted. Because of the low volume of the cells, the assay is mostly based on radiolabel counting, which as previously mentioned, can be disadvantageous in the early stage of development when a radiolabeled compound is unlikely to be available.

C. Everted Intestinal Rings

The use of intestinal rings for absorption measurement is not widespread, but still has its merits in terms of simplicity. In this method, a section of the intestine is isolated immediately after euthanizing the animal, washed in ice-cold buffer to remove debris and digestive products, and tied at one end with a piece of suture; now, the closed end is carefully pushed through the intestine using a glass rod, resulting in eversion of the intestine, which is then cut into small rings, typically 2–4 mm wide (30–50 mg wet weight). Any segment of the intestine can be selected, from the duodenum to the rectum, typically jejunum, ileum, and colon. Next the slices are incubated in a solution containing the compound under investigation, and shaken well in a waterbath. After a designated time interval the tissue slice is taken out of solution, blotted dry, and weighed, and then dissolved or processed for assay. The uptake of the compound is measured by radiolabel counting or other means.

Evertion of the tissue is performed to maximize the contact between the tissue at the uptake level and the solute. The everted segments are claimed to be viable for a period of 30–60 min, if they are maintained before use in a physiological buffer containing glucose (5).

Under appropriate conditions the in vitro uptake of a series of drugs into the rings closely parallels the known in vivo absorption of those drugs. Moreover the uptake is relatively independent of tissue origin and cosolvent; the latter was also shown in a recent paper showing the application of 1-methyl-

pyrrolidone as a cosolvent in transport measurements of poorly soluble compounds (6).

The uptake in slices or rings is determined as a function of time, and mostly here the waterbath shaking rate is also taken into account, because this has major influence on the uptake rate (7); from the plot of flux vs. shaking rate the unbiased membrane flux (J_0) can be estimated. The permeability P_0 is calculated from the unbiased flux (J_0), the concentration of the incubation medium (C), and a conversion factor for exposed tissue ($<cf>$) in cm^2/g for tissue/surface area from the equation: $J_0 = P_0 C <cf>$, where P_0 is expressed in cm/s (7).

The advantages of this method are the ease of preparation, as long as the appropriate conditions are met, and that from one piece of intestine an impressive set of slices can be prepared. In Fig. 3 a simple tool is shown to submerge five everted intestinal slices simultaneously into a buffer solution containing the permeant.

With this method both passive processes (2,8,9) and carried-mediated transport have been demonstrated (e.g., 5,7,8,10). A good correlation was reported for a set of 11 structurally unrelated compounds ranging from extremely low to very high bioavailability (Fig. 4). Both passively (trans- and paracellular) and actively transported compound are included in this set.

This method also has some drawbacks. The transport of the solute into the slices includes all areas accessed by the incubation solution, not only through the luminal membrane; connective tissue and muscle tissue are also exposed to drug solution and included in the calculation of ''uptake.'' In uptake experiments, the values must be corrected for nonspecific tissue binding (6). Furthermore, the paracellular and transcellular transport route cannot be distinguished using this method.

Osiecka et al. (2) compared permeability measurements using everted rings, BBMV, and isolated mucosal cells. One of the distinctive features of the enterocyte is its membrane polarity (mucosal or luminal versus serosal or basolateral): this polarity is lost in suspensions of isolated cells, presenting a factor that can change membrane transport in this model as compared with in vivo conditions. The interpretation of data resulting from cell suspensions might thereby be complicated. Similarly, both the mucosal and serosal surface of everted rings are exposed to the drug, leading to accumulation of passively diffusing compounds in the muscular as well as mucosal tissue. Actively transported compounds such as glucose or amino acids, on the other hand, were found in predominantly the mucosal tissue, indicating that the latter compounds were taken up mostly across the mucosal membrane, in contrast with the passively transported compounds (2).

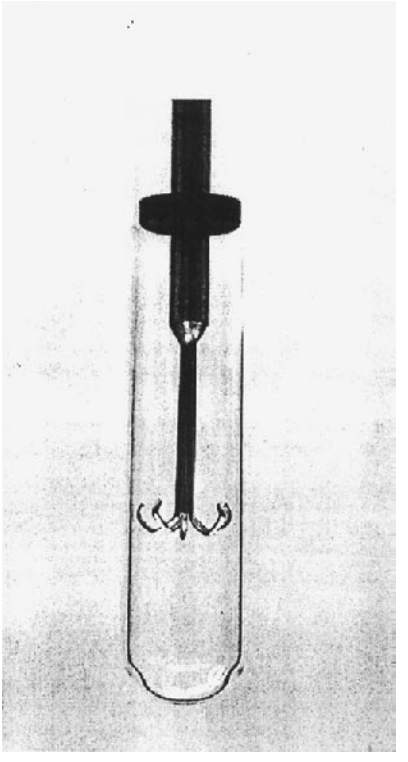

FIGURE 3 Five-arm anchor to submerge five everted intestinal rings simultaneously into buffer solution at the same shaking rate. (Courtesy JB Dressman.)

D. Everted Intestinal Sacs

In the everted intestinal sac method, a 2- to 4-cm section of the intestine is tied off at one end and everted using a glass rod or a thread, similar to the procedure described for the intestinal rings (11). As with the everted slices and rings, the mucosa becomes the outer side of the sac and is in contact with the incubation medium, but in contrast with the rings, only the mucosa is in contact with permeant. The sac is filled with buffer and put in a flask with oxygenated (95% O_2/5% CO_2) buffer containing the compound under investigation. At the end of the experiment the sac is cut and opened at one end, and the serosal fluid is collected (12). Viability of the sac can be monitored

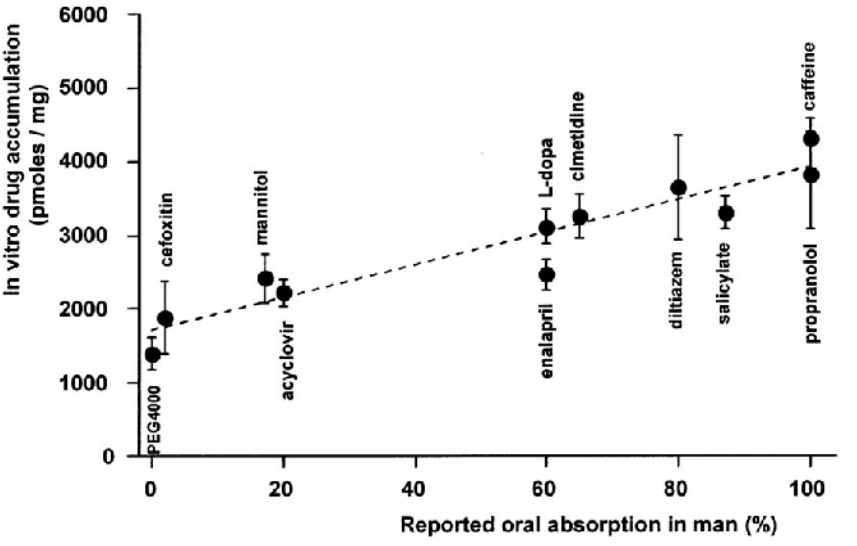

FIGURE 4 Correlation of reported oral availabilities in humans with measured uptake in vitro in everted intestinal rings ($n = 3$; ± s.d.). Initial drug concentration is 10 mM. (From Ref. 5.)

during the experiment by measuring the transport of a marker (e.g., trypan blue dye).

The transport decreases significantly within the first few minutes, if the animal is killed by cervical dislocation before removal of the segment (13). However, deterioration of the tissue can be avoided if the animal is anesthesized properly before isolation of the intestines, and euthanized only after harvesting the segment (13). With this modified procedure the type of anesthesia before isolation influences the translocation of calcium in the everted sacs.

Several improvements of the everted sac method have been suggested (e.g., 14, 15). In the first method (14) the tissue was kept in tissue culture medium, although it was still isolated after cervical dislocation. Mannitol transport showed a linear transport for as long as 75 min (Fig. 5) over a wide concentration range.

In another publication, the isolated segment was prepared and cannulated at both ends in a manner similar to the in situ Doluisio technique (15). A 10-mL syringe was attached to each cannula and the sac was suspended in 40 mL of phosphate buffer, which was stirred by continuous bubbling with

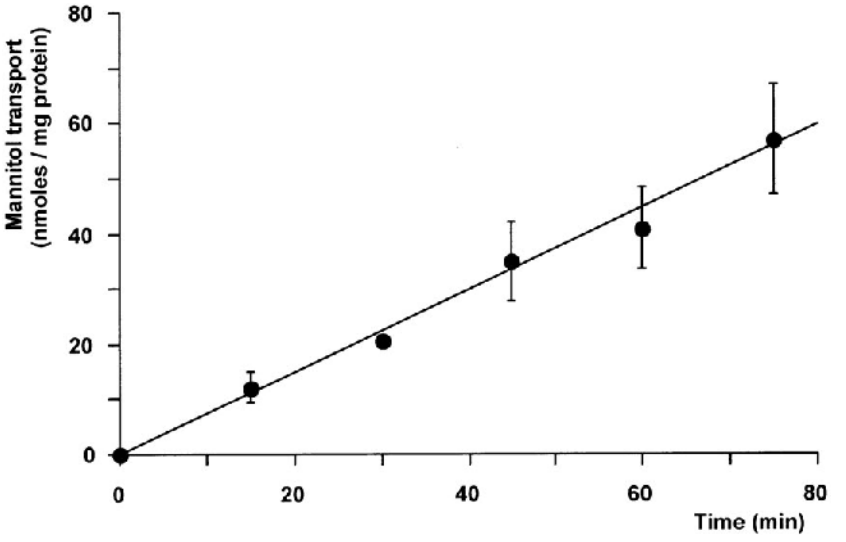

FIGURE 5 Time-dependent transport of mannitol at 10 mM concentration in everted sacs, according to an improved method. Data are the means of 6 sacs (± SEM). (From Ref. 14.)

carbogen. Using this approach, the investigators showed the influence of absorption promoters, such as sodium caprate and laurate, on the paracellular permeation route for cefmetazole and inulin (15). In contrast to rings, slices, and cell preparations, para- and transcellular diffusion can be discriminated, using everted sacs. In contrast with the everted slices and rings, the everted intestinal sac can be applied for the investigation of drug metabolism, as has been shown in several publications (see 16).

The everted sac method is an inexpensive technique that is also relatively simple and allows several experiments to be performed using tissue from just one intestine. One advantage is the low serosal volume compared with the area for absorption, which is especially advantageous with low-soluble drugs or low concentrations of drugs. This method has been a useful tool for studying mechanistical aspects of absorption and the influence of absorption enhancement. Also, by preparing the segment from different parts of the intestine, the absorption from different sites, such as small intestine and colon, can be compared.

E. Diffusion Cells Using Tissue

Since the early 1950s, side-by-side diffusion cells have been used to determine the transport of compound in living tissue, one of the first approaches being the so-called Ussing chambers (17). In this method small sections of the intestine (≈2 cm) are clamped between two glass chambers filled with buffer and nutrients such as glucose, at a temperature of 37°C. The buffer solutions at both sides of the membrane are gased continuously with carbogen (95% O_2/5% CO_2) to maintain the viability of the tissue and to ensure reproducible hydrodynamics (good mixing). A modification of the original method was published, using smaller acrylic chambers, allowing diffusion experiments with smaller amounts of compound (18); again in this method, carbogen bubbling is applied to increase viability and improve hydrodynamics. This cell is depicted in Fig. 6, in this example it is adapted for the use of tissue. The temperature is maintained by clamping the closed half-cells in a heating block.

The compound under study is added to one of the compartments (the ''donor'' compartment), either the serosal or the mucosal side, and the accumulation of the compound at the other side of the membrane (in the ''recep-

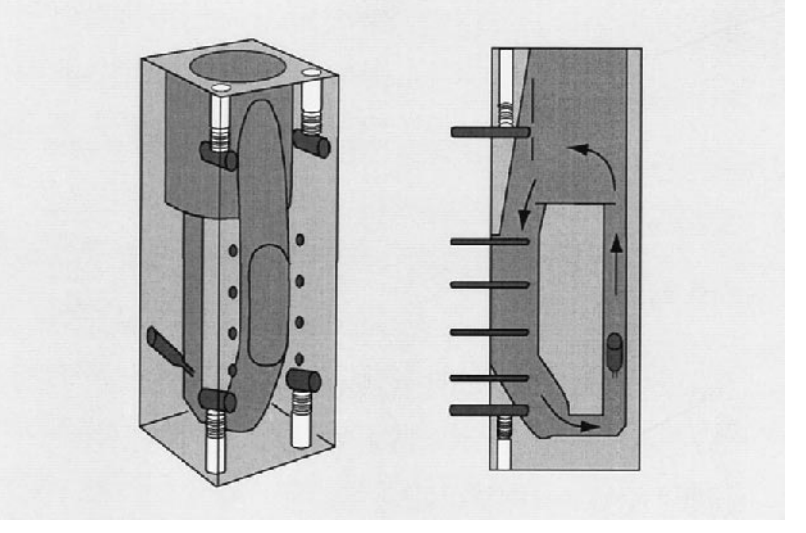

FIGURE 6 The Sweetana–Grass diffusion cell: this cell is designed for tissue that is mounted between two acrylic half-cells. Buffer is circulated by gas lift. (From Ref. 18.)

tor'') is measured as a function of time. From the appearance in the receptor compartment, the permeability of the compound is calculated according to equation: $P_{app} = dC/dt \times (V/A \times C)$, where dC/dt is the change in concentration in the receptor compartment per unit time, V is the receptor volume and A the area available for diffusion or transport. The P_{app} is usually expressed in centimeters per second (cm/s). In many studies the investigators prepare the intestinal tissue before mounting by stripping the serosa and the outer musculature (19); for studies designed to determine the mechanistics and rate of transport stripped tissue is claimed to be preferable because this resembles more closely the in vivo situation: in vivo, drug permeation occurs through the enterocytes and the basal membrane to the blood capillaries, and permeation through the serosa and musculature contributes little or nothing to the bioavailability.

In the original design of Ussing chambers (see Fig. 7), the setup was equipped with electrodes and a voltage clamp for monitoring epithelial potential difference and short-circuit current (*PD* and I_{sc}, resp.). Alternatively, the potential difference or current could be clamped to any value to investigate the influence of electrical driving force on the transport characteristics of the solute. These electrical parameters can be used to verify the viability of the tissue during and at the end of the experiment: at the end of the experiment a small amount of glucose is added to the mucosal bathing solution, and this glucose will be transported to the serosal side by the glucose transporter (only in the small intestine): this glucose transport is accompanied by the translocation of Na^+, which can be detected as a long-lasting increase in current. For colonic tissue, which does not have glucose transporters, prostaglandin E_1 (PGE_1) stimulates the Cl^- secretion which, in turn, also gives rise to an increase in I_{sc} (20). In our own laboratory we have observed viability of stripped and mounted tissue for at least 3–4 h using the same technique. In Fig. 8, a typical example of the electrical parameters over the membrane of rat duodenum is given. A constant value for the calculated resistance R over a 3-hr experiment was achieved (21). The electrical parameters are now widely accepted for monitoring the tissue viability and integrity in Ussing chambers.

The integrity of the tissue, especially after stripping, can also be followed using an integrity marker, in addition to and independent of monitoring the electrical parameters. Normally, a compound with low intrinsic permeability such mannitol, PEG_{4000}, inulin, or fluorescein is used. To overcome the environmental problems with radiolabeled compounds (the first three are, for ease of detection, applied mostly as labeled compounds), we apply fluorescein in a donor concentration of 5 μM and measure the concentration in the receptor

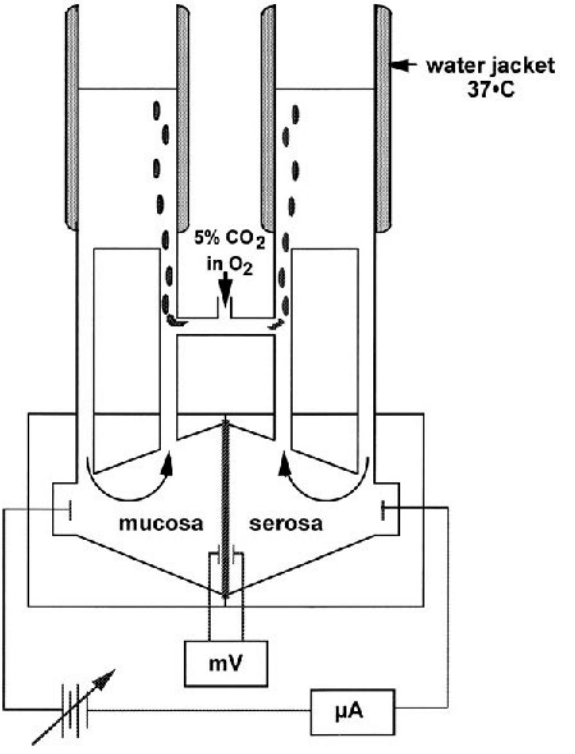

FIGURE 7 Schematic drawing of the original Ussing chamber, showing the half-cells with thermostated water jackets, gas lifts, and potential difference and current electrodes.

compartment with time using fluorescence spectrometry (after bringing the pH of the samples to $\approx$ 10 using NaOH).

It has been shown by several investigators that the tissue in Ussing chambers, as with everted sacs, can deteriorate within 30–60 min. Addition of energy sources such as glucose or L-glutamine can improve this life span considerably; proper handling and gasing with carbogen further improves the viability. Polentarutti et al. (21) reported that during an experiment in Ussing chambers using excised rat tissue, the morphology of the tissue changed, as did the permeation of the marker compounds investigated (propranolol and mannitol). Information on time-dependent structural changes would be necessary for a complete interpretation of the permeability data. However, ac-

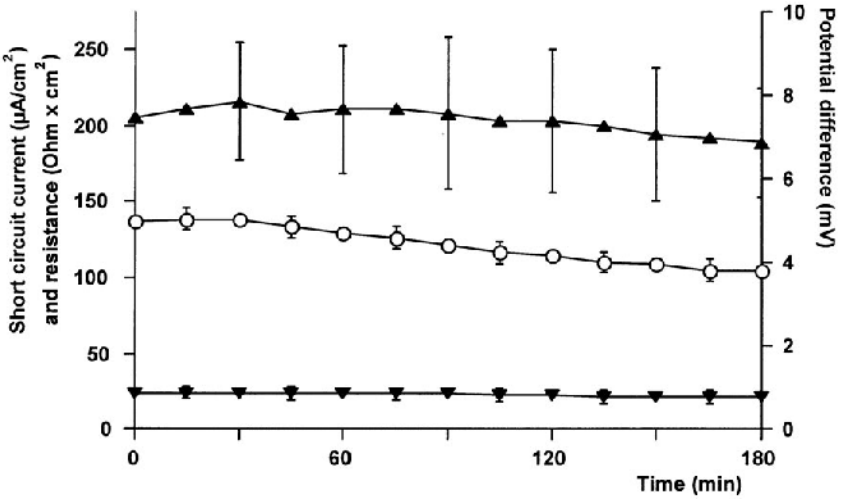

FIGURE 8 Mean electrical parameters, potential difference (○ PD, in mV), short-circuit current (▲ SCC, in μA/cm²), and resistance (▼ R, in Ohm × cm²) for rat intestinal tissue during 180-min experimental time. (From Ref. 21.)

cording to this and other publications it seems quite possible to perform transport experiments in Ussing chambers for at least 2–3 h, provided that the experimental conditions are adequately designed and that the permeation of the marker compounds into the receptor compartment is linear over the study period.

The Ussing diffusion chambers are now used by several groups, in some cases slightly modified, and have been useful tools for the determination of the permeability characteristics of drugs and for the selection of development candidates based on the in vitro permeability measurements (22–24).

The same method can be used for tissue other than intestinal tissue (e.g., buccal, esophageal, gastric, rectal, nasal, lung, and skin tissue). With a slight modification, the diffusional method, as described (18), can also be applied for monolayers of cells cultured on membranes fixed in inserts (25), but one of the advantages of the original approach using segments of excised tissue, is the possibility of studying differences in regional absorption of drugs. Moreover, the Ussing diffusion cell is especially applicable for mechanistic studies of paracellular transport, because the transport through the aqueous pores can be influenced rather easily.

F. Cultured Cells

Some decades ago, pharmaceutical scientists began to use cultured cells to study the transport of compounds. One of the advantages of cultured cells is that, when cultured as a monolayer, they exhibit polarized behavior, thus mimicking the situation in the intestine. Primary cell cultures have been attempted, but these lines have very poor viability and do not form a confluent monolayer in which the cells adhere closely together and form tight junctions (26). Instead, most cell culture models for the intestinal epithelium are based on immortalized cell lines that are derived from normal cells, from induced tumors, or from human colonic cancers. The cell lines derived from human colonic cancers are the most widely used, because they differentiate (either spontaneously or after induction) and readily form polarized and confluent monolayers in culture. Of these, the most widely used is the Caco-2 line, which was used for the first time in the 1970s (27), and has the advantage that it can be grown in culture on a porous support such as a filter insert on which it forms a polarized cell monolayer within a few days, and differentiates into absorptive intestinal cells with typical morphology, including some brush border enzyme activity and well-formed tight junctions.

Figure 9 illustrates the culturing system whereby the cells are seeded at a cell density of approx 60,000/cm^2, usually on polycarbonate filter supports. During culture the cells form confluent monolayers, resulting in increasing tightness of the cell layer, increasing epithelial resistance and decreasing mannitol (paracellular) transport. These cells show a fully developed monolayer with constant indices after 2 weeks; even more rapidly growing cell lines are now available.

The tight junctions in the Caco-2 monolayers resemble the junctions in the human colon, resulting in far higher transepithelial electrical resistance (TEER) of 150–450 Ω cm^2 (Fig. 10) than typical for small intestinal tissue (TEER in the range 25–40 Ω cm^2). The higher TEER makes the Caco-2 cell line a useful and widespread method for studying the influence of both pharmacological pretreatments and direct additives on cell integrity because the paracellular permeability of a typical nonpermeant, such as PEG 4000 or mannitol (see Fig. 10), can be easily monitored.

Although the TEER deviates from that of ‘‘normal’’ small intestinal tissue, the cultured Caco-2 monolayers express small intestinal brush border enzymes, and phase I and II metabolic enzymes (29). For this reason the Caco-2 monolayers have been suggested as an evaluation system for the metabolism of xenobiotics in intestinal tissue during the transport step (30).

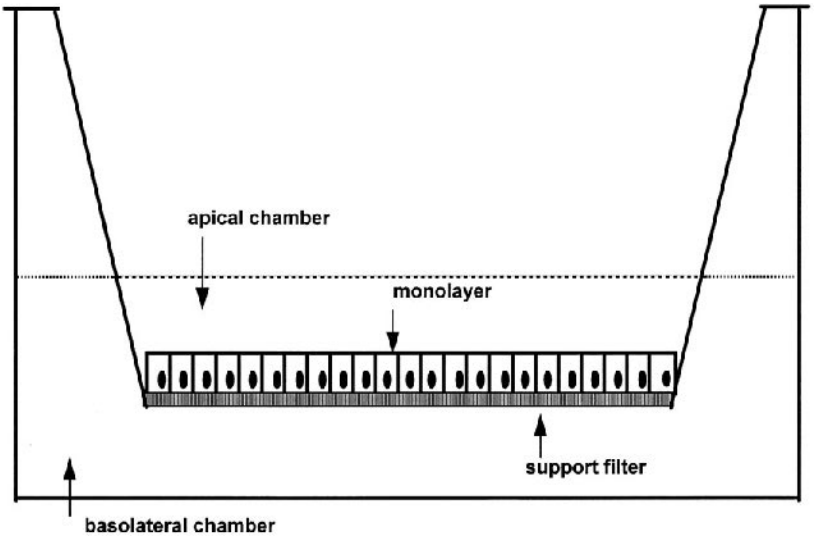

FIGURE 9 Cell monolayer cultured on polycarbonate filter. (From Ref. 28.)

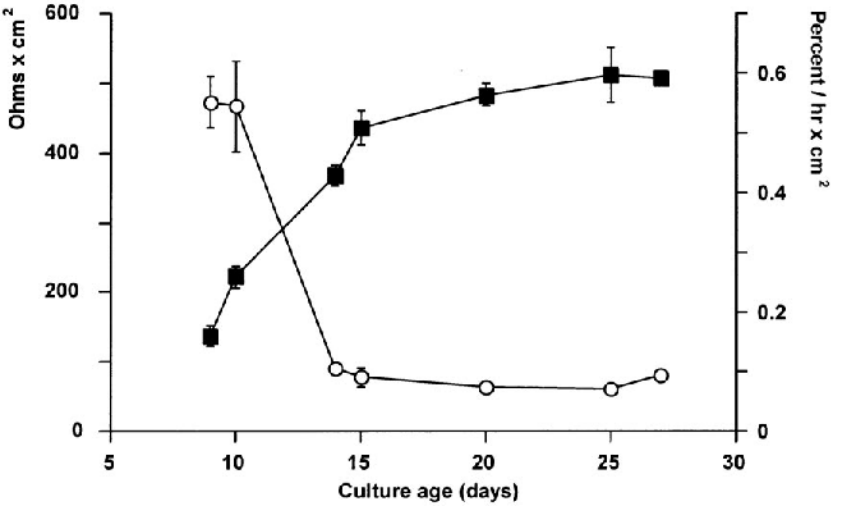

FIGURE 10 Transepithelial resistance (TEER: ■) and mannitol fluxes (○) as indices of monolayer integrity. (From Ref. 28.)

Moreover, after differentiation Caco-2 cells express several active transport systems, including amino acid transporters, small peptide, bile acid, glucose, and vitamin B_{12} transporters, as well as the P-glycoprotein efflux system. It should be emphasized that the Caco-2 cell lines originates from a colon carcinoma cell line, whereas the presence of the active carriers is a feature typical of small intestinal enterocytes.

Once grown on porous filter supports, the transport of pharmaceuticals can easily be measured using the original culture chamber, which is mounted on a shaker in an incubator. The culture medium is replaced by a donor medium containing the permeant, and an acceptor medium, respectively. Typical side-by-side diffusion chambers (see Fig. 6) can also be used if the monolayers are grown on Snapwell-type inserts. A concern with this method is the possible additional diffusional barrier that the polycarbonate filter supports might pose. Rubas et al. (31) estimated the permeability through the membrane support for hydrophylic solutes to be on the same order of magnitude as free diffusion in aqueous solution. This might, however, not be true for compounds such as strongly lipophilic ones, which may interact with the membrane.

One of the major advantages of the cultured cell method lies in its possible appliction to high-throughput screening (HTS) strategies; this model might have the best potential for HTS because the cells are rather simple to culture in high quantities, in a reproducible manner, and the results from the permeability experiments can also be highly reproducible (32).

Rubas et al. (31) compared the permeabilities of a series of compounds with poor intrinsic permeability (e.g., gamma interferon) in both Caco-2 cells and human large-intestinal tissue, and concluded that the cells well reflect the permeability characteristics of the large intestine (Fig. 11). Flux measurements across Caco-2 monolayers may therefore be predictive for permeabilities of the human colon and rectum (31).

Apart from these advantages, cultured cells based on the Caco-2 line also have striking disadvantages: first the Caco-2 is based on a colonic cell line that differentiates into a small intestinal-like tissue with tighter tight junctions than those present in the small intestine; indeed, the tight junctions in this cell line resemble the colonic tight junctions more closely. This might give rise to underprediction of the permeabilities of hydrophilic compounds with a low in vivo uptake. Second, although the cells show the expression of active transport systems (both in- and outward), this expression is quantitatively different for several transporters in comparison with excised intestinal tissue. An example is the glucose transporter, which is far less expressed in cultured cells. Also, although expression of these transporters is not a natural feature of colonic cells, it occurs spontaneously in the Caco-2 cell line: it remains to be seen whether other cellular features also differ from those of

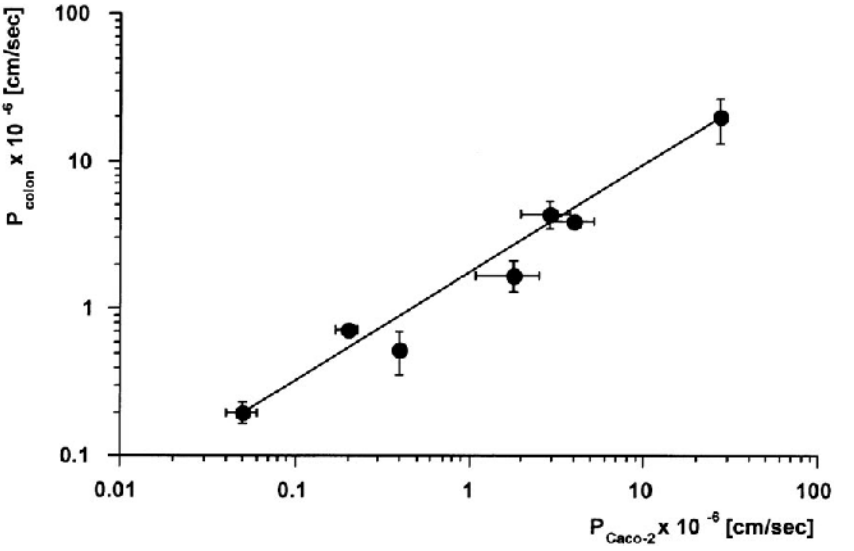

FIGURE 11 Relation of solute permeabilities of (from left to right) rhINFγ, rhIGF-1, rhGH, G4120, G6191, atenolol, and dexamethasone across Caco-2 monolayers and human large intestinal tissue (R^2 = 0.991). (From Ref. 31.)

the natural enterocytes. Third, between-laboratory, or even batch-to-batch variation in expression can occur. This may result in poor predictability of the permeabilities of both paracellularly transported and carrier-mediated compounds, and thus in a limited usefulness of these cells. On the other hand, in the near future, improvements in the engineering of the cells might lead to a more reproducible cell line with better and more realistic absorption characteristics, for all possible transport routes.

One of the advantages of the use of cultured cells is the application of cells in (partly) automated approaches as described recently (e.g., 32) or HTS purposes. Moreover, the cells have given qualitatively good information on drug interactions involving both CYP3A and P-glycoprotein, despite that quantitative information is still lacking (33).

III. DISCUSSION

A. Predictability of In Vivo Uptake

A good correlation has been shown with several of the methods described here, indicating that most of these can be used for prediction purposes. The

in vitro permeability coefficient in rat intestine in Ussing chambers or in some of the other methods has been a reliable predictor of oral absorption in humans. For all methods that have been discussed, it seems clear that a good discrimination can be made between the group of compounds with low to extremely low oral absorption ($< \approx 20\%$) and compounds with good oral absorption ($> \approx 80\%$). The intermediate group of compounds with moderate absorption after oral administration (in the 20–80% range) falls in the steep ascending part of the fraction absorbed versus permeability curve, making the estimation of the fraction absorbed more prone to error compared with the low- and high-absorption groups.

B. Variability

One of the major drawbacks of any in vitro system is the intrinsic variability that can be seen in the permeation data. This is immediately obvious when comparing data resulting from methods such as the Ussing chambers, but even more striking when data based on methods using cultured cells are compared between laboratories. The results obtained in several laboratories can differ by more than an order of magnitude, probably owing to the underlying variability in, for example, the culturing techniques. It has been suggested that an internal standard be included during permeability measurements, to deal with the intrinsic variability in the experimental system. Several suggestions have been made. For example, Dowty and Dietsch (34) used the permeability of mannitol as a normalizing agent to control intra- and intervariability in the rat. They claim that normalizing to an internal standard especially improves the predictive value for the intermediate group of moderate (20–80% absorbed) permeability, and indeed, this normalization procedure leads to a good correlation between intestinal permeability and oral absorption in rats (Fig. 12).

C. Comparison of Methods

Several groups have compared the various methods that are described in this and other chapters. Stewart et al. (35) compare three widely used intestinal absorption models: the rat in situ single-pass perfusion model, the rat everted intestinal ring method, and monolayers, based on Caco-2 cells, applying these methods to a series of small molecular size reference compounds. They concluded that both cell monolayers and single-pass perfusion combine the highest correlation between systems and most defined relation with fraction absorbed in humans.

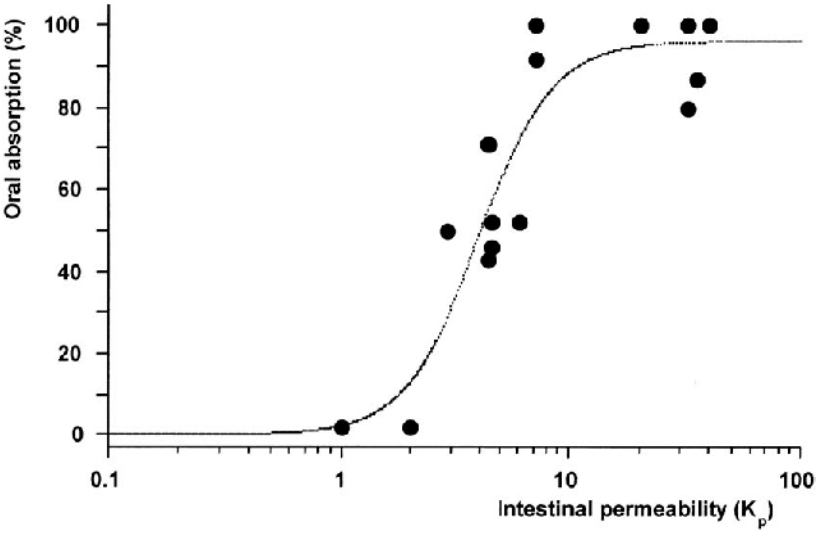

FIGURE 12 Correlation between rat intestinal permeability (K_p, in 10^{-4} cm/min) and percentage oral absorption in rats. (From Ref. 33.)

In a recent paper, the permeability of two componds transported by the large neutral amino acid carrier was studied (36). In the cell model, the two compounds showed permeabilities comparable with mannitol and failed to predict human absorption. One of the reasons might be that amino acid transport and metabolism differ strongly between normal tissue and cancer cells, thereby leading to poor predictions for compounds transported by amino acid transporters.

In a study during which the permeability characteristics of some hydrophilic markers were compared, the in vitro cell culture based on Caco-2 cells again showed a lower permeability in cultured monolayers compared with excised rat intestinal segments (37). Comparison of these data for permeabilities of polyetheleneglycols (PEGs) in humans and in in vitro methods indicate that the human intestine is more permeable than the in vitro methods suggest. In vitro underestimation of true absorption might be the result.

IV. SUMMARY

Several in vitro methods that are described in this chapter have been applied successfully to the predictive determination of human intestinal absorption of

drugs, and for mechanistic studies. The method of choice depends strongly on the nature of the question that has to be answered. Further reading in informative textbooks (e.g., 1) and many more publications than are cited here is strongly advised to assist in selection of the most appropriate in vitro model for a given study.

REFERENCES

1. RT Borchardt, PL Smith, G Wilson. Models for Assessing Drug Absorption and Metabolism. New York: Plenum Press, 1996.
2. I Osiecka, PA Porter, RT Borchardt, JA Fix, CR Gardner. In vitro drug absorption models. I. Brush border membrane vesicles, isolated mucosal cells and everted intestinal rings: characterization and salicylate accumulation. Pharm Res 1985; 2:284–293.
3. C Pidgeon, S Ong, H Liu, X Qiu, M Pidgeon, AH Dantzig, J Munroe, WJ Hornback, JS Kasher, L Glunz, T Szczerba. IAM chromatography: an in vitro screen for predicting drug membrane permeability. J Med Chem 1995; 38:590–594.
4. JA Fix. Intestinal rings and isolated intestinal mucosal cells. In: RT Borchardt, PL Smith, G Wilson, eds. Models for Assessing Drug Absorption and Metabolism. New York: Plenum Press, 1996; 51–66.
5. PS Leppert, JA Fix. Use of everted intestinal rings for in vitro examination of oral absorption potential. J Pharm Sci 1994; 83:976–981.
6. AS Uch, U Hesse, JB Dressman. Use of 1-methyl-pyrrolidone as a solubilizing agent for determining the uptake of poorly soluble drugs. Pharm Res 1999; 16: 968–971.
7. BH Stewart, AR Kugler, PR Thompson, HN Bockbrader. A saturable transport mechanism in the intestinal absorption of gabapentin is the underlying cause of the lack of proportionality between increasing dose and drug levels in plasma. Pharm Res 1993; 10:276–281.
8. KC Meadows, JB Dressman. Mechanism of acyclovir uptake in rat jejunum. Pharm Res 1990; 7:299–303.
9. PA Porter, I Osiecka, RT Borchardt, JA Fix, L Frost, C Gardner. In vitro drug absorption models. II. Salicylate, cefoxitin, α-methyldopa and theophylline uptake in cells and rings: correlation with in vivo bioavailability. Pharm Res 1985; 2:293–298.
10. JS Kim, RL Oberle, DA Krummel, JB Dressman, D Fleisher. Absorption of ACE inhibitors from small intestine and colon. J Pharm Sci 1994; 83:1350–1356.
11. TH Wilson, G Wiseman. The use of sacs of everted small intestine for the study of the transference of substances from the mucosal to the serosal surface. J Physiol 1954; 123:116–125.
12. A Yamamoto, T Kawaratani, K Kawashima, M Hashida, H Sezaki. Intestinal

transport of sulfanilic acid in rats immunized with protein–sulfanilic acid conjugate. Pharm Res 1990; 7:767–771.
13. JT Pento, GK Mousissian. Time-dependent deterioration of active transport in duodenal segments of rat intestine. J Pharmacol Methods 1988; 20:9–14.
14. L Barthe, JF Woodley, S Kenworthy, G Houin. An improved everted gut sac as a simple and accurate technique to measure paracellular transport across the small intestine. Eur J Drug Metab Pharmacokinet 1998; 23:313–323.
15. M Tomita, M Shiga, M Hayashi, S Awazu. Enhancement of colonic drug absorption by the paracellular permeation route. Pharm Res 1988; 5:341–346.
16. R Bouer, L Barthe, C Philibert, C Tournaire, J Woodley, G Houin. The roles of P-glycoprotein and intracellular metabolism in the intestinal absorption of methadone: in vitro studies using the rat everted intestinal sac. Fundam Clin Pharmacol 1999; 13:494–500.
17. HH Ussing, K Zerahn. Active transport of sodium as the source of electric current in the short-circuited isolated frog skin. Acta Physiol Scand 1951; 23:110–127.
18. GM Grass, SA Sweetana. In vitro measurement of gastrointestinal tissue permeability using a new diffusion cell. Pharm Res 1988; 5:372–376.
19. PL Smith. Methods for evaluating intestinal permeability and metabolism in vitro. In: RT Borchardt, PL Smith, G Wilson, eds. Models for Assessing Drug Absorption and Metabolism. New York: Plenum Press, 1996:13–34.
20. P-Y Yeh, PL Smith, H Ellens. Effect of medium-chain glycerides on physiological properties of rabbit intestinal epithelium in vitro. Pharm Res 1994; 11:1148–1154.
21. BI Polentarutti, AL Peterson, AK Sjöberg, EKI Anderberg, LM Utter, A-LB Ungell. Evaluation of viability of excised rat intestinal segments in the Ussing chamber: investigation of morphology, electrical parameters, and permeability constants. Pharm Res 1999; 16:446–454.
22. A–L Ungell, S Nylander, S Bergstrand, Å Sjöberg, H Lennernäs. Membrane transport of drugs in different regions of the intestinal tract of the rat. J Pharm Sci 1998; 87:360–366.
23. C–P Lee, RLA de Vrueh, PL Smith. Selection of development candidates based on in vitro permeability measurements. Adv Drug Deliv Rev 1997; 23:47–62.
24. BH Stewart, OH Chan, N Jezyk, D Fleisher. Discrimination between drug candidates using models for evaluation of intestinal absorption. Adv Drug Deliv Rev 1997; 23:27–45.
25. W Rubas, N Jezyk, GM Grass. Comparison of the permeability characteristics of a human colonic epithelial (Caco-2) cell line to colon of rabbit, monkey, and dog intestine and human drug absorption. Pharm Res 1993; 10:113–118.
26. L Barthe, J Woodley, G Houin. Gastrointestinal absorption of drugs: methods and studies. Fundam Clin Pharmacol 1999; 13:154–168.
27. J Fogh, JM Fogh, Orfeo T. 127 cultured human colon cell lines producing tumors in nude mice. J Natl Acad Sci USA 1977; 7:221–226.
28. IJ Hidalgo. Cultured intestinal epithelial cell models. In: RT Borchardt, PL

Smith, G Wilson, eds. Models for Assessing Drug Absorption and Metabolism. New York: Plenum Press, 1996:35–50.
29. L–S Gan, C Eads, T Niederer, A Bridgers, S Yanni, P–H Hsyu, FJ Pritchard, DR Thakker. Use of Caco-2 cells as an in vitro intestinal absorption and metabolism model. Drug Dev Ind Pharm 1994; 20:615–631.
30. L–SL Gan, DR Thakker. Applications of the Caco-2 model in the design and the development of orally active drugs: elucidation of biochemical and physical barriers posed by the intestinal epithelium. Adv Drug Deliv Rev 1997; 23:77–98.
31. W Rubas, MEM Cromwell, Z Shahrokh, J Villagran, T–N Nguyen, M Wellton, T–H Nguyen, RJ Mrsny. Flux measurements across Caco-2 monolayers may predict transport in human large intestinal tissue. J Pharm Sci 1996; 85:165–169.
32. P Garberg, P Eriksson, N Schipper, B Sjöström. Automated absorption assessment using Caco-2 cells cultured on both sides of polycarbonate membranes. Pharm Res 1999; 16:441–445.
33. SD Raessi, IJ Hidalgo, J Segura–Aquilar, P Artursson. Interplay between CYP3A-mediated metabolism and polarized efflux of terfenadine and its metabolites in intestinal Caco-2 (TC7) cell monolayers. Pharm Res 1999; 16:625–632.
34. ME Dowty, CR Dietsch. Improved prediction of in vivo peroral absorption from in vitro intestinal permeability using an internal standard to control for intra- and interrat variability. Pharm Res 1997; 14:1792–1797.
35. BH Stewart, OH Chan, RH Lu, EL Reyner, HL Schmid, HW Hamilton, BA Steinbauch, MD Taylor. Comparison of intestinal permeabilities determined in multiple in vitro and in situ models: relationship to absorption in humans. Pharm Res 1995; 12:693–699.
36. N Jezyk, C Li, BH Stewart, X Wu, HN Brockbrader, D Fleisher. Transport of pregabalin in rat intestine and Caco-2 monolayers. Pharm Res 1999; 16:519–526.
37. P Artursson, A-L Ungell, J-E Löfroth. Selective paracellular permeability in two models of intestinal absorption: cultured monolayers of human intestinal epithelial cells and rat intestinal segments. Pharm Res 1993; 10:1123–1129.

6
Animal Perfusion Studies

Hans Lennernäs
Uppsala University, Uppsala, Sweden

I. INTRODUCTION

The rate and extent of intestinal drug absorption (mass/time and mass/dose, respectively) in vivo are affected by several factors, such as dose/dissolution ratio, chemical instability, luminal localized metabolism, complex binding, intestinal transit, and effective permeability (P_{eff}) across the intestinal mucosa. The extent of drug absorption ($M(t)$/dose) (i.e., the fraction of drug disappearing from the intestinal lumen during a certain residence time, assuming no luminal reactions), at any time t is (1,2):

$$\frac{M(t)}{\text{dose}} = \int_0^t AP_{\text{eff}} C_{\text{lumen}} \cdot \mathrm{d}A\mathrm{d}t \tag{1}$$

where A is the available intestinal surface area, P_{eff} is the average value of the effective intestinal permeability in the gut region at which drug absorption occurs, and C_{lumen} is the drug concentration in the intestinal lumen available for absorption (1–5). Intestinal P_{eff} is one of the key variables controlling the overall intestinal absorption rate and extent, and may be used regard less of the transport mechanism(s) across the intestinal mucosa (1,2). Consequently, there are several reasons why this biopharmaceutical–pharmacokinetic variable should be investigated in both drug discovery and development.

The effective intestinal permeability (P_{eff}) is sometimes defined to include drug transport across the cytosol, basolateral membrane, interstitial fluid, and capillary wall to the portal blood flow (2–6). Consequently, such a definition also includes first-pass metabolism occurring in the cytosol of the enterocyte (for instance, by cytochromic P 450 [CYPp450] isoenzymes, and cytosolic-localized peptidases). It will particularly influence the fraction of the dose that reaches the portal vein in an intact form (6–11). However, according to the pharmacokinetic definition of bioavailability, drug metabolism localized in the enterocyte is a part of the total first-pass effect (gut wall metabolism, E_g, and hepatic extraction, E_h and not the absorption step (f_a) [$F = f_a (1 - E_g)$] $(1 - E_h)$ (12). Another and probably more accurate definition suggests that the intestinal epithelial P_{eff} for passive diffusion reflects the transport across the apical membrane of the enterocyte (13–15). Recently, it has also been reported that the permeability across epithelial cells is determined by the largest resistance, which is usually assumed to be the apical brush border membrane (13,14). Intestinal perfusion models, which measure the disappearance of the drug from the perfusion solution in the intestinal lumen, directly reflect the transport across the apical epithelial cell membrane (Fig. 1) (1,2). This means, strictly speaking, that the absorption variable, intestinal P_{eff}, represents transport of compounds into the enterocyte's cytosol (1,2). This view is cer-

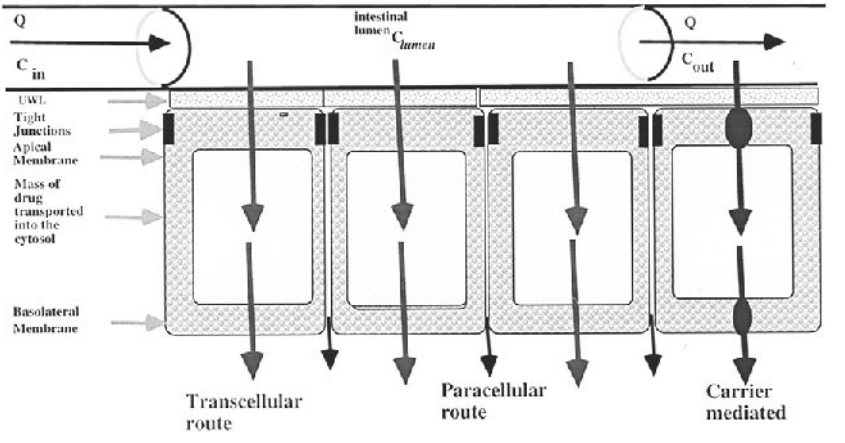

FIGURE 1 A schematic illustration of the membrane transport barriers for a drug molecule across the intestinal epithelium during a single-pass perfusion of the intestinal lumen. (UWL, unstirred water layer; Q, perfusion rate in lumen.)

tainly true for passive transcellular diffusion where the apical membrane is rate-limiting. However, it seems more likely that the basolateral membrane of the enterocyte is the slowest step in the overall transport from the intestinal lumen to portal blood for di- and tripeptides that are rapidly transported by the oligopeptide carrier (16).

Drug metabolism in the cell cytosol may influence the measured permeability if it is based on appearance of intact drug on the receiver side of the membrane (which corresponds to the portal blood), as in the Caco-2 and Ussing chamber models. However, it assumes that the intracellular enzymes are well expressed in these two models. For the perfusion method, which is based on disappearance, a special concern is peptides because they might be metabolized by membrane-bound enzymes (such as peptidases and esterases) in the brush border. These enzymatic processes in the lumen will increase the disappearance rate of the drug from the intestinal lumen during a perfusion experiment, and give an inaccurately high P_{eff} value (17). Therefore, it is crucial to be aware of the stability and which metabolic processes the investigated drug may take part in and account for them in any detailed model of the drug transport mechanism(s) across the mucosal membrane, as discussed earlier (2,6,18). This issue is crucial when investigating and developing principles for prodrugs and soft drugs. On the other hand, carrier-mediated efflux transport of drugs by P-glycoproteins (P_{gp}) or multidrug resistance proteins (MRP; or any other efflux proteins), which are located in the apical membrane of mature enterocytes, may result in a lower P_{eff}, even if the passive diffusion across the lipid membrane phase is high (19–25).

A third process that has been reported to affect the disappearance rate is binding of the drug to the intestinal tissue. Intestinal P_{eff} is measured at a steady-state, with the single-pass perfusion model, and the tissue-binding process that may influence (non–steady-state) drug permeation is quasi–steady-state, and does not contribute to the measured permeability (2,6). In addition, it is unlikely that the binding capacity will be high enough to affect the mass balance transport for most drugs. However, this may occur for drugs with extremely high distribution volumes, as this is indicative of extensive tissue binding.

This chapter will focus on animal models with which the effective permeability variable can be measured. The single-pass perfusion model in the rat is the model for which the largest database exists. The single-pass perfusion models of the chronically isolated intestinal segment in the rat and single-pass perfusion models of the chronically isolated intestinal segment in the rat and single-pass perfusion model of the dog will also be described briefly.

II. METHODS

A. In Situ Single-Pass Perfusion of the Rat Intestine (Acute Experiments)

Determination of the disappearance of drug from a perfusion solution passing through an isolated intestinal segment is a common method of estimating the effective intestinal permeability (P_{eff}) of drugs (see Fig. 1) (2,4,26). In humans, no validated models were available for estimation of P_{eff} until the Loc-I-Gut and Loc-I-Col perfusion techniques were introduced (a more detailed presentation of the techniques can be found in Chap. 7 (27–29). In rats the single-pass perfusion experiment is performed after surgery and under total anesthesia. The single-pass jejunal perfusion model in situ in rat has been validated against the human jejunal perfusion model (26). The rats usually weigh between 200 and 350 g (age 7–10 weeks), and are most often fasted overnight before the perfusion experiment. An intestinal segment (about 10 cm) is usually rinsed with 10–20 mL of saline solution to clear the segment before the test perfusion is started. A common perfusion rate is 0.2 mL/min, which is maintained by a syringe pump.

Over the age interval of 5–30 weeks, there is no effect of age on the jejunal P_{eff} in rat, either for passive diffusion of drugs or carrier-mediated transport by the D-glucose carrier (Fig. 2). However, age-dependent intestinal P_{eff} might, nevertheless, be an issue for very young and very old rats (30).

B. In Vivo Single-Pass Perfusion of the Rat Intestine (Chronically Cannulated)

The small intestine is exposed and a segment of 6–8 cm, with an intact blood flow supply and innervation, is isolated. The head–tail connection of the remaining intestine is restored by end-to-end anastomosis. Two polytetrafluoroethylene (Teflon) cannulas are inserted through the skin and attached to the abdominal wall by ligation. Outside the animal, silicon perfusion tubes are connected to these cannulas. Inside the animal, the loop is secured with an encircling silk suture. The single-pass perfusion is performed at a rate of 1.0 mL/min in the permanently isolated internal-loop model. The rats can move about freely in the cage between the perfusion experiments, but during a perfusion experiment each animal is placed in a restraining cage (31).

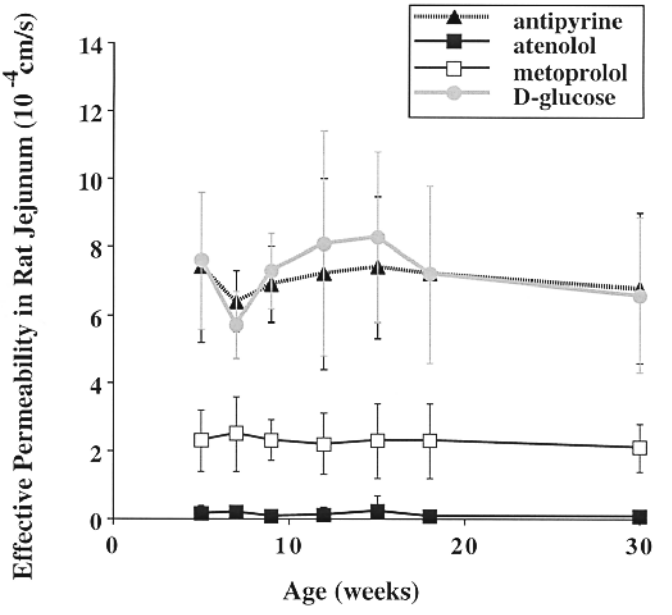

FIGURE 2 The effect of age on rat jejunal permeability for D-glucose, antipyrine, atenolol, and metoprolol.

C. In Vivo Single-Pass Perfusion of the Dog Intestine (Loc-I-Gut)

An in vivo intestinal perfusion technique has previously been developed and extensively used and validated for permeability investigations in humans (1,27,28). The experimental procedure using the tubes in humans is described in more detail in Chap. 7. Recently, the technique has been applied to drug absorption investigations in dogs (32). Beagle dogs were intubated in a standing position, using a wooden bite bar with a center opening to prevent the dog from chewing on the tube. The tube was inserted orally through the esophagus and then advanced slowly through the upper gastrointestinal tract. Upon reaching the proximal jejunum, the correct position of the tube was confirmed by X-ray and the two ballooons were inflated. The intestinal perfusion was then performed at a flow rate of 1.9 mL/min until steady-state was achieved, after which all calculations of the absorption variables were made (32).

1. Stability and Adsorption Tests

The chemical and enzymatic stability of each drug molecule has to be assessed by incubation in the perfusion solution (usually a buffer at a specific pH), as well as in aspirated intestinal fluid, before the intestinal perfusion experiment is performed (27). In addition, the binding of the compound to the tubing used in the perfusion experiments has to be investigated (27).

2. Functional Viability Tests During the Intestinal Perfusion

The intestinal barrier function (viability) has to be continuously monitored in any intestinal perfusion model. For instance, the intestinal viability may be assessed with the steady-state recovery of the nonabsorbable marker PEG 4000 ($PEG_{recovery}$), and by inspection of the steady-state P_{eff} levels of D-glucose (marker for active absorption) and antipyrine (marker for passive absorption) (26,33). The P_{eff} of antipyrine may also be used as an indicator of extensive changes in mesenteric blood flow (1,27). It is also important to check whether the P_{eff} values are stable over time, because this will indicate that no escalating viability changes have occurred. We have previously concluded that antipyrine is a suitable absorption marker since mass-balance between disappearance from the perfused segment and appearance in plasma of the drug can be achieved. This also suggests that antipyrine is not bound or concentrated in the intestinal tissue in any way (1,27).

3. Establishing a Permeability Method and the Use of Reference Compounds

To classify drugs according to the Biopharmaceutics Classification System (BCS) and to compare permeability data from different laboratories, the use of a series of reference compounds is necessary (2,34–36). Potential internal standards are metoprolol, antipyrine, polyethylene glycol, and mannitol. There is a list of compounds that are recommended for establishing a permeability model for use in the BCS context. These include ketoprofen, naproxen, verapamil, carbamazepine, propranolol, metoprolol, theophylline, caffeine, antipyrine, furosemide, hydrochlorothiazide, α-methyldopa, atenolol, and ranitidine (34–36).

4. Data Analysis of an Intestinal Perfusion Experiment

The steady-state effective intestinal permeability (P_{eff} cm/s) in rats is usually calculated using the parallel-tube model, because they are perfused from an

entrance in one end of the intestinal segment to an exit at the other end of the intestinal segment (for instance in the two rat models described earlier) [Eq. (2)] (5,18,26,38):

$$P_{\text{eff}} = \frac{-Q_{\text{in}} \ln(C_{\text{out}}/C_{in})}{A} \tag{2}$$

where C_{in} and C_{out} are the inlet and outlet, fluid-transport corrected, concentrations of the compound, respectively. Q_{in} is the perfusion flow rate, and A is the mass transfer surface area within the intestinal segment, which is assumed to be a cylinder with a length of 10 cm (27,37).

In the dog model, the permeability was calculated using the well-stirred model because it is assumed that the hydrodynamics are similar to the corresponding model in the human intestine. When the human intestine is perfused, we have shown by residence time distribution analysis that the hydrodynamics are best described by the well-mixed model (27,32,37). The appropriate equation for the calculation of P_{eff} in this case is

$$P_{\text{eff}} = \frac{Q_{\text{in}}(C_{\text{in}} - C_{\text{out}})/C_{\text{out}}}{A} \tag{3}$$

where C_{in} and C_{out} are the inlet and fluid–transport-corrected outlet concentrations of the compound, respectively. Q_{in} is the perfusion flow rate, and A is the mass transfer surface area within the intestinal segment, which is again assumed to be a cylinder with a length of 10 cm (27,32,37).

D. Absorption Investigations with the Single-Pass Perfusion Model in the Anesthetized Rat

An earlier study has shown that the extent of intestinal absorption in humans can be predicted from intestinal permeability values measured in situ in rats by single-pass perfusions (38). These authors investigated nine compounds and calculated the dimensionless permeability of each. Their main conclusion was that an intestinal permeability value can be used to estimate the extent of oral drug absorption in humans, regardless of the transport mechanism of the compound investigated (38).

Later, a direct comparison of the effective permeability values between human and rats was reported for a number of drugs (26). For passively transported compounds, the rank order was the same in perfused proximal jejunal segments of both humans and rats. The P_{eff} values for drugs transported by passive diffusion were on average 3.6 times higher in humans in vivo than in

the in situ model in rats, irrespective of the permeability classification of the drug (26). This ratio between human and rat intestinal permeability models has been subsequently verified for other drugs, such as fluvastatin and *R*/*S*-verapamil (39,40). Plausible reasons for the lower P_{eff} value in the rat model are differences in effective absorptive area within the perfused segment, or species differences affecting partitioning into the membrane, diffusion coefficient, or diffusion distance (26,41–43). The anesthesia will certainly also contribute to somewhat slower passive diffusion across the jejunal barrier. Carrier-mediated transported compounds, such as L-dopa and D-glucose, deviated from this linear relation between the two models, which clearly demonstrates that each carrier-mediated transported drug needs to be carefully investigated to elucidate the transport mechanism(s) involved and to obtain a scaling factor for direct comparisons of the two different species and models (26). However, both human and rat P_{eff} values predict the extent of intestinal drug absorption in vivo in humans (26) very well.

The cutoff value of the absorption half-life required to obtain a complete intestinal absorption seems to be about 30 min. In both rats and humans, the P_{eff} of metoprolol ($P_{eff} \approx 1.5 \times 10^{-4}$ cm/s) is on the lower end of the range

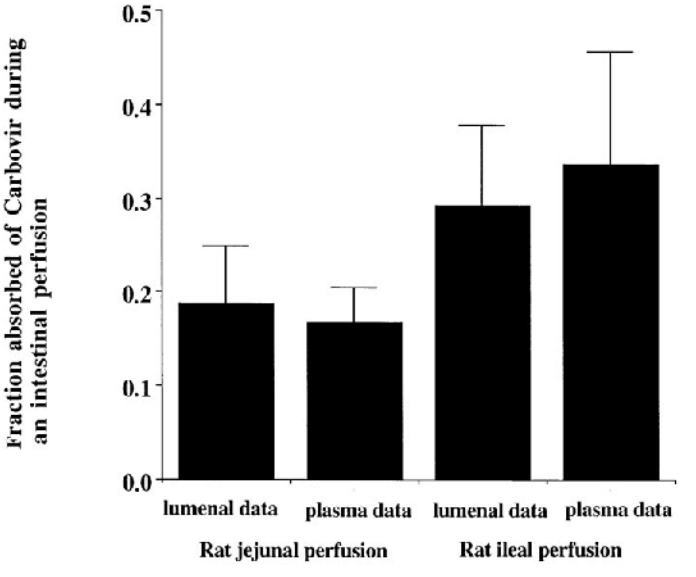

FIGURE 3 Mass balance of disappearance from the intestinal lumen and appearance rates in plasma for carbovir during perfusion of rat jejunum or rat ileum.

for the completely absorbed drugs (1,26). A half-life of approximately 30 min has also been previously suggested to be the cutoff value for complete absorption when the direct transmucosal transport rate of 13 drugs, representing a broad range of permeability values, was studied (43). The good agreement between different animal laboratories clearly demonstrates the robustness of the animal intestinal perfusion method.

The absorption and first-pass metabolism of carbovir was investigated in another experimental setup in which intestinal perfusion was carried out at the same time as plasma samples were taken from the portal vein (44). These authors found an agreement between the disappearance of carbovir from the intestinal lumen and the appearance of carbovir in the portal vein (Fig. 3). This mass balance between disappearance and appearance rates indicates that no metabolism of carbovir occurred in the gut wall. It also supports the conclusion that intestinal drug absorption can be determined by disappearance from the intestinal segment in the perfused rat model. Altogether, this report by Pithavala et al. in 1997 further demonstrates the great utility of the single-pass perfusion model in rats as a robust preclinical drug absorption model that can provide highly accurate permeability data (44).

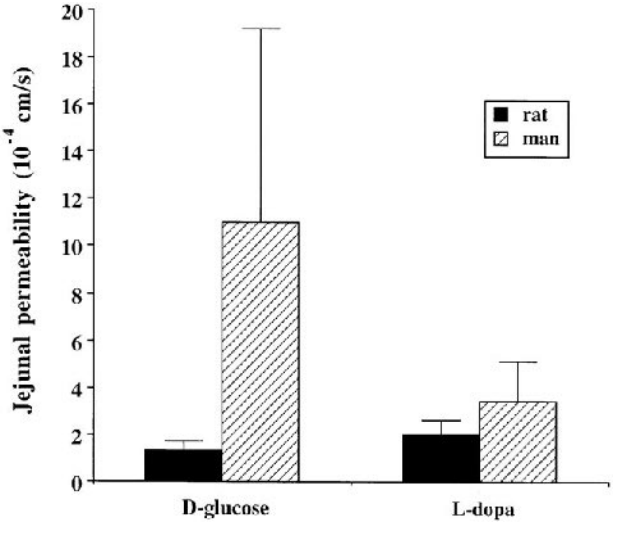

FIGURE 4 Jejunal permeabilities of D-glucose and L-dopa in humans and rats obtained by regional single-pass perfusion.

In general, the single-pass perfusion model in rats shows high permeability values for various model compounds that are transported through the hexose, amino acid, and oligopeptide carriers (2,26,45). The general opinion is that the transport properties for these carriers agree between rats and human (46,47). Jejunal permeability values for D-glucose and L-dopa are similar to the corresponding data in the human intestine (26) (Fig. 4). Accordingly, the single-pass perfusion model in the rat intestine is suitable for investigations of carrier-mediated drug transport. By contrast, the effective permeability values of carrier-mediated transported compounds, such as L-dopa, D-glucose, and L-leucine, are significantly slower, about 100- to 1000-fold, in Caco-2 cells than in human jejunum in vivo at the same concentrations (Fig. 5) (48). For instance, the carrier-mediated transport rate of L-dopa was approximately 340-fold slower in Caco-2 monolayers than in human jejunum. We cannot exclude the possibility that these compounds were partly transported by passive diffusion in the Caco-2 monolayers owing to saturation of the carrier (48). Nevertheless, the results are in agreement with previous studies in Caco-2 monolayers that show that this cell line displays a variable and generally lower expression of carrier-mediated transport than seen in vivo (49). This

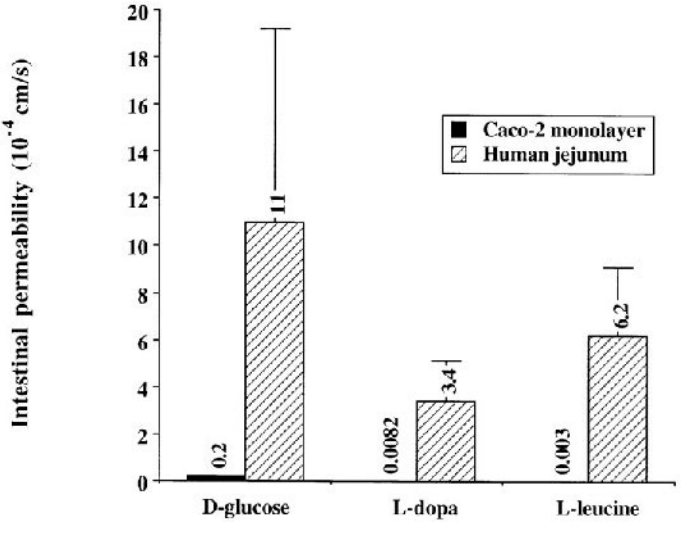

FIGURE 5 The relation between human jejunal permeability and Caco-2 monolayer permeability for D-glucose, L-dopa, and L-leucine. The number above each column is the permeability value.

is also consistent with the colonic origin of the Caco-2 cells. Quantitative prediction of carrier-mediated drug transport rate in humans, based on data generated in the Caco-2 model, therefore, will be possible only after characterization of each transport system, and subsequent introduction of the appropriate scaling factor to compensate for the different expression of the carrier in Caco-2 cells from that seen in vivo (18,48). Investigations of transport mechanisms (on a qualitative basis) for different drugs is still possible with the Caco-2 model with a high degree of predictivity, despite the lower expression of the transport proteins. Direct comparison of the oligopeptide-mediated transport for a model prodrug, D-asp-OBzl, has recently been reported by Steffansen et al. (50). D-asp-OBzl was transported 32 times slower in the Caco-2 model than from the rat jejunum (measured with a single-pass perfusion; Fig. 6) (50). This is most likely due to a significantly lower expression of the

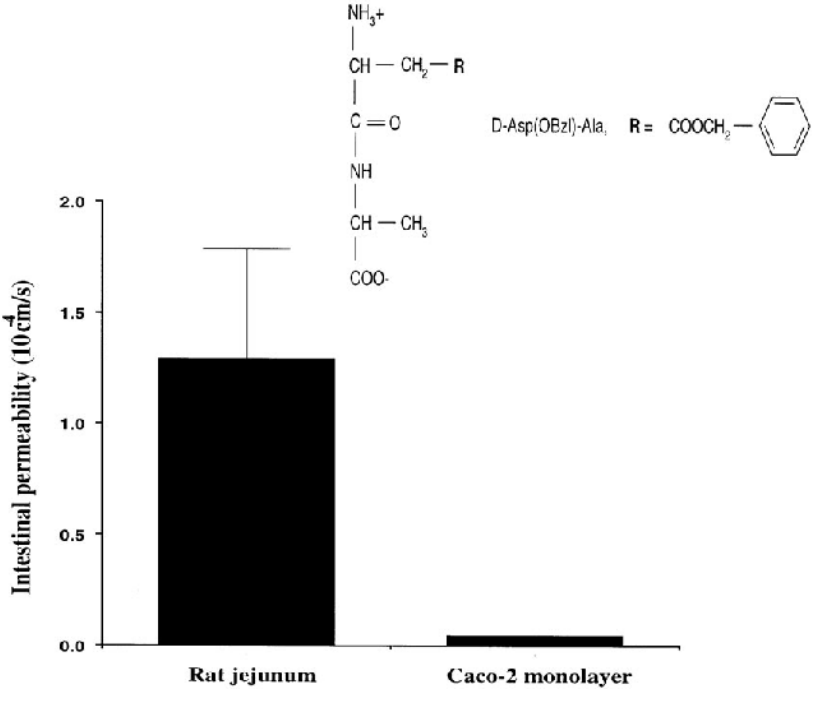

FIGURE 6 The permeability of a model prodrug for the oligopeptide carrier, D-Asp-OBzl, was 32 times lower in the Caco-2 model than in the rat intestinal single-pass perfusion model.

carrier in the cell culture (50). Passive drug absorption seems, however, to be equally well predicted with the Caco-2 model as with other permeability models.

Underprediction of the permeability of actively transported drugs is a limitation of the available cell culture (in vitro) transport models (such as Caco-2 model), because they have a low expression of various transport carriers (51). It is very important to consider this model difference, because some new drug molecules, intended to be used in oral drug products, seem to be absorbed by complex transport mechanisms, involving both passive diffusion and carrier-mediated transport in both directions across the intestinal barrier (carrier-mediated absorption and carrier-mediated efflux) (18,51).

III. DISCUSSION

A. Regional Intestinal Factors Affecting Absorption and Bioavailability

Absorption of the drug throughout the small intestine and certain regions of the large intestine is a prerequisite for drugs administered in controlled-release dosage forms. However, several physiological, anatomical, and biochemical factors that influence the dissolution, stability, absorption, and presystemic metabolism of the drug vary along the gastrointestinal tract. Consequently, it is crucial to investigate these processes in the intestinal regions of interest. One of the variables, intestinal P_{eff}, can easily be determined by applying the single-pass perfusion technique in various regions of the rat intestine.

The small intestine is the region of the gastrointestinal tract with the highest absorptive capacity and from which most drugs are mainly absorbed. The drug absorption from this region, which is specialized for rapid nutrient uptake, is high owing to a large surface area and a large number of different types of transport proteins (1,2,41,52–55). Drugs may also be absorbed to a significant extent from the colon, which is a necessary property for drug molecules that are to be given as controlled-release products (56). The extent and importance of colonic absorption are, however, difficult to predict. This is because of the highly variable transit time, conflicting results from animal in vitro or in situ studies on regional intestinal permeability, and a lack of human colonic permeability data (1). Available animal and human data have generally shown that the colon has a significantly lower permeability–absorptive capacity than the small intestine for hydrophilic to moderately lipophilic compounds (57–61). Furthermore, Kimura and co-workers found that a small drug of in-

termediate lipophilicity (acetaminophen, MW 151) was more rapidly absorbed from the small than from the large intestine in rats, whereas the P_{eff} of a highly lipophilic compound (indomethacin, MW 358) had similar permeabilities in these regions (68). Lower permeabilities are consistent with the lack of villi (smaller surface area), the lower membrane fluidity of the absorptive cells (colonocytes), lower mesenteric blood flow, less pronounced mixing of the luminal contents, and absence or low capacities of the specific transport systems for drug and nutrient absorption (57–64). However, the foregoing observations are in conflict with data obtained by other groups, who demonstrated a higher P_{eff} in the rat colon than the small intestine for hydrophilic compounds (65–67). The discrepancies in the results have not yet been clarified, but as previous animal in situ and in vitro studies have shown, they might be due to loss of the intestinal barrier function during the experimental procedure (26,33).

This inconsistency in the literature clearly demonstrates the need for using internal permeability standards and also to use several well-established model compounds when evaluating a permeability method. This is also necessary for comparison of regional permeability values between different laboratories. As discussed earlier, some animal in situ and in vitro studies have reported that the colon has a significantly higher permeability than the small intestine for lipophilic compounds, whereas others have observed that this is also true for hydrophilic molecules (61,64–70). The reasons for the different permeability patterns for hydrophilic and lipophilic compounds are unknown, but might be explained by a composition of colonocyte membranes that favors the uptake of lipophilic compounds, and an influence of the unstirred water layer adjacent to the intestinal wall, which is a diffusional barrier shown to have a considerable influence on the P_{eff} for highly permeable compounds in the perfused rat intestine in situ (71). Other factors such as paracellular absorption and solvent drag are less probable, because in this rat model neither solvent drag nor high luminal levels of D-glucose (up to 80 mM) influence the P_{eff} of compounds in this size range (72,73).

The approximately 20 and 100 times lower rat colonic P_{eff} values for D-glucose and L-dopa, respectively, compared with the rat jejunum are in agreement with observations for D-glucose in the human intestine in-vivo, and indicates an absence or low capacity of the glucose and amino acid transporters in the large intestine (1,29).

From the foregoing discussion and from several reports, it appears that there exists a similarity in intestinal drug absorption among human and rats. In a 1998 report by Chiou and Barve, found that data in the literature for the extent of intestinal absorption in humans was predictable on the basis of

corresponding data from the rat (74). The relation between human and rat absorption appeared to be linear for 64 drugs representing a wide range of different physicochemical and permeability properties. The extent of intestinal absorption ranged from approximately 20 to 100%. That the rat model is a good model is also supported in a study by He et al. in 1998, in which values of bioavailability of 16 oligomers of polyethylene glycol (PEG) with molecular weights between 280 and 950 were compared (75). As the compounds are not metabolized to any significant extent during first-pass, the bioavailability is assumed to reflect intestinal absorption. The bioavailability ranged between 14–79% and 21–56% in human and rats, respectively. Furthermore, the correlation between humans and rats was excellent ($r^2 = 0.975$). In contrast, dogs absorbed the same compounds significantly more efficiently and their extents of absorption were far less predictive of the absorption in humans ($r^2 = 0.449$) (75).

B. Intestinal Efflux and Drug Absorption

In the last few years, it has been discovered that drug transport across the intestinal barrier is affected not only by the interaction between the lipophilic membrane and the physicochemical properties of the drug molecule itself, but also by several and not yet fully understood carrier-mediated efflux mechanisms. This phenomenon, which is referred to as multidrug resistance (MDR), is mediated by the increased expression of energy-dependent drug efflux proteins such as P-glycoproteins (P_{gp}), multidrug resistance-associated proteins (MRP), or lung resistance proteins (LRP) (76–78). These ATP-binding cassette (ABC) transporters decrease the intracellular concentration of the drugs and their metabolites (if they are good substrates) by actively pumping them out of the cells. The P_{gp}, MRP, and LRP are expressed in various normal tissues (as well as in cancer cells), where they may influence the absorption, bioavailability, tissue distribution, and the elimination of drugs.

Several surfactants have been evaluated as reversers of MDR. It is not generally believed that these agents are substrates for P_{gp} or other efflux proteins, but rather, that they affect the proteins indirectly by inducing alterations in the physical state of the lipids in the plasma membrane (79).

The P-glycoproteins are encoded by two genes in humans (*MDR1* and *MDR2*) and three genes in rodents (*mdr1–3*). Only *MDR1, mdr1*, and *mdr3*, however, are involved in MDR (80). The 170-kDa P_{gp} is present in the apical membrane of intestinal epithelial cells of the small and large intestine, in the canalicular membrane of hepatocytes, and in the lumenal membrane of proximal epithelial cells in the kidney (81). These locations suggest that P_{gp} excretes

its substrates into the intestinal lumen, bile, and urine to eliminate these compounds from the body. It has also been reported that P_{gp} is present on the capillary endothelium of the brain, where it is a functionally important part of the blood–brain barrier (82,83).

The substrate specificity of P_{gp} appears to be very broad, as the protein is able to transport chemically and pharmacologically unrelated drugs such as vinca alkaloids (e.g., vincristine), calcium channel blockers (e.g., verapamil), the immunosuppressive agent cyclosporine, glucocorticoids (e.g., dexamethasone), the anthelmintic drug ivermectin, and β-receptor blocking agents (e.g., celiprolol) (80,82,84–85). Although the chemical structures recognized by P_{gp} are not fully determined, favored P_{gp} substrates appear to be cationic, hydrophobic molecules, with at least two planar rings, and a molecular weight of 400–1500 (80). It has been suggested that the interaction between P_{gp} and its substrates might involve the formation of several hydrogen bonds, separated by fixed distances of 2.3 ± 0.3 or 4.6 ± 0.6 Å (85). Klopman et al. (86) tested a data set of 609 diverse compounds as MDR reversal agents and reported that the C-C-N-C-C sequence was found in most of the active compounds, whereas the presence of a carboxylic acid or a quaternary ammonium was detrimental to reversal activity.

The tissue distribution of the 190-kDa MRP generally overlaps with that of the P_{gp} (87). The physiological role of MRP is probably to pump amphiphilic anions, such as phase II conjugates of glutathione, glucuronic acid, and sulfate, out of the cell (88). It has been suggested that drug efflux by the MRP might occur by a cotransport mechanism involving glutathione and possibly other anions (89,90). Whether the MRP is able to transport free drugs or not is, however, controversial and the subject of several ongoing investigations. Nevertheless, the MRP has been suggested to efflux calcein and several β-lactam antibiotics from the serosal to the apical side of rat intestinal segments in vitro (91–93). The MRP2, also called the canalicular multispecific organic anion transporter (cMOAT), is a homologue of MRP and is expressed in the liver as well as in the intestine (RNA expression), mainly in the duodenum (94). Furthermore, three new homologues of MRP and MRP2 have been identified: MRP3–5. The MRP3 is mainly expressed (RNA level) in the liver, MRP4 is expressed (RNA level) in only a few tissues (e.g., lung, kidney, and gallbladder), and MRP5 is expressed (RNA level) in almost every tissue (94). Their substrate specificities and potential roles in drug transport have not yet been established.

The tissue distribution of the 110-kDa LRP mainly overlaps with that of MRP (87). The potential role of LRP as an efflux transporter in normal (noncancer) tissues has not been reported.

In general, the presence of any efflux protein at the apical membrane of intestinal epithelial cells will efflux their substrates back into the intestinal lumen. At higher concentrations the efflux protein will be saturated, resulting in a higher fraction being absorbed and an increase in the bioavailability. It was suggested that this mechanism is the reason for the observed dose-dependent absorption of talinolol in humans and celiprolol in rats, and the concentration-dependent jejunal effective permeability of *R*/*S*-verapamil in humans and rats (25,95–97). There was an increase of rat jejunal P_{eff} from 0.42×10^{-4} to 0.8×10^{-4} cm/s ($p < 0.05$) at perfusate concentrations from 4.0 to 400 mg/L. Corresponding data in humans at the same perfusate concentrations increased from 2.5×10^{-4} to 6.8×10^{-4} cm/s ($p < 0.05$). In Fig. 7 a correlation is shown for the jejunal permeabilities of both enantioners of verapamil determined with single-pass perfusion of the rat and human jejunum. The jejunal P_{eff} of both enantiomers is about six to eight times lower in the perfused rat jejunum compared with human jejunum (25,97). The reason for this discrepancy might be that the rat intestine has a somewhat higher P_{gp}-mediated efflux activity than

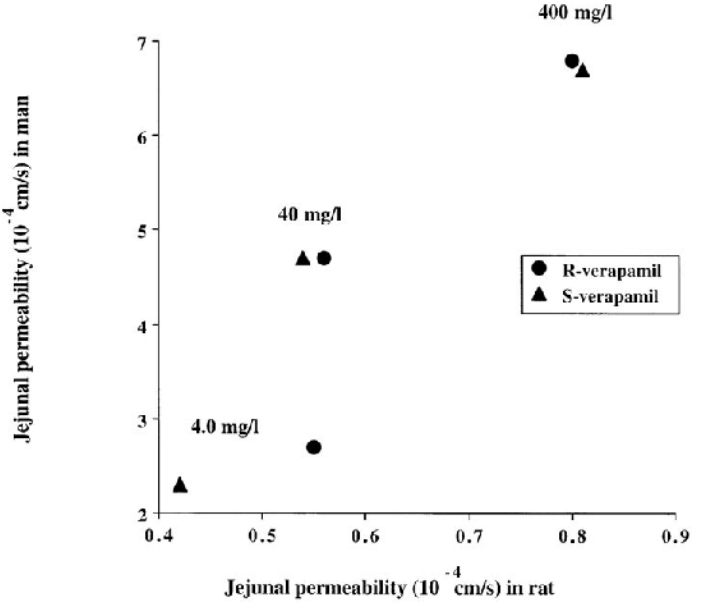

FIGURE 7 The relation between the jejunal permeabilities of each of the enantiomers of verapamil in rats and humans, respectively.

the human intestine. This is supported by our previously reported human–rat correlation for passively transported drugs for which the difference was about 3.6 times (26). However, the P_{eff}s for *R*- and *S*-verapamil in rats were still high enough to predict complete intestinal absorption. Interestingly, there was no detectable difference between the jejunal P_{eff} for *R*- and *S*-verapamil in humans in vivo or rats in situ (25,97). This has also been valid for the transport of *R*/*S*-verapamil in cancer cells in vitro. The lack of stereoselectivity of P-glycoprotein-mediated intestinal efflux transport, clearly demonstrated in humans and rats, is of utmost pharmacological importance to consider for the otherwise well-known stereoselective pharmacokinetics and pharmacodynamics for *R*/*S*-verapamil in humans (25,97).

However, even if *R*- and *S*-verapamil are substrates for P_{gp} in the small intestine in both rats and humans, the measured P_{eff}-values were sufficiently high to predict a complete intestinal absorption (26,97). This may be due saturation of the efflux carrier, and it appears that the P_{gp} transport activity might be saturated at luminal concentrations obtained after clinical doses. Earlier studies in humans and rats were performed as single-dose studies (without pretreatment of any P_{gp} inducer). Therefore, it is of great interest to specifically examine the effect on intestinal P_{eff} in rats pretreated with a well-known P_{gp} inducer. Rifampin has previously been shown to induce P_{gp} in human enterocytes in vivo and in cell cultures in vitro (99). In humans, the MDR1 mRNA expression in the enterocyte increased by an average of 4.3-fold following rifampin treatment for 7 days (100,101). In a rat intestinal perfusion investigation, the jejunal P_{eff} tended to decrease after treatment with rifampin (39). This is most probably attributable to increased expression of an efflux protein which, based on previous experience, should be the P-glycoprotein. However, even if the rat jejunal P_{eff} for *R*- and *S*-verapamil was affected by rifampin treatment, the reduction was too small to influence the extent of intestinal absorption of *R*- and *S*-verapamil (39). In another rat jejunal permeability investigation the animals were pretreated with artemisin, which is known to decrease its own bioavailability after repeated oral dosing to humans. However, multiple dosing of artemisin did not affect its permeability in the rat jejunum. Furthermore, rat jejunal P_{eff} of artemisin was not affected by addition of *R*/*S*-verapamil. Altogether this indicates that artemisin is not a P-glycoprotein substrate in rats and probably not in humans either (26,97,103). This in vivo model in rats also supports the use of Caco-2 model for efflux studies, because artemisin was not a substrate in that cell culture model (104).

In other studies it was shown that the bioavailability of the anticancer drug paclitaxel increased more than three-fold in mice lacking P_{gp} (mdrla−/−)

compared with wild-type mice (105). However, the quantitative role of efflux proteins for the bioavailability in vivo in humans is under debate in the literature, and remains to be definitively established (26,102,106).

The levels of mRNA expression of P_{gp} increase along the intestinal tract in humans. The P_{gp} is located on the apical membrane of the columnar epithelial cells, but not on the crypt cells in humans (81). A regional difference in transport activity of well-known P_{gp} substrates in rats (diffusion chamber), such as etoposide, vinblastine, or verapamil, has been reported: The ileum had a higher efflux capacity than either the jejunum or colon (107).

C. Enzymatic Activity of the Intestinal Wall

The intestinal expression of cytochrome P450 (CYP) isoenzymes in both humans and rats is highest in the duodenum and jejunum and lowest in the colon. The CYP3A4 accounts for most of the total CYP found in the human intestine, with duodenal, jejunal, ileal, and colonic concentrations (pmol/mg protein) of approximately 50, 30, 10, and 2% of that in the liver, respectively (108). The intrinsic clearance for CYP3A4 (midazolam 1′-hydroxylation) has been estimated to be 50, 144, and 19 mL/min in the duodenum, jejunum, and ileum, respectively (liver 15,800 mL/min) (109). CYP2C9 and CYP2D6 were detected only in the human small intestine, with concentrations approximately 5 and 20% of that of the liver, respectively (108). In rats, CYP2B1 is expressed in high concentrations in the duodenum (150% of that of the liver), lower in the jejunum (50%) and the ileum (25%), with only traces being found in the colon (108). It has been reported that the CYP3A enzymes are present throughout the gastrointestinal tract in rats, although at a lower concentration in the colon than in the upper small intestine (110). Zhang et al. reported in 1996 that CYP P450s, 1A1, 2B1, and 3A1, were detected in rat enterocytes (111). In addition, CYP P450s, 2C6 and sC11, were both constitutively expressed at low levels (111). In our own laboratories we have found that the mRNA expression of CYP P450s, 1A1, 2B1, 2C6, 2C11, 2D1, and P_{gp} was strong throughout the rat small intestine (Lindell, Lang, Lennernäs, unpublished data). Appearantly some controversies still exist regarding the expression of CYP P450s along the rat small intestine.

IV. CONCLUSION

Intestinal drug absorption can be determined by measuring disappearance rate of drugs from the intestinal segment in the perfused rat model. The high corre-

lation between rat and human jejunal permeabilities for drugs representing different chemical structures as well as transport mechanisms supports the great utility of the rat intestinal perfusion technique in preclinical research and development. Recent reports demonstrating mass balance between disappearance from the lumen and appearance rates of drug in the partial blood further support this conclusion.

REFERENCES

1. H Lennernäs. Human intestinal permeability: an overview. J Pharm Sci 1998; 87:403–410.
2. GL Amidon, H Lennernäs, VP Shah, J Crison. Theoretical considerations in the correlation of in vitro drug product dissolution and in vivo bioavailability: a basis for a biopharmaceutics drug classification. Pharm Res 1995; 12:413–420.
3. GL Flynn, SH Yalkowsky, TJ Roseman. Mass transport phenomena and models: theoretical concepts. J Pharm Sci 1974; 63:479–509.
4. NFH Ho, JY Park, PF Ni, WI Higuchi. Advancing quantitative and mechanistic approaches in interfacing gastrointestinal drug absorption studies in animals and humans. In: W Crouthamel, AC Sarapu, eds. Animal Models for Oral Drug Delivery in Man; In Situ and In Vivo Approaches. Washington, DC:, American Pharmaceutical Association, 1983:27–106.
5. I Komiya, JY Park, A Kamani, NFH Ho, WI Higuchi. Quantitative mechanistic studies in simultaneous fluid flow and intestinal absorption using steroids as model solutes. Int J Pharmaceut 1980; 4:249–262.
6. H Lennernäs, J Crison, GL Amidon. Permeability and clearance views of drug absorption: a commentary. J Pharmacokin et Biopharm 1995; 23:333–337.
7. S–X Wan, TA Sutfin, C Bärnhielm, CG Regårdh. Contribution of the intestine to the first-pass metabolism of felodipine in the rat. J Pharmacol Exp Ther 1989; 250:632–636.
8. CY Wu, LZ Benet, MF Hebert, SK Gupta, M Rowland, DY Gomez, VJ Wacher. Differention of absorption, first-pass gut and hepatic metabolism in man: studies with cyclosporine. Clin Pharmacol Ther 1995; 58:492–497.
9. J Samanen, G Wilson, PL Smith, C–P Lee, W Bondinell, T Ku, G Rhodes, A Nichols. Chemical approaches to improve the oral bioavailability of peptidergic molecules. J Pharm Pharmacol 1996; 48:119–125.
10. JC Kolars, WM Awni, RM Merion, PB Watkins. First-pass metabolism of cyclosporin by the gut. Lancet 1991; 338:1488–1490.
11. PS Burton, RA Conradi, NFH Ho, AR Hilgers, RT Borchardt. How structural features influence the biomembrane permeability of peptides. J Pharm Sci 1996; 85:1336–1340.

12. M Rowland, TN Tozer. Clinical Pharmacokinetics. 3rd ed. Baltimore: Williams & Wilkins, 1995:184–200.
13. MB Lande, NA Priver, ML Zeidel. Determinants of apical membrane permeabilities of barrier epithelia. Am J Physiol 1994; 267:C367–C374.
14. MB Lande, JM Donovan, ML Zeidel. The relationship between membrane fluidity and permeabilities to water, solutes, ammonia, and protons. J Gen Physiol. 1995; 106:67–84.
15. U Fagerholm, H Lennernäs. Experimental estimation of the effective unstirred water layer thickness in the human jejunum, and its importance in oral drug absorption. Eur J Pharm Sci 1995; 3:247–253.
16. D Meredith, CAR Boyd. Oligopeptide transport by epithelial cells. J Membr Biol 1995; 145:1–12.
17. E Krondahl, A Orzechowski, G Ekström, H Lennernäs. Rat jejunal permeability and metabolism of μ-selective tetrapeptides in gastrointestinal fluids from humans and rats. Pharm Res 1997; 14:1780–1785.
18. H Lennernäs. Human jejunal effective permeability and its correlation with preclinical drug absorption models. J Pharm Pharmacol 1997; 49:627–638.
19. F Thiebaud, T Tsuruo, H Hamada, MM Gottesman, I Pastan, MC Willingham. Cellular localization of the multi-drug resistance gene product P-glycoprotein in normal human tissues. Proc Natl Acad Sci USA 1987; 84:7735–7738.
20. A Tsuji, I Tamai. Carrier-mediated intestinal transport of drugs. Pharm Res 1996; 13:963–977.
21. JM Croop, M Raymond, D Haber, A Devault, RJ Arceci, P Gros, D Houseman. The three multidrug resistance (mdr) genes are expressed in a tissue-specific manner in normal human tissues. Mol Cell Biol 1989; 9:1346–1350.
22. PS Burton, RA Conradi, AR Hilgers, NFH Ho. Evidence for a polarized efflux system for peptides in the apical membrane of Caco-2 cells. Biochem Biophys Res Commun 1993; 190:760–766.
23. LZ Benet, C-Y Wu, MF Hebert, VJ Wacher. The importance of drug metabolism and antitransport processes: a paradigm shift in oral drug delivery. J Controlled Release 1996; 39:139–143.
24. IJ Hidalgo, J Li. Carrier-mediated transport and efflux mechanisms in Caco-2 cells. Adv Drug Deliv Rev 1996; 22:53–66.
25. R Sandström, A Karlsson, L Knutson, H Lennernäs. Jejunal absorption and metabolism of *R*/*S*-verapamil in humans. Pharm Res 1998; 15:856–862.
26. U Fagerholm, M Johansson, H Lennernäs. Comparison between permeability coefficients in rats and human jejunum. Pharm Res 1996; 13:1335–1341.
27. H Lennernäs, Ö Ahrenstedt, R Hällgren, L Knutson, M Ryde, LK Paalzow. Regional jejunal perfusion, a new in vivo approach to study oral drug absorption in man. Pharm Res 1992; 9:1243–1251.
28. L Knutson, B Odlind, R Hällgren. A new technique for segmental jejunal perfusion in man. Am J Gastroenterol 1989; 84:1278–1284.
29. H Lennernäs, U Fagerholm, Y Raab, B Gerdin, R Hällgren. Regional rectal

perfusion, a new in vivo approach to study rectal drug absorption in man. Pharm Res 1995; 12:426–432.
30. A Lindahl, E Krondahl, A-C Grudén, A-L Ungell, H Lennernäs. Is the jejunal permeability in rats age-dependent? Pharm Res 1997; 14:1278–1281.
31. FGJ Poelma, JJ Tukker. Evaluation of the chronically isolated intrajejunal loop in the rat for the study of drug absorption kinetics. J Pharm Sci 1987; 76:433–436.
32. E Lipka, H Spahn–Langguth, E Mutschler, GL Amidon. In vivo non-linear intestinal permeability of celiprolol and propranolol in conscious dogs. Evidence for intestinal secretion. Eur J Pharm Sci 1998; 6:75–81.
33. PDP Lundin, BR Weström, N Pantzar, BW Kalrsson. Bidirectional small intestinal permeability changes to different-sized molecules after HC-induced injury in the rat. Dig Dis Sci 1997; 42:677–683.
34. AS Hussain. Classifying your drug: The BCS guidance. In: GL Amidon, JR Robinson, RL Williams, eds. Scientific Foundations for Regulating Drug Product Quality. Alexandria, VA: AAPS Press, 1997:197–204.
35. LJ Lesko. Regulatory overview. In: GL Amidon, JR Robinson, RL Williams, eds. Scientific Foundations for Regulating Drug Product Quality. Alexandria; VA: AAPS Press, 1997:187–203.
36. RL Williams. In vitro bioequivalence standards. In: GL Amidon, JR Robinsson, RL Williams, eds. Scientific Foundations for Regulating Drug Product Quality. Alexandria, VA: AAPS Press, 1997:387–392.
37. H Lennernäs, I-D Lee, U Fagerholm, GL Amidon. A RTD analysis of the hydrodynamics within the human intestine during a regional single-pass perfusion: in vivo permeability estimation. J Pharm Pharmacol 1997; 49:682–686.
38. GL Amidon, PJ Sinko, D Fleisher. Estimating human oral fraction dose absorbed: a correlation using rat intestinal membrane permeability for passive and carrier-mediated compounds. Pharm Res 1988; 5:651–654.
39. R Sandström, H Lennernäs. Repeated oral administration of rifampicin decreases the jejunal permeability of *R*/*S*-verapamil in rats. Drug Metab Dispos 1999; 27:951–955.
40. A Lindahl, R Sandström, A–L Ungell, H Lennernäs. Concentration- and region-dependent intestinal permeability of fluvastatin in the rat. J Pharm Pharmacol 1998; 50:737–744.
41. HA Brasitus, K Dudeja. Regional differences in the lipid composition and fluidity of rat colonic brush-border membranes. Biochim Biophys Acta 1985; 819: 10–17.
42. WD Stein. Transport and Diffusion Across Cell Membranes. New York: Academic Press, 1986.
43. J Vonderscher, P Buri, J Deshusses, H Sucker. Absorption rate of drugs in rats—application of the improved modified Doluisio method to various classes of drugs. Acta Pharm Technol 1990; 36:133–138.
44. YK Pithavala, I Soria, CL Zimmerman. Use of the deconvolution principle in

the estimation of absorption and pre-systemic intestinal elimination of drugs. Drug Metab Dispos 1997; 25:1260–1265.
45. M Hu, GL Amidon. Passive and carrier-mediated intestinal absorption components of captopril. J Pharm Sci 1988; 77:1007–1011.
46. HK Han, DM Oh, GL Amidon. Cellular uptake mechanism of amino acid ester prodrugs in Caco-2/hPEPT1 cells overexpressing a human peptide transporter. Pharm Res 1998; 15:1382–1386.
47. H Lennernäs. Transcellular and paracellular transport mechanisms: consequences for bioavailability of peptides after oral dosing. In: S Frökjaer, L Christrup, P Krogsgard-Larsen, eds. Peptide and Protein Drug Delivery. Copenhagen: Munskgaard 1998;97–118.
48. H Lennernäs, K Palm, U Fagerholm, P Artursson. Comparison between active and passive drug transport in human intestinal epithelial (Caco-2) cells in vitro and human jejunum in vivo. Int. J Pharm 1996; 127:103–107.
49. M Hu, RT Borchardt. Mechanism of L-α-methyldopa transport through a monolayer of polarized human intestinal epithelial cells (Caco-2). Pharm Res 1990; 7:1313–1319.
50. B Steffansen, E–I Lepist, S Frökjaer, M Taub, H Lennernäs. Stability, metabolism and transport of D-ASP(OBZL)—a model prodrug with affinity for the oligopeptide transporter. Eur J Pharm Sci 1999; 8:67–73.
51. P Artursson, RT Borchardt. Intestinal drug absorption and metabolism in cell cultures: Caco-2 and beyond. Pharm Res 1997; 14:1655–1666.
52. VS Chadwick, SF Phillips, AF Hofmann. Measurements of intestinal permeability using low molecular weight polyethylene glycols (PEG 400). II. Application to normal and abnormal permeability states in man and animals. Gastroenterology 1977; 73:247–251.
53. DW Powell. Intestinal water and electrolyte transport. In: LR Johnson, ed. Physiology of the Gastrointestinal Tract, 3rd ed. New York: Raven Press, 1987: 1267–1306.
54. JL Madara, JS Trier. The functional morphology of the mucosa of the small intestine. In: LR Johnson, ed. Physiology of the Gastrointestinal Tract, 3rd ed. New York: Raven Press, 1994.
55. H Lennernäs, D Nilsson, S-M Aquilonius, Ö Ahrenstedt, L Knutson, LK Paalzow. The effect of L-leucine on the absorption of levodopa, studied by regional jejunal perfusion in man. Br J Clin Pharmacol 1993; 35:243–250.
56. B Abrahamsson, M Alpsten, M Hugosson, UE Jonsson, M Sundgren, A Svenheden, J Tolli. Absorption, gastrointestinal transit, and tablet erosion of felodipine extended-release (ER) tablets. J Pharm Res 1993; 10:709–714.
57. P Artursson, A-L Ungell, J–E Löfroth. Selective paracellular permeability in two models of intestinal absorption: cultured monolayers of human intestinal epithelial cells and rat intestinal segments. Pharm Res 1993; 10:1123–1129.
58. KKH Chan, A Buch, RD Glazer, VA John, WH Barr. Site-differential gastrointestinal absorption of benazepril hydrochloride in healthy volunteers. Pharm Res 1994; 11:432–437.

59. PJ Sinko, P Hu. Determination intestinal metabolism and permeability for several compounds in rats. Implications on regional bioavailability in humans. Pharm Res 1996; 13:108–113.
60. U Fagerholm, A Lindahl, H Lennernäs. Regional intestinal permeability in rats for compounds with different physico-chemical properties and transport mechanisms. J Pharm Pharmacol 1997; 49:687–690.
61. A–L Ungell, S Nylander, S Bergstrand, Å Sjöberg, H Lennernäs. Membrane transport of drugs in different regions of the intestinal tract of the rat. J Pharm Sci 1998; 87:360–366.
62. M Ashford, JT Fell. Colonic delivery of drugs. In: Current Status on Targeted Drug Delivery to the Gastrointestinal Tract. Capsugel Library, 1993.
63. M Mackay, I Williamson, J Hastewell. Cell biology of epithelia. Adv Drug Deliv Rev 1991; 7:313–338.
64. TT Kararli. Comparison of the gastrointestinal anatomy, physiology, and biochemistry of humans and commonly used laboratory animals. Biopharm Drug Dispos 1995; 16:351–380.
65. TY Ma, D Hollander, RA Erickson, H Troung, H Nguyen, P Krugliak. Mechanism of colonic permeation of inulin: is rat colon more permeable than small intestine? Gastroenterology 1995; 108:12–20.
66. D Hollander, S Koyama, V Dadufalza, DQ Tran, P Krugliak, T Ma, K-Y Ling. Polyethylene glycol 900 permeability of rat intestinal and colonic segments in vivo and brush border membrane vesicles in vitro. J Lab Clin Med 1989; 113: 505–515.
67. P Krugliak, D Hollander, CC Schlaepfer, H Nguyen, TY Ma. Mechanisms and sites of mannitol permeability of small and large intestine in the rat. Dig Dis Sci 1994; 39:796–801.
68. T Kimura, K Sudo, Y Kanzaki, K Miki, Y Takeichi, Y Kurosaki, T Nakayama. Drug absorption from large intestine: physicochemical factors governing drug absorption. Biol Pharm Bull 1994; 17:327–333.
69. N Jezyk, W Rubas, GM Grass. Permeability characteristics of various intestinal regions of rabbit, dog, and monkey. Pharm Res 1992; 9:1580–1586.
70. M Narawane, SK Podder, H Bundgaard, VHL Lee. Segmental differences in drug permeability, esterase activity and ketone reductase activity in the albino rabbit intestine. J Drug Target 1992; 1:7–17.
71. MD Levitt, T Aufderheide, CA Fetzer, JH Bond, DG Levitt. Use of carbon monoxide to measure luminal stirring in the rat gut. J Clin Invest 1984; 74: 2056–2064.
72. H Lennernäs. Does fluid flow across the intestinal mucosa affect quantitative oral drug absorption? Is it time for a reevaluation? Pharm Res 1995; 12:1573–1582.
73. U Fagerholm, D Nilsson, L Knutson, H Lennernäs. Jejunal permeability in humans in vivo and rat in situ: investigation of molecular size selectivity and solvent drag. Acta Physiol Scand 1999; 165:1–9.
74. WL Chiou, A Barve. Linear correlation of the fraction of oral dose absorbed of 64 drugs between humans and rats. Pharm Res 1998; 15:1792–1795.

75. YL He, S Murby, G Warhurst, L Gifford, D Walker, J Ayrton, R Eastmond, M Rowland. Species differences in size discrimination in the paracellular pathway reflected by oral bioavailability of poly(ethylene glycol) and D-peptides. J Pharm Sci 1998; 87:626–633.
76. MM Gottesman, I Pastan. Biochemistry of multidrug resistance mediated by the multidrug transporter. Annu Rev Biochem 1993; 62:385–427.
77. D Lautier, Y Carnitrot, RG Deeley, SPC Cole. Multidrug resistance mediated by the multidrug resistance protein (MRP) gene. Biochem Pharmacol 1996; 52: 967–977.
78. GL Scheffer, PLJ Wijngaard, MJ Flens, MA Izquierdo, ML Slovak, HM Pinedo, CJ Meijer, HC Clevers, RJ Scheper. The drug resistance-related protein LRP is the human major vault protein. Nat Med 1995; 1:578–582.
79. PK Dudeja, KM Anderson, JS Harris, L Buckingham, JS Coon. Reversal of multidrug resistance phenotype by surfactants: relationship to membrane lipid fluidity. Arch Biochem Biophys 1995; 319:309–315.
80. CR Leveille–Webster, IM Arias. The biology of the P-glycoproteins. J Membr Biol 1995; 143:89–102.
81. F Thiebaut, T Tsuruo, H Hamada, MM Gottesman, I Pastan, MC Willingham. Cellular localization of the multidrug-resistance gene product P-glycoprotein in normal human tissues. Proc Natl Acad Sci USA 1987; 84:7735–7738.
82. AH Schinkel, E Wagenaar, CAAM Mol, L van Deemter. P-glycoprotein in the blood–brain barrier of mice influences the brain penetration and pharmacological activity of many drugs. J Clin Invest 1996; 97:2517–2524.
83. C Cordon-Cardo, JP O'Brien, D Casals, L Rittman–Grauer, JL Biedler, MR Melamed, JR Bertino. Multidrug-resistance gene (P-glycoprotein) is expressed by endothelial cells at blood–brain barrier sites. Proc Natl Acad Sci USA 1989; 86:695–698.
84. J Karlsson S-M Kuo, J Ziemniak, P Artursson. Transport of celiprolol across human intestinal epithelial (Caco-2) cells: mediation of secretion by multiple transporters including P-glycoprotein. Br J Pharmacol 1993; 110:1009–1016.
85. A Sellig. How does P-glycoprotein recognize its substrates? Int J Clin Pharmacol Ther 1998; 36:50–54.
86. G Klopman, LM Shi, A Ramu. Quantitative structure–activity relationship of multidrug resistance reversal agents. Mol Pharmacol 1997; 52:323–334.
87. I Sugawara, S Akiyama, RJ Scheper, S Itoyama. Lung resistance protein (LRP) expression in human normal tissues in comparison with that of MDR1 and MRP. Cancer Lett 1997; 112:23–31.
88. M Kavallaris. The role of multidrug resistance-associated protein (MRP) expression in multidrug resistance. Anticancer Drugs 1997; 8:17–25.
89. RG Deeley, SPC Cole. Function, evolution and structure of multidrug resistance protein (MRP). Semin Cancer Biol 1997; 8:193–204.
90. SPC Cole, RG Deeley. Multidrug resistance mediated by the ATP-binding cassette transporters protein MRP. Bioessays 1998; 20:931–940.
91. T Fujita, H Yamada, M Fukuzumi, A Nishimaki, A Yamamoto, S Muranishi.

Calcein is excreted from the intestinal mucosal cell membrane by the active transport system. Life Sci 1997; 60:307–313.
92. H Saitoh, H Fujisaki, BJ Aungst, K Miyazaki. Restricted intestinal absorption of some beta-lactam antibiotics by an energy-dependent efflux system in rat intestine Pharm Res 1997; 14:645–649.
93. H Saitoh, C Gerard, BJ Aungst. The secretory intestinal transport of some beta-lactam antibiotics and anionic compounds: a mechanism contributing to poor oral absorption. J Pharmacol Exp Ther 1996; 278:205–211.
94. M Kool, M de Haas, GL Scheffer, RJ Scheper, MJ van Eijk, JA Juijn, F Baas, P Borst. Analysis of expression of cMOAT (MRP2), MRP3, MRP4, and MRP5, homologues of the multidrug resistance-associated protein gene (MRP1), in human cancer cell lines. Cancer Res 1997; 57:3537–3547.
95. U Wetterwich, LH Spahn, E Mutschler, B Terhaag, W Rosch, P Langguth. Evidence for intestinal secretion as an additional clearance pathway of talinolol enantiomers: concentration- and dose-dependent absorption in vitro and in vivo. Pharm Res 1996; 13:514–522.
96. SM Kuo, BR Whitby, P Artursson, JA Ziemniak. The contribution of intestinal secretion to the dose-dependent absorption of celiprolol. Pharm Res 1994; 11: 648–653.
97. R Sandström, A Karlsson, H Lennernäs. The absence of stereoselective P-glycoprotein mediated transport of *R*/*S*-verapamil across the rat jejunum. J Pharm Pharmacol 1998; 50:729–735.
98. G Mikus, M Eichelbaum, C Fischer, S Gumulka, U Klotz HK Kroemer. Interaction of verapamil and cimetidine: stereochemical aspects of drug metabolism, drug disposition and drug action. J Pharmacol Exp Ther 1990; 253:1042–1048.
99. EG Schuetz, WT Beck, JD Schuetz. Modulators and substrates of P-glycoprotein and cytochrome P4503A coordinately up-regulate these proteins in human colon carcinoma cells. Mol Pharmacol 1996; 49:311–318.
100. B Greiner, M Eichelbaum, P Fritz, HP Kreichgauer, O von Richter, J Zundler, HK Kroemer. The role of intestinal P-glycoprotein in the interaction of digoxin and rifampin. J Clin Invest 1999; 104:147–153.
101. KS Lown, JC Kolars, M Ghosh, P Schmiedlin-Ren, PB Watkins. Induction of MDR1 expression in normal rat and human intestine in vivo. Gastroenterology 1996; 110: A344.
102. UI Schwarz, T Gramatté, J Krappweis, A Berndt, R Oertel, O von Richter, W Kirch. Unexpected effect of verapamil on oral bioavailability of the beta-blocker talinolol in humans. Clin Pharmacol Ther 1999; 65:283–290.
103. USH Svensson, R Sandström, Ö Carlborg, H Lennernäs M Ashton. High in situ rat intestinal permeability of artemisin unaffected by multiple dosing and with no evidence of P-glycoprotein involvement. Drug Metab Dispos 1999; 27: 227–232.
104. P Augustijns, A D'Hulst, J Van Daele, R Kinget. Transport of artemisin and sodium artesunate in Caco-2 intestinal epithelial cells. J Pharm Sci 1996; 85: 577–579.

105. A Sparreboom, AJ van Mayer, AH Schinkel, JW Smit, DK Meijer, P Borst, WJ Nooijen, JH Beijnen, O van Tellingen. Limited oral bioavailability and active epithelial excretion of paclitaxel (Taxol) caused by P-glycoprotein in the intestine. Proc Natl Acad Sci USA 1997; 94:2031–2035.
106. R Sandström, L Knutson, T Knutson, B Jansson, H Lennernäs. The effect of ketoconazole on jejunal permeability and CYP 3A4 metabolism of *R*/*S*-verapamil in humans. Br J Clin Pharmacol 1999; 48:180–189.
107. VD Makhey, A Guo, DA Norris, P Hu, J Yan, PJ Sinko. Characterization of the regional intestinal kinetics of drug efflux in rat and human intestine and in Caco-2 cells. Pharm Res 1998; 15:1160–1167.
108. I de Waziers, PH Cugenec, CS Yang, JP Lerous, PH Beaune. Cytochrome. P450 isoenzymes, epoxide hydrolase and gluthathione transferase in rat and human hepatic and extrahepatic tissues. J Pharmacol Exp Ther 1990; 253:387–394.
109. MF Paine, M Khalighi, JM Fisher, DD Shen, KL Kunze, CL March, JD Perkins, KE Thummel. Characterization of interintestinal and intraintestinal differences in human CYP 3A-dependent metabolism. J Pharmacol Exp Ther 1997; 283: 1552–1562.
110. JC Kolars, RP Schmiedlin, W Dobbins, J de Schuetz, SA Wrighton, P Watkins. Heterogenity of cytochrome P450IIIA expression in rat gut epithelia. Gastroenterology 1992; 102:1186–1198.
111. Q-Y Zhang, J Wikoff, D Dunbar, L Kaminsky. Characterization of rat small intestinal cytochrome P450 composition and inducibility. Drug Metab Dispos 1996; 24:322–328.

7
Human Perfusion Studies

Hans Lennernäs
Uppsala University, Uppsala, Sweden

I. INTRODUCTION

The extent of absorption (*fa*) can be defined in terms of all processes, from the dissolution of the solid dosage form to the uptake of the drug into the intestinal tissue (i.e., transport across the apical membrane of the enterocyte). This general definition for the extent of absorption does not include metabolic first-pass effects in the gut or liver or biliary excretion in the liver (E_G and E_H) (1,2). The bioavailability (F) of a compound is a consequence of all these processes, as shown in Eq. (1).

$$F = fa\ (1 - E_G)\ (1 - E_H) \tag{1}$$

More explicitly, the extent of drug absorption *fa* from the small and large intestine takes into account the following factors: dose/dissolution ratio, chemical degradation–metabolism in the lumen, complex binding in the lumen, intestinal transit, and effective permeability (P_{eff}) across the intestinal mucosa (1,2). Drug transport across the intestinal barrier occurs by passive diffusion or active transcellular transport. Frequently, the P_{eff} is considered to be the rate-limiting step in the overall absorption process. However, with the advent of several new pharmacological targets in drug discovery, for instance, intracellularly localized receptors, it is expected that more lipophilic compounds will be developed (3). This means that drug disintegration and dissolution in the gastrointestinal fluids will be a crucial step in the design, development and optimization of a solid oral drug product. Nevertheless, it will be necessary

to establish that uptake into the intestinal tissue is not a limitation to oral bioavailability. The limited access to direct measurements of in vivo drug absorption means that not all important factors affecting drug absorption in the gut lumen and in the enterocyte membrane are known (1,4).

Our human intestinal perfusion approach has been useful for generating knowledge about the direct in vivo membrane transport (1,5). This clinical tool also allows investigation of the following research issues in humans: (a) the first-pass effect of drugs in the liver, (b) drug metabolism in intestinal tissue (by measurement of metabolite[s] in the outlet perfusate), (c) in vivo dissolution of drugs, (d) local pharmacological studies of drugs, (e) nutrient absorption, (f) biological mechanisms of different gastrointestinal diseases, (g) food–drug interactions, and (h) intestinal secretion of drugs and endogenous compounds (1,5–10).

The goal of this chapter is to demonstrate the usefulness of direct in vivo investigations in humans of important biopharmaceutical and pharmacokinetic properties, such as dissolution, intestinal permeability, mechanisms of drug transport, and metabolism.

II. MEASURING DRUG ABSORPTION AND BIOAVAILABILITY IN HUMANS

The most common way to investigate drug absorption–bioavailability in humans today is to perform standard pharmacokinetic studies. More elaborate methods include various intubation techniques, remote-controlled capsules, and pharmacoscintigraphy studies. Commonly used pharmacokinetic approaches to evaluate rate and extent of drug absorption have been summarized (11,12). All these methods are based on plasma concentration–time data and cannot be used to explicitly investigate the transport rate across intestinal epithelium (permeability) or drug dissolution in vivo. In contrast, single-pass perfusion of an intestinal segment is an approach that makes it possible to perform mechanistic investigations of drug absorption in humans.

Clinical investigations with direct measurements of in vivo dissolution are rare. In humans various approaches have been used. The most common way is to calculate the in vivo dissolution by using the deconvolution method of plasma concentrations after oral administration of solution and solid dosage forms. Other ways to investigate these processes are to utilize pharmacoscintigraphy and gastroscopic techniques (4).

A. The Validation of Intestinal Perfusion Techniques in Humans

A recently developed in vivo drug absorption technique for single-pass perfusion experiments in human subjects, the Loc-I-Gut, has been used for permeability investigations (5,13). This in vivo perfusion technique requires a 175-cm–long, sterile polyvinyl tube (external diameter 5.3 mm) with six inner channels. At the distal end of the tube there are two elongated latex balloons, placed 10 cm apart (5,13). The tube is inserted and positioned in the human proximal jejunum under the guidance of a fluoroscopic technique. This procedure is performed in the fasted state (10-h fasting). Air (24–32 mL) is used to inflate the two balloons, creating a 10-cm–long jejunal segment (Fig. 1). The positioning of the tube usually takes 1 h, after which the single pass perfusion at a rate of between 2.0 and 3.0 mL/min is started. A more detailed description of the positioning procedure and the perfusion technique can be found elsewhere (5,13). With Loc-I-Gut it has been possible to perform accurate and direct in vivo determinations of the local absorption rate in humans

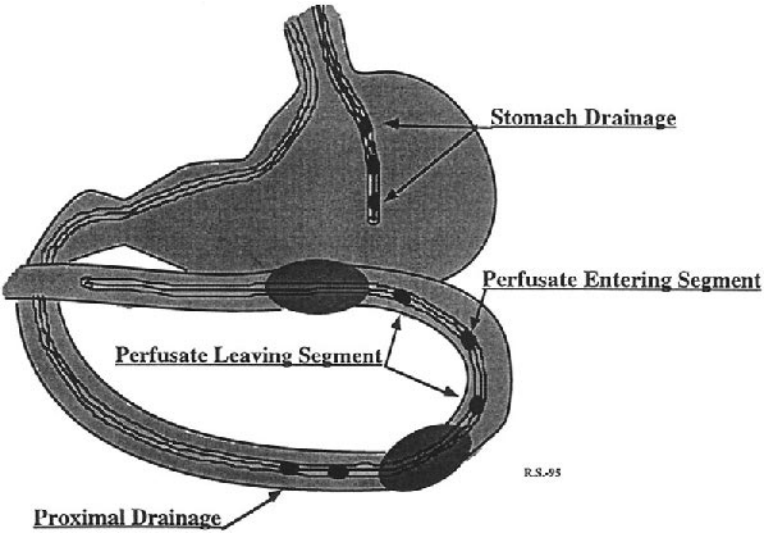

FIG. 1 The multichannel tube system with double balloons allowing segmental jejunal perfusion. The balloons are filled with air when the proximal balloon has passed the ligament of Treitz. Gastric suction is obtained by a separate tube. Polyethylene glycol (^{14}C-PEG 4000) is used as a volume marker.

(i.e., P_{eff} [cm/s]; see Fig. 1) (5,13). The hydrodynamics in the perfused segment are best described by a well-stirred model according to residence time distribution analysis (14). The intestinal effective permeability (P_{eff}) is calculated using Eq. (2) (5,14):

$$P_{eff} = \frac{(C_{in} - C_{out})Q_{in}}{C_{out}\,(2\pi\, rL)} \tag{2}$$

The surface of the cylinder ($2\pi\, rL$) of the jejunal segment is estimated from the intestinal radius ($r = 1.75$ cm) and the length ($L = 10$ cm) of the segment. That this estimate of the human jejunal radius is accurate for the perfused segment has been shown by a recently performed fluoroscopic investigation (Knutson et al., personal communication).

When single-pass perfusion experiments are performed at a perfusion rate of 2.0–3.0 mL/min, the recovery of the nonabsorbable volume marker polyethylene glycol (PEG) 4000 in the perfusate leaving the intestinal segment is more than 95% (1,5). This indicates that the intestinal tissue is intact, because it is generally viewed that the quantitative uptake of large hydrophilic molecules is diagnostic for decreased tissue viability and integrity in vivo (15). Whether the motility is altered by the presence of two balloons, and whether the blood supply to the perfused segment is influenced has also been discussed (16–19). It is known that distension of the canine intestine at a pressure of 20 mmHg does not reduce the capillary area open for tissue blood flow (19). However, an increase in the intraluminal pressure to 100 mmHg significantly affected capillary blood flow in the mesenteric circulation in same dogs (19). As a comparison, the regional perfusion jejunal segment with two balloons in humans—each with a pressure of about 20 mmHg—shows a very rapid absorption of both passively and actively transported high-permeability compounds (such as D-glucose, antipyrine, L-leucine, L-dopa, or carbamazepine) (1). The absorption of D-glucose (a marker for active absorption) and antipyrine (a marker for passive transcellular absorption and mesenteric blood flow) was stable over time, which indicates that no progressive changes in viability occurred (1,5). From these observations, we concluded that no major change in blood flow exists, for it has been reported that the absorption of antipyrine is sensitive to changes in mesenteric blood flow (1,5).

The mass balance of the transport of drugs and other compounds across the jejunal barrier during the single-pass perfusion cannot be directly assessed because it is not possible to measure the concentration of a drug in the cytosol of the enterocyte or in the vena porta in humans. Instead, the peripheral venous

blood has been used as the in vivo reference on the receiver side. In our first study we clearly demonstrated that the peripheral plasma concentration is about 100 times less than the luminal concentration for antipyrine (5). These data suggest that sink conditions apply: antipyrine is a drug with a small volume of distribution—approximately 40 L in a 70-kg person—and is assumed to be evenly distributed in the body (5). Furthermore, the liver extraction of fluvastatin—a CYP2C9 substrate—was identical following jejunal perfusion and intravenous infusion, which also supports the hypothesis that mass balance between disappearance from the lumen and appearance in blood exists for drugs investigated with the Loc-I-Gut system (1,6). Finally, we have established an excellent correlation between the measured jejunal P_{eff} and extent of intestinal absorption for low-, intermediate-, and high-permeability drugs (Fig. 2) (1,20). A major advantage with this clinical tool is that it is possible to

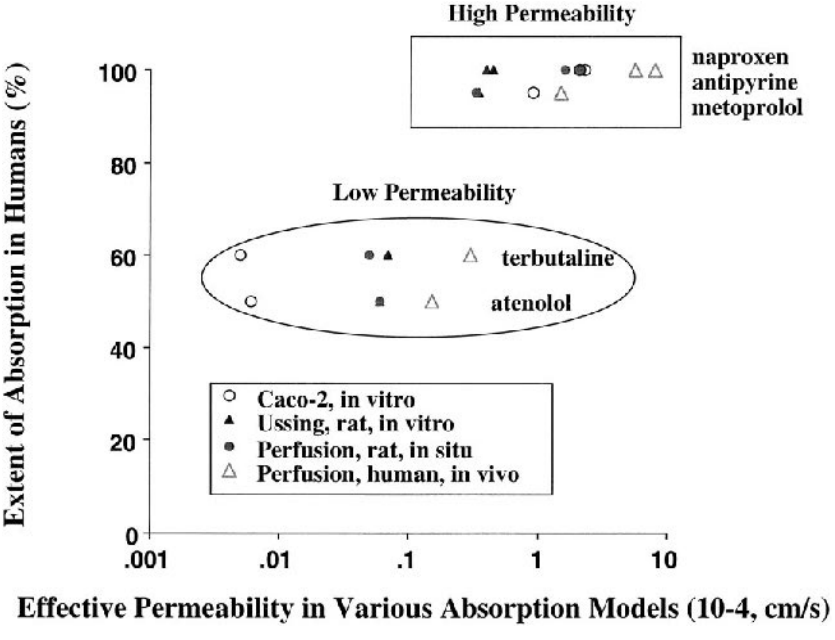

FIG. 2 The effective permeability of five drugs with different physicochemical properties in the Caco-2 monolayer, rat jejunal segment in the Ussing chamber, the perfused rat jejunum, and the human jejunum.

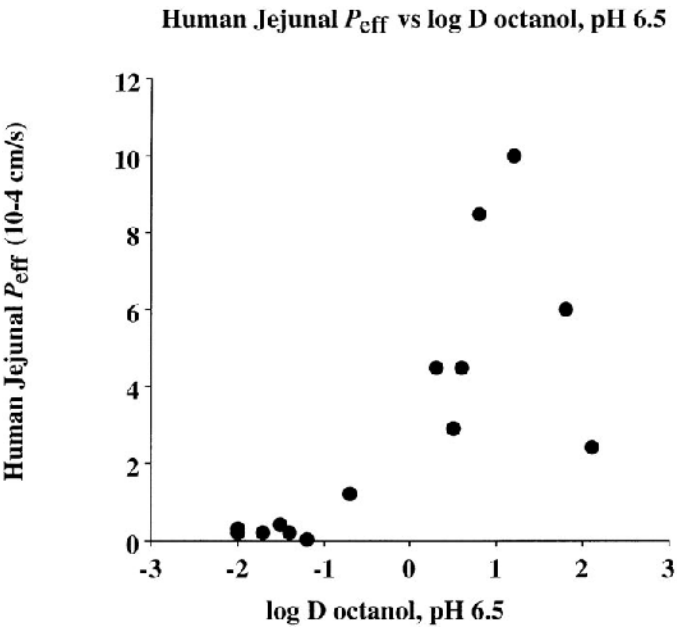

FIG. 3 The relation between human effective permeability (in vivo) and log *D* (octanol/phosphate buffer at pH 6.5) for passively absorbed drugs.

measure the intestinal transport and metabolism of drugs and their metabolites immediately adjacent to the tissue where these processes occur (10).

III. PERMEABILITY DETERMINATIONS

In Fig. 2 the relations between human in vivo P_{eff} values and their corresponding data determined in commonly used preclinical permeability models such as Caco-2 monolayer, single-pass perfusion in rat jejunum, and excised rat jejunal segment mounted in a diffusion chamber (Ussing model) are depicted (20–23). The permeability of passively transported compounds are predicted with a particularly high degree of accuracy. Because of the relative large interlaboratory variability in the permeability estimates, a set of reference drugs must be used to be able to compare P_{eff} values among different laboratories. Otherwise, only the rank order can be compared. The reference values make it possible to compensate for both the inter- and as well intralaboratory varia-

tions that exist for preclinical permeability models. Special care must be taken for drugs with a carrier-mediated transport mechanism, for which a scaling factor must be used.

In our work with the Biopharmaceutical Classification System (BCS) for immediate-release oral products we have determined the P_{eff} for a large number of drugs (1,20,23–27). The drugs for which we have performed permeability measurements represent several pharmacological classes and are shown in Table 1. The relation between measured human jejunal P_{eff} values and the extent of intestinal absorption (*fa*) is characterized by a steep curve in the permeability range $0.4–1.2 \times 10^{-4}$ cm/s (Fig. 2). The BCS is based on the qualitative variables solubility (*S*) and permeability (P_{eff})(2). The long-term goal of the human permeability project is to obtain quantitative values of the jejunal effective permeabilities (P_{eff}). In combination with solubility data, the P_{eff} enables the drug to be classified according to the BCS. The major advantage of the BCS is that, by identifying the key variables (*S* and P_{eff}) controlling drug absorption, it will be possible to simplify drug regulation (28–30) of immediate-release products for oral administration.

The interindividual variability in the estimate of the human jejunal P_{eff} was reduced for high-permeability drugs when antipyrine (a high-permeability drug that is absorbed by passive transcellular diffusion) was used as a reference marker. However, the interindividual variability was not decreased for low-permeability drugs. This observation is in accordance with the fact that intestinal absorption of the high-permeability drugs and antipyrine is influenced by the same factors. A plausible reason why the interindividual variability for low-permeability drugs was not affected is probably due to the fact that their transport is influenced by other factors.

TABLE 1 The Effective Jejunal Permeability Has Been Determined for the Following Drugs by Single-Pass Perfusion Experiments at Uppsala University. These Drugs Have Then Been Classified According to the Biopharmaceutics Classification System (BCS)

Cardiovascular system agents: metoprolol, atenolol, propranolol, lisinopril, α-methyldopa, losartan, and verapamil
NSAIDS: naproxen and ketoprofen
CNS agents: desipramine and carbamazepine
Anti-infective: amoxicillin
Urinary tract system agents: hydrochlorotiazide, furosemide, and amiloride
Gastroenterological agent: cimetidine

The jejunal P_{eff}s for 22 compounds with diverse structures have been correlated with both experimentally determined lipophilicity values and calculated molecular descriptors (31). Lipophilicity values were obtained using the pH-metric technique. Both pK_a values, log P and, if necessary, log P_{ion} values were determined. With these values log D values were calculated at pH 5.5, 6.5, and 7.4. Of these 22 compounds some were omitted because they are actively or paracellularly transported. The remaining compounds were included in a multivariate analysis to derive models that correlate passive intestinal permeability with physicochemical descriptors. Figure 3 demonstrates the relation between human jejunal P_{eff} for the passively transported drugs and their corresponding log $D_{6.5}$ values. The best model, based on 13 passively transcellularly transported compounds, used the variables HBD (number of hydrogen bond donors), PSA (polar surface area) and either log $D_{5.5}$ or log $D_{6.5}$ (distribution coefficient at pH 5.5 or 6.5, respectively). A good predictive model for human in vivo P_{eff} was also obtained using only theoretical parameters. Finally, it is possible to predict passive intestinal membrane diffusion in vivo for compounds that fit within the defined property space. However, these models are not applicable for predictions of effective in vivo human permeability for peptides, polysaccharides, or other compounds that do not fit into the defined property space (31).

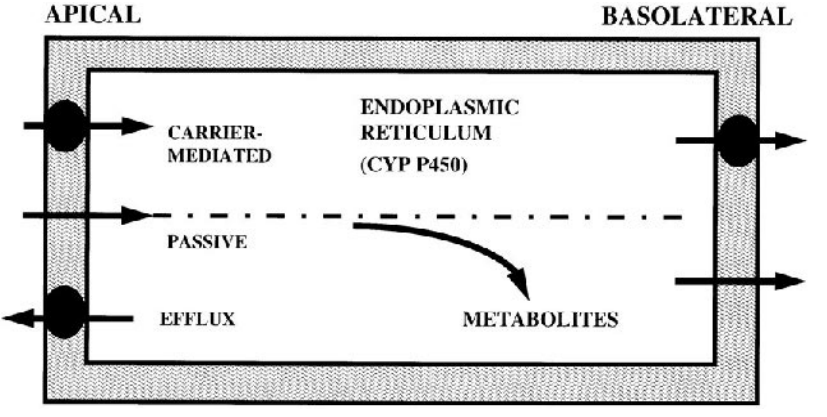

FIG. 4 An illustration of the transport of compounds across the intestinal membranes and how the intracellularly formed metabolites may interact with the cellular transport processes.

IV. INTESTINAL TRANSPORT AND METABOLISM IN VIVO IN HUMANS

Figure 4 illustrates the rather complex interplay that seems to exist during intestinal absorption of drugs between various processes, such as passive diffusion, carrier-mediated transport (in both directions), metabolism, and formed metabolites that may interact with efflux–metabolism.

A drug molecule enters the enterocyte by transport across the apical membrane, which for passively transported drugs is considered to be the rate-limiting step to intestinal transport (32). Membrane efflux proteins, such as P-glycoprotein, are located in the apical enterocyte (33). Metabolism by the cytochrome P450 (CYP) enzymes occurs inside the enterocyte, and the formed metabolites may also be substrates for any efflux protein. For carrier-mediated transported compounds, the carrier may be available at the basolateral as well as the apical membrane.

The gut wall metabolism of drugs (by CYP3A4) has been reported to be a significant part of the total first-pass effect following oral administration of drugs such as verapamil, midazolam, felodipine, and cyclosporine (34–37). It has been suggested that there is a considerable overlap in substrate specificity between the CYP3A enzymes and P-glycoprotein (P-gp), which further suggests that these two biological processes can cooperate to protect the organism from potentially toxic xenobiotics in the intestine, as well as in other tissues (efflux of drugs and metabolites may be considered as a phase-III process) (38–39). A hypothesis for the function of P-glycoprotein in the intestine is that it slows down the absorption rate (apical recycling), thereby reducing the concentration of the drug in the cytosol of the enterocytes. Accordingly, it may decrease the risk of enzymatic saturation of the intracellularly localized CYP3A enzymes (39). The tissue distribution of P-glycoprotein and CYP3A has been reported to be similar, which suggested that the expression of the two are linked in some way (38). However, in a further study of the expression of both CYP3A and P-gp in human enterocytes, no correlation between the tissue levels of CYP3A and P-gp was found (40). The same absence of correlation has been seen for the concentrations of CYP3A in the intestine compared with CYP3A in the liver (41). This indicates that the regulation of the expression of the enzyme and of the transport protein is not directly linked, even though the same drug can induce the expression of both these biological proteins. For example, rifampin has been reported to induce the expression of P-glycoprotein in the intestine and the metabolism in both the intestine and liver (36,42). There is only one human study in which the expression of P-glycopro-

tein in the intestine has been shown to influence the bioavailability of a drug (40). In that study, when cyclosporine was given to kidney transplant patients, P-glycoprotein expression contributed 17% of the variability in the apparent oral clearance of cyclosporine (40). In animal studies, the oral bioavailability of paclitaxel (Taxol) was higher in mice lacking both genes for *mdrla*, a gene coding for the intestinal P-glycoprotein, than in the wild-type mice (43). Some cooperation has also been found between P-glycoprotein transport and CYP3A metabolism of cyclosporine in an in vitro cell culture (Caco-2 monolayer) (44). However, it is unclear if the interplay between P-glycoprotein efflux and intracellular metabolism of CYP3A is of any clinical importance for other drugs with similar substrate specificity for these proteins. Accordingly, more in vivo pharmacokinetic–biopharmaceutic studies are needed to better understand the clinical relevance of the P-glycoprotein efflux mechanism.

In a human perfusion study with an open-perfusion technique, intestinal secretion of talinolol (a P-glycoprotein substrate) was reported (45). Other in vivo and in vitro studies have presented evidence that intestinal secretion is the reason behind the concentration- and dose-dependent absorption of talinolol (46). By using the Loc-I-Gut technique we have performed several single-pass perfusion studies in human jejunum with *R*/*S*-verapamil at different luminal concentrations. Verapamil is a lipophilic model drug (log *D* 2.7, octanol/H_2O; pH 7.4; MW 455 Da) that has been extensively used as a model substrate for P-glycoprotein(s) in cancer cells. *R*/*S*-Verapamil was chosen as model drug for three reasons: (a) it is a well-known substrate for P-glycoprotein; (b) it is metabolized to a major metabolite (*R*/*S*-norverapamil) by CYP3A4; and (c) it has a well-established stereoselective first-pass metabolic extraction (10,47). We have measured the jejunal P_{eff} of each enantioner of verapamil at 4.0, 40, 120, and 400 mg/L (of the racemate) (10,47). A luminal concentration of 400 mg/L is expected to be achieved in the upper part of the small intestine after oral administration of a 100-mg dose of verapamil in an immediate-release dosage form. The remaining concentrations represent decreased fractions of the dose left to be absorbed. The human jejunal P_{eff} increased with an increasing concentration of *R*/*S*-verapamil in the perfused intestinal segment. This is consistent with a saturable efflux mechanism mediated by P-glycoprotein located in the human jejunal epithelium. Furthermore, there was no difference between the *R*- and *S*-form of verapamil at any luminal concentration. This suggests that the efflux transport, most likely mediated by *P*-glycoprotein, cannot discriminate between the *R*- and *S*-forms of verapamil. The P_{eff} values for both enantioners at each of the concentrations (4.0, 40, 120, and 400 mg/L) were 2.5×10^{-4}; 4.7×10^{-4}; 5.5×10^{-4}; and 6.7×10^{-4} cm/s, respectively.

It is also interesting to note that the measured human jejunal P_{eff} (in vivo) was high enough at all four perfusate concentrations ($> 2.0 \times 10^{-4}$ cm/s) to predict complete intestinal absorption following oral dosing. In addition, ketoconazole (a well-known inhibitor of CYP3A4 metabolism and a P-glycoprotein modulator) did not enhance the P_{eff} of *R*/*S*-verapamil when they were coperfused through the human jejunal segment (*R*/*S*-verapamil at 120 mg/L and ketoconazole at 40 mg/L). However, in the same study we confirmed that CYP3A4 metabolism was affected, which suggests that ketoconazole is less potent as a P-glycoprotein than as a CYP3A4 inhibitor in humans (10,47).

The relative contributions of CYP3A4 to the presystemic metabolism in the gut and liver differ (40). For instance, cyclosporine has been reported to be mostly dependent on hepatic CYP3A4, whereas the intestinal CYP3A4 metabolism is crucial for the first-pass extraction of felodipine (37). These results might be due to factors other than the 3A4 enzymatic activity: (a) other CYP3A enzymes may be differently expressed in the intestine and the liver, (b) the functional role of P-glycoprotein as a transport barrier or apical recycling mechanism may vary with drug. The difference might also be due to a yet unrecognized efflux protein that contributes to the reported variability. In the present human jejunal perfusion study with the Loc-I-Gut technique, the liver extractions (E_h) were 0.63 $\pm$ 0.14 and 0.79 $\pm$ 0.16 for *R*- and *S*-verapamil, respectively. The estimated extractions in the gut wall (E_g) were 0.49 $\pm$ 0.18 and 0.68 $\pm$ 0.19 for *R*- and *S*-verapamil, respectively. The total first-pass extractions (calculated as $1 - F$) estimated from the whole jejunal perfusion experiment were 0.82 $\pm$ 8.2 and 0.94 $\pm$ 0.05 for *R*- and *S*-verapamil, respectively (47). Our perfusion data in humans confirm previously reported data that gut wall metabolism of CYP3A4 substrates contribute significantly to the total first-pass effect of drugs after oral administration (36,47). The biopharmaceutical–pharmacokinetic data obtained by single-pass perfusion of the human jejunum strengthen the earlier conclusions, because in the perfusion studies the extent of intestinal absorption [see *fa* in Eq. (1)] is estimated, resulting in a more accurate gut wall extraction value (E_G) for use in Eq. (1). In a further jejunal perfusion study in humans, the contribution of the intestine to the total first-pass effect was negligible for fluvastatin (a CYP2C9 substrate), suggesting that it is mainly CYP3A4 substrates that are metabolized in the gut wall (6,47).

In the perfusion study we also found an increased absorption rate of *R*/*S*-verapamil into the systemic circulation (by deconvolution) when ketoconazole was added to the perfusate, a finding that can be explained by inhibited metabolism in the human enterocyte. When the extraction values in the gut

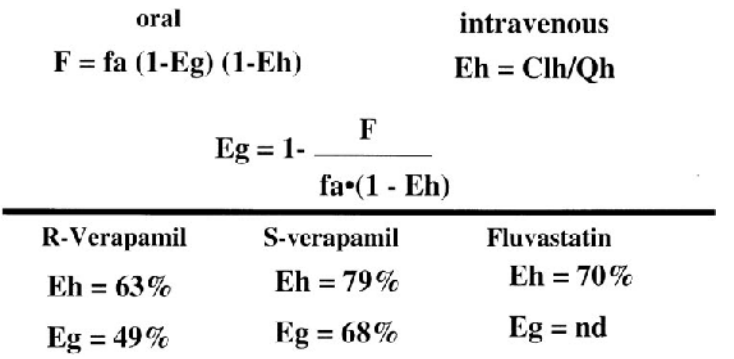

FIG. 5 The first-pass extraction in the intestine and the liver in humans of drugs that are metabolized with different enzyme systems. *R/S*-verapamil is metabolized mainly by CYP3A4 and fluvastatin by CYP2C9.

wall and the liver were separated [using Eq. (1)], it was clear that the gut wall contributed significantly to the first-pass elimination of both *R*- and *S*-verapamil (Fig. 5).

The main results of the present study in humans clearly demonstrate that the potent CYP3A4 inhibitor ketoconazole affects the presystemic metabolism of both *R*- and *S*- verapamil, but to different degrees. In addition, based on the unchanged P_{eff} of *R*/*S*-verapamil, it appears that ketoconazole did not influence the P-glycoprotein–mediated efflux of *R*/*S*-verapamil in the human enterocyte, indicating that ketoconazole is not a potent P-glycoprotein inhibitor.

VI. A NOVEL APPROACH FOR DIRECT INVESTIGATIONS OF IN VIVO DRUG DISSOLUTION IN THE HUMAN INTESTINE

We previously developed a novel approach for direct determination of the in vivo dissolution of drugs in humans (4,7). The major driving force for development of this human method was the need for further improved understanding of the in vivo dissolution of low-solubility compounds. Disintegration and dissolution of drugs is a crucial consideration in the drug development process, and is predicted to become even more important as more lipophilic drug candidates are pursued (3). Until recently, the most common approach

to investigate the in vivo dissolution rate has been to apply indirect methods, such as deconvolution of plasma profiles (4). It is also important to improve our understanding of the complex physicochemical composition of the gastrointestinal fluids and its intra- and interindividual variability. We have, therefore, characterized the content in these two regions of the gastrointestinal tract (48). The reported values showed the interindividual variability in gastrointestinal factors, such as bulk pH, osmolality, and the concentrations of electrolytes, proteins, and bile acids during fasting conditions. In addition, we examined potential gender differences for these physicochemical properties of the gastrointestinal fluids. In total we intubated 24 healthy volunteers, 12 women and 12 men, and fluids from the stomach and upper jejunum were collected separately (48).

The physicochemistry of the gastrointestinal fluid is complex and depends on the nutritional status (49). Disintegration and dissolution is started in the stomach and the proximal small intestine and is expected to show large inter- and intraindividual variability. The settings of in vitro dissolution standards must be done on the basis of the knowledge of the conditions existing in vivo in humans. The intubation studies showed that the content of the stomach and proximal jejunum varied significantly in all measured entities, except the total concentration of proteins. In Fig. 6 osmolality and the total concentration of bile acids are shown from both stomach and proximal jejunum for both men and women. Furthermore, we observed a pronounced day-to-day variation in the same individual, which may contribute to the large intraindividual variability seen for some oral drug products. By contrast, gender differences appear to be unimportant (48).

A new method for in vivo dissolution was evaluated by perfusing a semiopen segment localized in the proximal human jejunum (48). In these perfusion experiments only the distal balloon is inflated (see Fig. 1). In both studies we used carbamazepine as a model drug (4,7). Carbamazepine is an antiepileptic drug, which is classified as a class II drug (low solubility and high intestinal permeability) according to the Biopharmaceutical Classification System (2,7). The effective jejunal permeability (P_{eff}) in humans for carbamazepine has been determined to be approximately 4×10^{-4} cm/s (2). The direct measurement of the in vivo dissolution of carbamazepine agreed very well with in vivo dissolution obtained by the deconvolution approach using plasma concentrations of carbamazepine (Fig. 7). Bönlökke et al. have also found that the in vivo dissolution was significantly higher in terms of both rate and extent, compared with the in vitro dissolution (see Fig. 7) (4). The in vitro method was a flow-through cell using perfusion solution both with and without bile acids as dissolution media, at a flow rate of 2.5 mL/min and a temperature

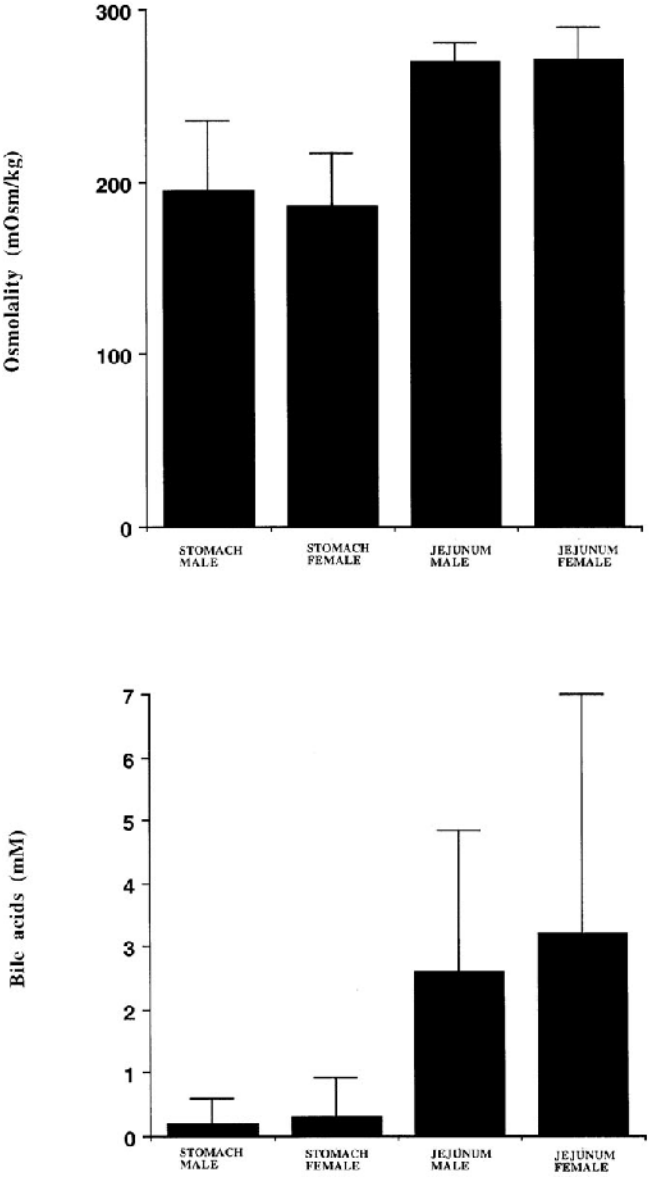

FIG. 6 The concentrations of different constituents (osmolality and bile acid) of gastric and jejunal fluids during the fasted state in males and females.

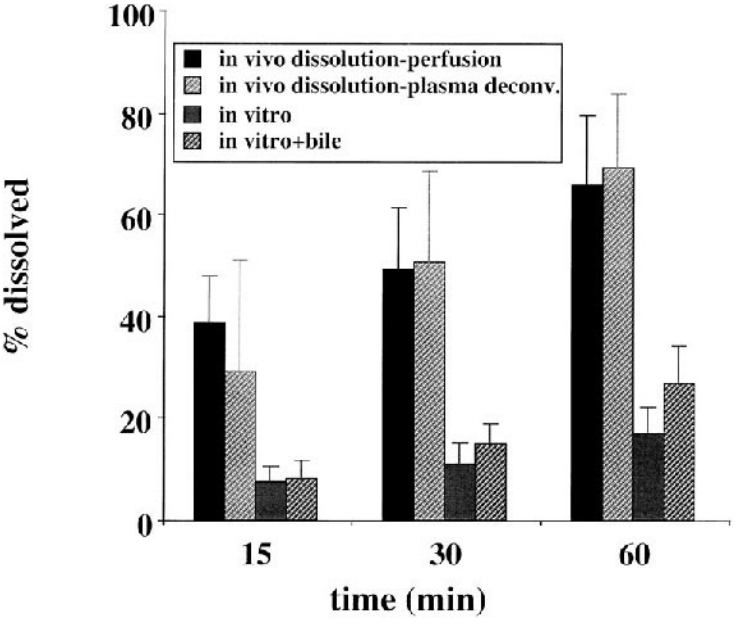

FIG. 7 The in vivo dissolution rate obtained by two different methods: (a) single-pass perfusion in the jejunum and (b) deconvolution of the plasma concentrations. These two in vivo approaches were compared with in vitro dissolution (flow-through cell method) with (3 mM) and without bile acids present in the dissolution medium.

of 37°C. We found that the dissolution rate was lower, despite the addition of bile acids to the in vitro dissolution medium at a physiological relevant concentration (3 mM) for the fasted state. This observed difference between in vivo and in vitro dissolution is probably a consequence of several factors, such as other important components of the luminal content, more efficient physiological stirring (hydrodynamics), and a high intestinal permeability of carbamazepine. The stirring and the continuous drug absorption most likely provide sink conditions in vivo. The suggestion that factors other than the bile acids are important for in vivo dissolution of drugs was supported by the observation that there was no correlation between direct in vivo dissolution in the jejunal lumen and measured concentrations of bile acids in the human jejunal lumen (4).

VIII. CONCLUSION

In conclusion, the main purposes of using the Loc-I-Gut jejunal perfusion technique in humans are to classify a drug as having low or high permeability, investigate the transport mechanism(s), examine the presystemic metabolism involved, and to measure the in vivo drug dissolution. For mechanistic investigations of transport and metabolism, these can also be designed to focus on issues such as drug–drug, food–drug, and drug–pharmaceutical excipient interactions. Furthermore, dissolution studies performed with the perfusion approach will add new insight to processes such as solubilization, hydrodynamics, and sink conditions.

REFERENCES

1. Lennernäs H. Human intestinal permeability: an overview. J Pharm Sci 1998; 87:403–410.
2. Amidon GL, Lennernäs H, Shah VP, Crison J. Theoretical considerations in the correlation of in vitro drug product dissolution and in vivo bioavailability: a basis for a biopharmaceutics drug classification. Pharm Res 1995; 12:413–420.
3. Lipinski CA, Lombardo E, Dominy BW, Feeney PJ. Experimental and computational approaches to estimate solubility and permeability in drug discovery and development settings. Adv Drug Delivery Rev 1997; 23:3–25.
4. Bönlökke L, Hovgard L, Kristensen HG, Knutson L, Lindahl A, Lennernäs H. A comparison between direct determination of in vivo dissolution and the deconvolution technique in humans. Eur J Pharm Sci 1998; 8:19–27.
5. Lennernäs H, Ahrenstedt Ö, Hällgren R, Knutson L, Ryde M, Paalzow LK. Regional jejunal perfusion, a new in vivo approach to study oral drug absorption in man. Pharm Res 1992; 9:1243–1251.
6. Lindahl A, Sandström R, Ungell A-L, Abrahamsson B, Knutson L, Knutson T, Lennernäs H. Jejunal permeability and hepatic extraction of fluvastatin in humans. Clin Pharm Ther 1996; 60:493–503.
7. Bönlökke L, Christensen F-N, Hovgard L, Kristensen HG, Lennernäs H. A new approach to study in vivo dissolution of drugs in humans. Pharm Res 1997; 14: 1490–1492.
8. Lennernäs H, Nilsson D, Aquilonius S-M, Ahrenstedt Ö, Knutson L, Paalzow LK. The effect of L-leucine on the absorption of levodopa, studied by regional jejunal perfusion in man. Br J Clin Pharmacol 1993; 35:243–250.
9. Lennernäs H. Does fluid flow across the intestinal mucosa affect quantitative oral drug absorption? Is it time for a reevaluation? Pharm Res 1995; 12:1573–1582.

10. Sandström R, Karlsson A, Knutson L, Lennernäs H. Jejunal absorption and metabolism of *R*/*S*-verapamil in humans. Pharm Res 1998; 15:856–862.
11. Cutler D. Assessment of rate and extent of drug absorption. Pharm Ther 1981; 14:123–160.
12. Tucker GT. The determination of in vivo drug absorption rate. Acta Pharm Technol 1983; 29:159–164.
13. Knutson L, Odlind B, Hällgren R. A new technique for segmental jejunal perfusion in man. Am J Gastroenterol 1989; 84:1278–1284.
14. Lennernäs H, Lee I-D, Fagerholm U, Amidon GL. A RTD analysis of the hydrodynamics within the human intestine during a regional single-pass perfusion: in vivo permeability estimation. J Pharm Pharmacol 1997; 49:682–686.
15. Lundin PDP, Weström BR, Pantzar N, Kalrsson BW. Bidirectional small intestinal permeability changes to different-sized molecules after HCl-induced injury in the rat. Dig Dis Sci 1997; 42:677–683.
16. Phillips SF, Summerskil WHJ. Occlusion of the jejunum for intestinal perfusion in man. Mayo Clin Proc 1966; 41:224–231.
17. Modigliani R, Ramboud JC, Bernier JJ. Digestion 1973; 9:176–192.
18. Whalen GE, Harris JA, Geenen JE, Soergel KH. Gastroenterology 1966; 51: 975–984.
19. Öhman U, Shepherd AP, Granger DN, eds. In: Physiology of the Intestinal Circulation. New York: Raven Press, 1984:321–334.
20. Lennernäs H. Human jejunal effective permeability and its correlation to preclinical drug absorption models. J Pharm Pharmacol 1997; 49:627–638.
21. Lennernäs H, Palm K, Fagerholm U, Artursson P. Comparison between active and passive drug transport in human intestinal epithelial (Caco-2) cells in vitro and human jejunum in vivo. Int J Pharm 1996; 127:103–107.
22. Fagerholm U, Johansson M, Lennernäs H. The correlation between rat and human small intestinal permeability to drugs with different physico-chemical properties. Pharm Res 1996; 13:1335–1341.
23. Lennernäs H, Nylander S, Ungell A-L. Correlation of effective drug permeability measurements in vitro using the Ussing chamber and the human jejunal perfusion. Pharm Res 1997; 14:667–671.
24. Lennernäs H, Knutson L, Knutson T, Hussain A, Lesko L, Salmonson T, Amidon GL. Human effective permeability for five cardiovascular drugs: atenolol, metoprolol, hydrochlorothiazide, furosemide and *R*/*S*-verapamil. Pharm Res 2000; (submitted).
25. Lennernäs H, Knutson L, Lesko L, Salmonson T, Amidon GL. Human jejunal permeabilities comparison of α-methyldopa and L-dopa: two carrier mediated drugs. Pharm Res 1996; 13:S-329.
26. Lennernäs H, Knutson L, Knutson T, Hussain A, Lesko L, Salmonson T, Amidon GL. The effective jejunal permeability of amiloride and amoxicillin in humans. Clin Ther Pharmacol 2000; (submitted).
27. Takamatsu N, Welage LS, Liu D-Y, Idkaidek NM, Lee P I-D, Hayashi Y, Rhie JK, Lennernäs H, Barnett JL, Shah VP, Lesko L, Amidon GL. Human intestinal

permeability of piroxicam, propranolol, phenylalanine and PEG 400 determined by jejunal perfusion. Pharm Res 1997; 14:1127–1132.
28. Hussain AS. Classifying your drug: the BCS guidance. In: Amidon GL, Robinson JR, Williams RL, eds. Scientific Foundations for Regulating Drug Product Quality. Alexandria: AAPS Press, 1997:197–204.
29. Lesko LJ. Regulatory overview. In: Amidon GL, Robinson JR, Williams RL, eds. Scientific Foundations for Regulating Drug Product Quality. Alexandria: AAPS Press, 1997:187–203.
30. Williams RL. In vitro bioequivalence standards. In: Amidon GL, Robinson JR, Williams RL, eds. Scientific Foundations for Regulating Drug Product Quality. Alexandria: AAPS Press, 1997:387–392.
31. Winiwarter S, Bonham N, Hallberg A, Lennernäs H, Karlén A. Correlation of human jejunal permeability (in vivo) with experimentally and theoretically derived parameters. A multivariate data analysis approach. J Med Chem 1998; 41: 4939–4949.
32. Lande MB, Donovan JM, Zeidel ML. The relationship between membrane fluidity and permeabilities to water, solutes, ammonia, and protons. J Gen Physiol 1995; 106:67–84.
33. Thiebaut F, Tsuruo T, Hamada H, Gottesman MM, Pastan I, Willingham MC. Cellular localization of the multi-drug resistance gene product P-glycoprotein in normal human tissues. Proc Natl Acad Sci USA 1987; 84:7735–7738.
34. Wu CY, Benet LZ, Herbert MF, Gupta SK, Rowland M, Gomez DY, Wacher VJ. Differentiation of absorption and first-pass gut and hepatic metabolism in humans: studies with cyclosporine. Clin Pharmacol Ther 1995; 58:492–497.
35. Thummel KE, O'Shea D, Paine MF, Shen DD, Kunze KL, Perkins JD, Wilkinson GR. Oral first-pass elimination of midazolam involves both gastrointestinal and hepatic CYP3A-mediated metabolism. Clin Pharmacol Ther 1996; 59:491–502.
36. Fromm MF, Busse D, Eichelbaum M. Differential induction of prehepatic and hepatic metabolism of verapamil by rifampin. Hepatology 1996; 24:796–801.
37. Regardh CG, Edgar B, Olsson R, Kendell M, Collste P, Shansky C. Pharmacokinetics of felodipine in patients with liver disease. Eur J Clin Pharmacol 1989; 36:473–479.
38. Wacher VJ, Wu CY, Benet LZ. Overlapping substrate specificities and tissue distribution of cytochrome P450 3A and P-glycoprotein: implications for drug delivery and activity in cancer chemotherapy. Mol Carcinog 1995; 13:129–134.
39. Benet LZ, Wu CY, Hebert MF, Wacher VJ. Intestinal drug metabolism and antitransport processes: a potential paradigm shift in oral drug delivery. J Controlled Release 1996; 39:139–143.
40. Lown KS, Mayo RR, Leichtman AB, Hsiao HL, Turgeon DK, Schmiedlin RP, Brown MB, Guo W, Rossi SJ, Benet LZ. Role of intestinal P-glycoprotein (mdr 1) in interpatient variation in the oral bioavailability of cyclosporine. Clin Pharmacol Ther 1997; 62:248–260.

41. Lown KS, Kolars JC, Thummel KE, Barnett JL, Kunze KL, Wrighton SA, Watkins PB. Interpatient heterogeneity in expression of CYP3A4 and CYP3A5 in small bowel. Lack of prediction by the erythromycin breath test. Drug Metabol Dispos 1994; 22:947–955.
42. Lown KS, Kolars JC, Ghosh M, Schmiedlin-Ren P, Watkins PB. Induction of MDR1 expression in normal rat and human intestine in vivo. Gastroenterology 1996; 110:A344.
43. Sparreboom A, van Mayer AJ, Schinkel AH, Smit JW, Meijer DK, Borst P, Nooijen WJ, Beijnen JH, van TO. Limited oral bioavailability and active epithelial excretion of paclitaxel (Taxol) caused by P-glycoprotein in the intestine. Proc Natl Acad Sci USA 1997; 94:2031–2035.
44. Gan LSL, Moseley MA, Khosla B, Augustijns PF, Bradshaw TP, Hendren RW, Thakker DR. CYP3A-like cytochrome P450-mediated metabolism and polarized efflux of cyclosporine in Caco-2 cells: interaction between the two biochemical barriers to intestinal transport. Drug Metab Dispos, 1996; 24:344–349.
45. Gramatté T, Oertel R, Terhaag B, Kirch W. Direct demonstration of small intestinal secretion and site-dependent absorption of the beta-blocker talinolol in humans. Clin Pharmacol Ther 1996; 59:541–549.
46. Wetterwich U, Spahn LH, Mutschler B, Terhaag B, Rosch W, Langguth P. Evidence for intestinal secretion as an additional clearance pathway to talinolol enantiomers: concentration- and dose-dependent absorption in vitro and in vivo. Pharm Res 1996; 13:514–522.
47. Sandström R, Knutson L, Knutson T, Jansson B, Lennernäs H. The effect of ketoconazole on jejunal permeability and CYP3A metabolism of *R*/*S*-verapamil in humans. 1999; 48:180–189.
48. Lindahl A, Ungell A-L, Lennernäs H. Characterization of fluids from the human stomach and proximal jejunum in the fasted state. Pharm Res 1997; 14:497–502.
49. Dressman JB, Amidon GL. Reppas C, Shah VP. Dissolution testing as a prognostic tool for oral drug absorption: immediate release dosage forms. Pharm Res 1998; 15:11–22.

8

The Role of Permeability Studies in Preclinical Evaluation

Philip L. Smith
SmithKline Beecham Pharmaceuticals, Collegeville, Pennsylvania

I. INTRODUCTION

In the pharmaceutical industry, it has been estimated that discovery and development of therapeutic agents requires approximately 5000 preclinical compounds to provide 5 compounds for clinical trials. Of those 5 compounds entering clinical trials, only 1 becomes a marketed product. Costs associated with this process can amount to more than 300 million dollars, and the process can take up to 15 years to complete (1). Navia and Chaturvedi have presented examples of the process that show that from a total of 314 angiotensin-converting enzyme (ACE) inhibitors evaluated only 15 progressed to preclinical studies, 12 advanced to clinical trials, and 11 were launched (2). However, those 11 marketed compounds represent only 3% of the compounds evaluated. This is actually an impressive record compared with more recent examples (e.g., HIV protease inhibitors and renin inhibitors) (2). In the case of human immunodeficiency virus (HIV) protease inhibitors, 351 compounds were evaluated. Nineteen moved into preclinical studies, 6 progressed to clinical trials, and only 3 were launched. Despite being launched, these HIV protease inhibitors presented significant developmental challenges related to their pharmacokinetic properties (3,4). For renin inhibitors, from 976 compounds evaluated, none have been launched, despite that 35 have been progressed through preclinical studies and 11 have been evaluated in clinical trials (2). This is a poor commentary on the development of therapeutic agents and highlights the need

for improvement in approaches to identify compounds that can be successfully developed. The reasons for the long developmental times and high costs associated with the drug development process are related to the complexities involved. For a compound to move from the laboratory to the clinic, many hurdles must be overcome. These include (a) identification of a potent and selective compound that will interact with the specified target (e.g., a membrane surface receptor or intracellular enzyme); (b) appropriate physicochemical properties to allow dissolution and absorption at a rate optimal for drug action as well as stability in an appropriate dosage form; (c) pharmacokinetic properties (e.g., metabolic stability, clearance, distribution) that are sufficient to provide a relevant concentration at the site of action for the required length of time; and (d) an adequate safety margin (5).

II. THE DEVELOPMENT PROCESS

The traditional paradigm used for identifying and evaluating drug candidates involves identification and selection of an appropriate target, followed by configuration of a high-throughput screen to select compounds for further in vitro and in vivo pharmacological assessment (Fig. 1). A limited number of compounds with the greatest pharmacological effect are then progressed to development. At this stage, pharmaceutical and pharmacokinetic evaluation may identify issues, such as poor absorption, rapid clearance, inappropriate distribution, or issues related to the side effect profile of the compound. Any of these findings could result in recycling back to the lead identification stage of the process, adding more time to the development program. Additionally, low or variable absorption can result in additional resources being devoted to identification of an optimized dosage form with appropriate excipients to provide the desired dissolution and absorption characteristics. Development of optimized dosage forms can lead to an increase in the cost of goods, additional bioequivalence studies, and further resource requirements. These activities can add to development costs through an increase in the numbers and length of clinical trials and the potential for safety issues, including drug–drug interactions.

For these reasons, the paradigm for drug development has been changing over the past decade. According to the new paradigm for drug development, absorption and pharmacokinetic screens are completed earlier in the discovery–development process to provide compounds for development with characteristics optimized not only for interaction at the target site, but also for absorption–delivery and pharmacokinetic properties (Fig. 2). Although not as

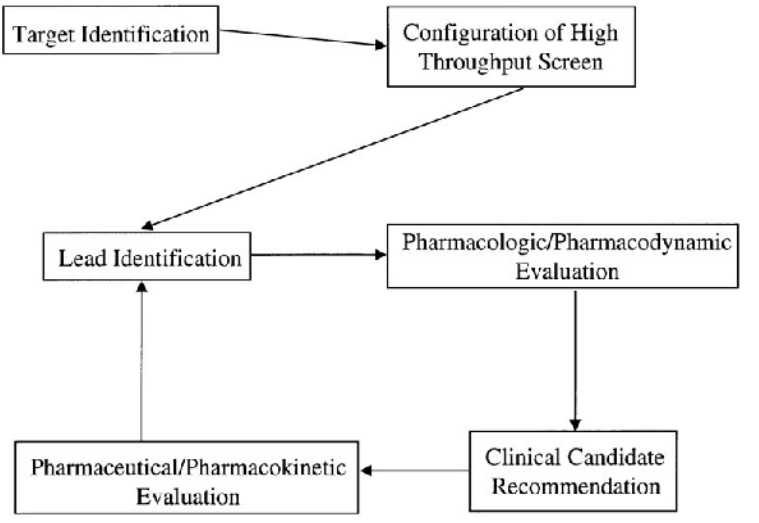

FIG. 1 Traditional paradigm for identification of a drug candidate: According to this scheme, pharmaceutical, drug delivery, and pharmacokinetic evaluation is conducted after selection of the lead candidate.

advanced as the absorption and pharmacokinetic screens, screens for assessment of potential safety issues and physicochemical characteristics of a compound, including potential stability issues, are being developed and will be integrated into the discovery process as soon as they have been validated and configured to a higher throughput format. As presented in Table 1, the increased need for preclinical studies has been precipitated by several factors. First, novel targets are being provided by the explosion in molecular biology (6). Incorporation of gene sequencing and bioinformatics into the drug discovery process has provided a plethora of potential targets. In the drug development process, receptors expressed from novel genes are employed to identify lead compounds that can be synthesized by combinatorial chemistry approaches and whose pharmacological potential can be identified by high-throughput screening (7). These approaches have tended to result in compounds with greater molecular weight and increased hydrophobicity (8). In many instances, the pharmacokinetic–pharmacodynamic relations for these novel receptors are determined late in preclinical development or not at all. Additionally, for many of these novel receptors–targets that are being identified through molecular biological approaches, dose and dosing frequency can-

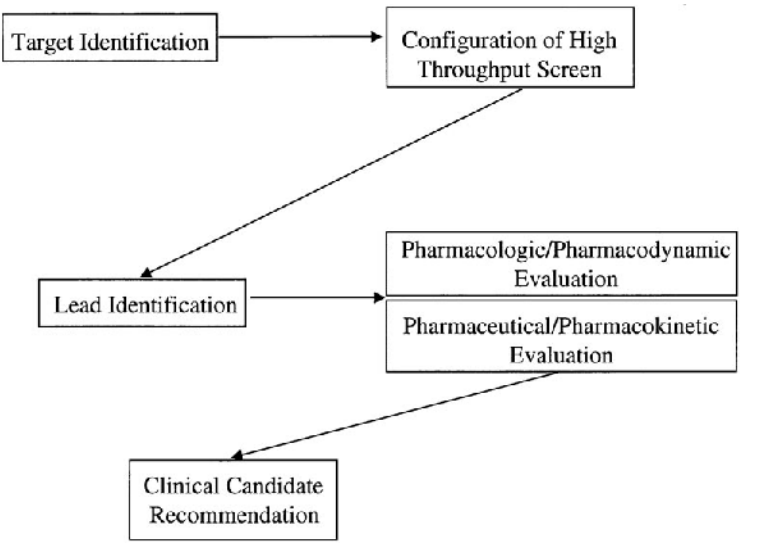

FIG. 2 Current paradigm for identification of a drug candidate: Pharmaceutical, drug delivery, and pharmacokinetic evaluation are conducted simultaneously to enhance clinical candidate characteristics before recommendation for further development.

not be determined from preclinical studies. Thus, for successful development to occur in a timely manner, it is necessary to develop approaches to identify issues early in the process.

What then are the approaches to these problems? How can compound selection be optimized, not only for potency, but also for absorption and pharmacokinetics? How can additional information relating dose and dosing fre-

TABLE 1 Increased Need for Preclinical Studies in Drug Development

Novel targets from gene sequencing and bioinformatics
Incorporation of high-throughput screening for compound evaluation
Incorporation of combinatorial chemistry approaches for compound synthesis
Higher molecular weight of drug candidates
Increased hydrophobicity of drug candidates
Lack of information on pharmacokinetic–pharmacodynamic relations
Lack of information on dose and dosing frequency

quency be obtained earlier in the discovery–developmental process? The latter question will not be addressed in this chapter, but is the subject of intense research to investigate and implement novel analytical and imaging approaches and to identify surrogate markers that can be employed to reduce the time required to optimize the dosing regimen in the clinical setting. For pharmaceutics, drug delivery, and pharmacokinetic evaluation, the challenge has been to develop approaches to measure or predict these parameters more rapidly to provide the medicinal chemists with timely information to aid in compound design. These activities require additional resources, but are already providing a new paradigm for the way we select candidates for development (9) (see Fig. 2). Thus, instead of depending just on in vitro and in vivo pharmacological assessment to identify a potential compound for development, there will be in vitro and in vivo pharmacological assessment, together with evaluation of drug absorption and pharmacokinetic properties, to provide a total package that then aids in the selection of a compound to be progressed to development.

The advantages of integrating development screens early in the discovery process include (a) rapid feedback for the medicinal chemists, and (b) selection of better development candidates relative to pharmaceutics, drug delivery, and pharmacokinetics (the hypothesis being that compounds with appropriate solubility, permeability, and pharmacokinetics should allow more facile dosage form design; thus, more rapid, cost-effective development). The ultimate benefit of these activities should be earlier registration of an optimized dosage form that has the potential for decreased side effects and increased compliance.

What strategies are being employed to increase capacity for development screens? Major advances have occurred in analytical approaches (e.g., LC/MS/MS) (10). The combination of mass spectroscopy with experimental approaches involving the inclusion of multiple compounds per dosing has allowed a much more rapid evaluation of the pharmacokinetics of drug candidates and a concomitant reduction in the time required to provide feedback to the medicinal chemists. Another advance has been the incorporation of physicochemical, in vitro, and computational approaches for predicting drug absorption (8,11–15). Although approaches to employ physicochemical properties of compounds for progression in discovery and development have been employed for many years, our understanding of the role of transporters in drug absorption, distribution, and clearance have dictated that additional techniques be developed and applied to these issues (11,16–18). For computational approaches for predicting drug absorption, the limited number of compounds that have been reported employing these approaches does not permit a critical

evaluation. Application of computational approaches to larger numbers of compounds from structurally diverse chemical classes is required before these will be generally accepted in the drug discovery and development process. Thus, this chapter will focus on the use of in vitro permeability measurements to aid in selection of compounds for development. Simply stated, the significance of employing permeability measurements is that absorption cannot occur from the gastrointestinal tract (or any other site) without membrane permeability. The converse of this statement is not true (i.e., permeability does not ensure absorption and bioavailability). This is due to the myriad of complicating factors involved in the absorption process (e.g., dissolution, metabolism, and clearance).

III. PERMEABILITY: BACKGROUND AND METHODS

A compound may traverse the intestinal epithelial barrier by a variety of routes. These are presented in Fig. 3. The first of these (A) is the passive transcellular transport pathway. For a compound to traverse this route, it must have sufficient hydrophobicity to interact with the lipid bilayer of the cell membrane. This is probably the most significant pathway for transport of a compound across the intestinal epithelium because the cell membrane surface area makes up more than 99% of the total surface area of the intestine. Additionally, the passive transcellular route of transport is an efficient route for a compound to traverse the intestinal epithelium along its entire length, unlike some carrier transport mechanisms that are localized within specific regions of the intestine (e.g., bile acid transporter in the ileum). For highly efficient absorption, the passive transcellular route is the preferred pathway because it is not as likely to be influenced by genetics as carrier-mediated transport pathways, and it is not a saturable pathway. Prediction of permeability in the transcellular route has been modeled based on physicochemical properties of compounds, and these approaches have met with some success (11–15). However, the presence of active and passive carrier-mediated transport pathways in the intestinal epithelium have precluded compound selection based on physicochemical properties alone.

The second transport pathway or permeability depicted in Fig. 3 is the paracellular pathway, which is essentially an aqueous channel, the access to which is restricted by the presence of tight junctional elements at the apical pole of the epithelial cells. This pathway accounts for less than 1% of the surface area of the intestinal epithelium, and transepithelial transport through this pathway is restricted by size. The estimated pore radius is approximately

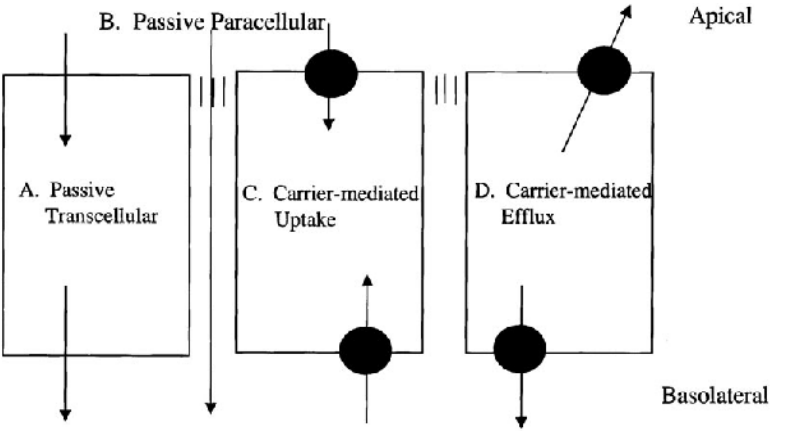

FIG. 3 Permeability pathways for drugs across epithelial (and endothelial) cells: (A) Passive transcellular transport pathway that is dependent on the ability of a compound to partition into the lipid bilayer of the cell membrane and traverse the barrier. (B) The paracellular route is the pathway through the tight junctions and the lateral intercellular space. This route is essentially an aqueous channel with restrictions on the size of the compound that can traverse the junctional complex. (C) Carrier-mediated transmembrane transport involving a carrier in the absence (passive) or presence of ATP (active). (D) Carrier-mediated efflux mechanisms that can also be either passive or active.

8 Å, but it varies with disease and along the length of the gastrointestinal tract (19). There have been several reports of investigations designed to identify approaches to enhance the permeability of the intestinal epithelium by regulation of the junctional complexes (20,21). However, this approach has met with limited success. In general, delivery of a compound through the paracellular pathway will be successful only if the compound is low dose and has a size appropriate to allow passage through the junctional complex.

The two other pathways presented in Fig. 3 are both carrier-mediated pathways (i.e., C and D). Permeability pathways, labeled C, are carrier-mediated transporters that may be located at either the apical or basolateral membrane and function to transport substrates from the cell exterior to the cytoplasm. Examples of transporters located at the apical membrane include the sodium-dependent sugar and amino acid transporters, proton-dependent peptide transporters, nucleoside transporters, and bile acid transporters that aid in the absorption of nutrients presented to the gut wall from the intestinal lumen (19). Additionally, for the proton-dependent peptide transporter, it has been

demonstrated that this pathway is responsible for the absorption of various classes of drugs including antibiotics and ACE inhibitors (18). At the basolateral membrane, there are transporters that translocate substrates, such as organic anions and cations (22,23). These transporters are present not only in the epithelial cells of the gastrointestinal tract, but they are also found in epithelial cells in the kidney and liver and may also be present in the endothelial cells that constitute the blood brain–barrier (23). Pathway D represents efflux mechanisms that have been identified in the epithelial cells of the intestine. These include P-glycoprotein at the apical membrane and amino acid carriers at the basolateral membrane (17,19). P-glycoprotein has been demonstrated to be an important mechanism for limiting absorption of a variety of therapeu-

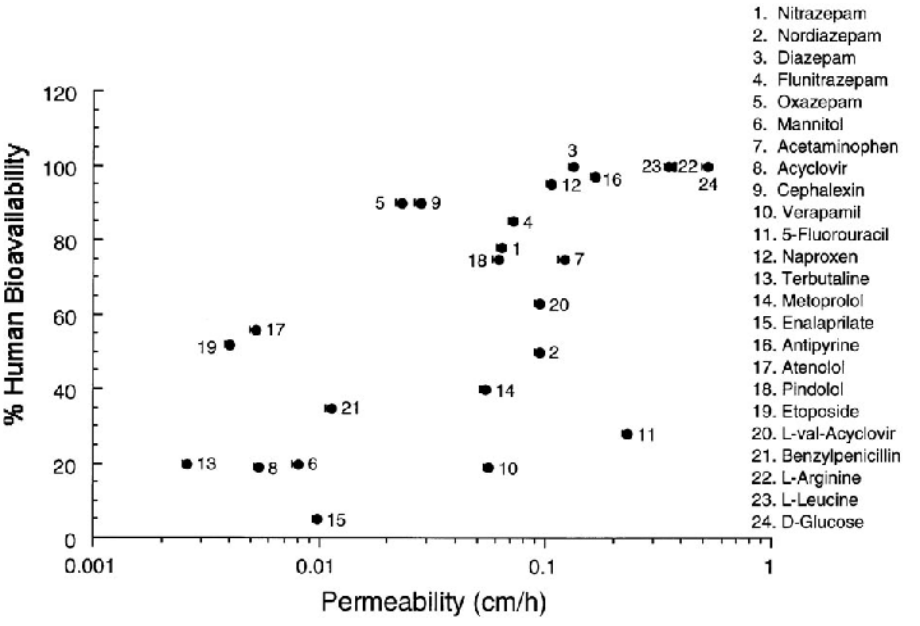

FIG. 4 Correlation between human bioavailability and rabbit ileal permeability for nutrients and marketed drugs. From studies with rabbit ileum, both passive and carrier-mediated transport mechanisms can be observed. Examples of compounds transported by passive transcellular mechanisms are oxazepam, flunitrazepam, diazepam, and antipyrine. Compounds transported by carrier-mediated mechanisms include L-leucine, cephalexin, L-val-acyclovir, and etoposide. Mannitol is an example of a passively transported paracellular compound.

tic agents and in combination with cytochrome P-450 (CYP), has been proposed to be a significant factor in limiting toxic agents from accessing the circulation (24). These carrier-mediated transport processes may be directly (primary active) or indirectly (secondary active) dependent on adenosine triphosphate (ATP) for optimal function.

Intestinal tissues and intestinal cells grown as confluent monolayers have been routinely employed, for many years, for studies directed at understanding the mechanisms and regulation of salt and water transport in the gastrointestinal tract. Over the past decade, these approaches have been applied to the study of drug transport in the intestine and in other tissues. In vitro cell culture models involve growing cells on a semipermeable support, placing them in a diffusion chamber, and determining the transport of drug from the solution bathing one side of the cell culture monolayer to the bathing solution on the other side of the monolayer (25,26). Tissue studies differ only in the use of animal tissues in place of cultured cell monolayers (27,28). With this general approach, cell or tissue viability can be evaluated by measuring the spontaneous transepithelial potential difference. The potential difference is generated by

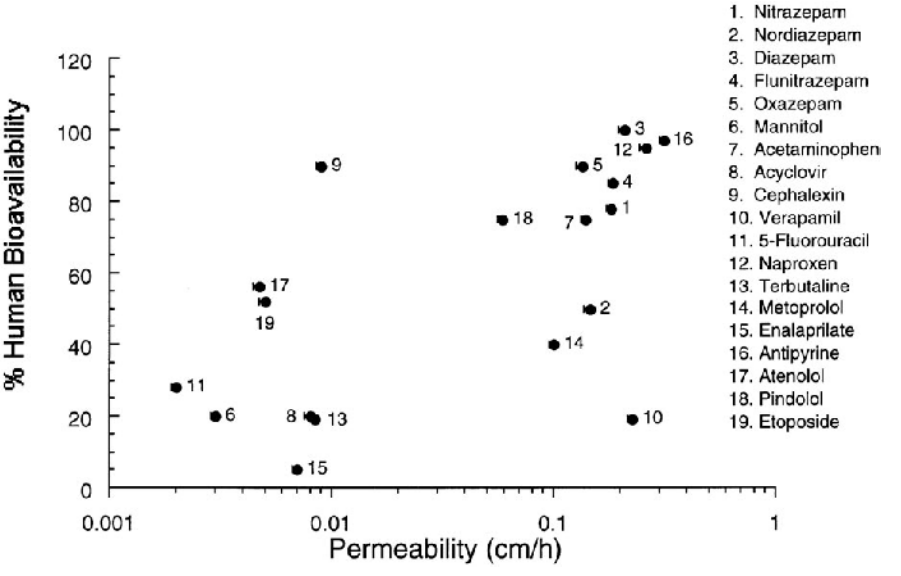

FIG. 5 Correlation between human bioavailability and rabbit distal colonic permeability for marketed drugs: From studies with rabbit distal colon, only passive transcellular and paracellular transport mechanisms can be evaluated.

the movement of ions. This process requires ATP. ATP production, measured as the establishment and maintenance of a transepithelial potential difference, is thus a measure of tissue viability. Alternatively, the short-circuit current can be measured to evaluate viability (27,28). Tissue and cell monolayer integrity can be monitored through measurement of the transepithelial conductance–resistance (27,28), or with the use of paracellular markers (e.g., mannitol) (27,28).

Biochemical approaches have also been employed for verifying cell and tissue viability (27). The permeability of a compound is determined by introducing a drug on one side of the tissue and measuring its appearance on the opposite side. Advantages to using tissues and cell monolayers include (a) ease of use; (b) relative analytical simplicity; (c) ability to study mechanisms; and (d) correlation with human absorption. The relation between in vitro permeability and absorption has been demonstrated in a variety of laboratories and is shown for rabbit intestinal tissues in Figs. 4 and 5. Correlations between permeability with Caco-2 cell monolayers and fraction absorbed have also been provided by a number of laboratories (29).

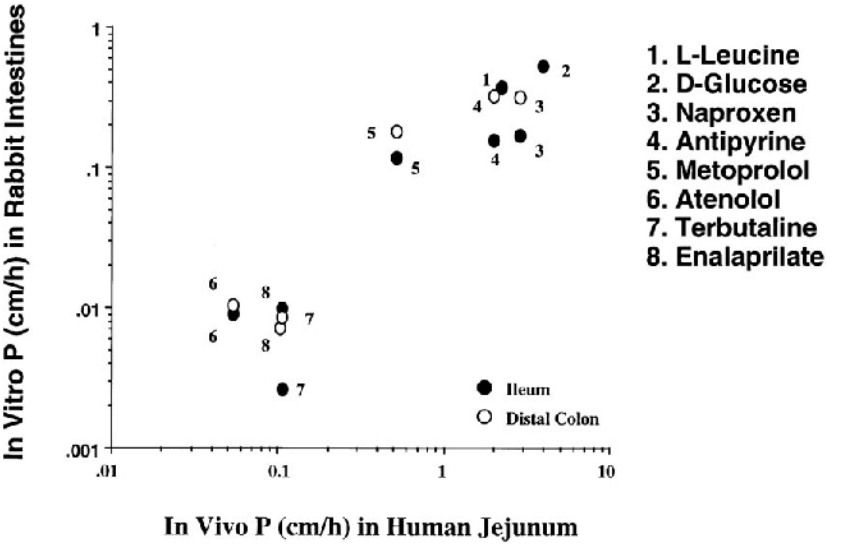

FIG. 6 Correlation between intestinal permeabilities determined in human and rabbit ileal or distal colonic tissues: Values for intestinal permeabilities in humans were taken from Lennernäs (36).

Although the correlation between permeability and bioavailability has significant scatter, owing to the myriad of metabolic and other clearance mechanisms, Fig. 6 demonstrates that there is an excellent agreement between permeabilities determined in rabbit intestinal tissues and in humans. From these results, it is obvious that although scaling from animals to humans in terms of absolute bioavailability may not be predictive owing to species differences in metabolism and clearance, intestinal epithelial permeability currently appears to be less variable between species. If this trend continues as more data accumulates, it will provide a convincing argument for generating permeability data early in the discovery process for selecting development candidates.

IV. CASE HISTORIES

Case histories to demonstrate the increased integration of pharmaceutical discovery and development have been recently presented (9). In the following discussion, examples of the role of permeability studies in preclinical evaluation and compound selection will be presented. The first example is the identification of an orally active endothelin receptor antagonist. Endothelin (ET) is a potent vasoconstrictor peptide that has been implicated in the pathophysiology of disease (30). Development of nonpeptide endothelin receptor antagonists has been undertaken to alleviate the pathophysiological effects associated with endothelin interaction at its receptors. Potent and selective nonpeptide endothelin receptor antagonists have been developed (e.g., SB 209670; Fig. 7). However, when administered orally in animals, the bioavailability of SB 209670 was low (31,32). To better understand the reasons for the low bioavailability seen with SB 209670, in vitro studies were designed to evaluate intestinal permeability of this compound. In these studies the intestinal permeability of SB 209670 was less than 0.01 cm/h in both Caco-2 cells and rabbit intestinal tissues (32). From results from a large number of intestinal permeability studies, 0.01 cm/h has been employed as the cutoff value for selection and further evaluation of potential development candidates. In the permeability studies with SB 209670 the unidirectional fluxes were similar, suggesting that SB 209670 is transported across the intestinal epithelium by a passive process. An examination of the structure of SB 209670 reveals that it is a dicarboxylic acid (see Fig. 7). From the estimated pK_a values for these carboxylic acid groups of less than 5.5, it was proposed that ionization of these groups could be responsible for the limited permeability and oral bioavailability seen with SB 209670. Comparison of the permeability of SB 209670 with that of an inactive, monocarboxylic acid analogue, SB 202994 (see Fig. 7), demonstrated

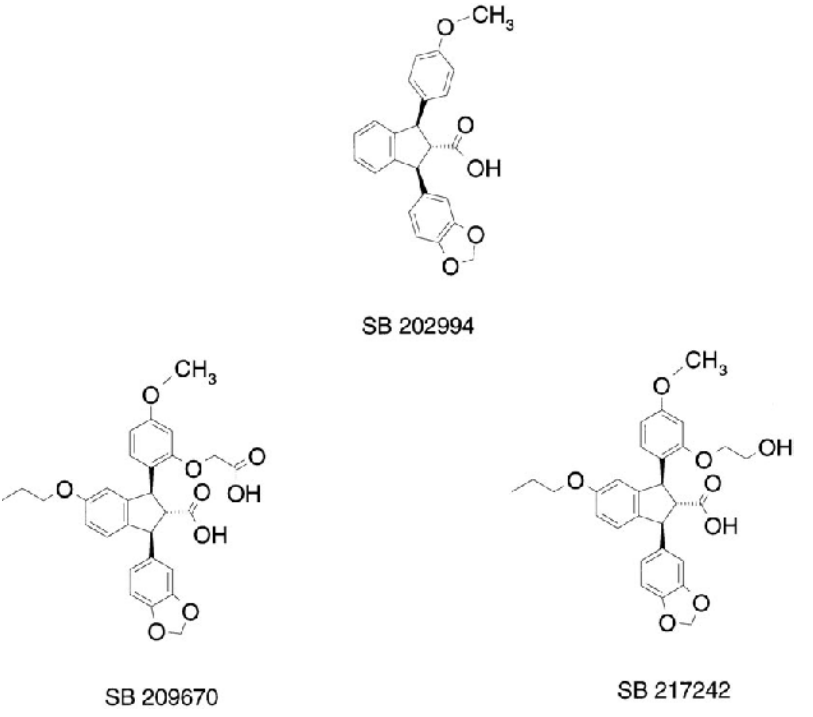

FIG. 7 Structures of endothelin receptor antagonists.

that permeability in the presence of a single charged group was approximately 0.2 cm/h in rabbit intestine. This permeability value is similar to that found with drugs demonstrating bioavailabilities greater than 90%. Further support for the hypothesis that the presence of two charged groups impedes passage across the gut wall was provided by the observation that SB 217242 (see Fig. 7), a highly potent monocarboxylic acid analogue of SB 209670, also has high intestinal tissue permeability (~0.1 cm/h). From a variety of studies conducted with SB 217242, it was demonstrated that this compound traverses the intestinal epithelium through a transcellular pathway and that transport is increased approximately tenfold as the bathing solution pH is reduced from 8 to 5.5 (32). Thus, from these in vitro studies and from pharmacological evaluation, it was possible to identify a highly potent, orally bioavailable endothelin receptor antagonist, of which the characteristics for development, in terms of delivery and pharmaceutics, have been enhanced.

Another example of the role of permeability studies in preclinical evaluation is the development of GPIIb/IIIa antagonists (33). These antagonists are being developed as an approach to prevent thrombosis (33). Initial studies focused on the development of stabilized arginine–glycine–aspartic acid (RGD) peptides and resulted in the identification of compounds such as SKF 107260, a cyclic peptide that is a potent GPIIb/IIIa receptor antagonist (34) (Fig. 8). However, from a variety of in vitro and in vivo studies it was demonstrated that this compound has low permeability in rabbit ileum (< 0.003 cm/h) and also low bioavailability ($< 5\%$) in animals (34). In light of these findings, efforts were directed at identifying compounds that would have similar potency, but enhanced bioavailability. From these studies, SB 207488 was identified (see Fig. 8). This compound is a nonpeptide mimetic with good potency for antagonism at the GPIIb/IIIa receptor, but with less than 0.001 cm/h permeability in rabbit ileum. From inspection of the structure of SB 207488, it can be seen that at physiological pH, both the carboxylic acid func-

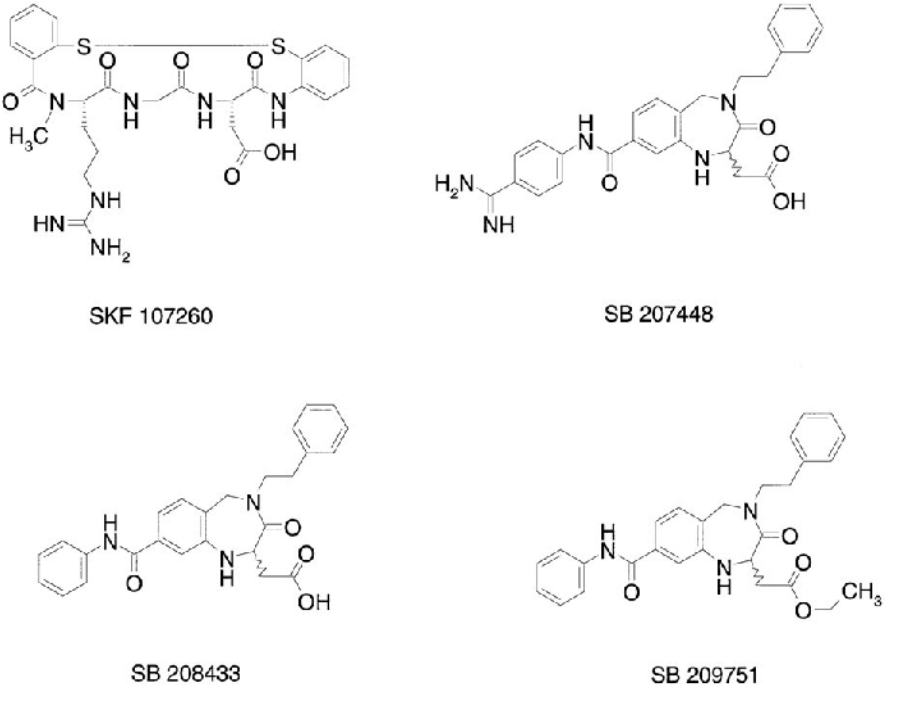

Fig. 8 Structures of GPIIb/IIIa receptor antagonists.

tion and the amine function will be charged. In an attempt to identify what approaches could be taken to enhance permeability, SB 208433 and SB 209751 were synthesized (see Fig. 8). Permeability of these analogs was determined in vitro in an attempt to identify what was the limiting factor for passage across the intestinal epithelial cells (i.e., the amino-terminus or the carboxylic acid function). From these studies, it was found that the permeability of SB 208433 (0.02 cm/h) is 20-fold greater than the permeability of the parent compound, SB 207448, whereas the permeability of SB 209751 (0.04 cm/h) is only two-fold greater than SB 208433.

These results suggest that the major contributing factor to the limited permeability of SB 207488 is the charged amino group and that attempts to modify this functional group should have a significant influence on the permeability of this class of compounds. In subsequent studies designed to produce receptor antagonists for related integrin receptors, compounds with less basic amino-terminal functions were synthesized (Fig. 9). Despite the reduction in basicity of the amino-terminal group, SB 223245 has low permeability (< 0.01 cm/h) in rabbit intestinal tissues. Because SB 223245 is still a zwitterionic compound and does not have significant intestinal permeability, the carboxyl group was modified to produce the metabolically stable methyl ester SB 223243 (see Fig. 9). SB 223243 has a high permeability in the basolateral (blood)-to-lumenal direction (0.22 cm/h). However, the lumen-to-blood permeability is less than 0.01 cm/h in rabbit intestine. These results suggest that in modifying the structure to enhance permeability, the compound has become a substrate for an active efflux mechanism. The presence of an active efflux process for SB 223243 could limit intestinal absorption and also contribute to other development issues, such as drug–drug interactions, high variability in absorption, and food effects (16). These results highlight the importance of conducting a variety of studies with compounds to understand the routes

FIG. 9 Structures of osteoclast vitronectin receptor antagonists.

and mechanisms by which they are transported across the intestinal epithelial cells.

V. FUTURE DIRECTIONS

As can be seen from the previous discussions, integration of development screens into the discovery process has provided approaches to identify and eliminate issues that previously would not have been observed until late in the process of development. Further advances in analytical methods, molecular biological approaches, and computational modeling should provide the increase in capacity required to meet the needs of the next millennium.

REFERENCES

1. DiMasi JA, Hansen RW, Grabowski HG, Lasagna L. Cost of innovation in the pharmaceutical industry. J Health Econ 1991; 10:107–142.
2. Navia MA, Chaturvedi PR. Design principles for orally bioavailable drugs. Drug Dis Today 1996; 96:179–189.
3. Lee CG, Gottesman MM, Cardarelli CO, Ramachandra M, Jeang KT, Ambudkar SV, Pastan I, Dey S. HIV-1 protease inhibitors are substrates for the MDR1 multidrug transporter. Biochemistry 1998; 37:3594–3601.
4. Kim AE, Dintaman JM, Waddell DS, Silverman JA. Saquinavir, an HIV protease inhibitor, is transported by P-glycoprotein. J Pharmacol Exp Ther 1998; 286: 1439–1445.
5. Benet LZ, Kroetz DL, Sheiner LB. Pharmacokinetics: the dynamics of drug absorption; distribution, and elimination. In: Hardman JG, Limbird LE, Molinoff PB, Ruddon RW, Gliman AG, eds. Goodman and Gilman's The Pharmacological Basis of Therapeutics. New York: McGraw-Hill, 1996:3–27.
6. Haseltine WA. Discovering genes for new medicines. Sci Am 1997; March, 92–97.
7. Wilson SR, Czarnik AW. Combinatorial Chemistry: Synthesis and Application. New York: John Wiley & Sons, 1997.
8. Lipinski CA, Lombardo F, Dominy BW, Feeney PJ. Experimental and computational approaches to estimate solubility and permeability in drug discovery and development settings. Adv Drug Deliv Rev 1997; 23:3–25.
9. Borchardt RT, Freidinger RM, Sawyer TK, Smith PL. Integration of Pharmaceutical Discovery and Development: Case Histories. New York: Plenum Press, 1998.

10. Whitney JL, Kerns EH, Rourick RA, Hail ME, Volk KJ, Fink SW, Lee MS. Accelerated structure profiling using automated LC–MS and robotics. Pharm Technol 1998; 22:76–82.
11. Camenisch G, Folkers G, van de Waterbeemd H. Review of theoretical passive drug absorption models: historical background, recent developments and limitations. Pharm Acta Helv 1996; 71:309–327.
12. van de Waterbeemd H, Camenish G, Folkers G, Raevsky OA. Estimation of Caco-2 cell permeability using calculated molecular descriptors. Quant Struct Act Relat 15:480–490, 1996.
13. Palm K, Luthman K, Ungell A, Strandlund G, Artursson P. Correlation of drug absorption with molecular surface properties. J Pharm Sci 1996; 85:32–39.
14. Palm K, Stenberg P, Luthman K, Artursson P. Polar molecular surface properties predict the intestinal absorption of drugs in humans. Pharm Res 1997; 14:568–571.
15. Krarup LH, Christensen IT, Hovgaard L, Frokjaer S. Predicting drug absorption from molecular surface properties based on molecular dynamics simulations. Pharm Res 1998; 15:972–978.
16. Lown KS, Mao RR, Leichtman AB, Hsiao H-L, Turgeon K, Schmiedlin-Ren P, Brown MB, Guo W, Rossi SJ, Benet LZ, Watkins PB. Role of P-glycoprotein (mdr 1) in interpatient variation in the oral bioavailability of cyclosporine. Clin Pharmacol Ther 1997; 62:248–260.
17. Schinkel AH, Smit JJM, van Tellingen O, Beijnen JH, Wagenaar E, van Deemter L, Mol CAAM, van der Valk MA, Robanus–Mandaag EC, te Riele HPJ, Berns AJM, Borst P. Disruption of the mouse *mdr1a* P-glycoprotein gene leads to a deficiency in the blood–brain barrier and to increased sensitivity to drugs. Cell 1994; 77:491–502.
18. Smith PL, Eddy EP, Lee C-P, Wilson G. Exploitation of the intestinal oligopeptide transporter to enhance drug absorption. Drug Deliv 1993; 1:103–111.
19. Powell DW. Intestinal water and electrolyte transport. In: Johnson LR, ed. Physiology of the Gastrointestinal Tract. New York: Raven Press, 1987:1267–1305.
20. Ritschel WA. Microemulsions for improved peptide absorption from the gastrointestinal tract. Methods Find Exp Clin Pharmacol 1993; 13:205–220.
21. Swenson EC, Curatolo WJ. Intestinal permeability enhancement for proteins, peptides and other polar drugs: mechanisms and potential toxicity. Adv Drug Deliv Rev 1992; 8:39–92.
22. Tsuji A, Tamai I. Carrier-mediated intestinal transport of drugs. Pharm Res 1996; 13:963–977.
23. Zhang L, Brett CM, Giacomini KM. Role of organic cation transporters in drug absorption and elimination. Annu Rev Pharmacol Toxicol 1998; 38:431–460.
24. Lampen A, Zhang Y, Hackbarth I, Benet LZ, Sewing KF, Christians U. Metabolism and transport of the macrolide immunosuppressant sirolimus in the small intestine. J Pharmacol Exp Ther 1998; 285:1104–1112.
25. Artursson P, Karlsson J, Ocklind G, Schipper N. Studying transport processes

in absorptive epithelia. In: Shaw A, ed. Cell Models of Epithelial Tissues—A Practical Approach. Oxford: IRL, 1996:111–133.
26. Hidalgo IJ. Cultured intestinal epithelial cell models. In: Borchardt RT, Smith PL, Wilson G. eds. Models for Assessing Drug Absorption and Metabolism. New York: Plenum Press, 1996:35–50.
27. Ungell A-L. In vitro absorption studies and their relevance to absorption from the GI tract. Drug Dev Ind Pharm 1997; 23:879–892.
28. Smith PL. Methods for evaluating intestinal permeability and metabolism in vitro. In: Borchardt RT, Smith PL, Wilson G, eds. Models for Assessing Drug Absorption and Metabolism. New York: Plenum Press, 1996:13–34.
29. Artursson P, Karlsson J. Correlation between oral drug absorption in humans and apparent drug permeability coefficients in human intestinal epithelial (Caco-2) cells. Biochem Biophys Res Commun 1991; 175:880–885.
30. Ruffalo RR Jr. Endothelin Receptors from the Gene to the Human. Boca Raton, FL: CRC Press, 1995.
31. Ohlstein EH, Nambi P, Lago A, Hay DWP, Beck G, Fong K-L, Eddy EP, Smith PL, Ellens H, Elliott JD. Nonpeptide endothelin receptor antagonists. VI. Pharmacological characterization of SB 217242, a potent and highly bioavailable endothelin receptor antagonist. J Pharmacol Exp Ther 1996; 276:609–615.
32. Ellens H, Eddy EP, Lee C-P, Dougherty P, Lago A, Xiang J-N, Elliott JD, Cheng H-Y, Ohlstein E, Smith PL. In vitro permeability screening for identification of orally bioavailable endothelin receptor antagonists. Adv Drug Deliv Rev 1997; 23:99–109.
33. Nichols AJ, Vasko JA, Koster PF, Valocik RE, Samanen JM. GPIIb/IIIa antagonists as novel antithrombotic drugs: potential therapeutic agents. In: Metcalf BW, Dalton BJ, Poste G, eds. Cellular Adhesion: Molecular Definition to Therapeutic Potential. New York: Plenum Press, 1994:213–237.
34. Samanen J, Wilson G, Smith PL, Lee C-P, Bondinell W, Ku T, Rhodes G, Nichols A. Chemical approaches to improve the oral bioavailability of peptidergic molecules. J Pharm Pharmacol 1996; 48:119–135.
35. Samanen JM, Lee C-P, Smith PL, Bondinell WE, Calvo RR, Jakas DR, Newlander KA, Parker M, Uzinskas I, Yellin TO, Nichols AJ. The use of rabbit intestinal permeability as an in vitro assay in the search for orally active GPIIb/IIIa antagonists. Adv Drug Deliv Rev 1996; 23:133–142.
36. Lennernäs H. Human intestinal permeability. J Pharm Sci 1998; 87:403–410.

9

Solubility as a Limiting Factor to Drug Absorption

Raimar Löbenberg* and Gordon L. Amidon
College of Pharmacy, The University of Michigan, Ann Arbor, Michigan

Michael Vieira
Port Systems LLC, Ann Arbor, Michigan

I. INTRODUCTION

The oral route is the preferred way of dosing, because this is the easiest and most convenient way of noninvasive administration. Most drug substances that are applied orally today are small molecules that can permeate the intestinal gut membrane by transcellular passive diffusion. This process is determined by physicochemical laws and by the properties of the intestinal cells. In addition to its permeability through the gut wall, the availability of a drug in the body depends on its ability to dissolve in the gastrointestinal (GI) fluids. This too can be influenced by both physiological and physicochemical factors. This chapter will focus on the prediction of fraction dose absorbed, based on solubility, for drugs that are transported across the gut wall by passive mechanisms.

II. FRACTION DOSE ABSORBED OF POORLY SOLUBLE DRUGS

The Biopharmaceutics Classification System (BCS) (1) combines physicochemical properties of compounds and physiological factors to predict the

* *Present affiliation*: College of Pharmacy, The University of Alberta, Edmonton, Alberta, Canada.

fraction dose absorbed from the gastrointestinal transit. The permeability of a given drug determines the upper limit of its extent of absorption. The interaction of the physiological environment (e.g., intestinal pH, transit time, gastrointestinal motility, luminal metabolism, endogenous substances, such as bile salts, and exogenous substances, such as nutrients) with physicochemical characteristics of the drug (e.g., pK_a, solubility in the gut lumen, dissolution rate, aqueous diffusivity, partition coefficient, and chemical and enzymatic stability in the intestine) can have an influence on the availability of the drug at the absorption site (Fig. 1).

A simple theoretical approach to estimate the extent of oral absorption is based on a steady-state mass balance of a drug in a defined segment of the gastrointestinal tract (1–3). Fick's first law applied to the gut membrane is shown in Eq. (1).

$$J_w = P_w C_w = \frac{\mathrm{dM}}{\mathrm{dt}} \frac{1}{A} \tag{1}$$

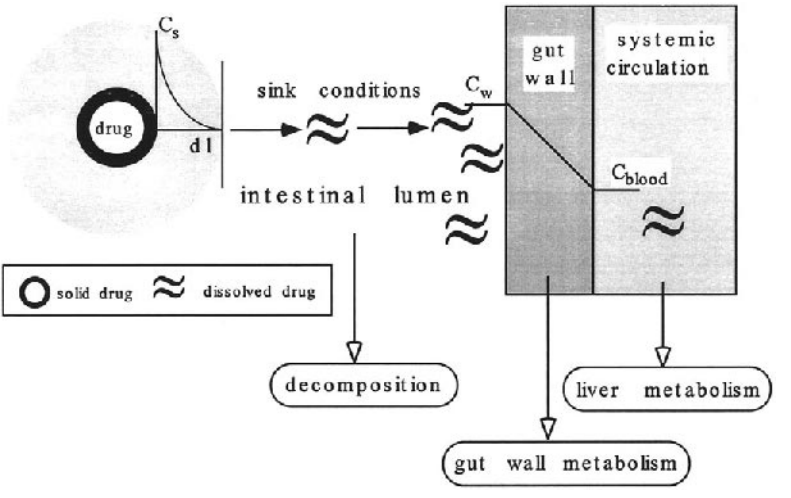

FIG. 1 Drug dissolution, where C_s is the saturation concentration of the drug, d*l* is the diffusion layer, C_w is the concentration at the gut wall, and C_{blood} the concentration in the blood. Further factors influencing the systemic availability are hydrolytic and enzymatic decomposition of the drug in the intestinal lumen, in the gut wall, and metabolism in the systemic circulation.

J_w is the mass transport across the gut wall, P_w can be defined as the effective permeability and C_w is the concentration of the drug at the membrane. In this approach, the stomach is assumed to be an infinite reservoir, with constant output rate relative to concentration and volume, while the small intestine is assumed to be a cylindrical tube with the surface area of $2\pi RL$, where R is the radius and L is the length of the tube (Fig. 2).

When permeability is the limiting factor for drug absorption (low P_w value) structural modification of the molecule is generally the most promising way to improve its absorption rate (2–4).

No difference in the fraction dose absorbed is expected for two drugs, if they have the same permeability and their dissolution and solubility are not limiting (i.e., same C_w). But if their physicochemical properties are different, in that the solubility is low enough for dissolution to be the limiting step to gastrointestinal uptake, a difference in the fraction dose absorbed for the two compounds is expected.

Four dimensionless parameters are fundamental variables for the estimation of the fraction dose absorbed (*Fa*) from the intestine (5): initial saturation (*Is*), absorption number (*An*), dose number (*Do*), and dissolution number (*Dn*). Physicochemical properties of a drug and physiological factors of the intestine are incorporated into these parameters (1–4).

To estimate the extent of drug absorption, it is assumed that the dose ingested is the sum of the initial amount dissolved (*Is*) and the remaining drug, which is present in the form of solid particles.

$$Is = \frac{C_w}{C_s} \tag{2}$$

I_s is defined as the ratio of the drug initially dissolved and available for absorption at the membrane (C_w) to the solubility (C_s) (5).

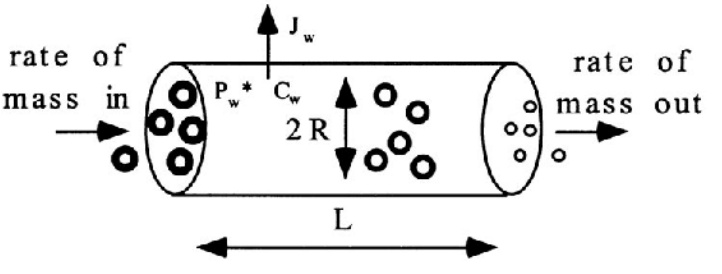

Fig. 2 Mass balance in the intestine. (From Ref. 18.)

An estimation of I_s is often difficult because it is influenced by parameters that are stipulated by the dosage form (e.g., disintegration, dissolution) and by gastrointestinal parameters (e.g., gastric emptying and food effects). Because the physiological solubility in vivo is difficult to measure, the aqueous solubility in vitro may be used as an estimate. However, this may cause significant errors owing to the potential differences between in vitro and in vivo estimations (5).

Three different cases are conceivable. In the first case, the administered dose is dissolved completely, in the second, the dose cannot be completely dissolved within the GI passage, and the third case is a combination of the first and second cases. At the beginning of the gut there is still undissolved drug present, but at the end, all of the drug is dissolved.

In the first case, the fraction absorbed (Fa) of a highly soluble drug can be calculated from Eq. (3).

$$Fa = 1 - e^{(-2\langle T_{si}\rangle R^{-1} Peff)} = 1 - e^{(-2An)} \tag{3}$$

where An is defined as the ratio of the mean transit time $\langle T_{si}\rangle$ to the absorption time $R\,P_{eff}^{-1} = \langle T_{abs}\rangle$, R is the radius of the small intestine and P_{eff} is the effective permeability, that is,

$$An = \left(\frac{\mathrm{P}_{eff}}{R}\right)\langle T_{si}\rangle = \frac{\langle T_{si}\rangle}{\langle T_{abs}\rangle} \tag{4}$$

Equation (3) shows that the fraction dose absorbed is approximated by an exponential function of An (Fig. 3). The absorption number and the permeability represent the primary variable for predicting oral absorption, assuming that dose and dissolution do not limit the oral absorption. Parameters, such as partition coefficient or pK_a of a compound, are useful guides, but are not fundamental parameters to predict Fa (1,4).

The Fa of a compound with $An = 1$ (transit time = absorption time) is about 86% (5). Complete absorption can be expected only if $An > 1$ which means that the absorption time is shorter than the transit time through the absorptive site of the gut.

In the second case, in which the drug is too poorly soluble to completely dissolve within the gut passage $\langle T_{si}\rangle$, Fa can be calculated as shown in Eq. (5).

$$Fa = \frac{2An}{Do} = \frac{2(P_{eff}/R)\langle T_{si}\rangle}{(D/V_o)/C_s} \tag{5}$$

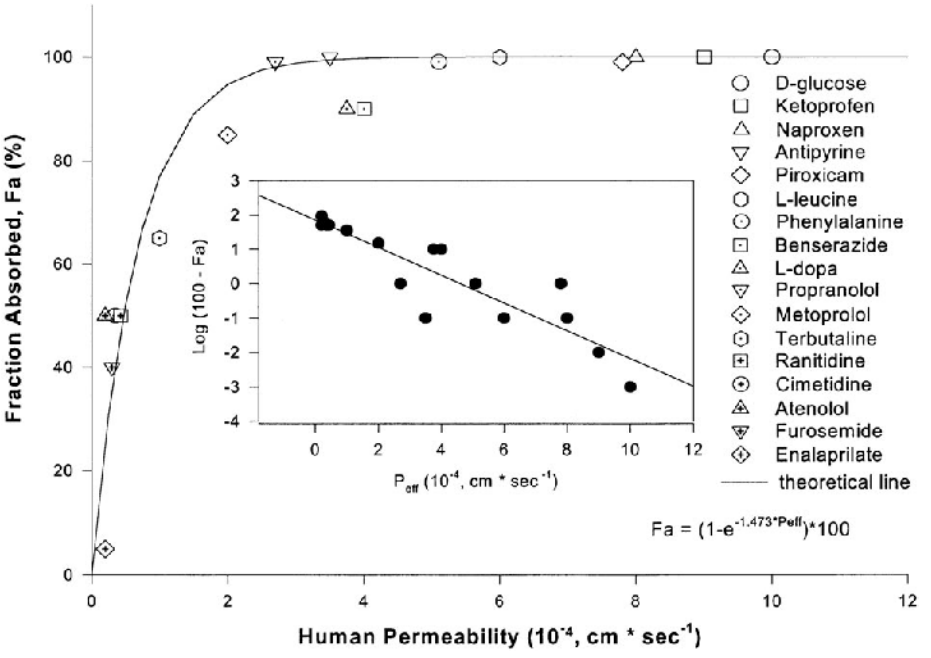

FIG. 3 Correlation between human permeability and fraction dose absorbed of a diverse series of therapeutic compounds: The solid line represents the predicted curve based on the complete radial mixing model. The inset shows the log–linear relation between permeability and fraction dose absorbed, with the slope representing the intestinal fluid velocity. (From Ref. 1.)

Here the assumption is made that $Do > 2\ An$, and that the dissolution rate is faster than the rate of drug absorption across the intestinal membrane, and thus the concentration in the solution can be assumed to equal the solubility of the drug (5).

The fraction dose absorbed for such compounds is not only a function of An, it also depends on the dose number (Do) (1). Do is defined as the ratio of dose concentration to drug solubility, Eq. (6).

$$Do = \frac{D/V_0}{C_s} \tag{6}$$

where (C_s) is the solubility, (D) is the dose, and (V_o) is the volume of water taken with the dose, which is generally set to be 250 mL (4,6).

Table 1 shows the values of C_s, at a given *An* of 1 or 10, which correspond to *Fa* values of 0.01, 0.1, and 0.5.

In the third case, the concentration of a drug at the beginning of the intestine is higher than its solubility and solid drug is present, whereas at the end of the intestine all drug is in solution. To facilitate the analysis, the intestine can be divided into two regions. In the proximal region, solid drug still exists, which is equal to the second case described in the foregoing, and in the distal region only dissolved drug is present, which corresponds to the first case (4).

The last dimensionless parameter to consider is the dissolution number *Dn*, which includes solubility C_s, diffusivity *D*, density ρ, initial particle radius *r* of a compound and the intestinal transit time. It can be defined as the ratio of residence time $\langle T_{si} \rangle$ to dissolution time $\langle T_{diss} \rangle$.

$$Dn = \left(\frac{3D}{r^2}\right)\left(\frac{C_s}{\rho}\right)\langle T_{si}\rangle = \frac{\langle T_{si}\rangle}{\langle T_{diss}\rangle} \tag{7}$$

The dissolution of a poorly soluble compound is normally low ($Dn < 1$), whereas for many poorly soluble compounds *An* and *Do* are high. The relation of dose number and dissolution number at a given absorption number to the fraction dose absorbed is shown in Fig. 4.

According to Fig. 4 the fraction dose absorbed of a poorly soluble compound may be low because the dose number is high, whereas the compound's dissolution number is low. But there are some possibilities to alter the values of these two parameters within certain ranges. For example, *Do* can simply be decreased by taking more water with the administered dose. A smaller dose number will always improve the fraction dose absorbed, but the dose of a drug is determined from pharmacokinetic and pharmacodynamic considerations outside of pharmaceutical control, and the initial amount of water that

Table 1 C_s **Values in μg/mL, for** *An* **= 1 or 10, Corresponding to** *Fa* **Values of 0.01, 0.1, and 0.5**

	An = 1			*An* = 10		
Fa	*D* 5 mg	50 mg	500 mg	5 mg	50 mg	500 mg
0.01	0.1	1	10	0.01	0.1	1
0.1	1	5	100	0.1	1	10
0.5	5	50	500	0.5	5	50

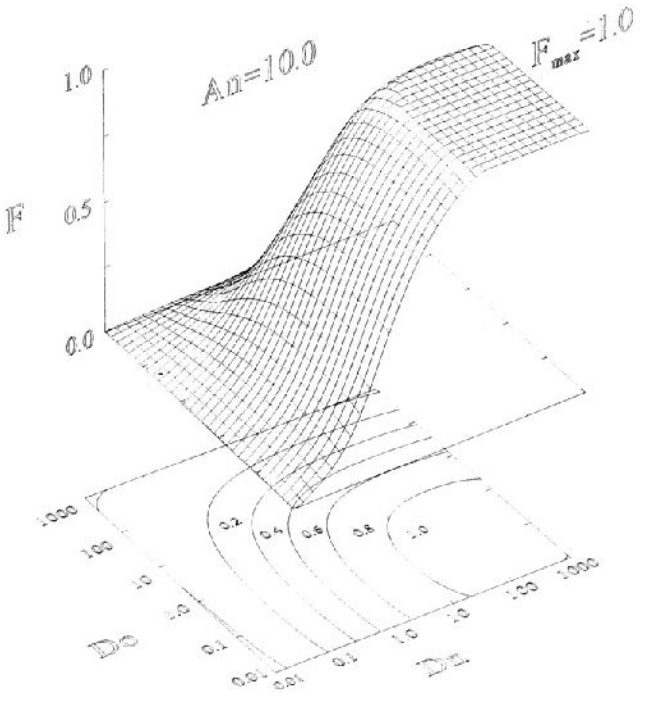

FIG. 4 Estimated fraction dose absorbed (*F*) vs. dissolution number (*Dn*) and dose number (*Do*) for a highly permeable drug: The absorption number (*An*) = 10 corresponds to a drug with a permeability approximately that of glucose. (From Ref. 1.)

is taken with the dosage form is also limited by patient compliance and the anatomical volume of the stomach. On the other hand, *Dn* can be increased by reducing the particle size and other formulation approaches designed to accelerate dissolution from the dosage form. However, Fig. 4 also points out that if *Do* and *Dn* are approximately 1 at *An* = 10, great variability in the fraction dose absorbed can result from small changes in the value of one or both variables. Drugs with these characteristics may exhibit highly variable behavior, even when administered under well-controlled conditions.

Classic examples for the influence of these two parameters on the bioavailability are digoxin and griseofulvin (7). Both drugs are poorly soluble

Table 2 Calculated Parameters for Representative Drugs

Drug	Dose (mg)	C_s[a] (mg/mL)	V_{sol}[b] (mL)	Do[c]	Dn[d] (estimated intrinsic)
Piroxicam	20	0.007	2,857	11.4	0.15
Glyburide	10	0.0034	2907	11.6	0.074
Cimetidine	800	6.000	133	0.53	129
Chlorthiazide	500	0.786	636	2.54	17.0
Digoxin	0.5	0.024	20.8	0.08	0.52
Griseofulvin	500	0.015	33,333	133	0.32
Carbamazepine	200	0.260	769	3.08	5.61

[a] Minimum physiological solubility in the pH range 1–8 and at 37°C.
[b] Volume of solvent required to completely dissolve the dose at minimum physiological solubility.
[c] Do = dose/V_0/C_s^{min}, initial gastric volume = 250 mL.
[d] Assumptions: r = 25 μm, D = 5×10^{-6} cm²/s, ρ = 1.2 mg/cm³ = 180 min.
Source: Ref. 1.

within the physiological pH range (Table 2). A typical dose of digoxin is 0.5 mg which will dissolve in approximately 21 mL water, whereas griseofulvin is dosed 1000-fold higher at 500 mg and about 33 L are necessary to dissolve the dose. Thus, the huge difference in dose results in a low *Do* for digoxin and a high *Do* for griseofulvin.

The limiting factor for digoxin is its dissolution: the dose can theoretically be dissolved by the volume of fluid available in the gut lumen. Studies varying the particle size of digoxin show that the bioavailability of digoxin directly depends on the particle size (7,8). If micronized powder (7 μm) was used for manufacture, the tablet was bioequivalent to a hydro-alcoholic solution of digoxin. When, however, the particle size of the drug in the tablet was 102 μm, bioequivalence with the solution could not be reached (9). For drugs, such as digoxin, achieving an equivalent of *Dn* with two different formulations should result in their bioequivalence (10).

The volume of fluid necessary to dissolve a normal dose of griseofulvin (33 L) is limiting to *Fa*. For this drug the solubility limits absorption, and reducing the particle size cannot achieve 100% absorption. Only solubilization enhancement sufficient to reduce the *Do* of griseofulvin significantly can raise the *Fa*. Consequently, the possibilities for formulation approaches to improve the bioavailability are more limited for drugs similar to griseofulvin than for drugs similar to digoxin.

III. GASTROINTESTINAL PHYSIOLOGY AND IN VITRO MICELLE SYSTEMS

Before a substance can be absorbed it has to be dissolved. Most drugs are not administered as solutions, but as solids (e.g., tablet or capsule) together with water. Here, the formulation has to release the drug, which usually occurs by disintegration followed by dissolution and absorption.

The GI fluids have to be taken into account when dosing of drug substances orally because there could be a deficit in the volume available to dissolve a dose of a poorly soluble substance as shown previously for griseofulvin. As shown in Fig. 5, about 1.2 L of fluids is ingested orally per day, a volume that varies according to the individual. The fluid volume of the stomach in the fasted state is about 20–50 mL. The secretions of the paragastrointestinal organs (salivary gland, liver, and pancreas) are received by the first portion of the duodenum. Approximately 1.5 L of pancreatic juice and 500 mL of bile are secreted into the duodenum within 1 day (11). The sum of

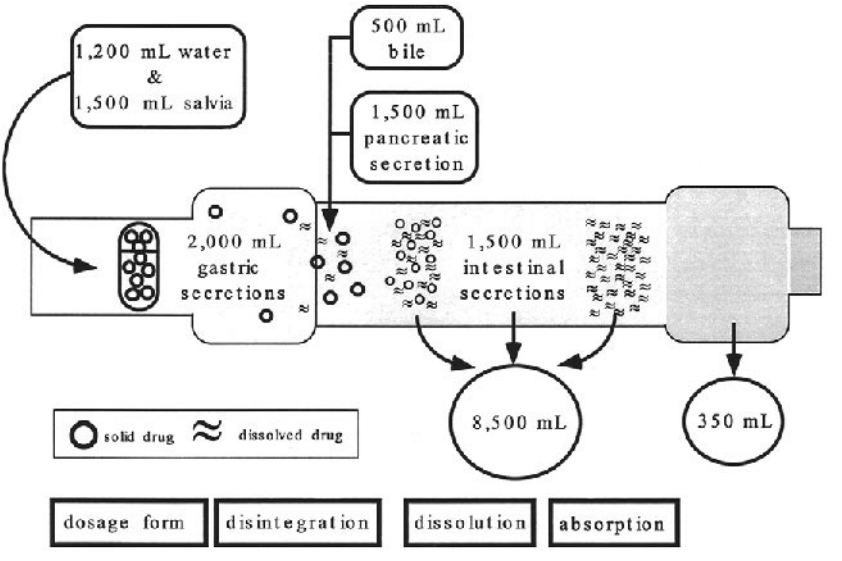

FIG. 5 Gastrointestinal transit of a dosage form and the volume of gastrointestinal fluids available to dissolve the drug.

these secretions is about 5–6 L/day, and they are essential for the digestion of food.

These fluids offer an enormous spectrum of pH-dependent hydrolysis and enzymatic activities that a drug has to withstand. The influence of such enzymatic and hydrolytic degradation on the calculation of fraction dose absorbed has been reviewed (4). On the other hand, the composition of these intestinal fluids offers a high capacity for solubilization of lipophilic and poorly soluble drugs to facilitate their uptake (12,13). A simulation of these in vivo conditions can be used to predict the availability of a drug. An in vitro dissolution medium that can simulate the in vivo dissolution would be an important tool for the prediction of bioequivalence or in vitro–in vivo correlations of poorly soluble drugs.

Many of the pharmaceutically useful surfactants and emulsifiers are efficient solubilizers (14). Surfactants that have been used for this purpose include sodium lauryl sulfate (SLS), dodecyltrimethylammonium bromide (DTAB), and Tween 20 (TW20). In addition to the solubilization of drugs into micelles, the ability of these substances to form emulsions can increase the dissolved amount of a lipophilic drug.

The micelle-facilitated dissolution is shown in Eq. (8).

$$\begin{aligned} \phi &= J_{\mathrm{Tot}}/J_s = (D_{\mathrm{eff}}^{2/3}/D_s^{2/3})(C_{\mathrm{tot}}/C_s) \\ k^* &= C_{sm(0)}/C_{s(0)}C_{m(b)} \end{aligned} \tag{8}$$

where J_{Tot} is the total flux, J_s is the flux in the solvent, D_{eff} is the effective diffusivity, D_s the diffusivity in the solvent, C_{tot} is the total concentration, and C_s is the solubility. The equilibrium coefficient is k*, $C_{\mathrm{sm(0)}}$ is the concentration of the drug-loaded micelle, the subscript (0) denotes the surface for the solid, and $C_{\mathrm{m(b)}}$ is the concentration of surfactant in the bulk solution.

As shown in Fig. 6 the enhancement of solubilization using surfactants can be up to 140-fold compared with simple aqueous solution. The highest solubility enhancement was achieved in this experiment using 0.06 M SLS, whereas TW 20 showed only a 20-fold enhancement. The effect of electrolytes, such as sodium chloride, on the solubility of griseofulvin was small, but for other drugs could also be significant.

Compared with the high enhancement of solubility, the flux enhancement of the micelle system is only up to 40-fold (15). The reason that the dissolution rate was increased only 40-fold while the solubility was increased 140-fold is because the diffusion coefficient of the micelle system is about one-third to one-fourth of the diffusion coefficient of a solution (14). At high surfactant concentrations the solute is in the micelle and the micelle, owing to its size, diffuses more slowly.

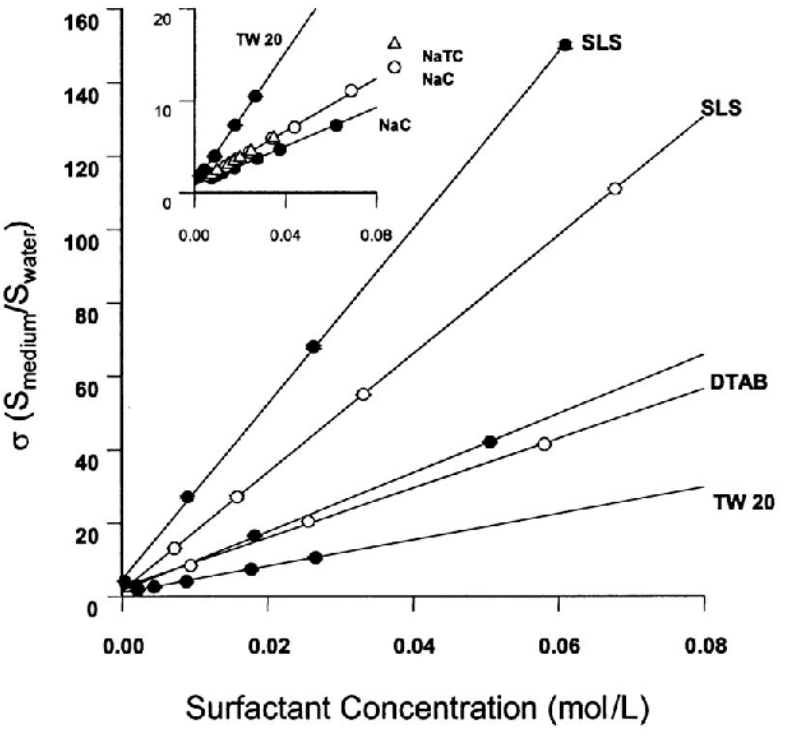

FIG. 6 σ (griseofulvin solubility enhancement factor at 37°C) as a function of surfactant concentration (total surfactant; CMC) in water (●) and in 0.15 NaCl (○). (From Ref. 18.)

In the gut, the presence of bile salts, lecithins, and other lipids can increase the solubility of drug substances (11,12), but often with less efficiency than pharmaceutical surfactants and their grade of purity (16), as shown in Fig. 6. Another factor to consider is that in vivo the micelle formation is dependent on several physiological factors (e.g., pH, bile concentration, and lecithin content). The intake of food results in greater secretion of bile, leading to an increase in the formation of micelles and, consequently, in the solubility of many drugs (17).

The next step to simulate the in vivo situation is to investigate oil–water (O/W) emulsion systems and their influence on the dissolution rate and solubility enhancement of drugs. In a micelle system surfactants group in relatively small clusters, whereas an O/W emulsion is characterized not only by

the presence of micelles, but also much larger lipid droplets, which are encased and stabilized by surfactants. The drug can diffuse into the lipid phase of the emulsion or can be solubilized by the micelles. Modeling drug behavior in O/W emulsions is complex because, owing to the surfactant and its structure at the interface between water and lipid phase, we have to consider the interfacial barrier as well as diffusion within the lipid droplet as potential resistances (18). Furthermore, in an emulsion, we expect a lower micelle concentration at a given total surfactant concentration because some surfactant is consumed by the lipid droplets. The droplet size and the viscosity of the emulsion system could also result in a decrease in the diffusivity, as shown before for micellar

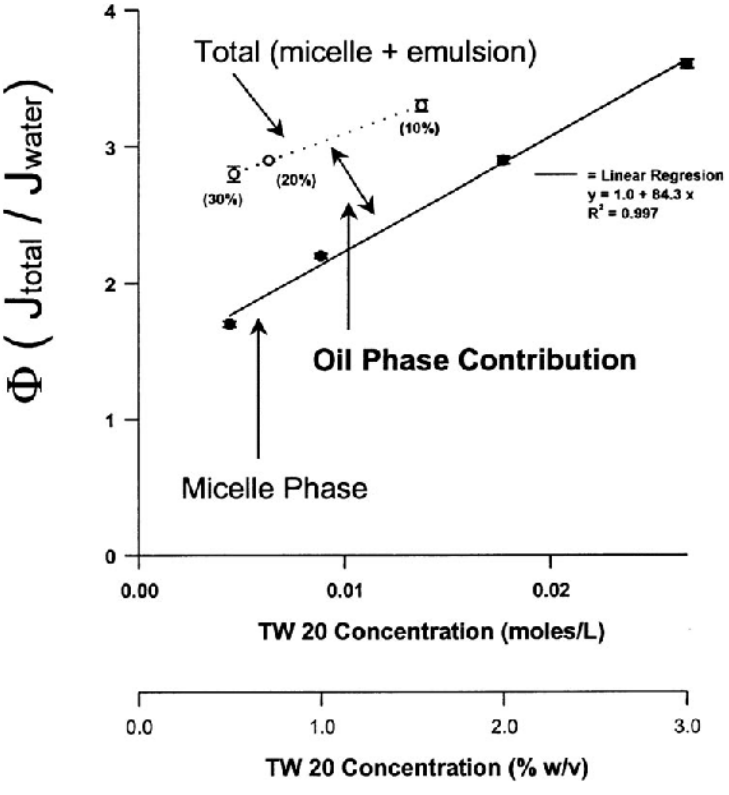

FIG. 7 Φ (griseofulvin flux enhancement factor): Closed symbols represent TW 20 solutions, open symbols represent emulsions plotted as a function of the apparent TW 20 concentration in the emulsion aqueous phase. (From Ref. 15.)

systems. In summary, an overall slower mass transport in an emulsion compared with that in a micellar system is expected.

Figure 7 shows the contribution of the oil phase on the flux of griseofulvin at the same surfactant content. From these results it can be concluded that the flux of a drug can be increased by its incorporation in an emulsion. The high efficiency of the oil phase to solubilize lipophilic drugs combines with solubilization by the micelle system to outweigh the expected decrease in the diffusivity. In general, an emulsion medium will have only a small effect on the dissolution rate, but offers a significant improvement in the overall solubilization of a lipophilic drug.

IV. IN VITRO–IN VIVO CORRELATIONS

In vitro–in vivo correlations (IVIVC) are becoming more and more important because bioequivalence of changes in drug products can be approved by in vitro tests according to the SUPAC (scale-up and postapproval changes) guidelines. In the future it can be expected that generic drug products will be approved solely on the basis of in vitro data if an IVIVC has been established. This will accelerate the regulatory process, because bioequivalence studies will not always have to be conducted.

To establish IVIVC it is necessary that the chosen in vitro method can reflect the in vivo plasma profile. A precise knowledge of the in vivo situation is key to determining whether an IVIVC can be established, with drug solubil-

TABLE 3 In Vitro–In Vivo Correlation Expectations for Immediate-Release Products Based on the Biopharmaceutics Classification Scheme

Class	Solubility	Permeability	IVIV correlation expectation
I	High	High	IVIV correlation if dissolution rate is slower than gastric emptying rate, otherwise limited or no correlation.
II	Low	High	IVIV correlation expected if in vitro dissolution rate is similar to in vivo dissolution rate, unless dose is very high.
III	High	Low	Absorption (permeability) is rate-determining and limited or no IVIV correlation with dissolution rate.
IV	Low	Low	Limited or no IVIV correlation expected

ity, dissolution, and gastrointestinal permeability as the fundamental parameters for correlating the in vitro with the in vivo data. On the in vivo side, we have to consider that, in addition to the permeability, the motility can also impinge on the availability of the drug (Table 3).

For poorly soluble drugs the transit time at the absorption site is an important factor for bioavailability. The transit time of dosage forms was investigated (19), and the mean transit time in the small intestine was determined as about 4 h. On the other hand, these results pointed out that the gastric emptying was very variable. The gastric emptying depends on the phase of the interdigestive migrating myoelectric complex (IMMC) and the amount of coadministered water (Fig. 8); 200 mL of water generally caused a faster gas-

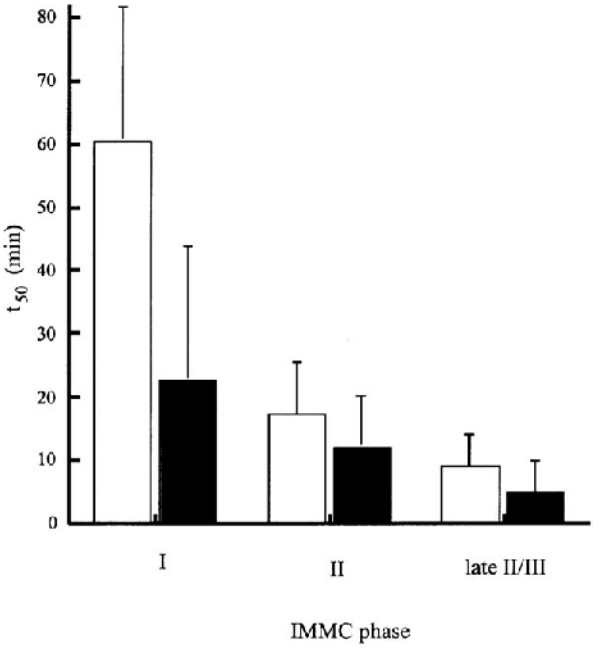

FIG. 8 Comparison of gastric emptying half-time (T_{50}) after administration of 50- (open bars) and 200-mL (filled bars) volumes in IMMC phase I, II, and late II/III. Data are expressed as mean ± SD. There was a statistical difference in T_{50} between 50- and 200-mL volumes during phase I and late II/III. These results show that differences in gastric emptying rates depend on the volume administered in addition to the extant IMMC phase. (From Ref. 25.)

tric emptying than did 50 mL (20). The total transit time of a dosage form in the gastrointestinal tract was investigated (21) using the nondegradable Oros pump system. The average passage time of this dosage form was about 1 day to 30 h, which shows that the transit time in the major absorption site, the small intestine, is less than one-sixth of the total residence time in the GI tract.

In consequence, the absorption pattern in the colon of poorly soluble drugs and drugs in controlled-release dosage forms have to be determined to estimate the fraction dose absorbed and to establish IVIVC. In the colon, the absorption as well as enzymatic and bacterial decomposition of drugs varies compared with the small intestine (22,23).

Presently, for the low-solubility, high-permeability drugs that commonly come from drug discovery, we expect an IVIVC if the in vitro dissolution rate is similar to the in vivo dissolution rate. Here in vitro dissolution and in vivo dissolution are important parameters unless the dose is very high.

In contrast with poorly soluble drugs and controlled-release dosage forms, the gastric-emptying and small-intestine–transit time will not influence the fraction dose absorbed of highly soluble, highly permeable drugs because those drugs will normally be absorbed within the gut passage. For these compounds, the gastric emptying will alter T_{max} and probably also C_{max}, and, if this occurs, it is unlikely that a satisfactory IVIVC can be achieved.

In general, an IVIVC can be expected if the dissolution rate of a drug is slower than gastric emptying (class II and IV). Otherwise there is limited or no correlation because the absorption rate of a class I drug will be regulated by the variable gastric emptying and, for a class III drug, the permeability limits the uptake.

REFERENCES

1. Amidon GL, Lennernas H, Shah VP, Crison JR. A theoretical basis for a biopharmaceutic drug classification: the correlation of in vitro drug product dissolution and in vivo bioavailability. Pharm Res 1995; 12:413–420.
2. Sinko PJ, Leesman GD, Amidon GL. Predicting fraction dose absorbed in humans using a macroscopic mass balance approach. Pharm Res 1991; 8:979–988.
3. Sinko PJ, Leesman GD, Waclawski AP, Yu H, Kou JH. Analysis of intestinal perfusion data for highly permeable drugs using a numerical aqueous resistance–nonlinear regression method. Pharm Res 1996; 13:570–576.
4. Yu LX, Lipka E, Crison JC, Amidon GL. Transport approaches to the biopharmaceutical design of oral drug delivery systems: prediction of intestinal absorption. Adv Drug Deliv Rev 1996; 19:359–376.

5. Oh DM, Curl RL, Amidon GL. Estimating the fraction dose absorbed from suspensions of poorly soluble compounds in humans: a mathematical model. Pharm Res 1993; 10:264–270.
6. Dressman JB, Amidon GL, Fleisher D. Absorption potential: estimating the fraction absorbed for orally administered compounds. J Pharm Sci 1985; 74:588–589.
7. Dressman JB, Fleisher D. Mixing-tank model for predicting dissolution rate control or oral absorption. J Pharm Sci 1986; 75:109–116.
8. Greenblatt DJ, Smith TW, Koch-Weser J. Bioavailability of drugs: the digoxin dilemma. Clin Pharmacokinet 1976; 1:36–51.
9. Jounela AJ, Pentikainen PJ, Sothmann A. Effect of particle size on the bioavailability of digoxin. Eur J Clin Pharmacol 1975; 8:365–370.
10. Oh DM, Curl R, Yong C, Amidon GL. Effect of micronization on the extent of drug absorption from suspensions in humans. Arch Pharm Res 1985; 18:427–433.
11. Dressman JB, Amidon GL, Reppas C, Shah VP. Dissolution testing as a prognostic tool for oral drug absorption: immediate release dosage forms. Pharm Res 1998;15:11–22.
12. Bakatselou V, Oppenheim RC, Dressman JB. Solubilization and wetting effects of bile salts on the dissolution of steroids. Pharm Res 1991; 8:1461–1469.
13. Mithani SD, Bakatselou V, TenHoor CN, Dressman JB. Estimation of the increase in solubility of drugs as a function of bile salt concentration. Pharm Res 1996; 13:163–167.
14. Crison JR, Shah VP, Skelly JP, Amidon GL. Drug dissolution into micellar solutions: development of a convective diffusion model and comparison to the film equilibrium model with application to surfactant-facilitated dissolution of carbamazepine. J Pharm Sci 1996; 85:1005–1011.
15. Vieira M. Dissertation. University of Michigan, 1998.
16. Crison JR, Weiner ND, Amidon GL. Dissolution media for in vitro testing of water insoluble drugs: effect of surfactant purity and electrolyte on in vitro dissolution of carbamazepine in aqueous solutions of sodium lauryl sulfate. J Pharm Sci 1997; 86:384–388.
17. Charman WN, Porter CJ, Mithani SD, Dressman JB. The effect of food on drug absorption—a physicochemical and predictive rationale for the role of lipids and pH. J Pharm Sci 1997; 86:269–282.
18. Amidon GL, Choe SY, Vieira M, Oh DM. Solubility, intrinsic dissolution and solubilization: influence on absorption. In: Amidon GL, Robinson JR, Williams RL, eds., Scientific Foundations for Regulating Drug Product Quality. Alexandria: AAPS Press, 1997:99–113.
19. Davis SS, Hardy JG, Fara JW. Transit of pharmaceutical dosage forms through the small intestine. Gut 1986; 27:886–892.
20. Oberle RL, Amidon GL. The influence of variable gastric emptying and intestinal transit rates on the plasma level curve of cimetidine; an explanation for the double peak phenomenon. J Pharmacokinet Biopharm 1987; 15:529–544.

21. John VA, Shotton PA, Moppert J, Theobold W. Gastrointestinal transit of Oros drug delivery systems in healthy volunteers: a short report. Br J Clin Pharmacol 1985; 19:203S–206S.
22. Ashford M, Fell JT. Targeting drugs to the colon: delivery systems for oral administration. J Drug Target 1994; 2:241–257.
23. Dressman JB, Bass P, Ritschel WA, Friend DR, Rubinstein A, Ziv E. Gastrointestinal parameters that influence oral medications. J Pharm Sci 1993; 82:857–872.
24. Lipka E, Crison J, Amidon GL. Transmembrane transport of peptide type compounds: prospects for oral delivery. J Controlled Release 1996; 39:121–129.
25. Oberle RL, Chen TS, Lloyd C, Barnett JL, Owyang C, Meyer J, Amidon GL. The influence of the interdigestive migrating myoelectric complex on the gastric emptying of liquids. Gastroenterology 1990; 99:1275–1282.

10

Dissolution Testing of Immediate-Release Products and Its Application to Forecasting In Vivo Performance

Jennifer B. Dressman
Johann Wolfgang Goethe University, Frankfurt on Main, Germany

I. GOALS OF DISSOLUTION TESTING

The goal of dissolution testing is to assure the pharmaceutical quality of the product. By pharmaceutical quality we mean not only the ability to manufacture the product reproducibly and to ensure that it maintains its release properties throughout the shelf life, but also that the product's biopharmaceutical characteristics, such as rate and extent of absorption, can be relied on. It would, therefore, be desirable to develop dissolution tests that can assess the ability of the dosage form to release the drug completely and to simultaneously indicate how the product will perform in vivo.

A. Quality Control Tests

Current compendial dissolution tests were for the most part developed with the aim of studying the physical properties of the dosage form. The overriding concern for the quality control test is to use conditions under which 100% of the drug can be released. Further important considerations are the reliability and reproducibility of the test and, particularly, for high-volume products, the possibility of automating the test. Consequently, the use of the simplest medium possible is preferred.

B. Biopharmaceutical Studies

In recent years the costs of pharmacokinetic studies have increased dramatically. Substitute studies in whole-animal models are often unsatisfactory. Although several species have gastrointestinal (GI) tracts that are similar in many ways to that of humans (see Chapter 6) differences in seemingly minor details can lead to a lack of correlation between results in animals and those in humans. Furthermore, ethical considerations demand that the number of animals used in research be minimized. Therefore, there is increasing interest in the development of dissolution tests to establish in vitro–in vivo correlations (IVIVC). When the dissolution test is to indicate the biopharmaceutical properties of the dosage form, it is more important that the test closely simulate the environment in the GI tract than necessarily produce sink conditions for release. Consequently, it is not always possible to meet the needs of both quality assurance and biopharmaceutical aspects with one dissolution test.

II. WHICH FACTORS CAN LIMIT BIOAVAILABILITY AFTER ORAL ADMINISTRATION?

As the diagram in Fig. 1 illustrates, a variety of factors can determine the rate and extent of drug absorption following oral administration. These include

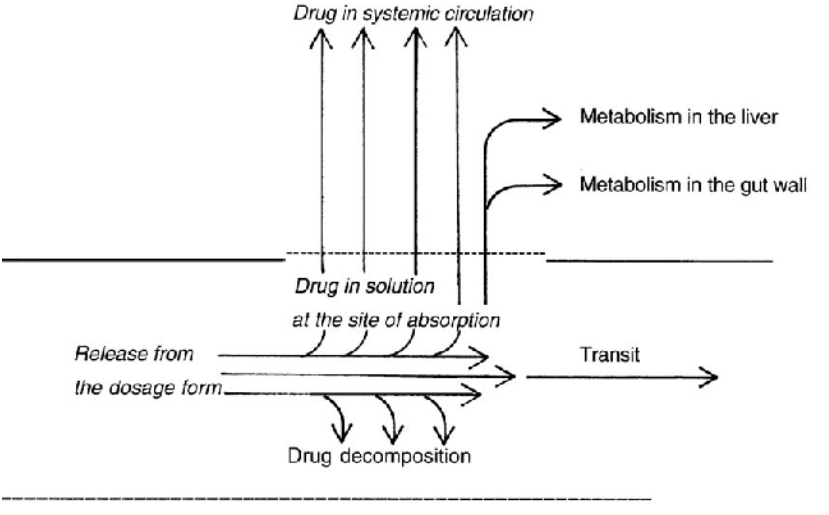

FIG. 1 **Factors that can limit the oral bioavailability of drugs.**

Table 1 The Biopharmaceutics Classification Scheme (BCS)

Class 1	Class 2
High solubility	Low solubility
Good permeability	Good permeability
Class 3	Class 4
High solubility	Low solubility
Poor permeability	Poor permeability

Source: Ref. 1.

slow release of the drug from the dosage form, instability of the drug in the GI tract, poor permeability of the GI mucosa to the drug, and first-pass metabolism of the drug in the gut wall or liver. In principle, dissolution tests can be used to predict the in vivo performance of the dosage form when release of the drug is the limiting factor in the absorption process. There are two classic cases in which release is limiting to absorption: controlled-release (CR) dosage forms and immediate-release (IR) dosage forms containing drugs that are poorly soluble.

The Biopharmaceutics Classification Scheme (Table 1) (1) can be used as a guide to determine whether an IVIVC can be expected for an immediate-release product.

According to the BCS, drugs are classified according to their permeability and solubility to assess whether or not an IVIVC can be attained. The intent of the BCS was originally to determine whether a biowaiver could be made on the basis of dissolution tests for a product that had undergone a scale-up or postapproval change (2). Classification of a drug according to the BCS can also be used as a practical starting point to select suitable dissolution test conditions for new drug products. The remainder of this chapter will be devoted to the selection of appropriate dissolution tests on the basis of the BCS classifications.

III. SELECTION OF DISSOLUTION TEST MEDIA BASED ON THE BCS

A. Class 1 Substances

Substances that belong to class 1 possess good aqueous solubility and are easily transported through the GI mucosa. Their bioavailability after oral dos-

ing, therefore, is usually close to 100%, provided they are not decomposed in the GI tract and do not undergo extensive first-pass metabolism. Acetaminophen and metoprolol are typical examples of class 1 drugs (Fig. 2).

Dissolution behavior of class 1 substances is typified by the release profiles shown in Fig. 3 (3). Irrespective of the medium, close to 100% release is quickly achieved. Because the absorption rate of a class 1 substance is usually limited by nondosage–form-related factors, such as gastric emptying, it is rarely possible to achieve an IVIVC for immediate-release dosage forms of class I substances. Nevertheless, dissolution testing can be used to verify that the dosage form functions sufficiently well that release is not a limiting factor to absorption. As a result, the U. S. Food and Drug Administration (FDA) now recommends a one-point test in a simple medium, with 85% or more of the drug to be released within 30 min for immediate-release dosage forms of class 1 drugs. Satisfactory release behavior under these conditions can then form the basis for a biowaiver in a scale-up or postapproval change (SUPAC) in the formulation.

After administration, the dosage form quickly passes into the stomach and, usually, disintegrates there, so it is logical to use a dissolution medium that reflects the gastric conditions. Simulated gastric fluid [SGF; *USP* 24 (4)], without enzymes, is suitable for many immediate-release dosage forms of class I compounds. For some capsules, an enzyme (pepsin) may have to be added to the medium to ensure timely dissolution of the shell. Alternatively, dissolu-

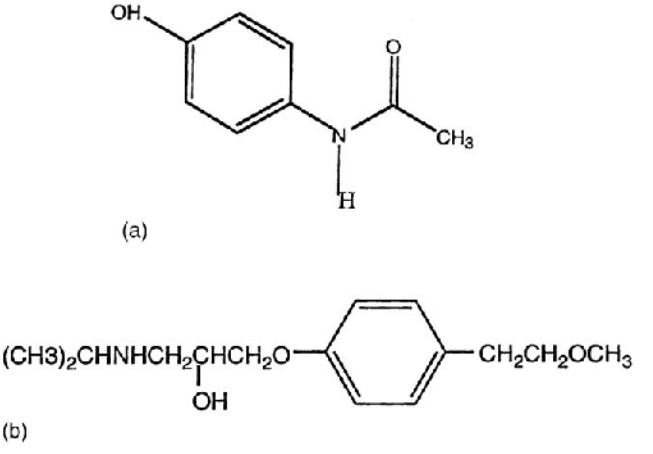

FIG. 2 Structures of (a) acetaminophen and (b) metoprolol.

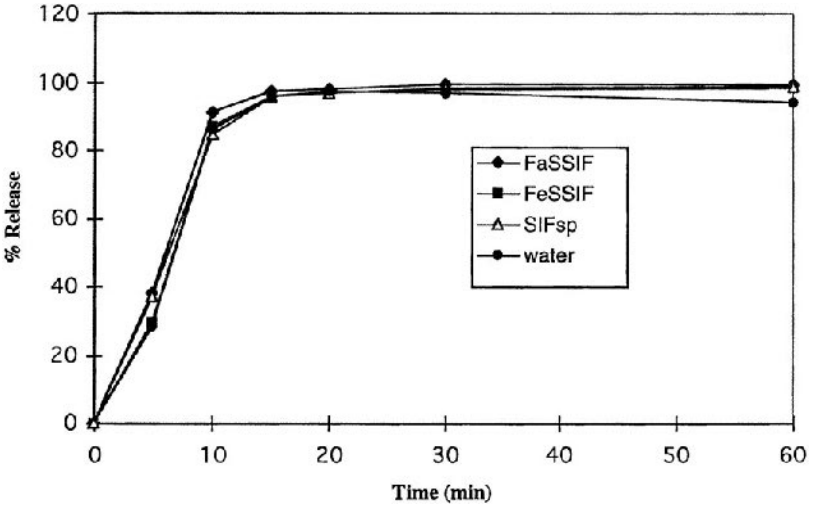

FIG. 3 Dissolution of acetaminophen (Panadol) tablets in water SIF_{sp} (*USP*), FaSSIF, and FeSSIF at 100 rpm in a paddle apparatus. (From Ref. 3.)

tion in a simple medium formulated at the pH of the small intestine (e.g., simulated intestinal fluid, *USP*, without enzymes) can be used. This medium is particularly suitable for formulations containing weak acids, the dissolution of which may be hampered by the low pH of SGF. Water is a less suitable medium than the aforementioned buffers, because it has a nominal buffer capacity of zero; therefore, the pH may vary during the test, if any of the excipients or drug(s) have acid or base properties, as well as from test to test. [One of the few justifiable applications of water as a dissolution medium for immediate-release dosage forms would be for the simulation of dissolution under hypochlorhydric conditions.] More complex, biorelevant media (e.g., FaSSIF and FeSSIF; see Sect. III.B.3.) are unnecessary for dissolution of class 1 drugs, and because of their expense and the more time-consuming preparation and analysis required, their use for the dissolution of class I drugs is not warranted.

B. Class 2 Substances

Class 2 drugs are poorly soluble in aqueous media, but are easily transported across the gut mucosa. This is a common combination, because the poor solubility of many compounds is directly associated with good lipophilicity which, in turn, encourages transport of the molecule across the lipid bilayer of the

absorptive cells lining the intestine. Examples may be found in a wide variety of therapeutic categories, including antifungals, steroids, nonsteroidal anti-inflammatory drugs (NSAIDs), cardiovascular agents, and antidiabetics (Fig. 4).

Compounds can be defined as being poorly soluble when their dissolution rate is the limiting factor to their oral bioavailability. An aqueous solubil-

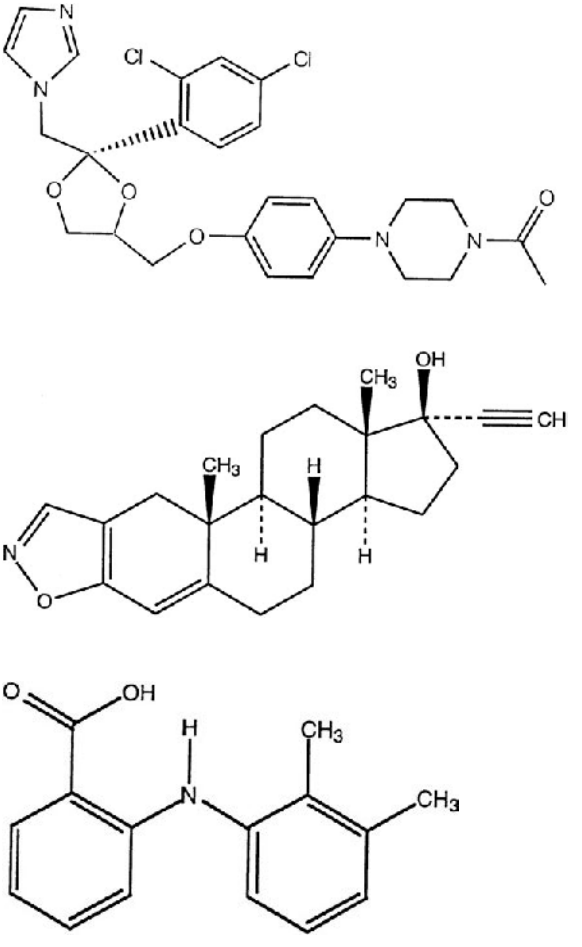

FIG. 4 Some examples of poorly soluble, lipophilic compounds (probably class II), top to bottom: ketoconazole, danazol, and mefenamic acid.

ity of less than 100 μg/mL is often a signal that dissolution of the drug will be problematic in vivo. The *dose/solubility* ratio, defined as

$$D/S = \frac{\text{dose (mg)}}{\text{aq. solubility (mg/mL)}}$$

indicates whether conditions in the GI tract are optimal for drug dissolution. It yields the volume of liquids, in milliliters, that is required to dissolve the entire dose of the drug. When this ratio exceeds the actual volume of GI fluids available, one can expect that dissolution and, therefore, absorption will not be complete. The FDA uses a *D*/*S* of 250 mL in its SUPAC guidance (2) as the cutoff value for compounds with good solubility. When the *D*/*S* exceeds 250 mL, it is probable that sink conditions do not prevail in vivo and that dissolution will be a limiting factor to the compound's absorption.

To illustrate the behavior of a class 2 drug, the dose/solubility ratio for griseofulvin can be calculated. Its aqueous solubility of 15 μg/mL at 37°C combined with a dose of 500 mg, results in a *D*/*S* of approximately 33 L. On the basis of griseofulvin's *D*/*S* and distribution coefficient of log $P = 2.18$, it is reasonable to assume that griseofulvin falls under class 2 of the BCS, a classification that is in agreement with the demonstrated dependency of griseofulvin absorption on its particle size (5) and formulation (6).

Suitable, biorelevant media for class 2 drugs include SGF_{sp} plus surfactant, to simulate fasted state in the stomach, Ensure or milk (3.5% fat) to simulate fed state in the stomach, and two newly developed media, FaSSIF and FeSSIF, to simulate fasted and fed state in the small intestine, respectively.

1. SGF_{sp} Plus Surfactant

SGF_{sp} plus surfactant is particularly suitable for weak bases, because these are most soluble under acidic conditions (Fig. 5).

Typical examples of class 2 bases include ketoconazole (pK_a values = 6.5 and 2.9) and dipyridamole ($pK_a = 6.4$). Their structures are shown in Figs. 4 and 6, respectively. In the fasted state, the absorption of both compounds is highly dependent on gastric pH (7,8). Hypochlorhydria, either as a result of aging or cotherapy with gastric acid blockers, is associated with very poor absorption. In addition, the presence of surfactant in the gastric fluids may play a role in the wetting and solubilization of poorly soluble acids in the stomach. Figure 7 shows data for the pH and surface tension of aspirated gastric fluids in humans (9). The low surface tension in the gastric juice was first reported by Finnholt et al. in 1968 (10). Recently, those results were verified by Efentakis (9), who also demonstrated a lack of correlation between

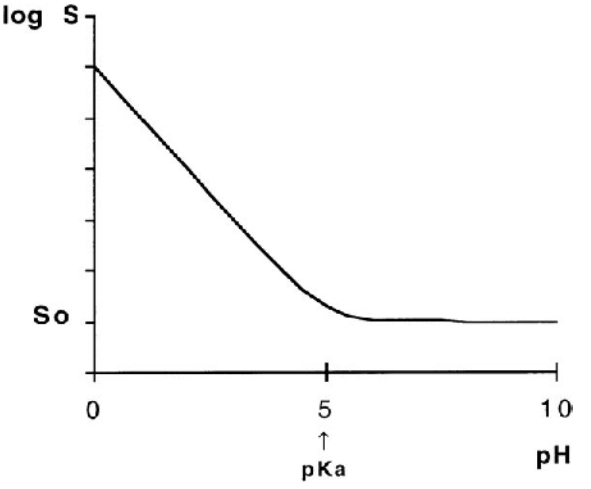

FIG. 5 Relation between the solubility of a weak base and the pH value of the medium.

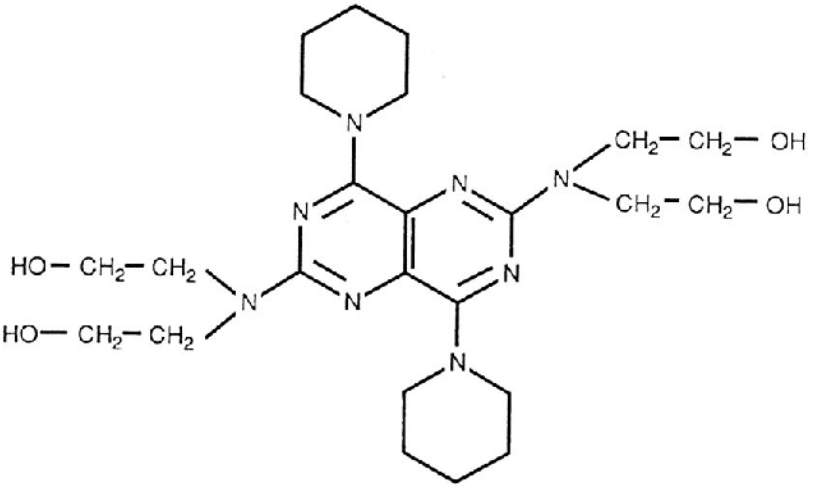

FIG. 6 Structure of dipyridamole.

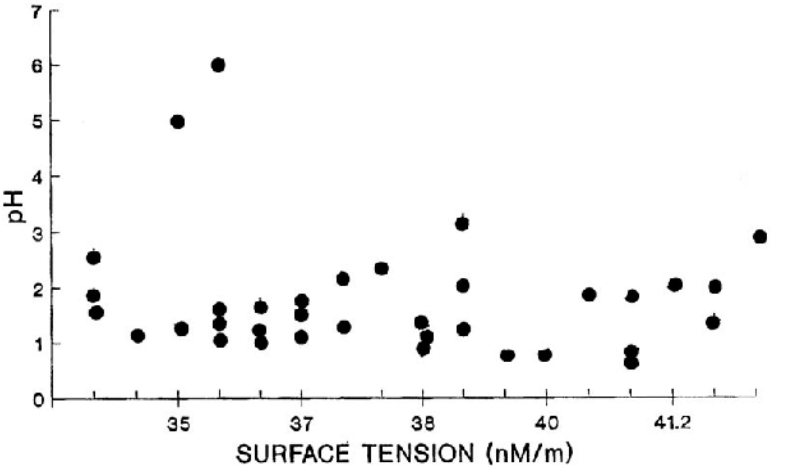

FIG. 7 pH and surface tension in the stomach in the fasted state. (From Ref. 9.)

the lower surface tension and presence of bile salts in the aspirate. These results indicated that other sources of surfactant besides refluxed bile must exist, but these have not yet been identified. Meanwhile, to simulate the gastric fluids better than is possible with the standard compendial medium, one can use a synthetic surfactant system to lower the surface tension appropriately.

The surfactant must be able to reduce the surface tension to an appropriate value (35–40 mNm^{-1}). A sample composition for SGF_{sp} with surfactant is given in Table 2. The range of hydrochloric acid concentrations reflects the usual range of pH values found in young healthy volunteers (11). Although the composition is given for 1 L, the volume of fluids in the fasted stomach is usually only on the order of 30–50 mL. Adding the contribution from the coadministered fluid, one reaches a total volume of about 250–300 mL, suggesting that the lowest volume practicable (300–500 mL) should be used with the *USP* I or II method to obtain physiologically representative results.

TABLE 2 Sample Composition for SGF_{sp} with Surfactant

HCl	0.01–0.05 M
Triton X-100	0.01% (equiv. to 40 mN/m)
NaCl	0.2%
Water	qs. ad 1 L

The solubilizing capacity of the surfactant is also important. If the surfactant solubilizes the drug too well, it may not be possible to discriminate adequately between formulations. Yet, if no surfactant is employed, the release rate may be lower in vitro than in vivo. Figure 8 illustrates the influence of the surfactant Triton X-100 on the release rate of several albendazole products in SGF_{sp} (12).

2. Ensure and Milk as Dissolution Media

Ensure and milk can be used during drug development to approximate conditions in the postprandial stomach. Both media contain similar ratios of protein/fat/carbohydrate to that found in a typical Western diet. Mechanisms by which Ensure and milk can improve drug solubility include solubilization of the drug in the fatty part of the fluid, solubilization in caseine micelles (milk) and, for weak acids, the favorably high pH values.

These two media are suitable only for IVIVC purposes: difficulties in filtering and separating the drug from the medium make these media unsuitable for routine quality assurance testing.

3. FaSSIF and FeSSIF

Two media have recently been developed to simulate intestinal conditions in the fasted and fed state. The compositions of these media, FaSSIF and FeSSIF, are given in Tables 3 and 4, and were based on literature and experimental data in dogs and humans (13) for the concentration of bile components, pH value, buffer capacity and osmolarity.

The two media are particularly useful for forecasting the in vivo dissolution of poorly soluble drugs from different formulations and for assessing potential for food effects on in vivo dissolution (see Sec. III.B.4). The closer simulation of physiological conditions makes them more suitable for IVIVC applications than the usual compendial media. Similar to Ensure and milk, they are intended for use at the development level and not for routine quality control purposes, owing to their expense and the amount of effort needed to separate the compound from the medium for analytical purposes.

The dissolution rate of a poorly soluble drug is often better in FaSSIF and FeSSIF than in simple aqueous buffers because of the increased wetting of the drug surface and micellar solubilization of the drug by the bile components. Examples of drugs for which addition of bile components to the media is known to improve dissolution rate include griseofulvin, digoxin, leukotriene-D_4 antagonists, gemfibrozil, diazepam, cyclosporine, pentazocine, and dana-

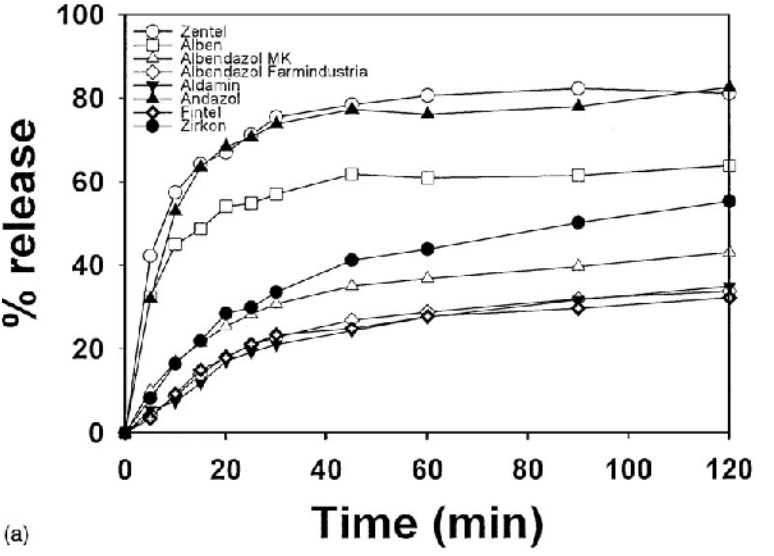

(a)

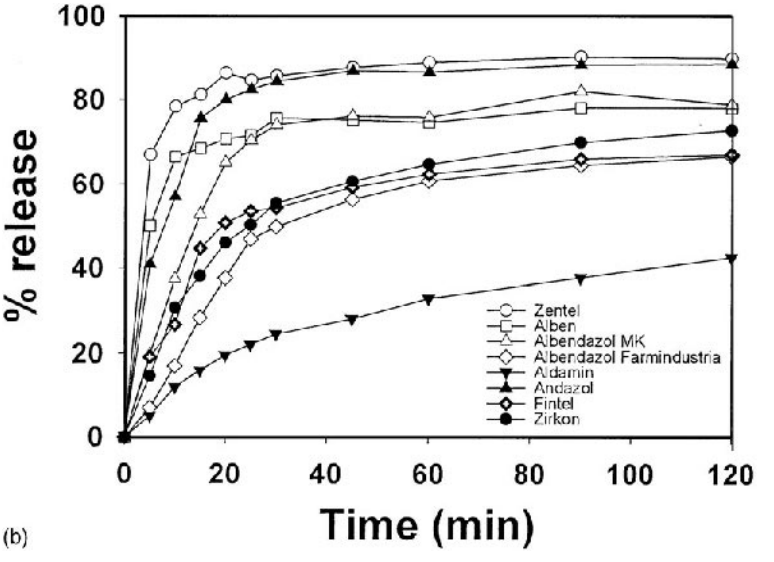

(b)

FIG. 8 Dissolution profiles of various albendazole products in acidic media (SGF_{sp}): upper panel without and lower panel with 0.1% Triton X-100.

Table 3 Composition of FaSSIF*

KH_2PO_4		3.9 g
Na taurocholate		3 mM
Lecithin		0.75 mM
KCl		7.7 g
NaOH	qs	pH 6.5
Distilled water	qs	1 L

* pH, 6.5; osmolarity, 270 ± 10 mOsm.

zol. Drug lipophilicity plays a role in the ability of bile salts to improve drug solubility. At log *P* values below about 1.5–2, the presence of bile salts appears to exert little effect on drug solubility. For more lipophilic compounds, however, there is a very close, log–log correlation between the partition coefficient and solubilization capacity of the bile salts for the drug. This relation is illustrated in Fig. 9 (14).

Because FaSSIF and FeSSIF combine a higher pH value with the possibility of micellar solubilization, they are especially suitable for studying the dissolution of poorly soluble weak acids. For example, many NSAIDs are weak acids, with pK_a values in the range 3.5–4.5. These drugs tend to dissolve very slowly under gastric conditions, but at intestinal pH and buffer capacity values, their dissolution rates can be several orders of magnitude higher.

The appropriate volume of medium to use depends on the conditions of administration. In the fasted state the intestine contains relatively little fluid, because the paraintestinal organs are secreting at essentially baseline rates. By contrast, when a drug is administered in the fed state, the volume of coadministered fluid is supplemented by the volume of fluid ingested with the meal and by secretions of the stomach, pancreas, and bile, all of which can easily

Table 4 Composition of FeSSIF*

Acetic acid		8.65 g
Na taurocholate		15 mM
Lecithin		3.75 mM
KCl		15.2 g
NaOH	qs	pH 5
Distilled water	qs	1 L

* pH, 5.0; osmolarity, 635 ± 10 mOsm.

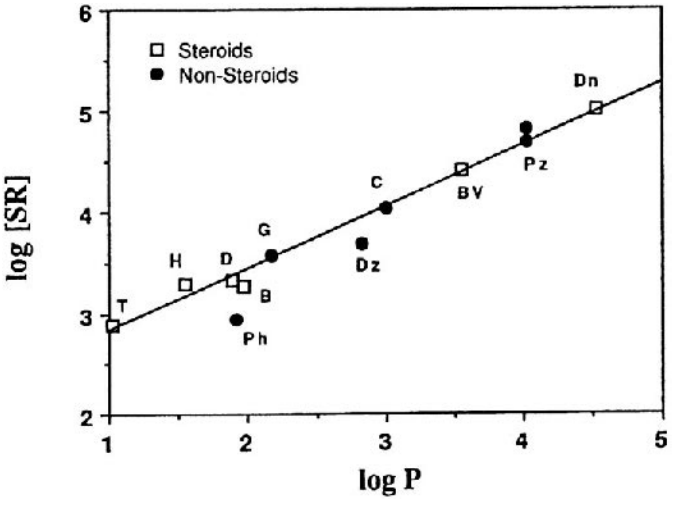

FIG. 9 Double logarithmic plot of the dependency of the solubilization capacity of sodium taurocholate for a drug on its lipophilicity (log *P* value). (From Ref. 14.)

achieve near maximal rates in response to meal intake. In addition, depending on whether the meal is hypo- or hypertonic, there may be net absorption or secretion of water across the intestinal wall. As a result, postprandial volumes in the upper small intestine as high as 1.5 L have been measured (15). These differences between fasted and fed state are particularly important when designing tests to assess the potential for food effects on in vivo release and absorption.

4. Dissolution Behavior of Various Class 2 Substances in the Different Media

The dissolution behaviors of ketoconazole, danazol, mefenamic acid, and troglitazone are shown in Fig. 10 (3,16).

In stark contrast to the behavior of class I compounds, the dissolution behavior of Class 2 compounds is highly dependent on the dissolution medium. Figure 10a shows that dissolution of the weak base ketoconazole is quickest under simulated fasted-state gastric conditions (900 mL), with practically no dissolution in FaSSIF (500 mL). Results also suggest that when the drug is taken after meals, the small intestine becomes an important site of dissolution (FeSSIF, 500 mL), accounting for the relatively good postprandial

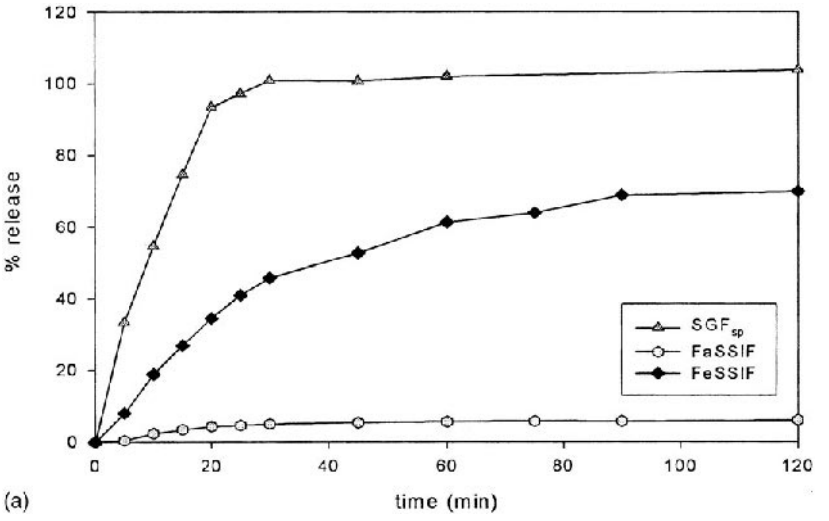

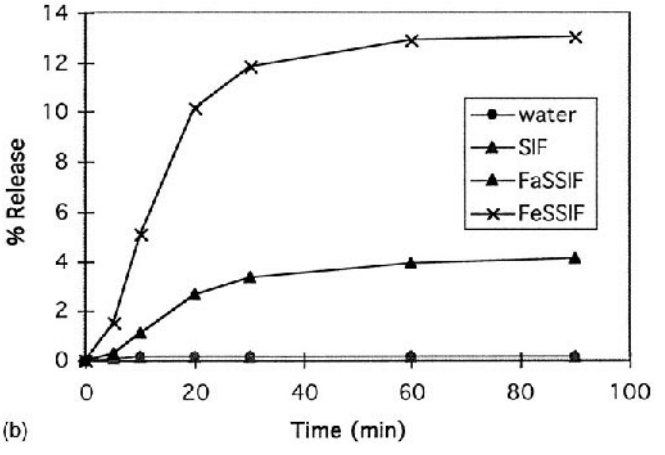

FIG. 10 Dissolution profiles of (a) ketoconazole, (b) danazol, (c) mefenamic acid, and (d) troglitazone in various media.

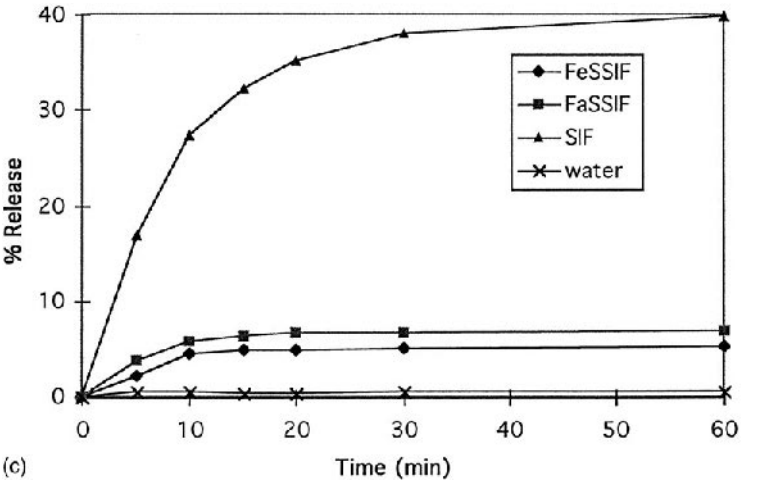

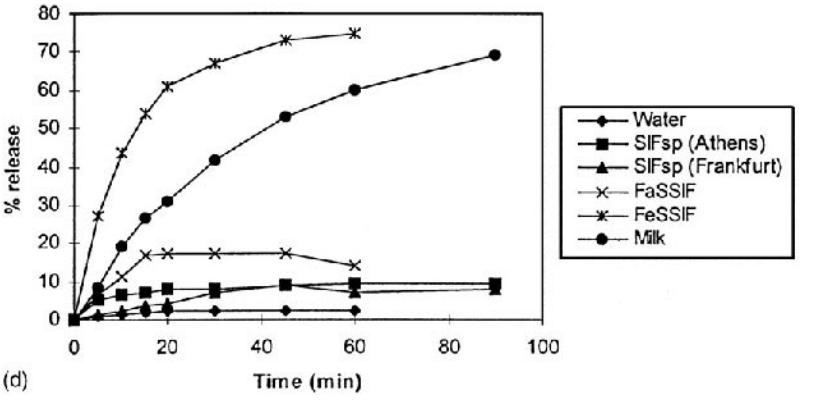

bioavailability of this compound. Had the volumes used been closer to the physiological values, the results would have concurred even more closely with results of bioavailability studies (8,17). Results with danazol in FaSSIF and FeSSIF were in excellent agreement with those of pharmacokinetic studies, which showed a threefold increase in C_{peak} and area under the concentration–time curve (AUC) when danazol was administered with food (18). By contrast, dissolution results in SIF incorrectly predicted a total lack of bioavailability for danazol.

Dissolution data for the two weak acids, mefenamic acid and troglitazone, make for an interesting comparison. Results in FaSSIF and FeSSIF for mefenamic acid (pK_a 4.2) were similar and agreed with the lack of influence of food on the absorption of this NSAID (3). By contrast, troglitazone dissolution was dramatically enhanced in FeSSIF compared with FaSSIF. These results were in accordance with the higher bioavailability of the antidiabetic agent when given with food (Fig. 11). Because of its higher pK_a values (pK_{a1} = 6.1; pK_{a2} = 12.0), the change in bile salt concentration from fasted- to fed-state conditions more than outweighed the unfavorable decrease in pH value. The influence of the higher pK_a values can also be seen in the low dissolution rate in SIF_{sp} (at the time of the study SIF_{sp} had a pH of 7.5) compared with mefenamic acid. In neither case, however, was the in vivo behavior predictable from the dissolution results in the compendial medium.

In summary, it is obvious that FaSSIF and FeSSIF are powerful tools for the assessment of in vivo dissolution behavior and food effects on the absorption of poorly soluble drugs. The data in milk also seems to be at least qualitatively predictive of food effects, but its use for predicting specific drug–food interactions has yet to be more thoroughly evaluated. Some refinements in the various biorelevant media, such as incorporating food digestion products in FeSSIF and simulating the digestion profile of Ensure or milk in the stomach, may be needed to optimize their predictive value. On the other hand, there is a need to simplify these media (for example, substitution of suitable

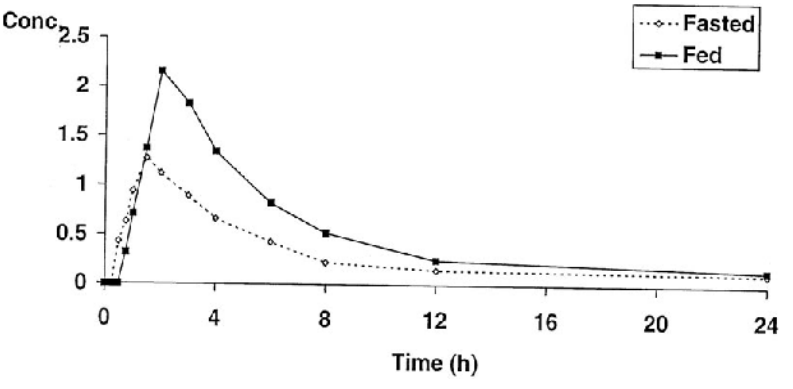

FIG. 11 Comparison of average pharmacokinetic profiles of troglitazone given before a meal and after a meal. (From Ref. 19.)

synthetic surfactants for the bile components in FaSSIF and FeSSIF) to be able to translate their use into the quality assurance area.

5. Use of Synthetic Surfactants in Dissolution Media

As alluded to earlier, the bile components (lecithin and bile salts) present some practical problems in terms of their purity and the time and effort required to prepare the medium and analyze the samples, not to mention their cost. For routine quality assurance, it would be far more practical to use a synthetic surfactant system that could match the surface tension lowering and solubilization properties of the bile components. The bile components lower the surface tension to about 45–50 mNm^{-1} (20), which is somewhat higher than the gastric surface tension. Therefore, no single surfactant–concentration combination can be applied for the simulation of both gastric and intestinal conditions. Furthermore, it is uncertain that the usual surfactants (SLS, Tweens, or other) solubilize drugs similarly to the bile components (21). The use of the wrong surfactant could lead either to over- or underdiscrimination among formulations. An example from the controlled-release literature is shown in Fig. 12, in which results in CTAB or Tween correctly predicted differences among three formulations in vivo, but SLS falsely predicted similarity among the three formulations (22). Not only the type, but also the concentration of surfactant could play a role here, and much work still needs to be done to identify a synthetic surfactant system that could be used as a general substitute for the bile components.

6. Hydroalcoholic Mixtures as Dissolution Media

Hydroalcoholic mixtures were popular at one time as dissolution media for poorly soluble drugs. A practical advantage of hydroalcoholic media over the use of surfactants in the medium is that they do not tend to foam, which makes deaeration and volume adjustment somewhat less frustrating. Furthermore, unlike some ionic surfactants, a wide range of pH values can be used without affecting the surface tension properties of the medium. Finally, the solubility of some drugs is more favorably influenced by alcohol than by surfactants, enabling sink conditions to be more easily achieved. Nevertheless, the use of hydroalcoholic media is widely frowned on these days because of the nonphysiological concentration of alcohol.

7. Duration of the Dissolution Test for Class 2 Substances

Because poorly soluble drugs dissolve more slowly than class 1 and 3 compounds, it is logical to study their dissolution over a longer, yet still physiologi-

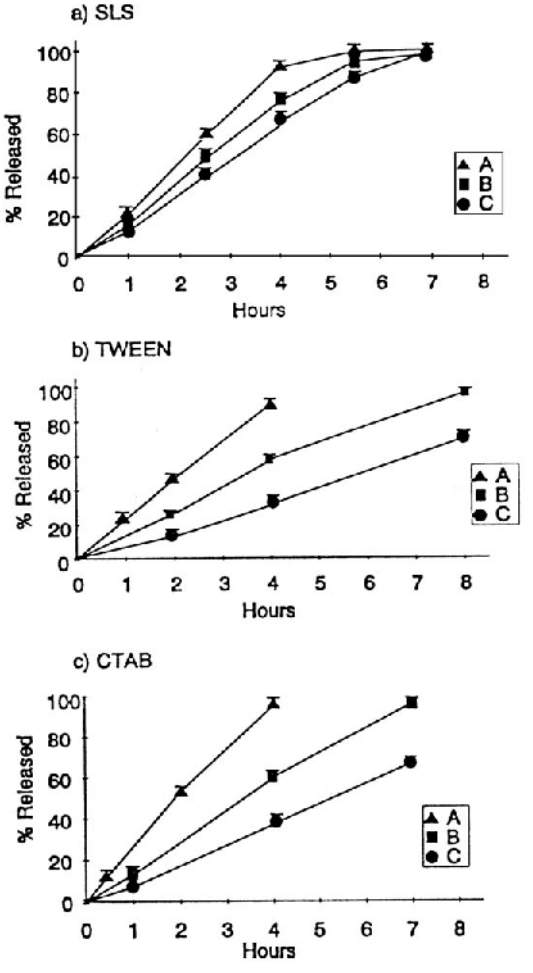

FIG. 12 Comparison of release from three CR products in (a) SLS, (b) Tween, and (c) CTAB. (From Ref. 22.)

cally reasonable period. Assuming that the drug is best absorbed from the small intestine and that absorption is rapid, test durations of up to 4 h are conceivable. This time represents the average transit time through the upper GI tract in the fasted state: if the formulation is to be administered in the fed state, durations of up to 6 h would be physiologically relevant, and if the

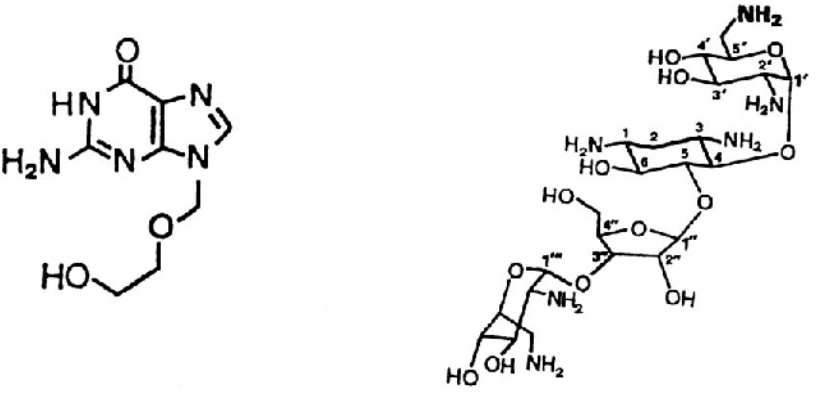

Fig. 13 Structures of (left) acyclovir and (right) neomycin.

compound is known to be absorbed well from the colon, tests as long as 8–10 h could be envisaged. Often, though, the percentage release reaches a plateau within 2 h, even for quite poorly soluble drugs, in the closed test systems (paddle and basket; see Fig. 10).

C. Dissolution Tests for Class 3 Substances

Despite their good aqueous solubility, Class III substances fail to achieve complete bioavailability after oral dosing because of their poor membrane permeability. Typical examples are the antiviral acyclovir ($S = 1.3$ mg/mL) and the aminoglycoside neomycin ($S = 15$ mg/mL) (Fig. 13).

As with class 1 compounds, a simple aqueous medium can be used for quality assurance dissolution testing of immediate-release products. A satisfactory IVIVC (level A, B, or C) is unlikely to be obtainable, on the one hand, because the release is typically faster than gastric emptying and, on the other

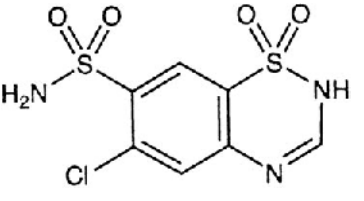

Fig. 14 Structure of chlorothiazide.

hand, because, for class III compounds, the membrane permeability is also a limiting factor to the absorption.

D. Dissolution Tests for Class 4 Substances

Class 4 drugs combine poor solubility with poor permeability. Therefore, similar to class 3 drugs, they usually do not approach complete bioavailability. Chlorothiazide (Fig. 14) provides an interesting example of a borderline case between class 3 and 4 behavior. Its bioavailability after a 100-mg dose is about 60%, yet at 500 mg, the bioavailability is only 20–30%. This behavior can be explained using the dose/solubility ratio calculation. The volume required to dissolve a 100 mg dose is 250 mL (S = 0.4 mg/mL), which puts it right on the borderline according to the BCS. At 500 mg, however, the D/S volume is 1250 mL, far in excess of the FDA's limit of 250 mL for a drug with good solubility.

As with class 3 drugs, IVIVC is unlikely for class 4 drugs, so recommendations can be limited to quality assurance media. These include the two compendial media (SGF_{sp} and SIF_{sp}), with the addition of a surfactant to assure that complete release of the drug is possible in the volume of medium to be used. Similar to class 2 drugs, release may have to be carried out over a somewhat longer duration than for class 1 and 3 drugs, to characterize the entire release profile.

IV. CHOICE OF DISSOLUTION EQUIPMENT

Currently there are four different dissolution test apparatus designs official in the *USP* for use with oral dosage forms: *USP* I (basket), *USP* II (paddle), *USP* III (Biodis), and *USP* IV (flow-through tester).

USP I and II are the apparatuses most often used for immediate-release dosage forms. The paddle apparatus is shown in Fig. 15.

The Biodis tester (*USP* III; Fig. 16) is most suitable when the pH of the medium is to be altered during the test; for example, for enteric-coated dosage forms.

The flow-through tester (*USP* IV; Fig. 17) is particularly suitable for extended-release dosage forms. The volume of medium required can be a problem when the test is of very long duration. Furthermore, it is not clear that the hydrodynamics in this system are any more representative of the GI tract than those in apparatuses I and II.

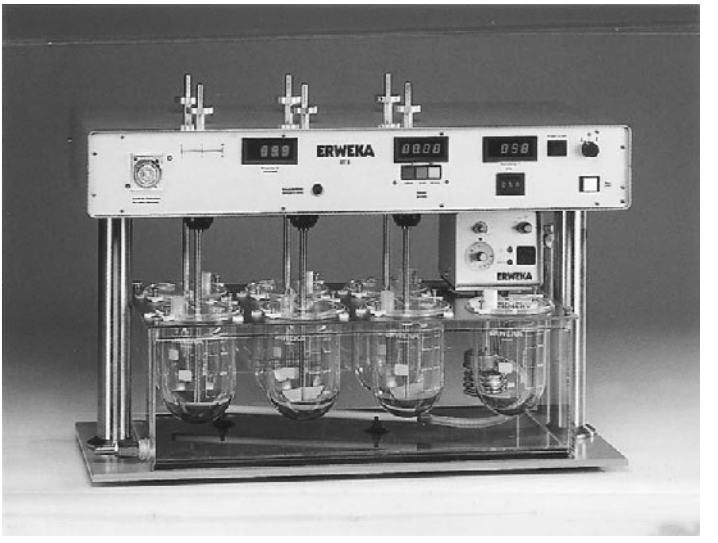

FIG. 15 *USP* II dissolution apparatus (paddle).

A. Selection of Agitation Rate

The most often used apparatus for immediate-release dosage forms is *USP* II. The volume of medium required for tests intended for development of IVIVCs should be based on the relevant physiological volumes (see Sects. III.B.1 and III.B.3). In addition, an appropriate rotational speed must be selected (23). If the rotation speed is *too low*, coning may occur, leading to artifactually low rates of dissolution. To avoid this problem, a higher rate of rotation or a peak vessel (Fig. 18) can be used.

If the rate of rotation is *too fast*, the test will not be able to discriminate between acceptable and not acceptable batches or formulations. Rotational speeds in the range 50–100 rpm appear to be suitable for the paddle method. Dissolution of class 1 compounds is relatively insensitive to variation in the paddle speed within this range (Fig. 19a), and even for class 2 compounds the effects are minimal (see Fig. 19b). If the basket method is to be used, a rotational speed of up to 150 rpm may be appropriate, as the linear velocity generated in the vessel is considerably lower for a given rotational speed for the basket than for the paddle (24). Rotational speeds in these ranges should also be appropriate for quality control tests.

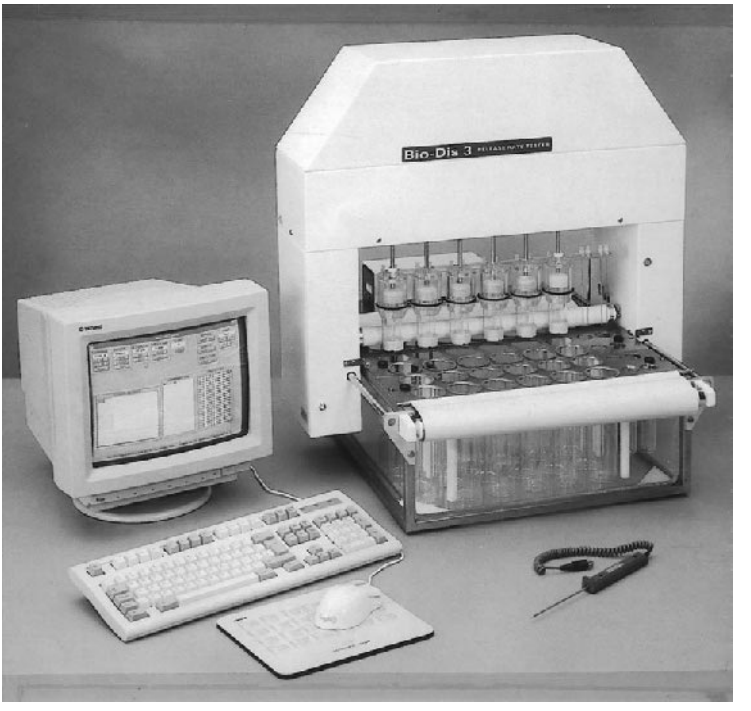

FIG. 16 The Biodis tester (*USP* III).

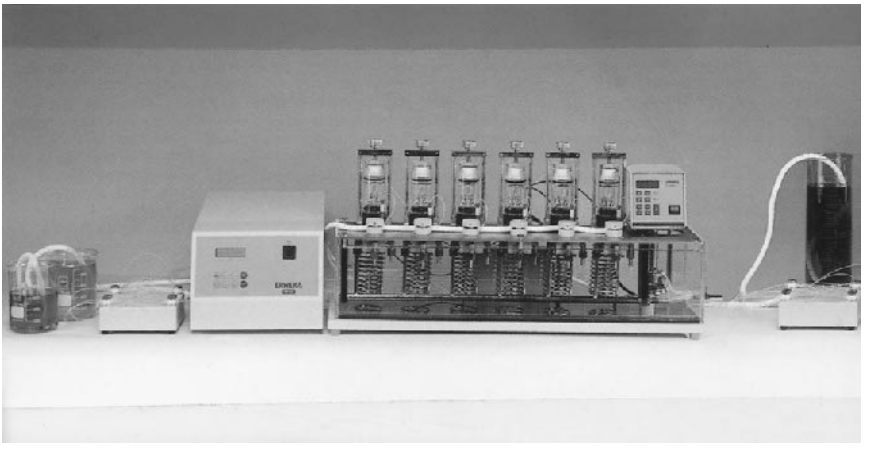

FIG. 17 The flow-through tester (*USP* IV).

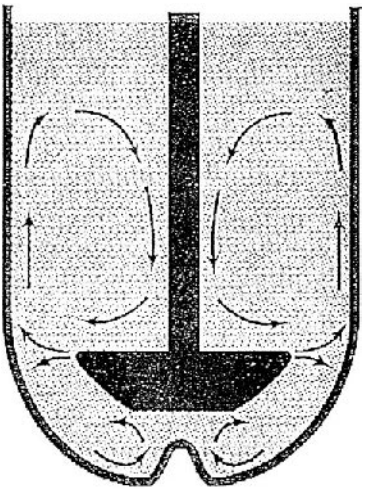

FIG. 18 Peak vessel.

V. SUMMARY

The choice of dissolution test for an immediate-release dosage form can be greatly facilitated by considering the classification of the drug according to the BCS. For class 1 and 3 compounds, the medium and method should be kept simple, regardless of whether the test is to be used for routine quality control or as the basis for a biowaiver. For class 2 compounds, the choice of test will depend on the objective to be met. For the development of IVIVCs, the new biorelevant media appear to offer significant advantages over the traditional compendial media in terms of being able to forecast the in vivo dissolution behavior. In the majority of cases, *USP* paddle will be the method of choice for the dissolution test, with medium volume chosen according to the intended administration conditions (fasted or fed) and the site where the drug will most likely dissolve in the GI tract. Although a correlation between rotational speed and in vivo hydrodynamics is still lacking, rotational speeds in the range 50–100 rpm appear to yield data that can be successfully used to develop IVIVCs. For routine quality control, simplified versions of the biorelevant media, utilizing substitute synthetic surfactant systems, need to be developed to avoid the costs and challenges associated with the preparation of the biorelevant media and attendant sample analysis.

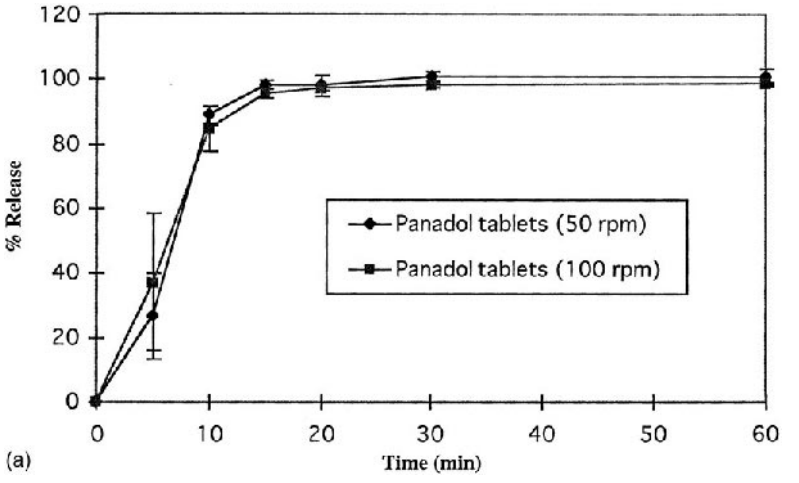

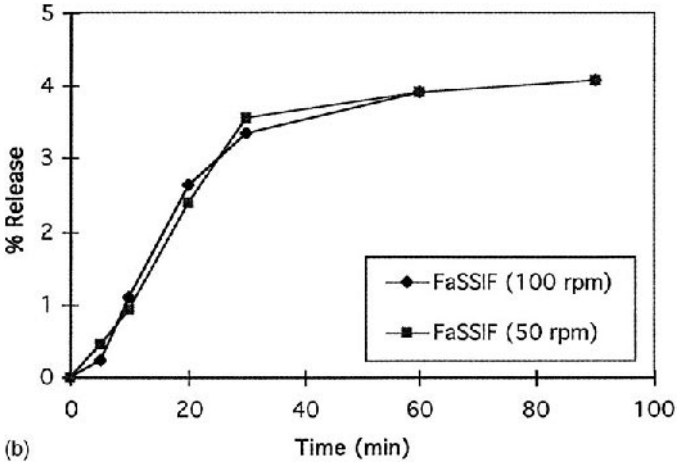

FIG. 19 Effect of rotational speed on the dissolution of (a) acetaminophen and (b) danazol from commercially available immediate-release dosage forms. (From Ref. 3.)

APPENDIX

A. Decision Tree for Dissolution Test Design

1. *Classify* the compound according to BCS.
2. Choose an *appropriate medium*.
   Class 1, 3: use the most simple yet reliable medium possible. Addition of surfactants is unnecessary.
   Class 2, 4: biorelevant media warranted
   for IVIVC SGF_{sp} plus surfactant, FaSSIF (fasted state). Ensure, milk, FeSSIF (fed state)
   for QC SGF_{sp}/SIF_{sp} plus suitable surfactant.
3. Choose an *appropriate medium volume*.
   In general, volumes for the fasted state will be lower than volumes for the fed state.
4. Choose an appropriate *test duration and sampling times*.
   Class 1, 3: short test (up to 30 min) with one-point sampling to verify that an appropriate amount (e.g., 90%) has dissolved.
   Class 2, 4: test duration depends on region of gut permeable to the drug and whether the drug is to be administered in a fasted or fed state. Multiple sampling required to define the dissolution profile [e.g., FIP guideline for ER products (25)].
5. *Apparatus: USP* II for IR products unless there is a strong reason for another tester type.
6. *RPM*: 50 or 75 rpm is usually suitable.
   In case of coning, go to 100 rpm or a peak vessel.
   In case of capsules, prevent floating with a sinker.

REFERENCES

1. Amidon GL, Lennernäs H, Shah VP, Crison JR. Theoretical basis for a biopharmaceutic drug classification: the correlation of in vitro drug product dissolution and in vivo bioavailability. Pharm Res 1995; 12:413–420.
2. Rudman A, Williams R. Guidance for Industry: Immediate Release Solid Oral Dosage Forms. Scale-up and post-approval changes: Chemistry, manufacturing and controls, in vitro dissolution testing and in vivo bioequivalence documentation. Center for Drug Evaluation and Research, Food and Drug Administration, Nov. 1995.
   See also Draft Guidance for Industry: Waiver of In Vivo Bioavailability and

Bioequivalence Studies for Immediate Release Solid Oral Dosage Forms Based on a Biopharmaceutics Classification Scheme. FDA, 1999. (http://www.fda.gov/cder/guidance/index.htm)
3. Galia E, Nicolaides E, Hörter D, Löbenberg R, Reppas C, Dressman JB. Evaluation of various dissolution media for predicting in vivo performance of class I and II drugs. Pharm Res 1998; 15:698–705.
4. United States Pharmacopeia 24 and National Formulary 19. Rockville, MD: United States Pharmacopeial Convention, 1999.
5. Kabasakalian P, Katz M, Rosenkrantz B, Townley E. Parameters affecting absorption of griseofulvin in a human subject using urinary excretion data. J Pharm Sci 1970; 59:595–600.
6. Chiou WL, Riegelman S. Pharmaceutical applications of solid dispersion systems. J Pharm Sci 1971; 60:1281–1303.
7. Russell TL, Berardi RR, Barnett JL, O'Sullivan TL, Wagner JG, Dressman JB. pH-related changes in the absorption of dipyridamole in the elderly. Pharm Res 1994; 11:136–143.
8. Lelawongs P, Barone JA, Colaizzi JL, Hsuan AT, Mechlinski W, Legendre R, Guarniere J. Effect of food and gastric acidity on absorption of orally administered ketoconazole. Clin Pharm 1988; 7:228–235.
9. Efentakis M, Dressman JB. Gastric juice as a dissolution medium: surface tension and pH. Eur J Drug Metab Pharmacokinet 1998; 23:97–102.
10. Finholt P, Solvang S. Dissolution kinetics of drugs in human gastric juice: the role of surface tension. J Pharm Sci 1968; 57:1322–1326.
11. Dressman JB, Berardi RR, Dermentzoglou LC, Russell TL, Schmaltz SP, Barnett JL, Jarvenpaa KM. Upper gastrointestinal pH in young, healthy men and women. Pharm Res 1990; 7:756–761.
12. Galia E, Horton J, Dressman JB. Albendazole generics: a comparative in vitro study. Pharm Res 1999; 16:1872–1876.
13. Greenwood DE. Small Intestinal pH and Buffer Capacity: Implications for Dissolution of Ionizable Compounds. Doctoral dissertation. The University of Michigan, Ann Arbor, MI, 1994.
14. Mithani SD, Bakatselou V, TenHoor CN, Dressman JB. Estimation of the increase in solubility of drugs as a function of bile salt concentration. Pharm Res 1996; 13:163–167.
15. Fordtran JS, Lochlear T. Ionic constituents and osmolarity of gastric and small intestinal fluids after eating. Am J Dig Dis 1966; 11:503–521.
16. Nicolaides E, Galia E, Efthymiopoulos C, Dressman JB, Reppas C. Forecasting the in vivo performance of four low solubility drugs from their in vitro dissolution data. Pharm Res 1999; 16:1877–1883.
17. Daneshmend TK, Warnock DW, Ene MD, Johnson EM, Potten MR, Richardson MD, Williamson PJ. Influence of food on the pharmacokinetics of ketoconazole. Antimicrob Agents Chemother 1984; 25:1–3.
18. Charman WN, Rogge MC, Boddy AW, Barr WH, Berger BM. Absorption of danazol after administration to different sites of the gastrointestinal tract and the

relationship to single and double peak phenomena in the plasma profiles. J Clin Pharmacol 1993; 33:1207–1213.
19. Young MA, Lettis S, Eastmond R. Improvement in the gastrointestinal absorption of troglitazone when taken with, or shortly after, food. Br J Clin Pharmacol 1998; 45:31–35.
20. Stippler E. personal communication (University of Frankfurt).
21. Shah VP, Konecny JJ, Everett RL, McCullough B, Nooriazadeh AC, Skelly JP. In vitro dissolution profile of water-insoluble drug dosage forms in the presence of surfactants. Pharm Res 1989; 6:612–618.
22. Abrahamsson B, Johansson D, Torstensson A, Wingstrand K. Evaluation of solubilizers in the drug release testing of hydrophilic matrix extended-release tablets of felodipine. Pharm Res 1994; 11:1093–1097.
23. Dressman JB, Amidon GL, Reppas C, Shah VP. Dissolution testing as a prognostic tool for drug absorption: immediate release dosage forms. Pharm Res 1998; 15:11–22.
24. Diebold S. personal communication (University of Frankfurt).
25. Dissolution testing of solid oral products. A joint report of the Section for Official Laboratories and Medicines Control Services and the Section of Industrial Pharmacists of the Federation Internationale Pharmaceutique. Dissolution Tech 1997; 4:5–14.

11
Dissolution Tests for Extended-Release Products

Barbara Sievert and Martin Siewert
Aventis Pharma, Frankfurt on Main, Germany

I. INTRODUCTION

During the last decade many workshops have been devoted to in vitro dissolution testing of immediate- as well as modified-release formulations. Several guidelines have been created over the years, and all key pharmacopoeias now include a description of dissolution testing. It appears that the methods have mostly been settled, and that real news on the theme is becoming rare.

Looking at the biopharmaceutical learning curve (Fig. 1) the development of biopharmaceutical test procedures began in the early 1960s (1–4). In the 1980s (5–10) special problems, such as principles of correlation and food effects, were addressed. During the 1990s (11–16) several guidances have been created by the U.S. Food and Drug Administration (FDA) and by the International Pharmacists Federation (FIP) covering most of the relevant aspects of in vitro dissolution testing. Nevertheless, there are topics that are still open or that represent points of ongoing debate.

II. DISSOLUTION CONCEPTS

Different concepts of dissolution testing exist for different purposes in the pharmaceutical industry. During drug development in vitro dissolution testing

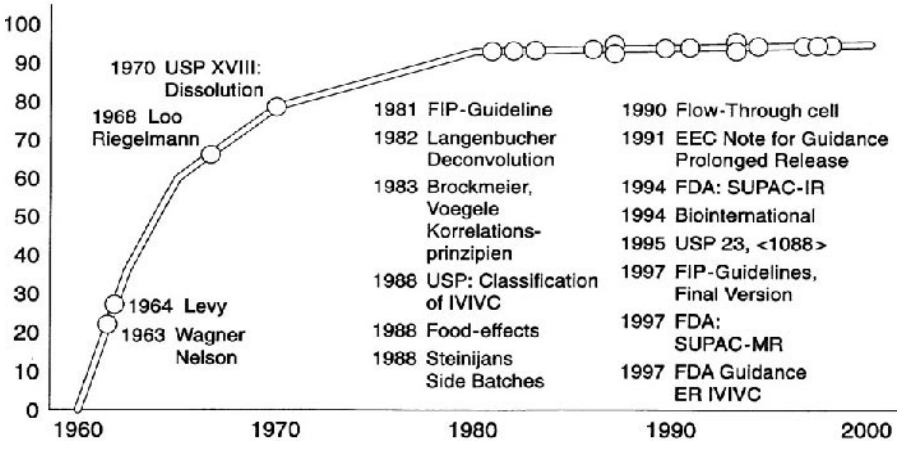

FIG. 1 Biopharmaceutical learning curve.

is an important tool in the development of the ''best'' formulation, in the understanding of the drug's biopharmaceutical characteristics, and in interpretation of possible risks, such as potential food effects on bioavailability or interaction with other drugs. The simulation of specific gastrointestinal conditions that may lead to potential therapeutic failure or adverse events is a further point of interest during drug development. At this stage, various models and test conditions for in vitro dissolution studies are applied to learn about the biopharmaceutical characteristics of early formulations and about the discriminating power of the test system. During development, in quality control and for postapproval changes, in vitro dissolution testing is an important part of stability studies. After the approval of a new drug it is common that only one test model is employed for routine quality control dissolution tests to assure the consistency of the manufacturing process and quality of finished product. In addition, pivotal batches are subjected to dissolution testing as part of follow-up stability studies. Postapproval, a drug product often undergoes changes in the production site, the manufacturing process, or the formulation. At this stage, and depending on the level of in vivo–in vitro correlation available, different sets of dissolution tests may be used (17) to demonstrate equivalence between the changed product and the previous product.

III. TEST PROCEDURES FOR DISSOLUTION TESTING

A. General Aspects

In principle, considerations should be made for testing conditions for extended-release (ER) formulations similar to those for immediate-release (IR) products. Solubility characteristics (''sink'') and the physiological environment have to be considered (16). Ranges are more important for ER products than for IR products to achieve special pharmacokinetic target profiles, especially for drug substances with a narrow therapeutic range. Because of the different concepts of slow-release formulations and the various therapeutic indications, ''standard'' specifications for extended-release formulations cannot be set (16).

B. Test Medium

An aqueous system as test medium is preferred. The instructions on pH differ slightly between the various pharmacopoeias (Fig. 2). Water as a dissolution medium is allowed by some guidances (16,18,19) but its use always needs to be justified. Additives (enzymes, salts, and surfactants) are also to be justified (16). A permissible additive (18) is sodium lauryl sulfate (up to 1%). For deaeration, a product-by-product validation must be performed (16). For the flow-through cell deaeration is, however, mandatory (19).

Volume	500 – 1000 ml	FIP, Ph. Eur.
pH	pH 1 – 6.8 (8), water (justification)	FIP, FDA
	pH 1 – 7.6, water (justification)	Ph. Eur.
Additives	Enzymes, salts, surfactants	FIP
	1% sodium lauryl sulfate possible	FDA
	Low concentration of surfactant allowed	Ph. Eur.
Deaeration	Product-by-product validation	FIP
	Mandatory for flow-through cell	Ph. Eur.

FIG. 2 Test media.

1. pH of Test Medium

For quality control purposes only one pH is usually used for dissolution testing. Exceptions are made only for delayed-release formulations. Different pH values are preferred in comparison with a pH gradient. In general, the decision to use a single pH value, rather than a pH gradient, is related to the apparatus (i.e., a gradient is used in conjunction with the Biodis [*U.S. Pharmacopeia; USP* App. 3] or the flow-through cell [*USP* App. 4]), whereas single pH values are preferred with basket and paddle (*USP* App. 1 and 2).

2. Apparatus

The most common types of apparatus used for ER formulations are the paddle and the basket method. Other methods, including the flow-through cell and the reciprocating cylinder (Biodis) can also be used. Full harmonization of the specifications for the dimensions of the paddles, baskets, and vessels in the various pharmacopoeias still represents an important challenge for the future. Automation of the process, including technical modifications (sampling valves), is possible, but must be validated on a product-by-product basis. If alternative apparatus or other modifications are used, evidence of their superiority to pharmacopoeial specifications is the only acceptable justification.

3. Agitation

Different rotation speeds are specified in the various pharmacopoeia and guidances. For basket and paddle, 50–100 (150) rpm are described (16,19), whereas 100 rpm for basket and 50–75 rpm for paddle are demanded by others (18). A scientifically based decision on the velocity of rotation does not exist and the rotational speed is set on a product-by-product basis.

4. Sinkers

With few exceptions, such as the Japanese pharmacopoeia (Ph. Jap.), no specifications for sinkers have been established. The FIP remains flexible on this issue and requires only that a justification be given (16).

5. Test Duration

At least 80% dissolution shall be reached within the test period. A direct determination of test duration from the dosage interval is scientifically justified only when the time axes in vitro and in vivo have a 1:1 relation. In special cases, an in vitro dissolution of less than 80% may be accepted if the test

duration is at least 24 h. In these cases, a recovery control has to be performed during development using dissolution profiles established under other test conditions.

IV. SETTING OF SPECIFICATIONS

For ER formulations the FIP guideline and Ph. Eur. demand at least three specification points (Fig. 3), the first after 1–2 h (about 20–30% drug release) to provide assurance against premature drug release. The second specification point has to be close to 50% (definition of the dissolution pattern). At the last point, the dissolution limit should be at least 80% to ensure almost quantitative release. Dissolution of less than 80% of the last point has to be justified and should be supported by results obtained over a test duration of at least 24 h (16). As can be seen, there are slight differences in the *USP* specifications (20), in which as few as two test points are required, depending on the individual monograph.

The purpose of establishing dissolution specifications is to ensure batch-to-batch consistency within a range that guarantees acceptable biopharmaceutical performance in vivo and to distinguish between good and bad batches. Specification limits, therefore, have to be defined based on experience gained during the drug development stage, especially during clinical development or in bioavailability–bioequivalence studies. The capability of the manufacturing process and the commonly accepted range of 95–105% of stated amount for average content of drug substance has to be taken into consideration (16).

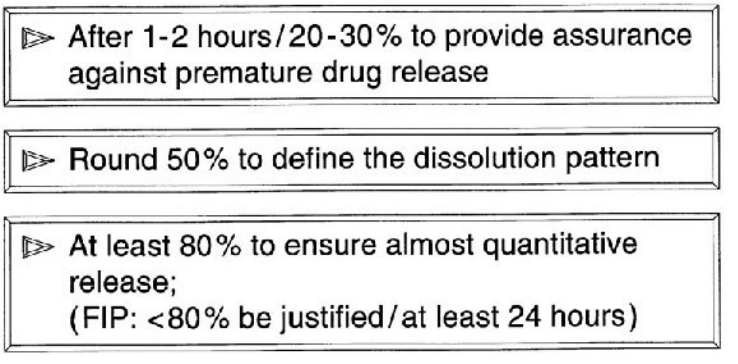
After 1-2 hours/20-30% to provide assurance against premature drug release
Round 50% to define the dissolution pattern
At least 80% to ensure almost quantitative release;
(FIP: <80% be justified/at least 24 hours)

FIG. 3 Dissolution specifications.

The *USP* approach for the acceptance criteria of ER formulations seems to be practical. Stage 3 testing (20) needs to be allowed, especially for stability testing and end of shelf-life considerations.

V. VERIFICATION OF SPECIFICATIONS (IVIVC)

For pharmaceutical development, especially of extended-release formulations, the relation between in vitro drug release and the biopharmaceutical performance in vivo needs to be confirmed as a valid and therapeutically relevant acceptance criterion. The application of in vitro dissolution tests to the control of critical production parameters, without establishing their relation with in vivo data, would represent a misunderstanding of biopharmaceuticals. In fact, the deduction of specification limits requires in vitro–in vivo comparison (IVIVC) studies. Relevant guidances demonstrate increasing consensus on in vitro–in vivo comparison techniques; however, some approaches are still significantly different. Agreement exists that the purpose of developing an in vitro test system is to distinguish between good and bad batches. The test specimen or batches need not be at full production scale. For CR or MR formulations with a level A correlation (independent drug release) at least one batch has to be tested. All other cases require testing of at least three batches under the following conditions: Profiles of at least 12 individual dosage units from each lot are required by the FDA (18), with a coefficient of variation of not more than 10%. The number of volunteers to be included in the bioavailability study should be at least 12 according to the FIP guidelines (16), whereas 6–36 are accepted by the FDA (18).

Different approaches concern the categories of in vitro–in vivo comparison. Whereas there is substantial agreement on the upper limits for level A, B, or C correlations, differences on what is acceptable as a lower limit remain. These limits are summarized in Fig. 4.

A rank order correlation (Fig. 5) according to FIP guidelines (16) is a sufficient verification of a specification under the assumption that no quantitative interpolation is necessary. In this case, the specifications have to be defined as experimentally obtained in vitro for a pair of batches that show in vivo bioequivalence.

Another approach for batches that have been manufactured and experimentally tested in vitro and in vivo for defining dissolution specifications (non–level A cases) is the side batch approach (Fig. 6). *Side batches* (16) represent batches that are created by modifications of manufacturing variables (e.g., during process validation studies) in a range expected to represent maxi-

A	FDA	FIP
B	FDA	FIP
Multiple C	FDA	–
C	FDA	FIP
Rank order	–	FIP
Without IVIVC	FDA	–

FIG. 4 Verification of specification vs. level of correlation.

mum variability during routine production. These batches are designed to show differences in their biopharmaceutical characteristics and to represent the upper and lower limits of the dissolution range, an approach that is required for level B and C correlations by the *USP*. According to the *USP* it must be demonstrated that these batches are acceptable by performing a bioavailability or bioequivalence study, but it is not ultimately required that the batches should be strictly bioequivalent. Another approach in case of correlation failure according to the EEC Note for Guidance (12) ''could consist of demonstrating bioequivalence of the proposed formulation to formulations with dissolution profiles at the upper and lower limits of the specification.''

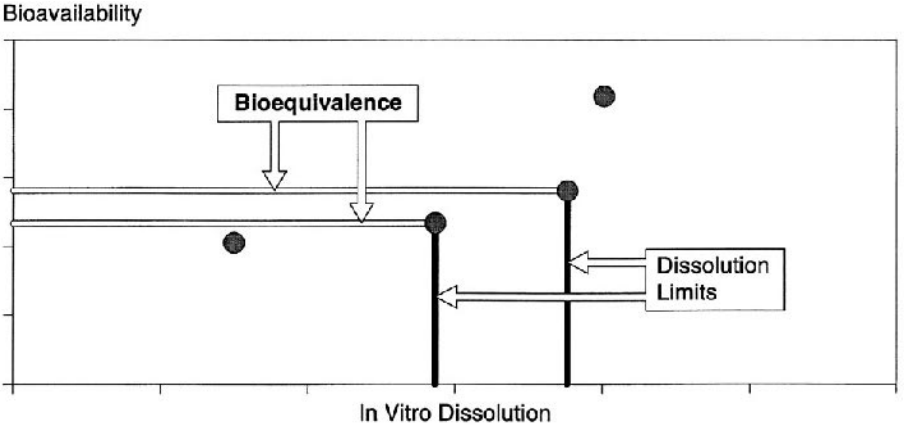

FIG. 5 FIP rank order.

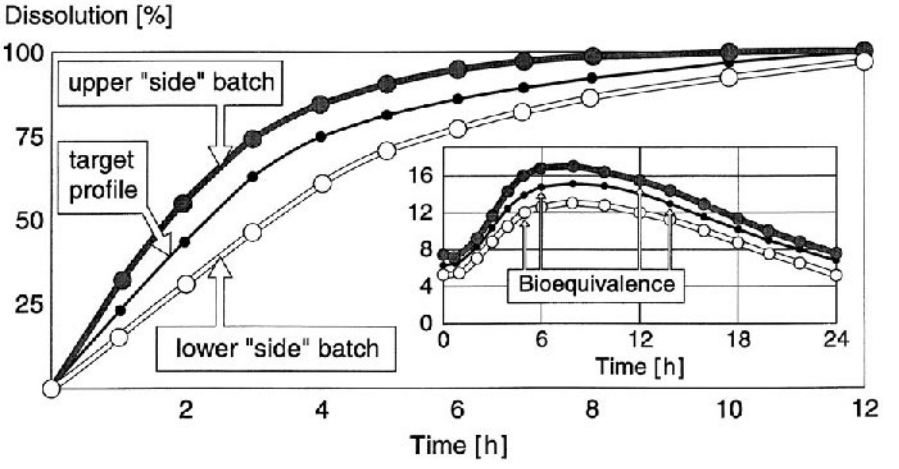

FIG. 6 FIP side batches.

Bioequivalence is strictly required, not between the side batches, but between the target profile and the profiles representing upper and lower specification limit.

VI. SETTING DISSOLUTION SPECIFICATIONS WITHOUT AN IVIVC

Without an IVIVC (18), the recommended range at any dissolution time point specification is ±10% relative to the mean dissolution profile obtained from the clinical–bioavailability lots. In certain cases deviations from the ±10% range may be accepted. The maximum deviation then would be 25% under the condition that bioequivalence of the side batches is proved. A minimum of three time points (early, middle, and late stages of the dissolution profile) are required, with a dissolution of 80% or more at the last time point.

The determination of the similarity factor f_2 of several dissolution profiles representing the ±10% and ±25%, respectively, of the target profile calculated according to the Guidance for Industry SUPAC-MR leads to the results shown in Fig. 7.

Because a similarity factor between 50 and 100 proves similar dissolution profiles, only the 90% vs. 100% and 110% vs. 100% are similar. In the

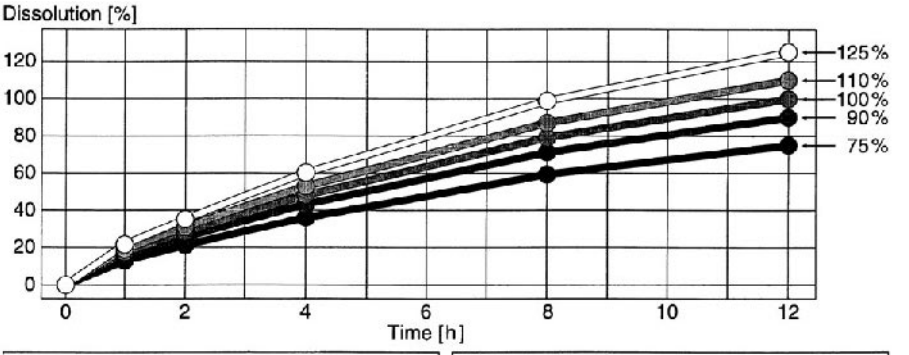

Similarity factor f_2		Similarity factor f_2	
59,85	90% vs. 100%, 110% vs. 100%	40,18	75% vs. 100%, 125% vs. 100%
45,12	90% vs. 110%, 110% vs. 90%	25,17	75% vs. 125%

FIG. 7 Setting dissolution specifications without an IVIVC (FDA).

other cases f_2 is less than 50, which means that the dissolution profiles are not necessarily similar.

VII. THE BIOPHARMACEUTICS CLASSIFICATION SYSTEM

For immediate-release solid oral dosage forms a Biopharmaceutics Classification System (BCS) is proposed (7) which introduces solubility and membrane permeability as two drug-related criteria that can be used to facilitate the understanding of the in vivo system and to approve in vitro–in vivo correlations.

For immediate-release oral dosage forms four biopharmaceutical classifications are proposed (Table 1).

The BCS can be used for immediate-release solid oral dosage forms as a helpful approach within the formulation-orientated, decision-making process

TABLE 1 The Biopharmaceutics Classification System

Class 1	High solubility	High permeability
Class 2	Low solubility	High permeability
Class 3	High solubility	Low permeability
Class 4	Low solubility	Low permeability

of drug development. For extended-release, solid oral dosage forms there always remains the influence of the characteristics of the dosage form, which was designed to obtain special dissolution characteristics.

Extended-release formulations are created to ensure a limited, controlled release out of the dosage form, with a controlled dissolution rate. Only the amount of drug released is available for solution and permeation across the gut wall.

Application of the special characteristics of extended-release dosage forms on the BCS would lead to the following correlation expectations (Table 2).

For class 1 drugs, an in vitro–in vivo correlation is expected because the active ingredient that is released out of the dosage form dissolves immediately and is available for absorption. Also for class 2 drugs an IVIVC can be expected because the released dose is low. The controlled release out of the dosage form avoids a high concentration of active ingredient in the gastrointestinal medium so that the released drug can easily dissolve in the available volume of dissolution medium.

Although release of a class 3 drug out of an ER dosage form is limited, the dissolution of the released active compound takes place quickly. Nevertheless, the absorption is influenced not only by the special characteristics of the dosage form, but also by the low permeability through the gut wall. An IVIVC, therefore, is limited or impossible.

This consideration is similar for class 4 drugs, for which again only a limited or no IVIV correlation can be expected because of the low permeability.

Summarizing the considerations, the BCS can also be used as an approach for extended-release, solid oral dosage forms; but owing to the addi-

Table 2 Likelihood of IVIVC, Based on the Biopharmaceutics Classification System

Class	Solubility	Permeability	IVIVC correlation expectation
1	High	High	IVIVC correlation because dissolution rate is slower than gastric-emptying time
2	Low	High	IVIVC correlation expected for similar in vitro and in vivo dissolution rates
3	High	Low	Absorption is rate-determining, therefore, limited or no IVIV correlation expected
4	Low	Low	Limited or no IVIV correlation expected

tional factor of the dosage form characteristics, the decision-making process is more complicated than that for immediate-release formulations.

VIII. POSTAPPROVAL CHANGES AND FOOD EFFECTS

Postapproval changes in site of manufacture, manufacturing process, or in the components of a composition take place during the whole life cycle of a product. For several products, sequential changes are carried out. In every case, reference is to be made to the biobatch (pivotal batch) considered in the in vitro dissolution. But is this so-called gold standard helpful in not losing track if there have been several incremental changes? Reference to the biobatch relative to similarity or dissimilarity is to be questioned when changes are applied after long time periods and the shelf life of the biobatch is exceeded.

After food intake, environmental conditions change in the gastrointestinal tract, which may cause an alteration of drug performance in vivo. In vitro tests under various experimental conditions have been used in an attempt to predict and evaluate potential risks during therapy. Effects on bioavailability of CR or MR formulations can be only partially simulated in vitro, and ''correlations'' with the results of in vivo studies are relatively poor. Results of various studies (in vitro vs. in vivo) show that a prediction of a food effect is

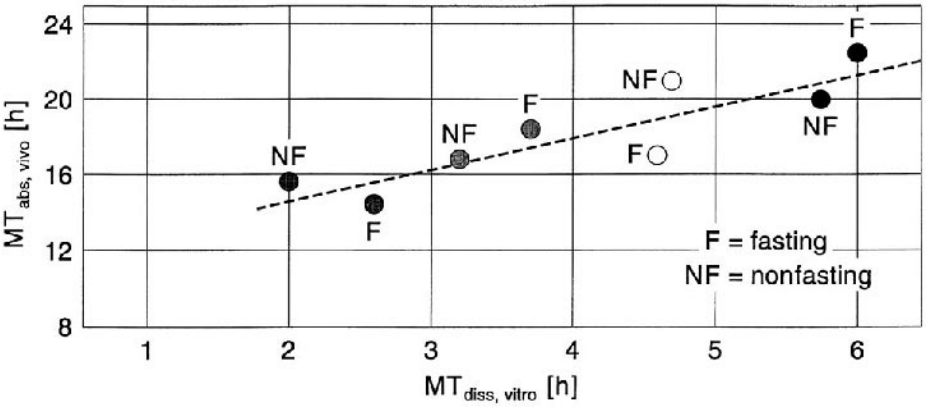

FIG. 8 In vivo–in vitro association of mean times for four theophylline controlled- or modified-release preparations after bioavailability studies and in vitro dissolution tests relative to food effects. (From Ref. 21.)

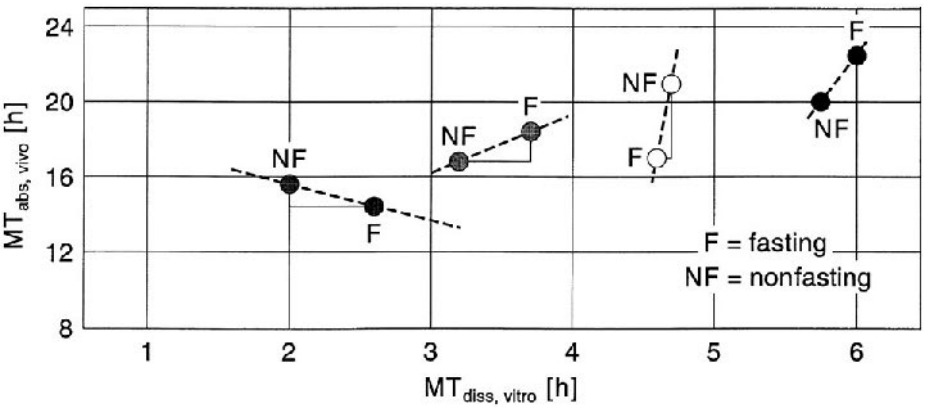

FIG. 9 In vivo–in vitro association of mean times for four theophylline controlled- or modified-release preparations after bioavailability studies and in vitro dissolution tests relative to food effects. (From Ref. 21.)

nearly impossible (see Figs. 8 and 9, representing different interpretations of the same study results).

IX. CONCLUSION

In conclusion, industry and regulatory authorities need to accept the consensus achieved so far and not try to go beyond. Also, industry and regulatory authorities need to focus on harmonization of ''geometries'' and ''acceptance criteria,'' to allow product-specific flexibility and to accept the need for product-specific justification.

REFERENCES

1. Wagner JG, Nelson E. Per cent absorbed time plots derived from blood level and/or urinary excretion data. J Pharm Sci 1963; 52:610–611.
2. Levy G. Effect of dosage form on drug absorption—a frequent variable in clinical pharmacology. Arch Int Pharmacodyn 1964; 152:59–68.
3. Loo JCK, Riegelman S. New method for calculating the intrinsic absorption rate of drugs. J Pharm Sci 1968; 57:918–928.
4. *U.S. Pharmacopeia (USP).* Dissolution, USP XVIII, 1970:934–935.

5. Joint Report of the Section for Control Laboratories and the Section of Industrial Pharmacists of FIP. Guidelines for dissolution testing of solid oral products. Pharm Ind 1981; 43:334–343.
6. Langenbucher F. Numerical convolution/deconvolution as a tool for correlating in vitro with in vivo drug availability. Pharm Ind 1982; 44:1166–1172.
7. Brockmeier D, Voegele D, van Hattingberg HM. In vitro–in vivo correlation, a time scaling problem? Arzneimittelforschung 1983; 33:598–601.
8. USP Subcommittee on Biopharmaceutics. In vitro/in vivo correlation for extended release oral dosage forms. Pharm Forum 1988; 14:4160–4161.
9. Karim A. Importance of assessing ''food effects'' in evaluating controlled-release formulations. In: Yacobi A, Halperin-Walega E, eds. Oral Sustained Release Formulations: Design and Evaluations. New York: Pergamon Press, 1988.
10. Steinijans VE, Dietrich R, Trautmann H, Sauter R, Benedikt G. A novel approach to the specification of in vitro dissolution boundaries based on regulatory requirements for once-daily administration. Arzneimittelforschung 1988; 38:1203–1209.
11. Nicklasson M, Langenbucher F. Description and evaluation of the flow cell dissolution apparatus as an alternative test method for drug release. Pharm Forum 1990; 16:532–540.
12. EEC Note for Guidance. Quality of prolonged release oral solid dosage forms, III/3172/91-EN 1991.
13. FDA Interim Guidance. Immediate Release Solid Oral Dosage Forms—Pre- and Post-Approval Changes. 1994.
14. Bio-International Conference, Munich, Germany, 1994.
15. USP. ⟨1088⟩ In vitro in vivo evaluation of dosage forms. USP 23, 1995.
16. FIP Guidelines for Dissolution Testing of Solid Oral Products. Pharm Ind 1997; 59:760–766.
17. Guidance for Industry SUPAC-MR: Modified-Release Solid Oral Dosage Forms Scale-Up and Post Approval Changes: Chemistry, Manufacturing, and Controls; In Vitro Dissolution Testing and In Vivo Bioequivalence Documentation. 1997.
18. FDA Guidance for Industry. Extended Release Solid Oral Dosage Forms. Development, Evaluation and Application of In Vitro/In Vivo Correlations. 1997.
19. European Pharmacopoeia
20. USP 23. 1995.
21. Maturu PU, Prasad VK, Worsely WN, Shiu GU, Skelly JP. Influence of a high fat breakfast on the bioavailability of theophylline controlled release formulations: an in vitro demonstration of an in vivo observation. J Pharm Sci 1986; 75:1205–1206.

12
Dissolution Testing in the Development of Oral Drug Products

Bertil Abrahamsson
AstraZeneca R&D, Mölndal, Sweden

I. INTRODUCTION

In vitro dissolution is perhaps the most important test method when developing solid dosage forms. Despite the apparent simplicity, it is no trivial matter to develop methods and use them rationally. To be successful, a multidisciplinary approach is needed, involving expertise from the fields of biopharmaceutics, formulation, analytical chemistry, and physical chemistry. Well-designed and accurately performed tests contribute to reducing development times, resource requirements, and the number of in vivo experiments, while ensuring a high quality biopharmaceutical product of benefit for clinical efficacy and safety.

In vitro dissolution testing is used from the start of dosage form development and throughout all subsequent phases. It is used for various purposes, as shown in Table 1, and the methods needed depend on the specific purpose of the test. For example, simplicity and robustness are crucial properties of a quality control method, whereas physiological relevance may overrule these factors if a method is to be used for in vivo predictions. This chapter will be focused mainly on the last aspect. The use of in vitro dissolution in most situations during development will be meaningless if the method does not provide some correlation with in vivo data or resemblance to the physiological conditions in the gastrointestinal (GI) tract. The interest in predictions of in vivo performance from in vitro dissolution data has also increased in recent years, after a period when the existence of meaningful in vitro–in vivo correla-

Table 1 Different Roles of In Vitro Dissolution Testing

Investigation of drug release mechanisms, especially for extended-release (ER) formualations
In formulation development to reach a predefined target release profile and robust drug release properties with respect to influence of physiological factors (e.g., pH and food)
To generate supportive data for interpretation of bioavailability studies
Validation of manufacturing processes
Storage stability studies
Batch quality studies
Batch quality control
As a surrogate for bioequivalence studies

tion (IVIVC) was questioned and dissolution testing was mainly viewed as a batch quality characteristic (1). This is very well reflected by some new regulatory guidelines that define situations for which bioequivalence studies can be replaced by in vitro dissolution testing. The renewed interest in in vivo predictive dissolution testing has also led to some new research and development initiatives for dissolution test methods that may further improve the possibilities for in vivo relevant in vitro tests in the future. This chapter will highlight some of these areas, including the importance of hydrodynamic conditions, special aspects for poorly soluble compounds, prediction of food effects, as well as give some general prerequisites for in vivo predictive dissolution tests. Several cases will be presented from the research and development of modified-release (MR) dosage forms at AstraHässle, Mölndal, Sweden.

II. PRINCIPLES AND PREREQUISITES FOR IN VIVO PREDICTIVE DISSOLUTION TESTS

The expression ''in vitro dissolution testing'' indicates that only the process of drug dissolution is studied. This is somewhat misleading because standard in vitro dissolution testing models not only the dissolution of a drug substance in the GI fluids, but also the drug release from a formulation. The release may occur by simple tablet disintegration for immediate-release tablets, or by more complicated mechanisms for MR dosage forms.

Ideally, the in vitro test methods employed should mimic all GI factors that could potentially affect both release and dissolution. Numerous GI factors

may need to be considered, such as pH, ions, surfactants, lipids, enzymes, volumes, flow rates, viscosity, and mechanical stress. In addition, the variation of these factors, owing to the different conditions in different parts of the GI tract, may also be included in the in vitro model. There are three different principles to handle this complex situation:

1. To develop an in vitro test method that provides the best correlation to in vivo data irrespective of the physiological relevance of the test conditions
2. To develop an in vitro test method that fully models the physiological conditions in the GI tract
3. To develop a formulation that provides release or dissolution that is insensitive to physiological factors

Approach 1 is a very pragmatic way to solve the problem. This can often be good enough, both from a development and regulatory point of view and successful examples have been presented in the literature (2). The main potential drawback of this approach is the risk that the in vitro–in vivo correlation is not valid for modifications of the formulation other than those included in the development of the test method.

The second approach, to completely mimic the in vivo situation, is a very valid aim. Dissolution test media that more closely resemble the GI fluids in the stomach and small intestine have been described (3). Even more complex systems are used in the area of food research for studies of nutrient absorption. Simulation of GI pH gradients, peristaltic movements, transit times, biliary and pancreatic secretions, and water absorption are examples of features in such dynamic in vitro test models (4). However, owing to the complexity and dynamics of the physiological conditions in the GI tract, it is not a realistic goal to completely model the in vivo situation. More physiologically based methods, therefore, cannot always be expected to provide in vivo relevant data; therefore, the need for other approaches to reach in vitro–in vivo correlations will remain.

The third approach may be viewed as optimal because the problem of modeling the highly complex conditions in the GI tract is avoided and simple standard methods can be used. In addition, a dosage form with release properties being independent of physiological factors is also highly desirable relative to biopharmaceutical quality (i.e., the drug will be delivered consistently without any contribution by the dosage form to the pharmacokinetic variability). Although this goal may be viewed as utopical, examples close to this ideal have emerged. One such case is the controlled-release formulation of metoprolol succinate, which will be presented in more detail in the following section.

To predict drug plasma concentration–time profiles from in vitro dissolution tests there are other requirements, outside the scope of the design of the test or the formulation, that must be fulfilled. Primarily, the drug substance should have absorption properties such that the drug dissolution or release becomes the rate-limiting step in the absorption process. Desirable substance characteristics include high permeability, lack of luminal complex-binding, and lack of active efflux from the enterocytes. In addition, the first-pass metabolism should be linear and independent of the absorption site in the GI tract. When these criteria are not met, one possibility to establish an in vitro–in vivo correlation is to use trace amounts of radionuclides in experimental formulations. The radionuclide should mimic the release of the drug from the formulation, and this process can then be monitored in vivo by gamma-scintigraphy. Successful examples of this approach have been described (5), and such data have also been used for in vitro–in vivo correlation (6).

A. Case Example: Metoprolol Succinate in Membrane-Coated Multiple-Unit Formulation (CR/ZOK)

Metoprolol succinate is a highly soluble (280 mg/mL), highly permeable, weak base (pK_a 9.5), without any identified or suspected interactions, efflux, or metabolism in the GI tract. The rate and extent of drug absorption in humans are almost identical over the entire GI tract, as determined by remote-controlled capsule and intubation studies (7,8). The extended-release (ER) formulation principle based on the membrane-coated multiple-units principle is illustrated in Fig. 1. The beads are embedded in a tablet that disintegrates immediately in the stomach. The drug-containing units are thereby liberated and dispersed in the GI tract, as documented by gamma-scintigraphy (9). The drug release, which is controlled by the polymeric membrane that surrounds each pellet, proceeds at an almost constant rate for 20 h. The mechanism of the drug-release process has been investigated in more detail (10).

In the development of this formulation, dissolution testing was performed not only by use of a standard control test, but also the robustness of the release profile toward different factors was repeatedly tested. A final formulation was obtained that was insensitive to various in vitro conditions, as exemplified by tests in different pH, agitation, apparatus, and buffer (Fig. 2). Under such circumstances, in vitro–in vivo correlation can be expected, irrespective of the in vitro test method used; hence, it should be possible to use a standard method with a plain buffer. The in vitro–in vivo correlation

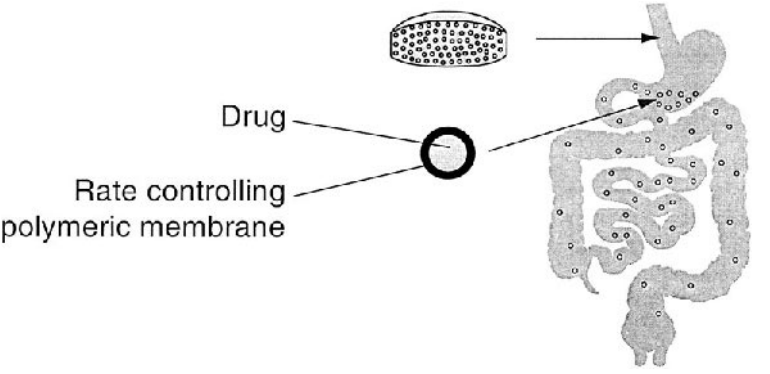

FIG. 1 Metoprolol CR/ZOK formulation principle.

of metoprolol dissolution for a standard *U.S. Pharmacopeia* (USP) II method with a phosphate buffer pH 6.8 was investigated. A human bioavailability study was performed that included three formulations in which the thickness of the membrane coating was somewhat altered (11). A type A correlation was obtained (i.e., the in vitro and in vivo dissolution time curves were almost superimposable; Fig. 3). Thus, the in vitro method was suitable for product quality control and for documentation of postapproval changes. In addition, the good correlation also supported the concept of a formulation being insensitive to physiological factors as a way to obtain in vivo predictive in vitro dissolution data.

After regulatory approval of the original product, the formulation was altered to avoid organic solvents in the production process and to make the process more efficient. The alterations included composition and manufacturing process for the polymeric membrane and the composition of the tablet matrix. This modified formulation was intended to be bioequivalent to the original product. The in vitro dissolution test was used as the primary surrogate variable to reach this goal. A model that described the relation between the in vitro dissolution time profile and the most important process and composition variables was established by use of a statistical experimental design. It was possible to obtain a modified product of which the dissolution properties were very similar to those of the original formulation. For documentary purposes, bioequivalence studies of the original and modified formulation were performed. Bioequivalence was proved in all studies according to 90% confidence interval (CI) within the 80–125% criteria for both C_{max} and area under the

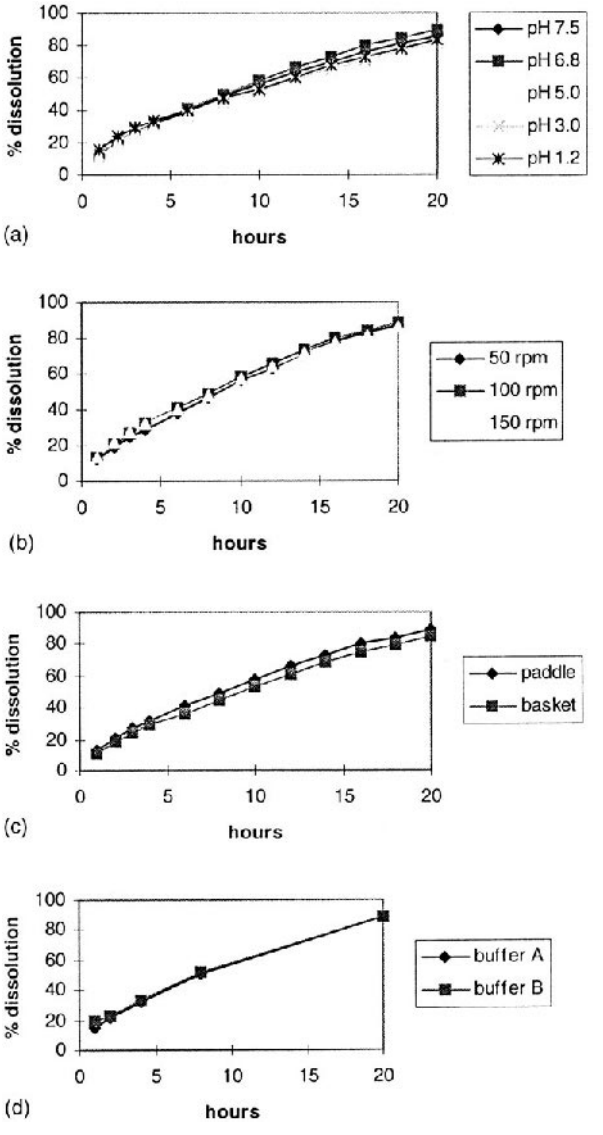

FIG. 2 In vitro dissolution of metoprolol from the CR/ZOK formulation at different test conditions.

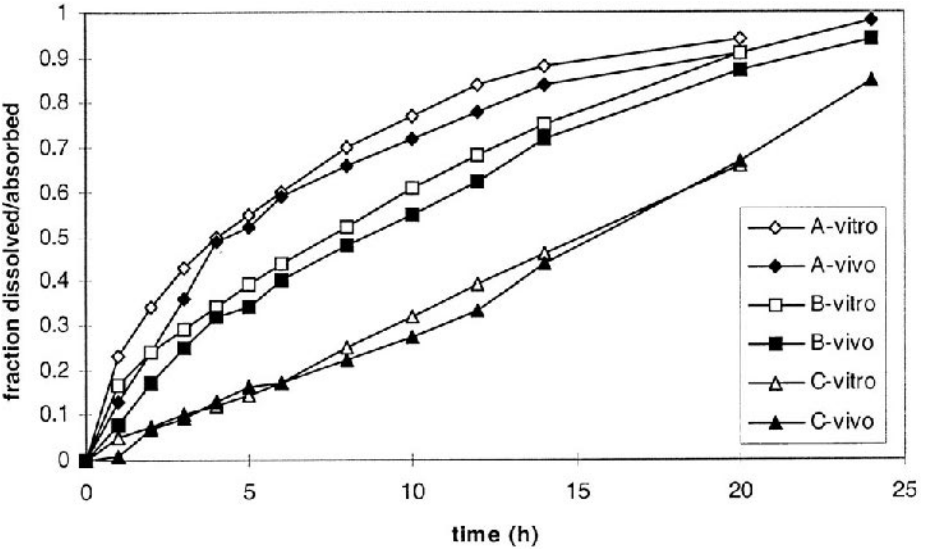

FIG. 3 Mean cumulative in vitro dissolution–and absorption–time profiles of three different metoprolol ER formulations (A, B, and C).

concentration–time curve (AUC). Thus, the usefulness of the in vitro dissolution in development was confirmed, and the use of in vitro dissolution as a surrogate for human bioequivalence studies when a solid in vitro–in vivo correlation has been established was also supported.

III. IMPORTANCE OF HYDRODYNAMICS

The hydrodynamic conditions in an in vitro dissolution experiment are defined by the design of the apparatus, agitation intensity, flow–volume, and viscosity of the test medium. The hydrodynamics can affect the dissolution in several different ways. For example, the dissolution rate of a crystalline drug substance will be affected by changes in the diffusion boundary layer around each particle and potentially also by different degrees of dispersion of particles, leading to changes in the surface area exposed to the solvent. The drug dissolution will also be affected by hydrodynamic effects on the formulation. The disintegration of an immediate-release tablet is an example of a process that may be affected. The situation for some MR formulations is perhaps even

more critical in this sense because the release–rate-controlling mechanism can be sensitive to variations in the hydrodynamics. Other effects related to the hydrodynamic conditions, such as whether the formulation or drug substance floats on surface of the test medium, sinks to the bottom of the vessel, or adheres to the equipment, will also affect the dissolution results.

Great emphasis has been placed on the hydrodynamic conditions to minimize the variability between repeated measurements. The pharmacopoeial methods are very well defined when it comes to dimensions of vessels and other related equipment, as well as tolerances for agitation. This is of especially great importance in the use of the dissolution as a batch release test in regular manufacturing because rejection of batches on false grounds is a costly mistake. However, in formulation development and documentation, there is a profound need for in vivo predictive results. To fulfill this necessity, the in vitro test conditions have to reflect the in vivo situation when the dissolution rate is dependent on the hydrodynamic conditions. If not, different kinds of misinterpretation of in vitro data may occur such as (a) lack of discrimination between formulations that are different in vivo; (b) the reverse situation, creation of a difference in vitro that does not exist in vivo; and (c) different duration and kinetics of drug release in vivo compared with in vitro. Unfortunately, the question of in vivo relevant hydrodynamics in in vitro tests has so far received little attention. A problem, which is perhaps the main reason for lack of research efforts within this area, is the complexity of the in vivo conditions. The motility pattern in the GI tract varies over time in a cyclic manner and the mixing of the GI fluids also varies between the stomach and the intestines. Other factors that are a part of normal life, such as intake of food and fluids, sleep, and exercise, also greatly affect volumes, motility patterns, and flow rates. Furthermore, it is not clear how to characterize the in vivo hydrodynamics in such a way that it is possible to translate this to in vitro test equipment. Currently used in vivo measurements, such as manometric and flow measurements, have so far provided limited guidance for design of in vitro methods.

The best possible approach at the early stage of development is still to obtain in vivo bioavailability data and then try to find the in vitro setting that provides the best in vitro/in vivo correlation. Wide variations in the hydrodynamic conditions can be obtained by use of the four different *USP* test methods: the rotating basket, the rotating paddle, the reciprocating cylinder, and the flow-through cell. In addition, different conditions can be obtained within one apparatus by changing the stirring rate, reciprocating frequency, or flow rate, respectively. If suitable correspondence to in vivo data cannot be obtained by these standard methods, other methods can be used, such as the

recently developed modified *USP* II method, with a peak in the bottom of the vessel, the rotating flask, or other noncompendial methods (12,13). Methods including addition of inert beads to the dissolution medium have also been described (14).

When formulations need to be compared (e.g., when a formulation has been changed or if a formulation has to be selected for further development among different candidates), a battery of different methods and test conditions might be the most successful approach. Consistent results for the comparison of two or more formulations in such a multiple test provides a reasonable confidence in the in vivo relevance, whereas if more conflicting results occur, in vivo pilot studies may be the only option. A multiple test also serves to investigate the relative sensitivity to hydrodynamic conditions for a series of candidate formulations, i.e., the formulation that is least affected is most likely to consistently provide the intended in vivo release profile. This approach will be further illustrated in the following case examples.

A. Case Example: Importance of In Vitro Hydrodynamics for Dense Pellets

The present case involves two similar enteric-coated MR pellets formulations containing a high-solubility, high-permeability drug. The two formulations, denoted D and E, consisted of dense pellets (1.4 and 1.3 g/cm^3, respectively), with a mean diameter of 0.4 and 0.6 mm, respectively. They were very similar in manufacturing process, composition of the drug core and the polymeric coating. The aim in the development of formulation D was to obtain the same release and bioavailability characteristics as those of E.

A standard *USP* II dissolution apparatus with a close to neutral buffer was initially used. However, the variability between individual dose units was unacceptably large for pellets D. Visual inspection of the in vitro dissolution test by video recording revealed that the new pellets were lumped together in the bottom of the vessel for long periods and then irregularly spread out for short periods. This problem also persisted at a more vigorous paddle stirring rate (100 rpm) than recommended by *USP* and generally accepted by FDA (Fig. 4). A recently developed modified *USP* II vessel with a peak in the bottom was tested to overcome this problem. The peak creates a turbulent flow below the axis of the paddle (Fig. 5) in contrast to the very low degree of agitation exerted in the standard method. The tested pellets did not form a heap with this method, and the variability in dissolution between individual units was also significantly lower in the modified vessel, as shown in Fig. 4.

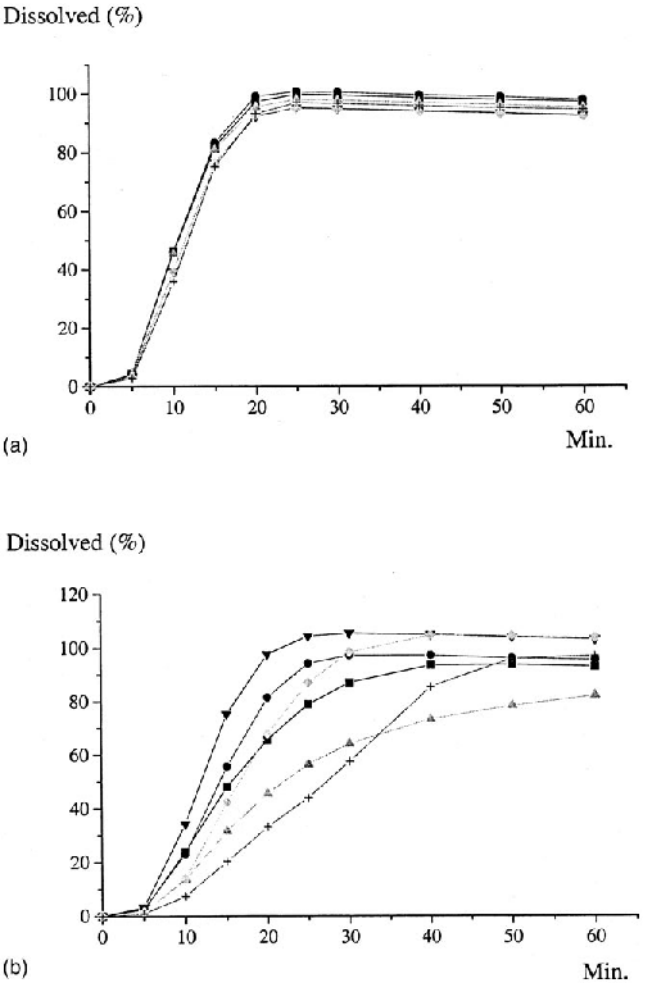

FIG. 4 Drug dissolution–time profiles for six individual doses of pellets D in the peak vessel (a) and in the standard *USP* II method (b) at a stirring rate of 100 rpm.

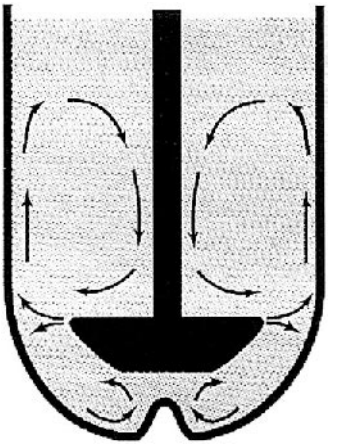

FIG. 5 The peak vessel with illustrations of flow patterns.

Essentially no difference was observed between the mean dissolution profiles of the different pellets in the peak vessel, whereas D was somewhat slower than E in the standard *USP* apparatus (Fig. 6). A human, single-dose, fasting bioavailability study with D and E was performed, and the formulations were not significantly ($p > 0.05$) different. In addition, no tendency toward a slower absorption for pellets E was revealed. Thus, the difference between the dissolution–time profiles observed in the standard method was not relevant to the in vivo situation. The slower-release profile obtained for pellets D in the standard method was most probably due to the gathering of pellets at the bottom vessel. This phenomenon, therefore, may be considered a pure hydrodynamic in vitro artifact that could be avoided by use of the peak vessel. These results may well be of relevance also for other pellet formulations that are poorly dispersed in the standard *USP* II method.

B. Case Example: Hydrophilic Matrix ER Tablets with Erosion-Controlled Drug Release

The hydrophilic matrix tablet is a common principle for obtaining extended drug release (15). Such a tablet gradually forms a gel layer from the surface of tablet toward its center in contact with the dissolution medium. The drug is released either by diffusion through the gel matrix or by erosion at the tablet surface. For poorly soluble compounds, the drug release is controlled entirely

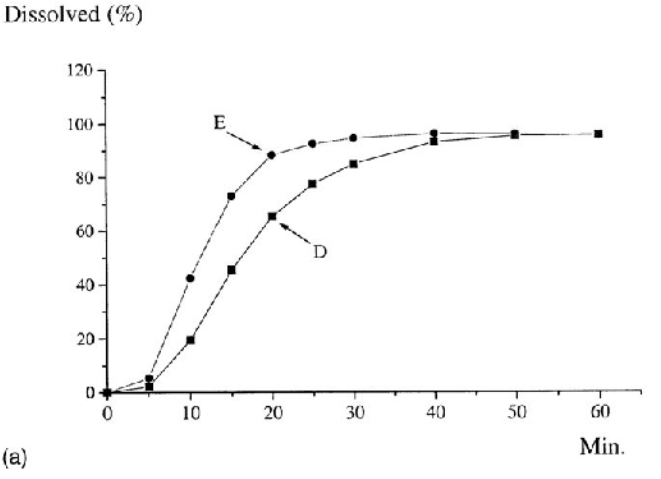

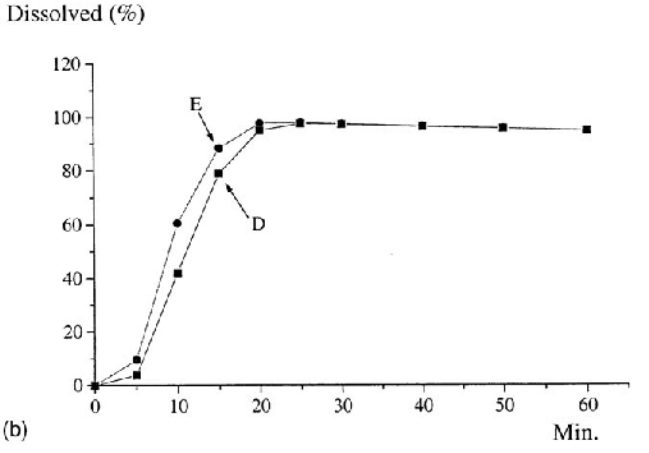

FIG. 6 Mean drug dissolution–time profiles of pellets D and E in (a) the standard *USP* II method and (b) in the peak vessel at a stirring rate of 100 rpm.

by the latter process. The present case comprises data for only matrices with erosion-controlled drug release.

The hydrodynamics play an important role in the dissolution testing of such formulations for several reasons. First, hydrophilic matrices can adhere to the glass walls of the dissolution test equipment and become stuck there for a long time. They may also float on the surface of the dissolution medium after gel formation. Both of these phenomena can create variable and irrelevant results. This must be considered when selecting a test apparatus. In the present case, a *USP* II apparatus, modified with a stationary basket (Fig. 7) containing the tablet was used to avoid this problem.

Another more complicated hydrodynamic effect for hydrophilic matrices is caused by the sensitivity of tablet erosion—and thereby, drug release—to the intensity of the agitation. For example, the drug-release rate could be twice as high at a paddle-stirring rate of 100 rpm as that at 50 rpm in the *USP* II apparatus. Therefore, in the development of products based on this principle, it is crucial to know which apparatus and agitation intensity provides release rates that correspond to the in vivo situation. Otherwise, the in vitro results could lead to misdirected formulation developmental work, consuming further time and resources before the final product is obtained.

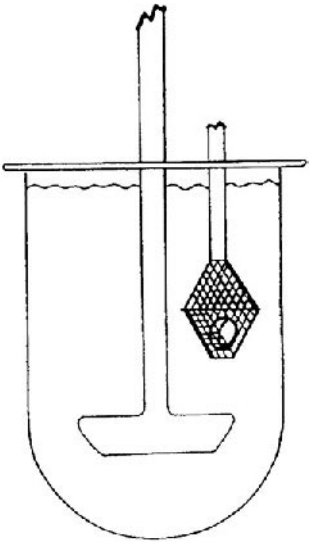

FIG. 7 *USP* II apparatus modified with a stationary basket.

Three different hydrophilic gel matrix tablets with different release rates were studied in a human bioavailability study (16) with administration under fasting conditions. All of the tablets had also been tested in vitro at paddle-stirring rates of both 50 and 100 rpm. The linear relation between the in vitro and in vivo dissolution rates, expressed as mean dissolution times (MDT), are given in Table 2. A close to 1:1 relation between the in vitro and in vivo release rates was obtained at 50 rpm, whereas at the higher agitation intensity the drug release rate in vitro was twice as high as that in vivo. From a practical standpoint it might still be desirable to use the higher agitation intensity, because the time required for an in vitro dissolution test can be shortened, thus increasing the efficiency of the dissolution test laboratory. Such an approach would be valid in a formulation development stage provided that the in vitro data are time-scaled to obtain a correct estimate of the duration of the in vivo profile. The faster paddle-stirring rate could also be justified when the test method is used as a batch quality control method, because the in vitro and in vivo correlation and discrimination between tablets with different release rates was as good as at the slower agitation rate. It might also be tempting to conclude from these data that paddle stirring at 50 rpm in a *USP* II beaker generally provides in vivo relevant hydrodynamic conditions. However, in other attempts to make similar comparisons, different results were obtained. For example, one study has indicated that in vivo relevant agitation was obtained at a paddle-stirring rate as low as 10 rpm using the *USP* II apparatus (17). Until more experience has been accumulated on this subject the identification of in vivo relevant hydrodynamics will need to be investigated on a case-by-case basis.

In the development of an ER tablet, in vitro dissolution testing may be used not only to reach the desired average release properties, but also to obtain

Table 2 Linear Regression Analysis of the Relation Between the Mean Dissolution Time (MDT) in vivo (y) and MDT in vitro (x) of Felodipine in a Modified *USP* II Apparatus at 50 and 100 rpm for Three Different ER Tablets

Stirring rate (rpm)	Relation	r^2
50	$y = 1.1x + 0.1$	0.94
100	$y = 2.1x - 0.5$	0.94

a formulation that has release properties that are relatively robust for the different physiological hydrodynamic conditions. For example, the intake of food can be expected to alter the hydrodynamics in the upper GI tract. This may affect the tablet erosion and, thereby, drug release. One in vitro test strategy that can be used to investigate such effects is to test under a wide variety of hydrodynamic conditions. In the present case, a more thorough investigation was performed on two different gel matrix tablets denoted B and G. Three different methods were used, including the modified *USP* II method, the *USP* III apparatus (reciprocating cylinder), and a rotating flask with baffles (12). All three apparatuses were operated at varying agitation intensities. In this set of experiments, tablet erosion was measured as a surrogate for drug dissolution. The times required for 50% tablet erosion of the different test conditions are given in Fig. 8 as a measure of the erosion–drug-release rate. The erosion rate of both tablets increased under more intense agitation in all apparatuses, as would be expected. However, the effect of agitation intensity was larger on tablet G. This was most apparent in the *USP* II apparatus and least obvious in the rotating flask. Tablets B and G were also investigated in humans under both fasting and fed conditions relative to both in vivo dissolution, as determined from plasma drug concentrations, and in vivo tablet erosion, as determined by gamma-scintigraphy (18,19). For tablet G, in vivo tablet erosion (see Fig. 8) and drug dissolution were strongly affected by food, whereas tablet

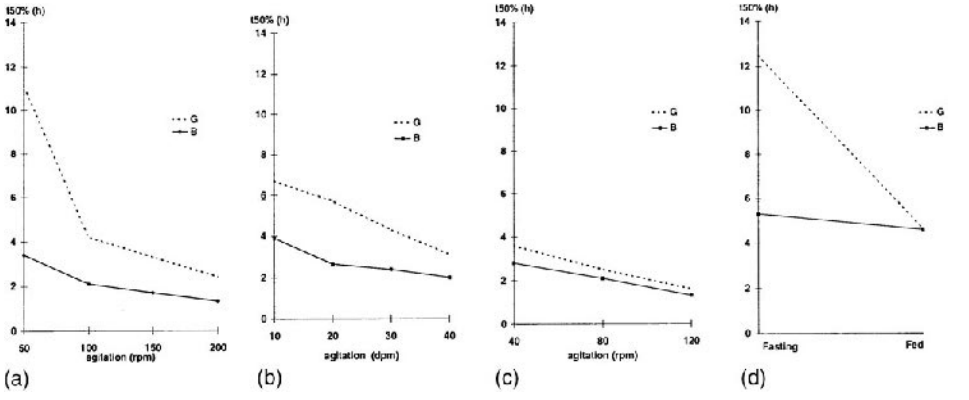

FIG. 8 Time to 50% (*t*50%) tablet erosion vs. agitation intensity in vitro in (a) *USP* II, (b) *USP* III, (c) rotating flask, and (d) in vivo apparatuses and *t*50% in vivo after administration under fasting and nonfasting conditions for two hydrophilic matrix tablets (B and G).

B was almost unaffected. Thus, the difference between the tablets in their response to hydrodynamic conditions indicated by the in vitro testing was a relevant measure for selecting the formulation with the most robust properties. In addition, it was noted that the modified *USP* II apparatus provided the most discriminative test, especially at moderate agitation intensities.

IV. POORLY SOLUBLE COMPOUNDS

Low water solubility is a substance property that may increase the difficulty of obtaining in vivo predictive results in in vitro dissolution testing. The dissolution rate (dm/dt) of a drug substance according to the Noyes–Whitney equation can be expressed as:

$$\frac{dm}{dt} = \frac{DS}{h}(C_s - C_t)$$

where D is the diffusion coefficient in the stagnant diffusion layer around each solid particle; h is the thickness of the diffusion layer; S is the effective surface area of the particles; C_s is the saturation solubility; and C_t is the concentration in the test medium at time t. All these factors can clearly be affected by the dissolution test conditions. For example, C_s and C_t are dependent on the composition of the test medium. Wetting effects may also result in variation of S with the test medium. In addition, S and h are dependent on the hydrodynamic conditions. The equation implies that to obtain an in vitro dissolution test that is relevant to the in vivo situation, all these variables must be set at a level that corresponds to the in vivo situation.

So far, the major issue in the development of dissolution tests for poorly soluble compounds has not been how to attain in vivo relevant dissolution conditions, but rather, how to obtain adequate solubility of the drug in the test medium. Generally, the goal has been to obtain ''sink conditions,'' which corresponds to a drug solubility (C_s) that is five to ten times the concentration reached when the complete dose has been dissolved. At sink conditions, the term C_t in the Noyes–Whitney equation can be neglected (i.e., the dissolution rate at all time points will be independent of the amount already dissolved. There are several good reasons why the concept of sink conditions has been so well established. First, testing under ''non–sink conditions'' may not discriminate for formulation effects exerted during the later part of the dissolution–time profile, because the dissolution rate will be influenced more by the amount of drug already in solution (C_t) than by the dosage form performance. The use of sink conditions can also be justified from an in vivo prediction point of view if it can be assumed that the C_t in the GI fluids is negligible

owing to rapid absorption of the drug over the gastric wall. This concept has been experimentally supported by an in vivo dissolution experiment in humans for a low-solubility, high-permeability drug (20). Finally, sink conditions are desirable for practical reasons, such as the possibility of using the same method and specification requirements for different dose strengths in quality control.

It is often a trivial task to obtain sink conditions in the in vitro dissolution test medium. In the first instance, the pH of the test medium can be adjusted to increase the solubility or the volume of the dissolution medium. There are several ways to increase volume, including use of the maximum volume in a standard vessel, use of larger vessels, use of the flow-through cell (*USP* IV) or other noncompendial methods when the dissolution medium is exchanged. However, such approaches may not provide sufficient solubility if the drug is aprotic or has a very low solubility in relation to the dose. In those cases, a surfactant in concentrations above the critical micelle concentration (CMC) or a cosolvent can be added. The use of surfactants is currently favored because this is felt to be a more in vivo realistic system, as surfactants, such as bile salts, are present in vivo (21). The solubility can sometimes be improved by several orders of magnitude using surfactants, with sink conditions easily reached at reasonably low surfactant concentrations.

Attainment of sink conditions, however, does not guarantee that the in vitro test will provide in vivo relevant results, as will be exemplified in the following case. To achieve the same dissolution rate in vitro and in vivo, the saturation solubility in the test medium should correspond to the in vivo situation, for the dissolution rate is dependent on the solubility (C_s). The in vivo solubility is dependent on bile salts, which are present primarily in the small intestine at varying concentrations depending on site and physiological state. This is not a well-defined system, as there is a mixture of different bile salts, and they form mixed micelles with lecithin and monoolein. In addition, a poorly soluble drug can also be dissolved in the fatty part of the emulsion droplets formed in the small intestine as a part of lipolysis, although there are indications that this effect has a negligible influence on the dissolution rate (22). It is clear that such a dynamic and complex system cannot be fully reconstituted in vitro. The most commonly adopted approach is to use a synthetic surfactant, especially sodium lauryl sulfate (SLS). The amount of surfactant to be used in the test method is often established by (a) solubility measurements to reach sink conditions, or (b) the ability to obtain discriminative in vitro dissolution results between drug particles of different size, or (c) achievement of in vitro–in vivo correlation for drug particles of different size or other product characteristic that is supposed to affect the dissolution rate. Another approach based on the concept to mimic the in vivo situation by use of physiologically relevant levels of bile salt and lecithin has been described recently

in the literature (3). Such methods may not provide sink conditions for all drugs, which probably makes them more suitable as developmental tools and for biopharmaceutical documentation of comparisons of formulations than for batch quality control.

There are some additional aspects on the use of surfactants in the in vitro dissolution test medium that have to be considered to obtain valid data. For example, the surfactant may interact with components of the dosage form in a way that affects the dissolution rate. If that kind of interaction has no physiological relevance, the correlation to in vivo data will be confounded. This will be further exemplified in the following case. Another potential problem concerning the use of surfactants, especially in batch quality control, is that the quality of the surfactants may affect the dissolution rate. This has been shown in a study using different purity levels of SLS (23). Even between-lot variations in a certain quality of a surfactant can be so significant that unacceptable variations in the dissolution results are obtained (24). Thus, the quality of the surfactants used in the dissolution tests may sometimes need to be further defined beyond the pharmacopoeial and manufacturer specifications.

A. Case Example: Felodipine ER Tablets

Felodipine is an aprotic, poorly soluble (0.001 mg/mL) drug, with complete absorption across the intestinal epithelium, although the systemic availability is reduced to 15% by first-pass extraction (25). Felodipine has good absorption over the entire GI tract, including the colon, as indicated by a pharmacoscintigraphic study and in absorption data for formulations with 24-h duration of drug release (19,26).

The rationale for developing an ER formulation of felodipine was very clear: the plasma drug elimination half-life is short, there is a direct relation between plasma drug concentrations and the antihypertensive effect, side effects may occur at high plasma drug peak levels, and the drug has good absorption properties even in the more distal parts of the intestines. The final ER formulation was of the hydrophilic matrix type, as described earlier in this chapter. To avoid poor dissolution of the drug in vivo, felodipine was solubilized in the tablet by use of dissolution enhancers. The success of this approach was verified by attainment of human bioavailability equivalent to that of an oral solution (16).

A series of studies were performed to better understand the dissolution process for these tablets, in particular, to identify critical dissolution and formulation parameters. The in vitro drug dissolution and tablet erosion, measured as loss of dry weight, were superimposable under different in vitro test

conditions, such as pH, ionic strength, osmolality, viscosity, surfactant concentration, or paddle-stirring rate. It was thus concluded that the drug release in vitro was entirely controlled by the erosion of the hydrophilic matrix and not directly dependent on the dissolution of the poorly soluble substance. Owing to the consistency of the erosion control, irrespective of the test conditions, it was assumed that tablet erosion was also the rate-limiting step in the drug dissolution process in vivo. To investigate this hypothesis, a pharmacoscintigraphic study was performed in humans, which included measurement of tablet erosion (19). There was a good resemblance between drug dissolution, as determined from plasma concentration data, and tablet erosion in vivo as well as in vitro. This further strengthened the hypothesis that tablet erosion was the most critical process in dissolution testing of these tablets.

The main in vitro dissolution method used in the development of this product was based on the modified *USP* II apparatus described earlier, with a close to neutral buffer, including 1% SLS to achieve sink conditions. This method was validated by an in vitro–in vivo correlation study that included three different ER tablets for which the release rate had been altered by changing the gel matrix composition (16). These three tablets were tested in humans and, despite the complex situation with a poorly soluble drug in an ER formulation, a good correlation between mean dissolution time (MDT) in vitro and in vivo was obtained (Fig. 9). The method was thus concluded to be suitable both as a tool for further development and for batch quality control.

At a later stage, it was decided to change the formulation of the felodipine ER tablet to reduce the tablet size. This could be achieved by using more viscous hydrophilic polymers. The in vitro dissolution method with 1% SLS, just described, was initially used as a developmental tool. A prototype formulation of a smaller size was developed that had an in vitro release profile similar to that of the original product, which was desirable because the aim was to achieve bioequivalence between the old and new product. However, a small pilot bioavailability study in humans showed very different plasma drug concentration profiles for the old and new formulation, i.e., the results from the in vitro test were misleading. Surfactants other than SLS were then tested in the dissolution medium to improve the in vivo prediction for the in vitro method. This was a successful approach and a satisfactory discrimination was obtained between the two tablets tested in vivo. A more thorough investigation was performed to better understand the underlying reasons for the differences bound between the various surfactants and to validate a new method (17). Three different tablets of the smaller size with different release rates (A, B, and C) were tested both in vitro with SLS, the cationic cetyltrimethylammonium bromide (CTAB), and a nonionic surfactant (Tween), respectively, and in a bioavailability study in humans. Three different concentrations of

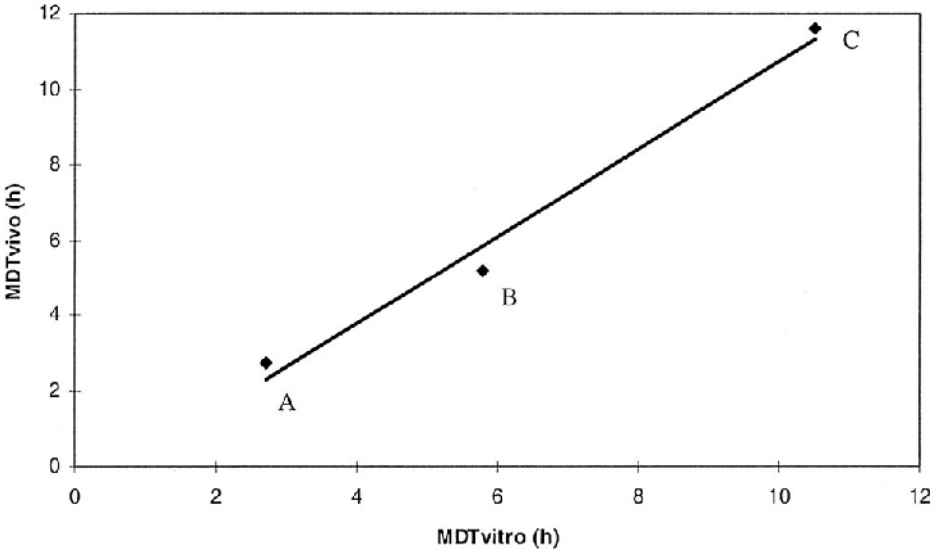

FIG. 9 Mean dissolution time (MDT) in vivo vs. MDT in vitro for three different felodipine ER tablets (A, B, and C).

each surfactant were used. At each level concentrations were chosen so that each surfactant provided approximately the same felodipine solubility. All surfactant concentrations were well above CMC and the amount needed for sink conditions. A close to linear in vitro release–time profile was obtained for all test media, but the rate for one of the tablets varied more than twofold between the different media. It was also clear that the difference between the three tablets was smaller when SLS was used than when the other two surfactants were used (Fig. 10). The differences in vitro among dissolution results obtained for the three surfactants were most probably due to different degrees of interaction between the surfactant and the gel-forming polymers. The most pronounced effect was exerted by SLS. The effect of SLS on tablet erosion was verified by tablet erosion experiments, and the surfactant–polymer interaction was also supported by cloud point measurements in diluted polymer solutions (27). Comparison of the in vitro and in vivo dissolution data showed a good correlation for all three surfactants (Fig. 11). However, a very steep relation was obtained with SLS, and it could thus be concluded that the interaction effect exerted by SLS on the hydrophilic matrix did not have any in vivo relevance. This implied that SLS was not adequately predictive, because a great difference in the in vivo performance was reflected by only a small

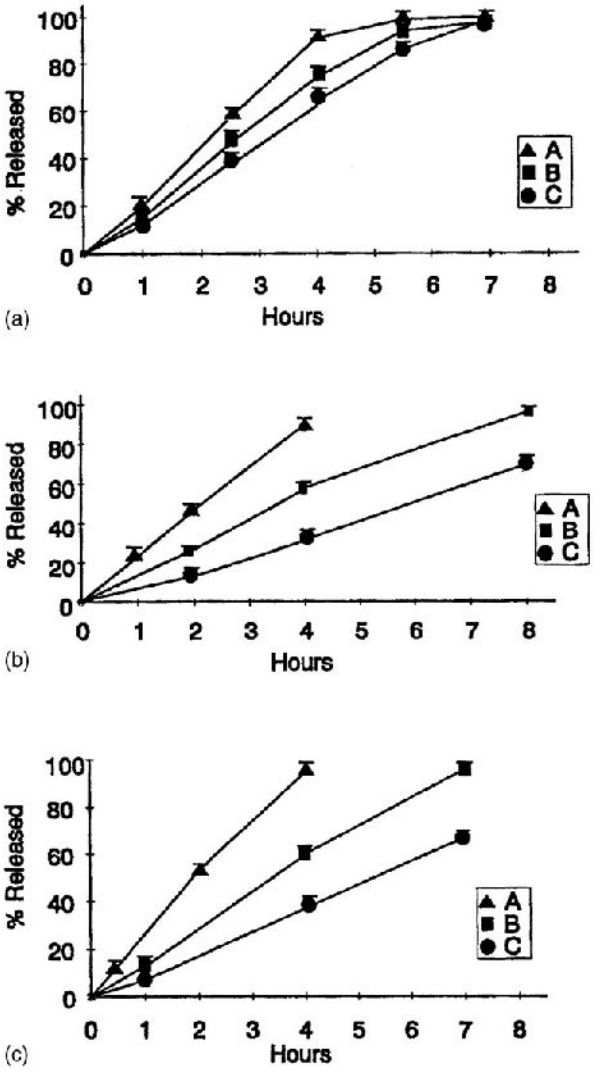

FIG. 10 Mean (SD) cumulative in vitro dissolution–time profiles of felodipine for three different ER tablets (A, B, and C) in dissolution test media either containing SLS (a), Tween (b), or CTAB (c).

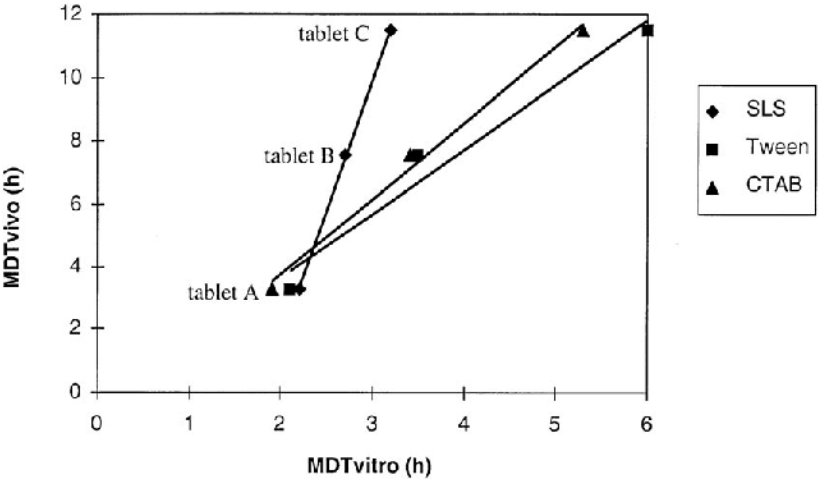

FIG. 11 Mean dissolution time (MDT) in vivo vs. MDT in vitro for three different surfactants, SLS, CTAB, and Tween in the dissolution test media. Each point in the graph represents mean data for one of three different ER tablets (A, B, and C) included in the study.

difference in vitro. This was also the reason for the failure in the initial development work on the small tablet (described earlier). In summary, it is clear that the use of a surfactant in the dissolution medium must be evaluated for interactions with release–rate-controlling excipients, and that SLS is not suitable for all products.

The foregoing data illustrate that the in vitro dissolution method can successfully predict the in vivo performance of felodipine ER tablets, especially after the exchange of SLS. However, as the next and final part of the felodipine example will illustrate, if the release mechanisms are changed, the in vivo prediction can be lost. An experimental tablet was manufactured that had exactly the same composition as the marketed product. However, the drug was included in a crystalline state in the experimental tablet in contrast with the solubilized form used in the product. The in vitro dissolution data for the two tablets were identical (Fig. 12) as might be expected from the fact that they contained the same gel matrix and, therefore, ostensibly the same tablet erosion rate. The two tablets were tested in a small bioavailability study in humans, and the resulting plasma drug concentration profiles are shown in Fig. 12. Almost no drug was absorbed from the experimental tablets. The lack of absorption was most likely caused by poor dissolution of the drug in vivo

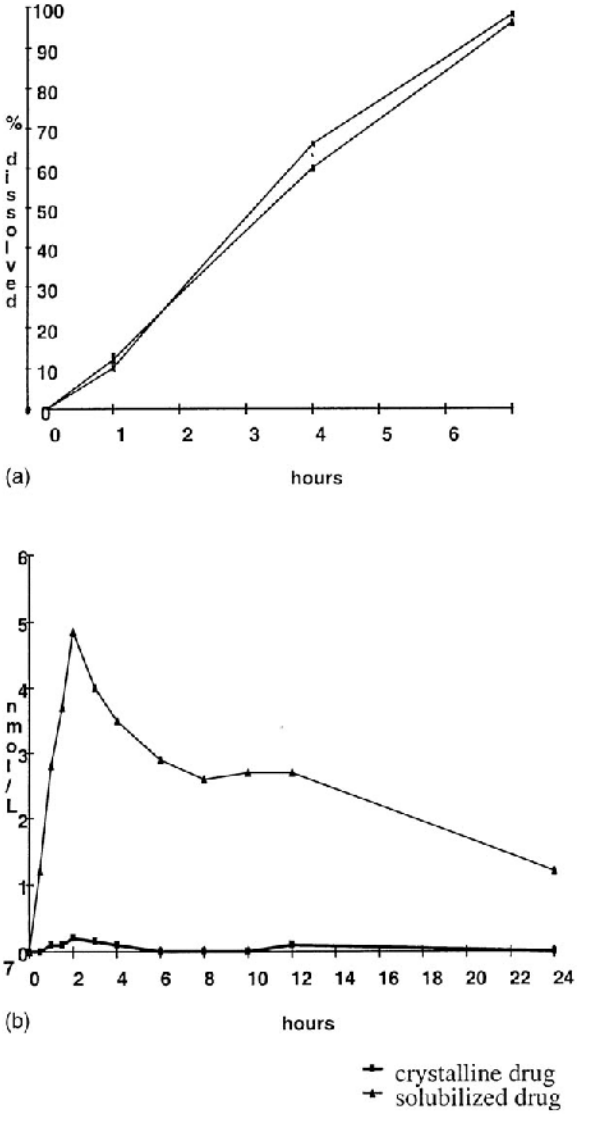

FIG. 12 Mean cumulative in vitro dissolution–time curves (a) and mean plasma drug concentration–time curves (b) for two felodipine ER tablets containing the drug in a crystalline or solubilized form.

(i.e., the drug dissolution was much slower than the tablet erosion). The use of the surfactant in amounts providing sink condition resulted in a lack of discrimination of such effects. An in vitro test medium providing more in vivo realistic dissolution enhancement would, therefore, be required here. Thus, it is important to identify the rate-limiting step in the dissolution process and to bear in mind that the concept of sink conditions may, under certain conditions, provide a solubility that is too favorable to obtain discriminative results.

V. PREDICTION OF FOOD EFFECTS

Food can directly or indirectly exert a wide range of effects on the drug dissolution from a solid product. Therefore, it is relevant at certain points in the developmental process of a new solid dosage form to evaluate food-induced effects on the in vitro drug dissolution. For example, an assessment could be performed in connection with an in vivo food interaction study to improve the interpretation of the bioavailability data obtained, or be used more proactively to select the least-affected candidate formulation for further development. A third situation could arise when the composition or manufacturing process has been altered, but the original and the modified product are meant to have the same properties. Thus, in vitro dissolution tests could clearly play a role in predicting the influence of food on drug dissolution.

The influence of food on drug dissolution may occur directly or by interaction with the dosage form. Such effects can be directly mediated by the food constituents or by secondary effects induced by the presence of food in the GI tract. Direct effects include changes in pH, osmolarity, viscosity, concentration of ionic and nonionic solutes, fats, carbohydrates, and proteins. Indirect effects, such as altered motility and increased secretory flow of bile salts and others, can lead to altered agitation, surface activity, and solubility. Several attempts to model food-induced effects on drug dissolution have been described, including use of the following (3,28–34):

Bile salt and lecithin
pH changes
Fat emulsions, such as Intralipid or milk
Well-defined nutritional drinks
Enzymes
Dynamic lipolytic models
Presoaking in oil
Viscosity enhancement
Inert beads to obtain a grinding effect similar to that of solid foodstuff

Good predictions of in vivo dissolution have also been reported for some methods. However, it is typical of all methods that they cover a limited number of potential food effects. This implies that no method described so far is generally applicable. The success of in vivo predictions for those methods will be dependent on the substance and formulation properties (i.e., prediction of food effects will be obtained when the critical in vivo factor is included in the in vitro test). Two approaches to studying food effects in vitro will be presented in the next example. They are intended to provide somewhat more generally applicable methods, although they are by no means close to the full complexity of the in vivo physiology.

A. Case Example: Food Effects on Tablet Erosion of Hydrophilic Matrix Tablets

Two in vitro food interaction studies were performed using different methods (35). Both studies included two different hydrophilic matrix tablets. One of the tablets (denoted A) had previously been shown to erode much faster in the GI tract after intake together with food than after administration under fasting conditions (20). The other tablet (denoted B) was almost unaffected by food (19), and it was included in the in vitro test to exclude false-positive results.

The first set of experiments was performed with a modified *USP* II apparatus, including test media designed to correspond to the in vivo fluids under fasting and fed conditions. The following test media and time intervals were used:

	Fasting	Fed
Stomach	1-h duration 0.1 M HCl	3-h duration Multicomponent nutritional liquid pH adjusted to 5.6 by HCl
Intestine	Krebs–Henseleit Ringer buffer pH 7.2 5 mM sodium taurocholate 0.5% fat emulsion (Intralipid)	Krebs–Henseleit Ringer buffer pH 7.2 20 mM sodium taurocholate 5% fat emulsion (Intralipid)

All test media were stable and homogeneous for at least 24 h at 37°C. The resulting erosion–time profiles for tablet A and B are shown in Fig. 13. The simulated food conditions slightly retarded the erosion rate for both tablets.

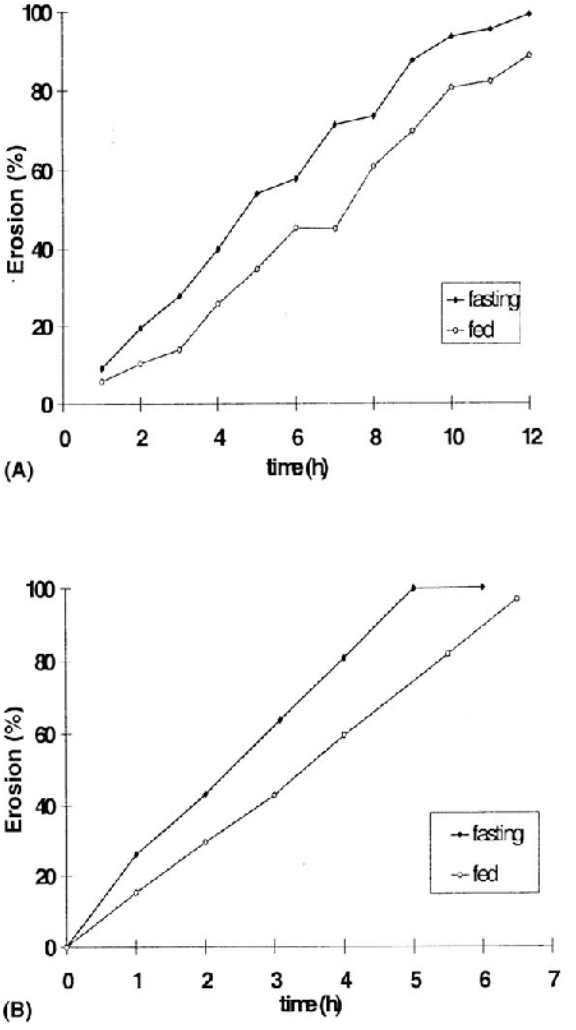

FIG. 13 Mean cumulative in vitro tablet erosion–time curves for two hydrophilic matrix ER tablets (A and B) tested under simulated fasted and fed conditions.

Factors, Settings, Physicochemical Characterizations of Test Media and Tablet Erosion Rate for All Experimental Runs ional 2^6 Factorial Design of Two Hydrophilic Matrix Tablets (A and B)

pH nominal	NaCl (M)	Brij (mM)	Urea (M)	HPMC (M)	Paddle speed (rpm)	pH measured	Ionic strength	Surface tension (mN/m)	Osmolarity (mOsM)	Viscosity (mPas)	Erosic rate (%/h A	
2.3	0.08	30	0.2	1	150	2.4	0.08	41	390	230	5	1
6.8	0.08	30	0	0	150	6.8	0.1	43	190	1	11	2
2.3	0.18	30	0	1	50	2.3	0.18	42	400	250	1.5	
6.8	0.18	30	0.2	0	50	6.7	0.2	43	600	1	2.9	1
2.3	0.08	0	0.2	0	50	2.4	0.08	72	360	1	4.8	1
6.8	0.08	0	0	1	50	6.8	0.1	49	190	270	2.9	1
6.8	0.08	0	0	1	50	6.8	0.1	45	190	280	3	1
2.3	0.18	0	0	0	150	2.3	0.18	72	350	1	13	2
2.3	0.18	0	0	0	150	2.3	0.18	71	350	1	13	2
6.8	0.18	0	0.2	1	150	6.7	0.2	48	580	260	5.2	2
6.8	0.18	0	0	1	50	6.7	0.2	48	370	230	2.2	1
2.3	0.18	0	0	1	50	2.3	0.18	50	390	250	2.7	1

Copyright © Marcel Dekker, Inc. All rights reserved.

Marcel Dekker, Inc.
270 Madison Avenue, New York, New York 10016

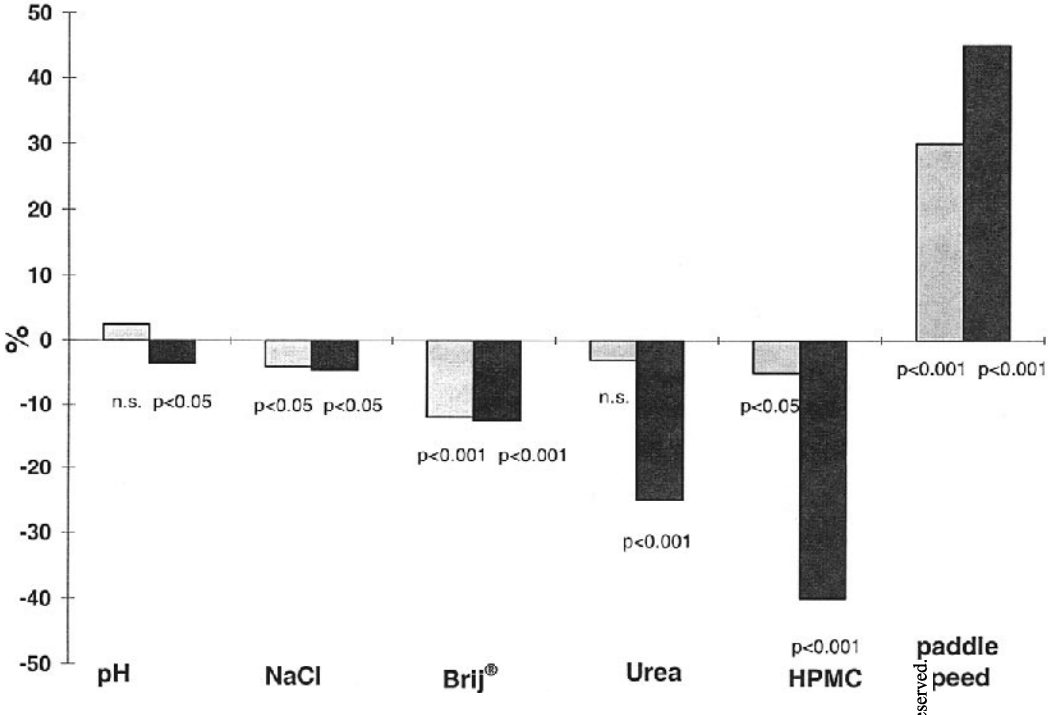

FIG. 14 Influence on the tablet erosion rate for two hydrophilic matrix tablets (A and B) of H, NaCl concent tion, surfactant concentration (Brij), urea concentration, HPMC concentrations in the dis ution test mediu and paddle-stirring rate. The influence of each factor is expressed as percentage char from low to h level used in a 2^6 fractional factorial experimental design (see Table 3). The statistica significances of different factors are also given.

Copyright © Marcel Dekker, Inc. All rights reserved.

MARCEL DEKKER, INC.
270 Madison Avenue, New York, New York 10016

A corresponding effect may occur for these formulations in vivo, but because this did not correspond with the in vivo data for the two tablets, factors other than those included in the present test must also play a role. This applies especially to tablet A, for which the erosion rate was drastically increased by food in vivo. This illustrates that, despite the use of rather complex test media, it was still not possible to predict an in vivo food effect.

The other set of experiments on tablets A and B were focused on the effects of different physicochemical factors that could be induced by a meal, such as pH, ionic strength, surface activity, osmotic pressure and agitation. Different physicochemical conditions were obtained mainly by agents of a nonphysiological origin, but the amounts used were set to correspond to the levels obtained in the GI tract after fasting and fed conditions. A fractional factorial design was employed for this investigation, and the different experimental conditions are given in Table 3, together with the resulting erosion rates. The relative effect of each variable on the erosion rate of tablets A and B is shown in Fig. 14. Table A, being sensitive to food effects in vivo, was also more affected by the different factors in vitro than tablet B, especially the osmotic pressure (urea), viscosity (hydroxypropyl methylcellulose; HPMC), and paddle-stirring rate. However, the paddle-stirring rate was the only factor that increased the erosion rate in accordance with the in vivo food effect. The far greater susceptibility of tablet A to changes in viscosity further supported the conclusion that this tablet was much more sensitive to hydrodynamic stress. Thus, this type of multifactorial studies may be very helpful in comparisons of robustness versus food effects between different formulations, and they also indicate which factors are of importance.

VI. CONCLUSION

In vitro dissolution is a very cost-effective tool in development of solid dosage forms provided that in vivo predictive results are obtained. To fulfill this requirement, physicochemical and pharmacokinetic properties of the substances, as well as the function of the dosage form and physiological factors, must be taken into consideration in design of dissolution tests and in predictions of in vivo performance based on in vitro data.

REFERENCES

1. Welling PG. In vitro methods to determine bioavailability: in vitro–in vivo correlations. In: Welling PG, Tse LST, Dighe SV, eds. Pharmaceutical Bioequivalence. New York: Marcel Dekker, 1991:223–232.

2. Abuzarur-Aloul R, Gjellan K, Sjölund M, Löfqvist M, Graffner C. Critical dissolution tests of oral systems based on statistically designed experiments. I. Screening of critical fluids and in vitro/in vivo modelling of extended release coated spheres. Drug Dev Ind Pharm 1997; 23:749–760.
3. Galia E, Nicolaides E, Horter D, Löbenberg R, Reppas C, Dressman JB. Evaluation of various dissolution media for predicting in vivo performance of class I and II drugs. Pharm Res 1998; 15:698–705.
4. Minekus M, Havenaar R. In vitro model of an in vivo digestive tract. US Patent 5525305, 1996.
5. Daly PB, Davis SS, Frier M, Hardy JG, Kennerley JW, Wilson CG. Scintigraphic assessment of the in vivo dissolution rate of sustained release tablet. Int J Pharm 1982; 10:17–24.
6. Abrahamsson B, Alpsten M, Bake B, Larsson A, Sjögren J. In vitro and in vivo erosion of two different hydrophilic gel matrix tablets. Eur J Pharmacol Biopharm 1998; 46:69–75.
7. Vidon N, Evard D, Godbillon J, Rongier M, Duval M, Schoeller JP, Bernier JJ, Hirtz J. Investigation of drug absorption from the gastrointestinal tract of man. II. Metoprolol in jejunum and ileum. Br J Clin Pharmacol 1985; 19(suppl 2): 107S–112S.
8. Godbillon J, Evard D, Vidon N, Duval M, Schoeller JP, Bernier JJ, Hirtz J. Investigation of drug absorption from the gastrointestinal tract of man. III. Metoprolol in the colon. Br J Clin Pharmacol 1985; 19(suppl 2):113S–118S.
9. Abrahamsson B, Alpsten M, Jonsson UE, Lundberg PJ, Sandberg A, Sundgren M, Svenheden A, Tölli J. Gastro-intestinal transit of a multiple-unit formulation (metoprolol CR/ZOK) and a non-disintegrating tablet with the emphasis on colon. Int J Pharm 1996; 140:229–235.
10. Ragnarsson G, Sanberg A, Johansson MO, Lindstedt B, Sjögren J. In vitro release characteristics of membrane-coated pellet formulation—influence of drug solubility and particle size. Int J Pharm 1992; 79:223–232.
11. Sandberg A, Abrahamsson B, Sjögren J. Influence of dissolution rate on the extent and rate of bioavailability of metoprolol. Int J Pharm 1991; 68:167–177.
12. Koch HP. The resotest apparatus. A universally applicable biopharmaceutical experimental tool. Methods Find Exp Clin Pharmacol 1980; 2:97–102.
13. Abdou HM. Dissolution, Bioavailability and Bioequivalence. Easton, PA: Mack Publishing, 1989.
14. Aoki S, Ando H, Tatsuishi K, Uesugi K, Ozawa H. Determination of the mechanical impact force in the in vitro dissolution test and evaluation of the correlation between in vivo and in vitro release. Int J Pharm 1993; 95:67–75.
15. Melia CD. Hydrophilic matrix sustained release systems based on polysaccharide carriers. Crit Rev Ther Drug Carrier Syst 1991; 8:395–421.
16. Abrahamsson B, Johansson D, Torstensson A, Wingstrand K. Evaluation of solubilizers in the drug release testing of hydrophilic matrix extended-release tablets of felodipine. Pharm Res 1994; 11:1093–1097.

17. Shameem M, Katori LN, Aoyagi N, Kojima S. Oral solid controlled release dosage forms: role of GI–mechanical destructive forces and colonic release in drug absorption under fasted and fed conditions in humans. Pharm Res 1995; 12: 1049–1054.
18. Abrahamsson B, Alpstein M, Hugosson M, Jonsson UE, Sundgren M, Svenheden A, Tölli J. Absorption, gastrointestinal transit and tablet erosion of felodipine extended-release (ER) tablets. Pharm Res 1994; 10:709–714.
19. Abrahamsson B, Alpsten M, Bake B, Jonsson UE, Eriksson-Lepkowska M, Larsson A. Drug absorption from a nifedipine hydrophilic matrix entended-release (ER) tablet—comparison with an osmotic pump tablet and effect of food. J Controlled Release 1998; 52:301–310.
20. Bönlökke L, Christensen FN, Hovgard L, Kristensen HG, Lennernäs H. A new approach to study in vivo dissolution of drugs in humans. Pharm Res 1997; 14: 1490–1492.
21. Shah VP, Konecny JJ, Everett RL, McCullough B, Noorizaden AC, Skelly JP. In vitro dissolution profile of water-insoluble drug dosage forms in the presence of solubilizers. Pharm Res 1989; 6:162–618.
22. Amidon GL. In: Biopharmaceutics Drug Classification and International Drug Regulation. Capsugel Seminars and Open Forums, Tokyo, Japan, 1997:13–27.
23. Amidon GL, Crison JR, Weiner ND. Dissolution media for in vitro testing of water-insoluble drugs: effect of surfactant purity and electrolyte on in vitro dissolution of carbamazepine in aqueous solutions of sodium lauryl sulfate. J Pharm Sci 1997; 86:384–388.
24. Data on file, Astra Hässle
25. Edgar B, Lundborg P, Regårdh. Clinical pharmacokinetics of felodipine. A summary. Drugs 1987; 34(suppl 3):16–27.
26. Wingstrand K, Abrahamsson B, Edgar B. Bioavailability from felodpinine extended-release tablets with different dissolution properties. Int J Pharm 1990; 60:151–156.
27. Löfroth JE, Johansson L, Norman AC, Wettström K. Interactions between solubilizers and polymers. I: HPMC. Prog Colloid Polym Sci 1991; 1–5.
28. Aoki S, Uesugi K, Tatsuishi K, Ozawa H, Kayano M. Evaluation of the correlation between in vivo and in vitro release of phenylpropanolamine HCl from controlled-release tablets. Int J Pharm 1992; 85:65–73.
29. Wearley L, Karim A, Pagone F, Streicher J, Wickman A. Food-induced theophylline release/absorption changes from controlled-release formulations: a proposed in vitro model. Drug Dev Ind Pharm 1988; 14:13–28.
30. Junginger HE, Verhoeven J, Peschier LJC. A new in vitro model to detect interactions between controlled release dosage forms and food. Acta Pharm Technol 1990; 36:155–160.
31. Maturu PK. Influence of a high fat breakfast on the bioavailability of theophylline controlled-release formulations: an in vitro demonstration of an in vivo observation. J Pharm Sci 1986; 75:1205–1206.
32. Das SK, Gupta BK. Simulation of physiological pH–time profile in in vitro dis-

solution study: relationship between dissolution rate and bioavailability of controlled release dosage form. Drug Dev Ind Pharm 1988; 14:537–544.
33. Macheras P, Koupparis M, Tsaprounis C. Drug dissolution studies in milk using the automated flow injection serial dynamic dialysis technique. Int J Pharm 1986; 33:125–136.
34. Jonkman JHG, Schoenmaker R, Grimberg N, Zeeuw RA. A new in vitro dissolution test for controlled-release theophylline tablets. Int J Pharm 1981; 8:153–156.
35. Abrahamsson B, Roos K, Sjögren J. Investigation of post-prandial effects on hydrophilic matrix tablets. Drug Dev Ind Pharm 1999; 25:765–771.

13
Analysis of Drug Dissolution Data

Christos Reppas and Eleftheria Nicolaides
University of Athens, Athens, Greece

I. THE NEED FOR MULTIPOINT ASSESSMENT OF DISSOLUTION CHARACTERISTICS OF SOLID ORAL DOSAGE FORMS

Apart from providing experimental evidence for the validity of dissolution theories, drug dissolution data can be very useful at various stages during development of drug products, at the regulatory level, and at the clinical level.

Single-point dissolution testing still remains the most frequently recommended quality control test of immediate-release (IR) oral solid dosage forms in most pharmacopoeias worldwide. However, various national and international organizations have recently issued guidelines indicating that this test is suitable as a routine quality control test only for highly soluble and rapidly dissolving drug products (1,2). Single-point dissolution data may also be considered adequate for waiving an in vivo bioequivalence study for these products (1,2), although the time allowed for complete dissolution and the definition of complete dissolution have yet to be universally agreed on. However, if the in vitro single-point test result differs from the specification, this does not automatically imply bioinequivalence (e.g., 3) and, therefore, it is highly desirable to carefully map out the bioequivalence region for these products (4).

For characterizing the quality of an IR drug product a two-point specification is nowadays more often recommended (1). A two-point dissolution specification is already stipulated by some pharmacopoeias (e.g., 5) as a routine quality control test of some IR products (on a drug substance basis) and

it seems that in the future it will be the norm for any slowly dissolving or poorly water soluble drug (1).

Characterization of the complete dissolution profile or multipoint dissolution data comparisons are currently recommended in the following cases:

- When establishing the quality of extended-release (ER) drug products (6)
- To define in vitro dissolution specifications for generic IR (1) and ER products (5,6)
- To waive bioequivalence requirements for lower strengths of an IR dosage form (1)
- To establish IR product sameness after level 2 postapproval changes in components and composition (except for high-solubility, high-permeability drugs for which a single-point test is appropriate), in batch size, and in manufacturing equipment (7)
- To establish modified-release (MR) product sameness after level 2 postapproval changes (8)
- To establish product sameness after level 3 postapproval changes of both IR and MR products (7,8)
- In developing point-to-point in vitro–in vivo correlations or predicting the entire in vivo plasma profile based on dissolution data, regardless of the type of product (1,5,6)

II. CONSTRUCTING A CUMULATIVE DISSOLUTION DATA SET

Test conditions and sampling procedures vary with the aim of the test and the experimental setup.

When dissolution experiments are performed for studying the theoretical aspects of the process, the test conditions will depend on the model under consideration. If the dissolution profile is to be used for quality assurance purposes and in absence of specific direction in a relevant pharmacopoeial monograph, attention should be paid to obtaining an adequate profile within a practical time frame, in an aqueous medium, using compendial experimental setups. If the dissolution profile is to be used for prediction of the in vivo performance the in vitro conditions should simulate the in vivo environment as closely as possible and, depending on the in vitro apparatus used, they may lead to incomplete dissolution of the dose. Physiological data relevant to the design of dissolution tests, particularly relative to the composition, volume,

flow rates, and mixing patterns of the fluids in the gastrointestinal tract have been recently summarized (9).

If the data are collected in closed systems, successive sampling will reduce the volume of the dissolution medium and will remove part of the dissolved substance. Volume replacement will maintain a constant volume of dissolution medium, but it may create problems in identifying the plateau level when the ratio of the dose to the volume of the test medium is greater than the drug's solubility. In any case, the sample volume should be kept as small as possible, and corrections for the amount of drug removed with each sample have to be made.

Regardless of the aim of the dissolution test or the experimental setup, the number and the location of the data points within a profile are of major importance for its accurate description. Together with the number of repetitions, the sampling schedule determines the methods that may be used for comparing profiles.

For complete characterization of a profile that asymptotically reaches a plateau level, several data points are required (usually six to nine are sufficient). For this, sampling times should not be equidistant, but distributed in roughly logarithmic sequence over the interval of ''complete'' dissolution (e.g., the series 0, 2, 4, 6, 12, 18, 24, 36, 48, 60 min) for a total interval of 60 min (10). Situations that require extra caution include rapidly dissolving products (appropriately spaced data points are often difficult to obtain), and products with initial lag times (for which appropriate early data should be obtained so that the lag phase can be adequately characterized). However, if multipoint dissolution data comparisons are performed without prior complete profile characterization, three to five data points ''meaningfully'' spaced are usually required (see Sec. III.B.1).

III. ANALYSIS OF CUMULATIVE DISSOLUTION PROFILES

A. Characterization of Dissolution Profiles

Cumulative dissolution profiles can be partly characterized with parameters estimated directly from the raw data (i.e., with model-independent parameters). Such parameters provide information on the extent of dissolution, the global rate of the process (by means of characteristic times) or both.

Provided that a closed system is used, the extent of dissolution is reported as the maximum percentage dissolved ($X_{d\%,\max}$) or the maximum cumulative mass dissolved ($X_{d,\max}$). Provided that several data points are available, characteristic times can be estimated by linear interpolation or according to

statistical moment theory. The time for 50% dissolution, $T_{50\%}$, is the most frequently reported characteristic time which is estimated by interpolation. Alternatively, the mean dissolution time (MDT) is the first statistical moment for the cumulative dissolution process (e.g., 11) and is defined by the Eq. (1) (Fig. 1 explains the symbols):

$$\text{MDT} = \frac{\int_0^\infty tX_d(t)dt}{\int_0^\infty X_d(t)dt} = \frac{\text{ABC}}{X_{d,\max}} \tag{1}$$

On a practical basis, MDT can be estimated from the cumulative mass dissolved vs. time profile by using Eq. (2) (e.g., 3):

$$\text{MDT} = \frac{\sum_{i=1}^{n} t_{\text{mid}}\Delta X_d}{\sum_{i=1}^{n} \Delta X_d} \tag{2}$$

where i is the sample number, n is the total number of sample times, t_{mid} is the time at the midpoint between i and $i - 1$, and ΔX_d is the additional mass of drug dissolved between i and $i - 1$.

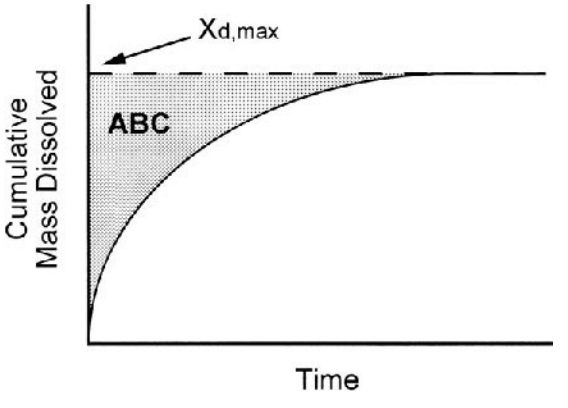

FIG. 1 Graphic presentation of the parameters used to estimate the mean dissolution time (MDT): $X_{d,\max}$ is the actual maximum cumulative mass dissolved, and ABC is the shaded area.

Finally, dissolution efficiency DE is a measure of both the extent and the overall rate of dissolution (12). *DE* is defined as the area under the dissolution curve up to a certain time *t*, expressed as a percentage of the area of the rectangle described by 100% dissolution in the same time. Provided that several data points are available, *DE* can be estimated with the trapezoidal rule (i.e., similar to the procedure presented for the estimation of ABC).

From the definitions it can be seen that two profiles may have identical *DE* values, or $X_{d,\max}$ and MDT values, and yet be quite different in shape. Therefore, unique characterization of the dissolution profile of a drug product usually requires the use of a model. Modeling is implicit when the theoretical aspects of dissolution are studied. It is also useful for setting dissolution specifications (13), for assessing the difference between two dissolution profiles (see Sec. III.B.2), and for predicting the entire in vivo plasma profile of the drug product (see Sec. III.C.1). Depending on the dosage form and the available theoretical basis for describing a specific dissolution data set, models can be built either according to the theoretical aspects of the process, or they can be (semi)empirical. Furthermore, depending on the complexity of the model, the procedure for profile characterization involves the fitting of a specific function to the data, or (less frequently) numerical solution of a differential equation.

1. *Dissolution Profile Description Based on the Theoretical Physicochemical Aspects of Dissolution*

These models are based on the Noyes–Whitney law of rate of solution of solid substances in their own solutions (14,15). Most frequently they are combined with the convective diffusion theory, and they are based on Eq. (3) (16,17).

$$\frac{dX_d}{dt} = \frac{D}{\delta} A\left(C_s - \frac{X_d}{V}\right) \tag{3}$$

where X_d is the mass of drug dissolved at time *t, A* is the surface area of the dissolving solid, *D* is the diffusion coefficient of the drug, δ is the effective diffusion boundary layer thickness, C_s is the total solubility in the dissolution medium, and *V* is the volume of the bulk solution. The usefulness of Eq. (3) in describing drug dissolution data depends on how well the various components of this equation can be monitored.

In the ideal case,

1. The process takes place in a closed system (i.e., the volume of dissolution medium can be maintained constant during the dissolution process).

2. Total solubility is independent of particle size.
3. The surface area of the dissolving solid remains unchanged throughout the process.
4. Dissolution is an isotropic process (i.e., the ratio D/δ, usually called the intrinsic dissolution rate constant, is constant in all directions).

Equation (3) can be integrated to give the following first-order equation:

$$X_d = VC_s[1 - e^{-(DA/\delta V)t}] \tag{4}$$

Also, under these conditions, for as long $X_d/V < 0.2C_s$ (i.e., for the period during which sink conditions prevail), X_d/V may be considered negligible and eliminated from Eq. (3). In this case, the resulting equation suggests that dissolution could be approximated as a zero-order process:

$$X_d = \left(\frac{DAC_S}{\delta}\right)t \tag{5}$$

Maintaining the volume of the dissolution medium constant does not usually constitute a problem, because it can be directly evaluated from the experimental conditions. The assumption of independence between solubility and particle size can also be considered rigid unless micronized powders are used, in which case the solubility dependence on particle size may need to be taken into consideration (18,19). Although the dissolving surface area can be held constant with certain appropriate experimental setups (e.g., 17), dissolution of drugs more usually takes place under both changing solid surface area and nonisotropic conditions (20–22). Therefore, the application of Eqs. (4) and (5) is somewhat limited.

a. Managing the Changing Surface Area. The surface area of a nondisintegrating, dissolving solid continuously decreases. However, pharmaceutical products are not usually formulated as such. Most frequently disintegration and deaggregation processes precede particle dissolution and lead to a temporary increase in the available surface area for dissolution. Modeling of the initial increase of the available surface area until now has been considered only with (semi)empirical functions (see Sec. III.A.2).

From the general form of Eq. (3), various investigators have derived working equations for treating particle dissolution data obtained under continuously decreasing surface area conditions (23–29). In most of these cases isotropicity was assumed. One further assumption in deriving the relevant equations is that the dissolving particles are isometric [i.e., the surface area is related to the volume by Eq. (6)].

$$A = \Gamma(V)^{2/3} \tag{6}$$

where Γ is a ''shape factor'' constant. Theoretically, this is a valid assumption for spheres, and it is a reasonably good assumption for solid particles that maintain their relative dimensions during the dissolution process (27). With this approach, the following equation can be written for a single solid particle:

$$A_{\text{part}} = \Gamma\left(\frac{m}{\rho}\right)^{2/3} \tag{7}$$

where A_{part} is the surface area of the particle at time t, m is the mass of the particle, and ρ is the density of the solid particle. Subsequent manipulations depend on the existence of sink conditions and the size distribution of the powder.

If the powder consists of N particles of approximately equal size, Eq. (7) becomes

$$A = \frac{N^{1/3}\Gamma X^{2/3}}{\rho^{2/3}} \tag{8}$$

in which case the surface area becomes a function of the mass remaining to be dissolved X. By combining Eqs. (3) and (8), and assuming that particle dissolution occurs isotropically, a linear (although complicated) equation can be derived. If sink conditions prevail the resulting equation becomes the well-known cube-root equation (30,31).

$$X_0^{1/3} - X^{1/3} = \frac{D\Gamma N^{1/3} C_s}{3\delta\rho^{2/3}} t \tag{9}$$

where X_0 is the initial mass of solid brought for dissolution. For polydisperse powders under both sink (25,27) and nonsink (29) conditions, similar approaches have been developed. The *sink conditions* approach (whenever justified) facilitates the derivation of equations that can be solved analytically. However, with the advancement of computer technology, this approach in many cases could and, where possible, should be avoided because it leads to an inexact approximation of the dissolution process.

It should be noted, however, that real particles are rarely spherical, but rather, often consist of needles, cuboids, or platelets. In these cases the shape factor changes during the process. Relevant data show that the shape factor of a single crystal changes significantly after about 50% has dissolved and this change is of particular importance for needles and platelets (31,32).

Provided that the initial disintegration–deaggregation step occurs very fast, and depending on the validity of other assumptions, it may be possible to use the equations referenced in this section to describe the dissolution profile of an IR product.

b. Managing the Changing Boundary Layer Thickness. With the diffusion coefficient considered constant in common aqueous dissolution media, the changing intrinsic dissolution rate constant is usually accounted for by managing the effective diffusion boundary layer thickness, δ. However, the study of particle dissolution data under changing δ conditions is still very limited. Perhaps this is because there is no clear-cut method for determining this change. In general, it is believed that for particles with sizes up to few tens of microns, δ is comparable with the particle radius, whereas for larger particles it reaches a plateau (20,21). The changing boundary layer thickness of a single particle is usually taken into consideration by Eq. (10) (29,33):

$$\delta = r_0\left(\frac{m_t}{m_0}\right)^{1/3} \tag{10}$$

where m_t is the mass of solid drug particle at time t, m_0 is the initial mass of drug particle, and r_0 is the initial radius of the particle. Particle size distributions are usually converted from spherical radii to other shapes of known geometry through the use of the shape factor constant and the assumption of equivalent volume (29). However, although the hypothesis of a time-dependent effective diffusion layer thickness seems realistic, the limited data simulations to date are not supportive (29). More work needs to be done to determine whether the assumption of a time-dependent diffusion layer thickness would generally lead to more accurate simulations.

2. Description of Dissolution Profiles with (Semi)empirical Models

The description of drug particle dissolution data with models based on convective diffusion theory requires the use of certain assumptions and still today (one century after the proposition of the leading law) represents more an active research area than a tool for describing drug particle dissolution data. Moreover, this approach can only be applied to rapidly disintegrating IR products that release the drug from particles and, obviously, it is not applicable to most ER products for which the release process is usually governed by various

product-specific technological factors. Consequently, pharmaceutical scientists frequently characterize dissolution profiles with (semi)empirical models.

For a given data set, the decision on how to describe the dissolution kinetics with the use of a semiempirical or an empirical model usually involves three steps. (These steps should also be considered when dissolution models based on the convective diffusion theory are used for describing dissolution profiles of drug products.) The first is the selection of several models that contain assumptions appropriate to their application to the specific data set. As a second step the goodness of fit of each model to the specific data is assessed. This is usually done on the basis of the tightness of the residual errors, the absence of systematic trends in the residual errors and the absence of overparameterization. The third step relates to the decision on which model best describes the data. Models that fit the individual specific data sets to a similar degree are compared on the basis of their goodness of fit. Various criteria have been suggested, of which the Akaike's Information Criterion is probably the most commonly used (e.g., 34). Additionally, a small coefficient of variation of parameter estimates from various data of identical formulations are indicative of the closeness of the estimated values to the true value of the parameters.

From the initial attempts of Higuchi (35) and Gibaldi and Feldman (36) to the latest population growth model (37) several semiempirical- or empirical-modeling approaches have been considered to describe the dissolution profiles of pharmaceutical products. Most of the proposed functions have been previously applied to other scientific fields to describe similar types of curves. These functions may be grouped in two main categories: The first category contains semiempirical functions that can be considered under certain conditions (35–40). The Higuchi model (35) and the Gibaldi and Feldman first-order exponential (36) require different assumptions about the releasing solid surface area and cannot be applied when nonsink conditions prevail or in case of S-shaped profiles. A further approach, the population growth model (37), cannot be applied to S-shaped curves. The so-called power law (38), the control factor approach (39), and the order model (40) can be applied only under sink conditions. The last three models have been useful for ER drug products for which sink conditions usually prevail in vitro for a long time. However, all three models should be employed cautiously, because additional limitations apply.

The second category of functions consists of empirical models. These models include the ''first-order series'' approach (41); the Hill equation (42,43); the Gomperz model (44); the quadratic model (e.g., 43); and models based on distribution functions, such as the log-normal distribution (45), the log-logistic distribution (e.g., 46), and the RRSBW distribution (commonly

known as the Weibull distribution) (10,47). These models may be more efficient than the semiempirical models because they can be applied without prior consideration of sink conditions or of the shape of the curves. An S-shaped curve may be due to the type of formulation, to a lag time before the initiation of the dissolution process, or to a combination of both. In general, four parameters are required for the complete description of these types of profiles: the initial lag time, the final plateau value, a rate parameter, and a parameter for the sigmoidicity of the curve. All empirical models cited in the foregoing permit estimation of four characteristic parameters. However, with some of them (i.e., the first-order series approach, the quadratic model, and the log-normal distribution) it is difficult to interpret the meaning of each estimated parameter. To date, experience suggests that the Weibull distribution is one of most useful functions for describing drug dissolution data: not only because each individual estimated parameter has distinct meaning (10), but also because it usually gives a better fit than other models (e.g., 13,48,49). The Weibull function is written as (10,47):

$$X_d = X_{d,\max}[1 - e^{-[(t-\gamma)/\tau_d]^\beta}] \tag{11}$$

where γ is the location parameter (which in dissolution experiments is identical with the lag time before the onset of the dissolution), τ_d is the time parameter (which provides information about the rate of the process and has units of [time]), and β is the shape parameter (which is dimensionless and indicative of the shape of the profile [$\beta = 1$ the curve is exponential, $\beta > 1$ the curve is S-shaped, and $\beta < 1$ the rate is initially faster than exponential]). An advantage of this function is that, in case of uncoated products (where no lag time is present) and provided $X_{d,\max}$ is experimentally measured, an S-shaped profile can be characterized entirely with only two parameters: τ_d and β. For products that are expected (from their type of formulation) to show lag time before the onset of dissolution, a procedure for identifying this has been also suggested with the Weibull function (10).

B. Comparison of Dissolution Profiles

Comparisons of cumulative dissolution profiles are performed to assess whether or not a drug product complies with preset specifications (e.g., in quality control testing) or to study the performance of various products under various experimental conditions (e.g., for research purposes). Dissolution profiles may be tested for similarity by virtue of similarity at individual sample time points (local similarity) or the overall profile similarity (global similarity).

In the first case, relevant procedures are model-independent and applied directly to the raw data. The second case involves comparisons of parameters estimated after fitting a model to the data. Before presenting an overview of current profile comparison methods, it should be mentioned that the testing of similarity of in vitro dissolution profiles of two dosage forms may or may not be equivalent to testing their bioequivalence. For this to be true, both of the following requirements must be fulfilled for the two dosage forms:

1. Dissolution process limits the overall absorption process
2. Either an in vitro–in vivo correlation (IVIVC) model has been previously developed and validated, or prediction of the plasma profile has been previously achieved and validated. In addition, the in vitro dissolution data used for the IVIVC model or for the prediction of plasma profile must have been collected under identical conditions with those used for obtaining the profiles to be compared.

1. Model-Independent Methods for Comparing Dissolution Profiles

A restriction common to model-independent methods is that they cannot be used for comparisons of profiles with nonidentical sampling schemes.

The *U.S. Pharmacopoeia/National Formulary* (*USP/NF*) sampling acceptance dissolution criteria constitute the simplest model-independent approach for comparing dissolution data (5). For multi–time-point dissolution specifications, the approach is to apply the *USP* criteria (defined as minimum, maximum, or range of percentage dissolved mean values at specific time points) independently at each individual time point. This approach has two weaknesses: (a) it does not take into account the repeated measurements over the course of time, and (b) it does not use all the information of the dissolution profile. The need for alternative acceptance sampling rules has been recently considered (13,50). Eliminating both weaknesses requires the use of modeling (13). During the last decade, various model-independent methods for the comparison of two dissolution profiles have been proposed, so that the repeated measurements over the time course of a dissolution process to be taken into account. These methods can be subgrouped into statistical and index approaches.

a. ''Statistical'' Approaches. Shah et al. (51) first proposed a repeated-measures (split-plot) analysis of variance by which it is possible to test both the hypothesis that two profiles do not differ relative to average dissolution (averaged over all time points), and the hypothesis that the two profiles are

essentially parallel. This method is similar to that previously discussed by Westlake (52) for the analysis of blood level measurements in a bioavailability study. A restriction of the proposed methodology, however, is that it is valid only when the variance–covariance matrix of residuals is uniform.

Tsong et al. (53) proposed a method for assessment of mean difference between two dissolution data sets based on multivariate Mahalanobis distance between the two data sets. The concept of this approach is that for two sets to be similar, the difference between a test and the reference set should be less or equal to the maximum expected difference between various reference data sets. Application of this method involves a sequence of steps that include the computation of the reference multivariate statistical distance (MSD) to define the similarity limits (based on earlier reference data sets), estimation of confidence limits for the true MSD between test and reference data sets, and comparison of confidence with similarity limits. However, this procedure becomes very complicated with nonidentical covariance structures of the similarity and confidence regions, especially when the number of dissolution data points is larger than three.

Chow et al. (54) suggested an alternative approach that could be more easily applied when many data points are to be compared. With this method, similarity testing is based on parameters after fitting a one-degree autoregression time series model. In this approach, a concept similar to that of bioequivalence is used to define lower (L) and upper (U) similarity limits for dissolution testing as (δ_L, δ_U), where $\delta_L = (Q - \delta)/(Q + \delta)$, $\delta_U = (Q + \delta)/(Q - \delta)$, and Q is the percentage drug amount dissolved as specified in the individual monograph of the *USP*. Two drug products are claimed to have similar dissolution profiles if the ratio of dissolution rates (estimated as $\%\text{dissolved}_{\text{test}}/\%\text{dissolved}_{\text{ref}}$ from the available data) is within (δ_L, δ_U) with 95% assurance. This method takes into account that the dissolution rates are dependent on time and that the dependency is a decreasing function of time. However, this method requires the existence of a Q value. Also, the response is based on the ratio of test over reference; if the role of two profiles is interchanged in the computation, the resulting confidence interval will vary. Finally, it is very sensitive to the variability of the data. If the variability is large the probability of declaring dissimilarity is large, even when the two profiles are identical (55).

b. Index Approaches. The concept in this approach is similar to that of the statistical approaches: a test profile is accepted as similar to a reference profile if the difference between them is no more than the average difference among various reference profiles. The distinction here is that the profile difference is assessed with an index estimated from the individual raw data of two profiles.

An index estimated from two mean sample profiles could be used as a point-estimate measure of the difference (or similarity) of the two test dissolution conditions provided that both of the following requirements are fulfilled: (a) for each data set, the variability at each sample time point is low (to allow the use of mean data); (b) an acceptable dissolution difference and its corresponding index value has been defined. Also, by testing difference (or similarity) with a point estimate and not based on a statistical hypothesis, false-negative or false-positive rates cannot be evaluated.

There are three commonly considered indices: the difference factor, the similarity factor, and the Rescigno index.

The difference factor f_1 is a measure of the relative error between the two curves and is defined by Eq. (12) (56):

$$f_1 = 100 \left[\frac{\sum_{i=1}^{n} |R_i - T_i|}{\sum_{i=1}^{n} R_i} \right] \tag{12}$$

where R_i, T_i are the percentage dissolved of the reference and test profile, respectively, at the ith time point (Fig. 2).

The similarity factor f_2 is a measure of the similarity in the percentage dissolution between the two curves and is defined by Eq. (13) (56):

$$f_2 = 50 \log \left[100 \left(1 \Big/ \sqrt{1 + \frac{1}{n} \sum_{i=1}^{n} (R_i - T_i)^2} \right) \right] \tag{13}$$

Assuming that the percentage dissolved values for two profiles cannot be higher than 100, the difference factor can take values from 0 (when no difference between the two curves exists) to 100 (when maximum difference exists; see Fig. 2). With the same assumption holding, the similarity factor can take values from 100 (when no difference between the two curves exists) to 0 (when maximum difference exists; see Fig. 2).

These two indices are recommended by U.S. Food and Drug Administration (FDA) (1,6–8), and they are also used by independent researchers (3,57) as point estimate measures of the difference or similarity of dissolution profiles of various batches of the same product tested under identical experimental conditions (i.e., in quality control testing). This is possible because the variability of the data in such types of dissolution testing is usually low and, also, a maximum acceptable difference between two dissolution sets can be set

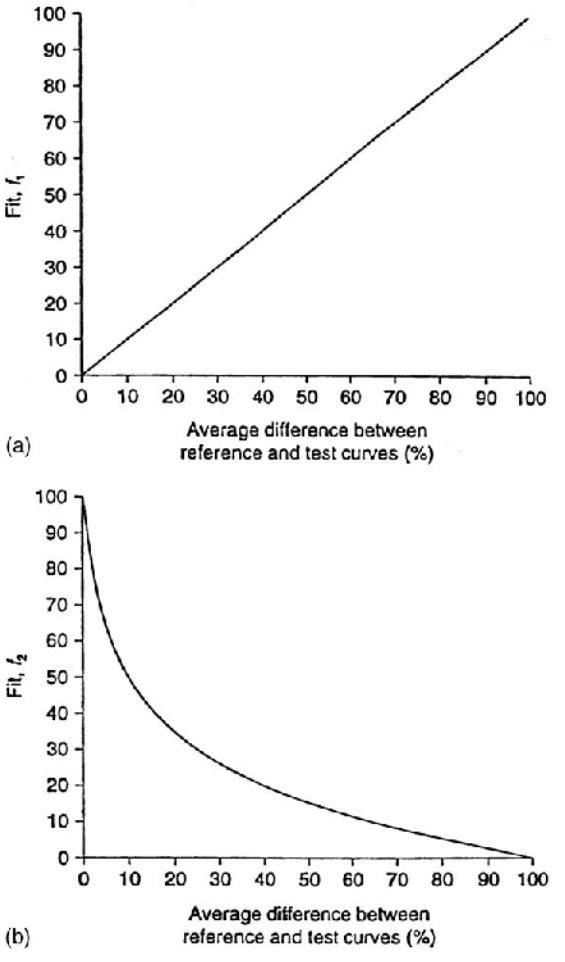

FIG. 2 Relation of the distance between curves and calculated values of (a) difference factor f_1, and (b) similarity factor f_2. (From Ref. 56.)

(based on current experience with dissolution profiles). Specifically, a coefficient of variation (CV) of no more than 20% at early time points (e.g., up to 15 min for IR products) and a CV of no more than 10% at other time points is considered acceptable (1). In general, if the CV is consistently higher than 15%, other methods for profile comparisons should be used (1). Also, a 10% difference between batches of the same formulation at all sample time points

is generally acceptable (1). Thus, according to Eq. (12) for an up to 10% difference between two curves, f_1 should be 15 at most, and from Eq. (13), for an up to 10% difference between two curves, f_2 should be at least 50. (Similarity limits could also be set on a product basis, rather than on the empirical basis of a 10% difference.) However, before using these indices as point estimates of difference or similarity, one should be aware of two technical issues; about four data points (preferably equally spaced) and only one after 85% dissolution of the test or the reference (whichever occurs first) should be used (1,6,8,55,58). Moreover, because of the sampling variation of the estimate, dissolution similarity of the test and reference batches may not be assessed by direct comparison of the estimated value of the index with the similarity limit, but rather, should be judged on a statistical basis. In general, this requires knowledge of the sampling distribution of the index under consideration. Only the similarity factor f_2 has been studied from this point of view. Initially, Liu et al. (58) suggested that, because a standard form of the estimated value of the similarity factor, $\hat{f}_2$, may not exist, the ratio of the sum of squared differences over the number of the data points tested might be a better alternative to be used for assessing similarity on a confidence interval basis (58). However, recently the criterion for average similarity of the dissolution profiles using the similarity factor has been formulated as an interval procedure (59). According to this method, by assuming that the expected value of $\hat{f}_2$ equals f_2; that is, $E(\hat{f}_2) = f_2$, one can compare the 90% lower confidence limit of $E(\hat{f}_2)$ with the similarity limit with a 95% likelihood of reaching the correct decision. The 90% confidence interval for the $E(\hat{f}_2)$ can be simulated by a bootstrap method (59). For nonstatisticians, the bootstrap is a relatively new, data-based simulation method for statistical inference (60), which can be actually performed with many commercially available statistical packages for personal computers, such as Matlab®, S-plus®, and others.

The Rescigno index (61) ξ_j was initially proposed for comparison of plasma concentration versus time curves and is defined by Eq. (14):

$$\xi_j = \left[\frac{\int_0^{t_{\text{last}}} |R_i - T_i|^j dt}{\int_0^{t_{\text{last}}} |R_i + T_i|^j dt} \right]^{1/j} \tag{14}$$

where j is a positive integer (usually 1 or 2). The Rescigno index can take values from 0 (when no difference between test and reference data exists) to 1 (which represents complete dissolution of one formulation before the other

begins to dissolve). Until now, this index has been used in dissolution profile comparisons only on a relative comparative basis and seldom as a point measure estimate of similarity (3,57). One important restriction is that the similarity limit of this index (based on the maximum accepted percentage difference between two profiles) depends on whether the test curve is greater or less than the reference curve. Furthermore, the statistical properties of this estimate have yet to be defined.

2. Model-Dependent Multivariate Analysis Procedure for Comparing Dissolution Profiles

The distinction from the model-independent multivariate analysis is that the testing is done by comparing the parameters estimated after fitting a specific model to the dissolution data instead of directly comparing the raw data. Sathe et al. (48,49) have given thorough presentations of this procedure using the estimated scale and shape parameters of the Weibull function to test the difference of a test batch from a reference batch. In these examples, the procedure was applied as follows:

1. Confirmation that both test and reference data sets can be completely (and better than other models) described with the Weibull function by using only the scale and shape parameters. [Obviously, if one parameter is adequate, the evaluation is further simplified. However, current experience with solid drug products indicates that this seldom occurs (12,48,49).]
2. Definition of the similarity region, based on the intra- or interbatch parameter variances of various earlier reference batches.
3. Computation of the multivariate statistical distance (using the M-statistic) in model parameters between test and reference batches.
4. Estimation of the 90% confidence region of the true difference between test and reference batches.
5. Comparison of the confidence region with the similarity region.

Model-dependent multivariate analysis procedures are more useful than the model-independent approach when the dissolution data consist of more than four data points and functions with up to three parameters to be estimated can be used. In such cases the model-dependent multivariate analysis procedures are less complicated, they allow for different sampling points between test and reference profiles, and they provide information of the kinetics of the dissolution process (since the profile is automatically characterized during estimation of the model parameters). If an adequate mathematical model cannot be fitted to both data sets, the ''principal component analysis'' approach may be considered. This approach compares the principal components gener-

ated by slicing the dissolution profiles into different sections, and it offers the possibility of avoiding a multipoint, multivariate model-independent procedure (13).

3. Multivariate Statistical Versus Index Approaches

With the multivariate approaches the variance–covariance structure of the raw data or of the estimated parameters is accounted for, in addition to the mean dissolution values. These approaches are useful when up to three pairs of raw data or estimated parameters are considered.

Of the index approaches, either the f_1 or the f_2 index could be used as point estimate measures, provided that the variability of the data is low and similarity limits can be set. However, as such, they do not account for the variance–covariance structure of the data. Also, false-negative or false-positive rates cannot be evaluated. The f_2 index can additionally be used on the basis of a confidence interval. However, experience in using the f_2 index in various types of dissolution data is still limited. For example, as with most of the proposed methods for profile comparisons, the f_2 index was originally proposed for assessing differences between two average cumulative percentages of dissolved versus time plots that both reach 100% dissolution. This may indeed be true in quality control testing, but frequently not in biorelevant dissolution testing. Furthermore, before using the bootstrap approach for simulating the confidence interval, it must be known that $\hat{f}_2$ is a consistent and unbiased estimate of f_2. These requirements may not be fulfilled when fewer than 12 replications per batch are available or the number of data points per curve differs greatly from four. When dissolution studies are run for general research purposes, only three to six replications are performed. When 85% dissolution occurs very quickly, there usually are only one or two usable data points. The other extreme is the ''data rich scenario'' for which the applicability of the bootstrap procedure still needs to be evaluated.

C. Treatment of In Vitro Dissolution Profiles for Predicting In Vivo Performance of Dosage Forms

Prediction of in vivo performance from in vitro dissolution data is usually based on a previously established IVIVC model, which traditionally can be constructed at three levels (5). The lowest two levels involve the establishment of a (usually linear) relation between one in vitro parameter (from the dissolution test) and one in vivo parameter (e.g., from the plasma levels). The third (highest) level of IVIVC (point-to-point correlation) is established between the entire in vitro dissolution and in vivo dissolution profile (which is usually

obtained by deconvolution techniques and is often assumed to be identical with the in vivo absorption profile). It is obvious that complete description of the in vivo profile is possible only where a point-to-point IVIVC model has been developed.

Less frequently, a point-to-point assessment of the in vivo performance is made by constructing the (simulated) plasma concentration versus time profile with convolution techniques and by using the entire in vitro dissolution profile as the input (absorption) profile.

Both deconvolution- and convolution-based techniques are discussed in other chapters of this book and have been very useful for many types of ER products. However, they often fail for IR products. Two main reasons are responsible for this. In ER products, dissolution (release) rate is by definition the rate-limiting step for absorption, whereas for IR products this is often not true. Another reason is that dissolution rates of IR products are generally more susceptible to the changing environment along the upper gastrointestinal (GI) tract or in response to food intake than the release rates from ER products. Because of the more robust release characteristics of ER products, in vitro conditions may not be as important for ER products as for IR products, making it easier to obtain an in vitro dissolution profile that is similar to the in vivo profile.

1. *Prediction of the In Vivo Profile of Sparingly Soluble and Highly Lipophilic Drugs Based on In Vitro Cumulative Dissolution Data*

With IR products, the chances of establishing a point-to-point IVIVC or predicting the in vivo plasma levels should be higher in cases where drugs with dissolution-limited absorption [i.e., class II drugs (62)] are considered and the dissolution medium is appropriately designed. Galia et al. recently showed (63) that with physiologically based dissolution media it is possible to forecast trends in the in vivo performance of class II drugs. Moreover, a complete description of the in vivo performance of class II drugs based on their in vitro dissolution behavior may be possible using a model-dependent approach for constructing the predicted plasma concentration versus time profile (64). The steps for applying such an approach with a class II drug are:

1. Obtain the plasma drug concentration versus time profiles after single-dose administration of the solid IR product to a small number of individuals.
2. Using the same individuals and the same dose, obtain the plasma

concentration versus time profiles after single-dose intravenous administration of the drug.
3. Estimate the disposition parameters of the drug (e.g., 34).
4. Perform physiologically based dissolution tests (9).
5. Simulate the average oral plasma concentration versus time profile, based on in vitro dissolution data population gastric-emptying data, absolute bioavailability, and disposition parameters of the drug.
6. Compare the simulated profile with the actual plasma concentration versus time profiles obtained after administration of the solid product.
7. If the simulated profile is similar to the actual profiles, the in vitro dissolution profile can be further used as a reference profile for future IR products of this drug. If dissolution profiles of future products are similar to the reference profile their in vivo performance will be known without extra biostudies. If the simulated profile is not similar to the actual profile, it may worth examining the in vitro test conditions to determine whether they need to be changed to more adequately simulate GI conditions.

It is apparent that this approach involves two different types of profile comparisons. Comparison of simulated versus actual plasma profiles can be based on absolute or root mean square errors using all the actual data points or on percentage prediction errors for C_{max} (e.g., 43). Alternatively, metrics that have been recently proposed for direct plasma curve comparisons could also be considered (61,65,66). However, although similarity can be judged according to cut-off values of percentage prediction errors for C_{max}, other metrics should be used cautiously because both the location and the number of the experimental data points may affect their value. The second profile comparison involves the comparison of two in vitro dissolution profiles. As a first approach, the model-dependent multivariate approach seems to be the most appropriate.

One weak point of the proposed method for predicting in vivo profiles of sparingly soluble drugs may be the use of population data for describing the gastric-emptying process. However, it should be made clear that this method is proposed as a tool for better predictions at the developmental level and not for regulatory requirements. In addition, in case of sparingly soluble and highly lipophilic weak acids or nonionizable compounds at fasted state, variations in gastric emptying are not expected to be of paramount importance for the construction of the plasma profile because gastric dissolution will be limited. If this is true, a level A correlation between the in vitro dissolution profile

[obtained in media simulating the small intestinal lumenal conditions (9)] and the in vivo absorption profile should be achievable.

a. Testing the Applicability of the Proposed Method. By using acetaminophen (paracetamol) as a negative control, and a weakly acidic drug with low solubility and highly lipophilic characteristics (GR92132X, GlaxoWellcome, UK), various features of the proposed model-dependent approach can be demonstrated (64).

By assuming negligible gastric uptake, simultaneous solid and liquid emptying from the stomach, and average population values for gastric-emptying rate (e.g., 9), and by knowing the absolute bioavailability and disposition parameters of the drug formulations, the scheme shown in Fig. 3 could be applied.

Figure 4 shows the average (mean) simulated and actual concentration versus time profiles of an acetaminophen IR product administered under fasted and fed state conditions.

The simulated profiles, shown in Fig. 4 were obtained by using the following:

1. First-order gastric-emptying half-life of 2.8 h^{-1} in fasted state and zero-order caloric–content-dependent gastric-emptying rate of 4 Kcal/min in fed state.

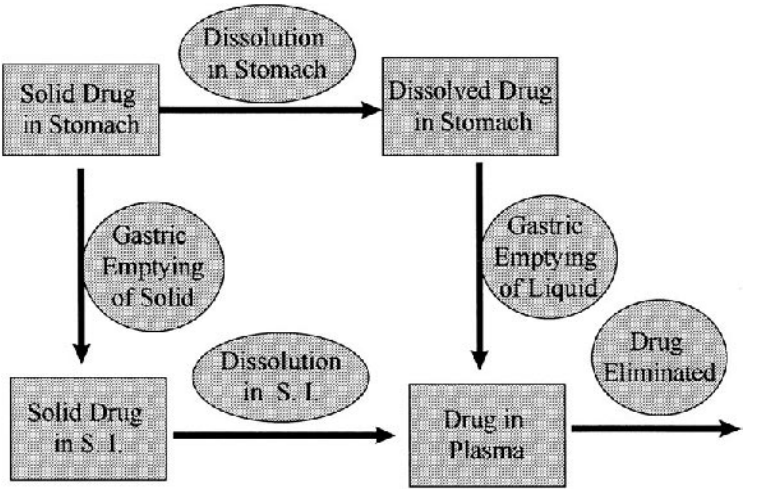

FIG. 3 Schematic of the proposed model for predicting the in vivo plasma profile of drugs with high intestinal permeability after oral administration. (From Ref. 64.)

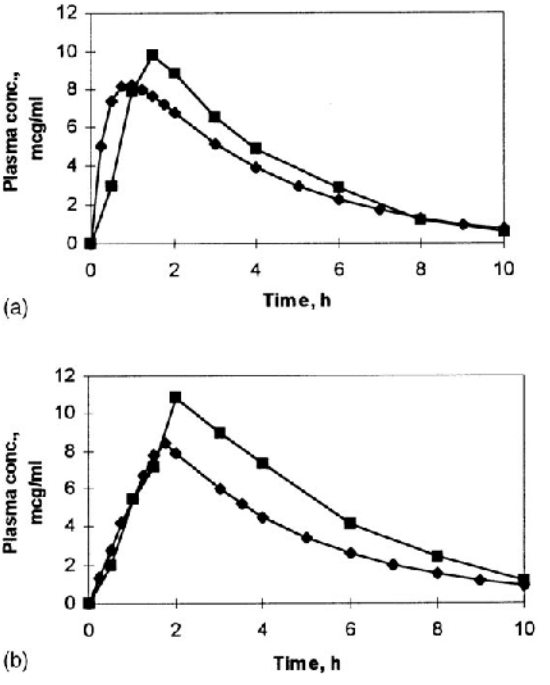

FIG. 4 Average simulated (◆) and actual (■) plasma concentration vs. time profiles of acetaminophen (paracetamol) under (a) fasted-state and (b) fed-state conditions. f_1 values are 26.9 and 26.5 for the fasted- and fed-state conditions, respectively. (From Ref. 64.)

2. The average (mean) in vitro dissolution kinetics in water and FaSSIF (to simulate the gastric and the intestinal dissolution, respectively, in the fasted state) and in milk and FeSSIF (to simulate the gastric and the intestinal dissolution, respectively, in the fed state) using the *USP* 2 apparatus at 100 rpm (63). Dissolution kinetics were introduced into the model using the shape factor constant approach (see Sec. III.A.1.a).

Holding the gastric emptying rate constant at a predetermined value, simulated in vivo profiles obtained with dissolution data at various agitation intensities in water (for simulating gastric dissolution) and in SIF_{sp} or FaSSIF (for simulating dissolution in small intestine) were further compared with the average (mean) actual profile obtained under fasted state conditions. The f_1 values

remained unchanged at 26.9, regardless of the data used (64). The same was also observed when the in vivo profile obtained under fed-state conditions was compared with various simulated profiles obtained by using in vitro dissolution data in water or milk (gastric dissolution) and SIF_{sp} or FeSSIF (dissolution in small intestine); f_1 values ranged from 26.4 to 27.3. In contrast, when the gastric-emptying rate constant varied (from 1.85 to 5.54 h^{-1} and from 2 to 6 Kcal/min for the fasted and fed state, respectively) and dissolution data in water/FaSSIF or milk/FeSSIF (*USP* 2 apparatus, 100 rpm) were used, f_1 values varied from 22.7 to 33.2 in the fasted state and from 26.5 to 39.2 in the fed state (64).

Figure 5 shows the average (mean) simulated and actual concentration versus time profiles of GR92132X under fed-state conditions. Simulated profiles were estimated using experimental dissolution data (67) and the same procedure as for the acetaminophen example under fed-state conditions (see Fig. 4b). Simulated profiles varied considerably with the dissolution kinetics (f_1 values ranged from 15.5 to 53.0 using various dissolution data, as with the acetaminophen example). Not surprisingly, the gastric-emptying rate also affected the simulated profile ($15.5 < f_1 < 41.4$); the driving force for gastric dissolution (i.e., solubility) increases, whereas gastric-emptying rates are slowed down so that the influence of these two factors becomes comparable.

In summary, the model described confirmed that acetaminophen absorption is not dissolution-dependent and that, regardless of the media composition, in vitro dissolution data are of no value in predicting the oral absorption

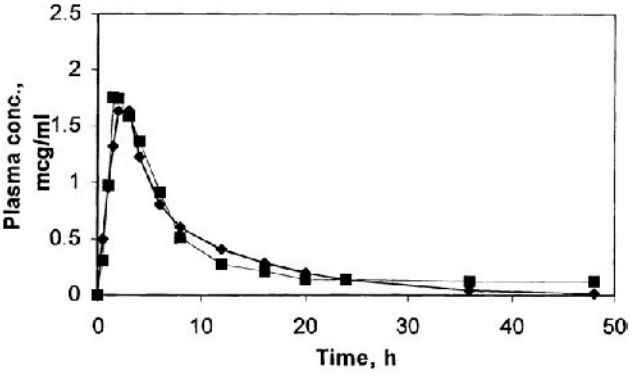

FIG. 5 Average simulated (◆) and actual (■) plasma concentration vs. time profiles (f_1 = 15.5) of a GlaxoWellcome drug with dissolution-limited absorption under fed-state conditions. (From Ref. 64.)

profile of this drug. Even in the fed state, for which the dissolution rate in the stomach was simulated with the in vitro dissolution data in milk [in which the dissolution rate can be substantially decreased (63,68)] gastric emptying seemed to be the process that determined the rate of absorption. In contrast, for the low-solubility, high-lipophilicity (class II) drug, the choice of physiologically relevant dissolution media was crucial for predicting the in vivo plasma profile in the fed-state conditions.

In the examples presented here, simulated profiles were compared with the mean actual profiles. However, given the high variability of plasma profiles of poorly soluble drugs, when the difference (or similarity) is assessed with an index, comparisons of the simulated profile with each individual actual plasma profile should rather be performed, and assessment of similarity should be based on the median value of the index.

REFERENCES

1. Guidance for Industry. Dissolution Testing of Immediate Release Solid Oral Dosage Forms. Rockville, MD: CDER, Food and Drug Administration, August 1997.
2. FIP guidelines for dissolution testing of solid oral products. Joint report of the section for official laboratories and medicines control services and the section of industrial pharmacists of the F.I.P. Pharm Ind 1997; 59:760–766.
3. Polli JE, Rekhi GS, Augsburger LL, Shah VP. Methods to compare dissolution profiles and a rationale for wide dissolution specifications for metoprolol tartrate tablets. J Pharm Sci 1997; 86:690–700.
4. Shah VP. Concept of mapping. Drug Inf J 1996; 30:1085–1089.
5. United States Pharmacopeial Convention, Inc. The United States Pharmacopoeia (USP 23). Rockville, MD, 1995.
6. Guidance for Industry. Extended Release Oral Dosage Forms: Development, Evaluation and Application of In Vitro/In Vivo Correlations. Rockville, MD: CDER, Food and Drug Administration, September 1997.
7. Guidance for Industry. Immediate Release Solid Oral Dosage Forms, Scale-up and Post-approval Changes: Chemistry, Manufacturing and Controls, In Vitro Dissolution Testing and In Vivo Bioequivalence Documentation. Rockville, MD: CDER, Food and Drug Administration, November 1995.
8. Guidance for Industry. Modified Release Solid Oral Dosage Forms, Scale-up and Post-approval Changes: Chemistry, Manufacturing and Controls, In Vitro Dissolution Testing and In Vivo Bioequivalence Documentation. Rockville, MD: CDER, Food and Drug Administration, September 1997.
9. Dressman JB, Amidon GL, Reppas C, Shah VP. Dissolution testing as a prognos-

tic tool for oral drug absorption: immediate release forms. Pharm Res 1998; 15: 11–22.
10. Langenbucher F. Parametric representation of dissolution-rate curves by the RRSBW distribution. Pharm Ind 1976; 38:472–477.
11. Langenbucher F, Moeller H. Correlation of in vitro drug release with in vivo response kinetics. Part II: Use of function parameters. Pharm Ind 1983; 45:629–633.
12. Khan KA. The concept of dissolution efficiency. J Pharm Pharmacol 1975; 27: 28–49.
13. Tsong Y, Hammerstrom T, Chen JJ. Multipoint dissolution specification and acceptance sampling rule based on profile modeling and principal component analysis. J Biopharm Stat 1997; 7:423–439.
14. Noyes AA, Whitney WR. The rate of solution of solid substances in their own solutions. J Am Chem Soc 1897; 19:756–761.
15. Noyes AA, Whitney WR. Ueber die Auflösungsgeschwindigkeit von festen Stoffen in ihren eigenen Lösungen. Z Phys Chem 1897; 23:689–692.
16. Nernst W, Brunner E. Theorie der Reaktionsgeschwindigkeit in heterogenen Systemen. Z Phys Chem 1904; 47:52–110.
17. Levich VG. Physicochemical Hydrodynamics. Englewood Cliffs, NJ: Prentice Hall, 1962.
18. Ostwald W. Studien über die Bildung und Umwandlung fester Körper. Z Phys Chem 1897; 22:289–330.
19. Higuchi WI, Rowe EL, Hiestand EN. Dissolution rates of finely divided powders II: Micronized methylprednisolone. J Pharm Sci 1963; 52:162–164.
20. Harriott P. Mass transfer to particles I. Suspended in agitated tanks. Am Inst Chem Eng J 1962; 8:93–101.
21. Higuchi WI, Hiestand EN. Dissolution rates of finely divided drug powders I. Effect of distribution of particle sizes in a diffusion-controlled process. J Pharm Sci 1963; 52:67–71.
22. Grijseels H, Crommelin DJA, de Blaey CJ. Hydrodynamic approach to dissolution rate. Pharm Weekbl (Sci Ed) 1981; 3:1005–1020.
23. Niebergall PJ, Goyan JE. Dissolution rate studies I. Continuous recording technique for following rapid reaction in solution. J Pharm Sci 1963; 52:29–33.
24. Short MP, Sharkey P, Rhodes CT. Dissolution of hydrocortisone. J Pharm Sci 1972; 61:1733–1735.
25. Carstensen JT, Musa MN. Dissolution rate patterns of log-normally distributed powders. J Pharm Sci 1972; 61:223–227.
26. Pothisiri P, Carstensen JT. Nonsink dissolution rate equation. J Pharm Sci 1973; 62:1468–1470.
27. Carstensen JT, Patel M. Dissolution patterns of polydisperse powders: oxalic acid dihydrate. J Pharm Sci 1975; 64:1770–1776.
28. Pedersen PV, Brown KF. Theoretical isotropic dissolution of nonspherical particles. J Pharm Sci 1976; 65:1437–1442.
29. Lu ATK, Frisella ME, Johnson KC. Dissolution modelling: factors affecting the dissolution rate of polydisperse powders. Pharm Res 1993; 10:1308–1314.

30. Hixcon AW, Crowell JH. Dependence of reaction velocity upon surface and agitation. I. Theoretical considerations. Ind Eng Chem 1931; 23:923–931.
31. Dali MV, Carstensen JT. Effect of change in shape factor of a single crystal on its dissolution behavior. Pharm Res 1996; 13:155–162.
32. Lai TY, Carstensen JT. Effect of shape factor on cube root dissolution behavior. Int J Pharm 1978; 1:33–40.
33. Hintz RJ, Johnson KC. The effect of particle size distribution on dissolution rate and oral absorption. Int J Pharm 1989; 51:9–17.
34. Wagner JG. Pharmacokinetics for the Pharmaceutical Scientist, New York: Technomic Publishing, 1993.
35. Higuchi T. Rate of release of medicaments from ointment bases containing drugs in suspension. J Pharm Sci 1961; 50:874–875.
36. Gibaldi M, Feldman S. Establishment of sink conditions in dissolution rate determinations. Theoretical considerations and application to non-disintegrating dosage forms. J Pharm Sci 1967; 56:1238–1242.
37. Dokoumetzidis A, Macheras P. A population growth model of dissolution. Pharm Res 1997; 14:1122–1126.
38. Peppas NA. Analysis of Fickian and non-Fickian drug release from polymers. Pharm Acta Helv 1985; 60:110–111.
39. Kervinen L, Yliruusi J. Modelling S-shaped dissolution curves. Int J Pharm 1993; 92:115–122.
40. Jørgensen K, Christensen FN. Shape modelling of dissolution profiles by non-integer kinetic orders. Int J Pharm 1996; 143:223–232.
41. Leary JR, Ross SD. Mathematical expression of tablet dissolution profiles. Int J Pharm 1983; 17:193–201.
42. Holford NHG, Sheiner LB. Understanding the dose-effect relationship: clinical application of pharmacokinetic–pharmacodynamic models. Clin Pharmacokinet 1981; 6:429–453.
43. Eddington ND, Marroum P, Uppoor R, Hussain A, Augsburger L. Development and internal validation of an in vitro–in vivo correlation for hydrophilic metoprolol tartrate extended release tablet formulation. Pharm Res 1998; 15:466–472.
44. Dawoodbhai S, Suryanarayan ER, Woodruff CW, Rhodes CT. Optimization of tablet formulation containing talc. Drug Dev Ind Pharm 1991; 17:1343–1371.
45. Wagner JG. Interpretation of percent dissolved–time plots derived from in vitro testing of conventional tablets and capsules. J Pharm Sci 1969; 58:1253–1257.
46. Goldsmith JA, Randall N, Ross SD. On the methods of expressing dissolution rate data. J Pharm Pharmacol 1978; 30:347–349.
47. Langenbucher F. Linearization of dissolution curves by the Weibull distribution. J Pharm Pharm 1972; 24:979–981.
48. Sathe PM, Tsong Y, Shah VP. In vitro dissolution profile comparison: statistics and analysis, model dependent approach. Pharm Res 1996; 13:1799–1803.
49. Sathe P, Tsong Y, Shah VP. In vitro dissolution profile comparison and IVIVR. Carbamazepine case. Adv Exp Med Biol 1997; 423:31–42.
50. Chen JJ, Tsong Y. Multiple-time-point dissolution specification for a sampling acceptance plan. J Biopharm Stat 1997; 7:259–270.

51. Shah VP, Yamamoto LA, Schuirman D, Elkins J, Skelly JP. Analysis of in vitro dissolution of whole vs. half controlled-release theophylline tablets. Pharm Res 1987; 4:416–419.
52. Westlake WJ. Use of statistical methods in evaluation of in vivo performance of dosage forms. J Pharm Sci 1973; 62:1579–1589.
53. Tsong Y, Hammerstrom T, Sathe P, Shah VP. Statistical assessment of mean differences between two dissolution data sets. Drug Inf J 1996; 30:1105–1112.
54. Chow SC, Ki FYC. Statistical comparison between dissolution profiles of drug products. J Biopharm Stat 1997; 7:241–258.
55. Ju HL, Liaw SJ. On the assessment of similarity of drug dissolution profiles—a simulation study. Drug Inf J 1997; 31:1273–1289.
56. Moore JW, Flanner HH. Mathematical comparison of dissolution profiles. Pharm Technol 1996; 6:64–74.
57. Polli JE, Rekhi GS, Shah VP. Methods to compare dissolution profiles. Drug Inf J 1996; 30:1113–1120.
58. Liu JP, Ma MC, Chow SC. Statistical evaluation of the similarity factor f_2 as a criterion for assessment of similarity between dissolution profiles. Drug Inf J 1997; 31:1255–1271.
59. Shah VP, Tsong Y, Sathe P, Liu J-P. In vitro dissolution profile comparison. Statistics and analysis of the similarity factor, f_2. Pharm Res 1998; 15:889–896.
60. Efron B, Tibshirani RJ. An Introduction to the Bootstrap. New York: Chapman & Hall, 1993.
61. Rescigno A. Bioequivalence. Pharm Res 1992; 9:925–928.
62. Amidon GL, Lennernäs H, Shah VP, Crison JRA. Theoretical basis for a biopharmaceutics drug classification: the correlation of in vitro drug product dissolution and in vivo bioavailability. Pharm Res 1995; 12:413–420.
63. Galia E, Nicolaides E, Hörter D, Löbenberg R, Reppas C, Dressman JB. Evaluation of various dissolution media for predicting in vivo performance of class I and II drugs. Pharm Res 1998; 15:698–705.
64. Nicolaides E, Galia E, Symillides M, Dressman J, Efthymiopoulos C, Reppas C. Prediction of the oral absorption of class II drugs from immediate release formulations. Proceedings of the 9th Panhellenic Pharmaceutical Conference, Athens, Greece, 1998.
65. Chinchilli VM, Elswick RK Jr. The multivariate assessment of bioequivalence. J Biopharm Stat 1997; 7:113–123.
66. Martson SA, Polli JE. Evaluation of direct curve comparison metrics applied to pharmacokinetic profiles and relative bioavailability and bioequivalence. Pharm Res 1997; 14:1363–1369.
67. Galia E, Nicolaides E, Efthymiopoulos C, Reppas C, Dressman JB. Physiologically based dissolution tests: experience with two poorly soluble GlaxoWellcome drugs [abstr.]. Pharm Res 1997; 14:S–491.
68. Macheras P, Koupparis M, Tsaprounis C. Drug dissolution studies in milk using the automated flow injection serial dynamic dialysis technique. Int J Pharm 1986; 33:125–136.

14

Convolution and Deconvolution Methods

Richard Süverkrüp
University of Bonn, Bonn, Germany

I. DEFINITIONS, APPLICATIONS, AND PROBLEMS

There are at least two approaches to convolution and deconvolution methods in biopharmaceutics and pharmacokinetics: an abstract one, for which mathematical methods suited to handle broad classes of problems are applied to elucidate the relations between plasma level curves and the underlying processes of drug release, absorption, and disposition, or to pharmacological effects. This approach is usually preferred by workers originally trained in mathematics or physics. Pharmacokineticists coming from a medical, chemical, or pharmaceutical background frequently prefer an approach oriented toward rate processes, in which physicochemical or physiological phenomena are expressed more specifically in mathematical terms. In this instance, the initial model is frequently inordinately complex in view of the number and the quality of the data available and has to be simplified stepwise until it can be used to solve particular problems.

Convolution and deconvolution are operations defined for pairs of functions, of which at least one is linear. In the context of pharmacokinetics, the relation between these functions and the processes of which they are abstractions should be kept in mind. In particular, assumptions concerning linearity and time invariance may not be perfectly valid, and such imperfections in structural models can cause problems. In addition, experimental scatter in the

observations can make it difficult to obtain reasonable estimates of the functions sought.

Although deconvolution is most commonly used to determine absorption-rate profiles from plasma concentration data when individual disposition kinetics are given, this is by no means the only application: under favorable circumstances it may be possible to reconstruct the kinetics of in vivo drug release. Less ambitious is the determination of the unit impulse response function, which is characteristic of a linear pharmacokinetic system, from the time course of plasma levels if the input function is known (e.g., after infusion of the drug at a constant rate).

In abstract terms, we are dealing with linear, causal, and time-invariant systems, in which the unit impulse response of the system $g(t)$ completely determines its response $h(t)$ to any input rate function $f(t)$. We shall take causality here for granted. The relation is established by a Volterra-type integral equation:

$$h(t) = \int_0^t f(\tau)g(t - \tau)d\tau \tag{1}$$

Here, $g(t)$ is the unit impulse response function of the linear system, which is sometimes called the system function or, for reasons that will become apparent later, weighting function. In a more general context, the notation

$$h(x) = \int f(x)K(y, x)dx \tag{2}$$

is common, where $K(y, x)$ is called the convolution kernel.

The function $h(t)$ is observed after exposure of the system to an input function $f(t)$. An abbreviated notation for the convolution operation is

$$h(t) = f(t) * g(t) \tag{3}$$

The linearity of the system, which is the condition for the superposition principle to hold, is most concisely expressed in the homogeneity property: let a be a real coefficient of the input function, then

$$af(t) * g(t) = ah(t) \tag{4}$$

An impulse is a paradoxical kind of input function: it is the limiting case of all input rate functions by which a given dose D enters the system as the length of the time interval during which it enters the system approaches zero. Expressed in terms of a constant absolute rate (zero-order) process, which is called a pulse if Δ is sufficiently short, this is expressed by Verrotta (1) as follows:

$$\delta_\Delta(t - t_1) = \begin{cases} 0 & \text{for} \quad t < t_1 \\ \dfrac{1}{\Delta} & \text{for} \quad t_1 \le t \le t_1 + \Delta \\ 0 & \text{for} \quad t > t_1 + \Delta \end{cases} \tag{5}$$

If Δ vanishes, and the dose is unity, the limiting function is called Dirac's delta function δ, and its integral is the unit-step function.

The rate function of an impulse cannot be represented graphically because it approaches infinity as Δ approaches zero. The different lengths of the vertical lines in Fig. 1a indicate that we are dealing with pulse functions, where Δ is still finite. On the other hand, the step functions representing cumulative amounts (see Fig. 1b) are the integrals of impulses.

The input rate function and its integral, the cumulative amount input function, are two representations of input kinetics that can be viewed in statisti-

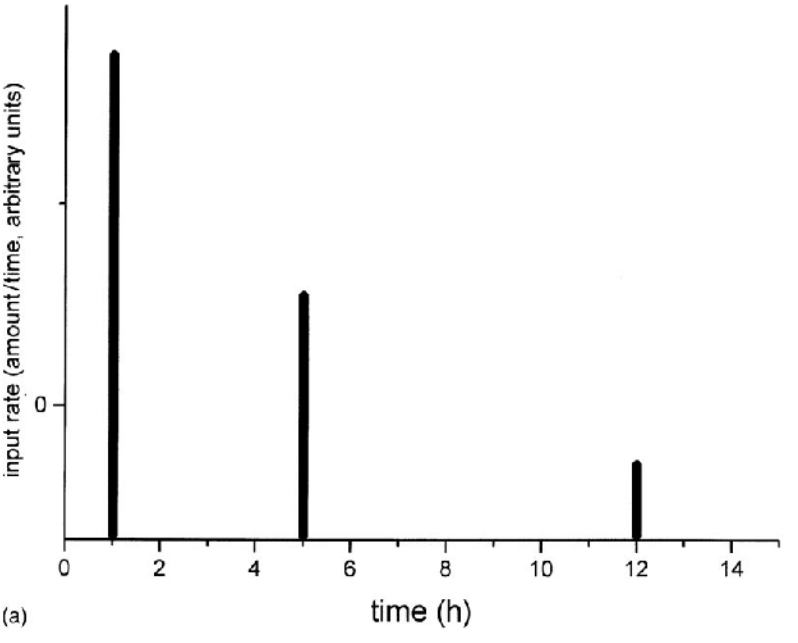

FIG. 1 Impulse train input: (a) approximate input rate function; (b) cumulative input function; (c) plasma concentration response function (one-compartment model).

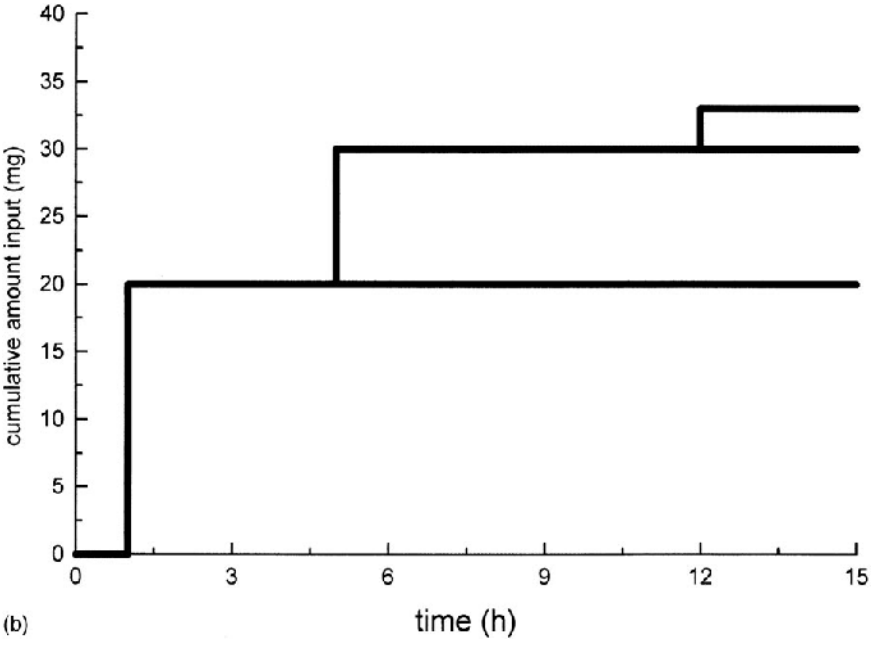

(b)

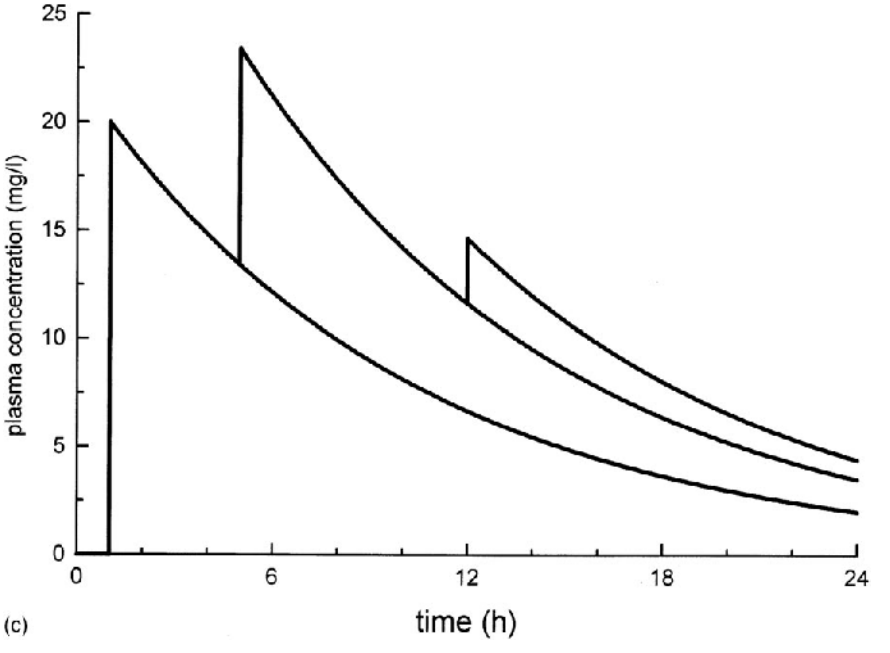

(c)

FIG. 1 Continued

cal terms as the density function and the distribution function of a residence time distribution. The convolution of the input rate function and the monoexponential disposition function corresponding to a one-compartment open body model (see Fig. 1c) show how the input is ''smeared'' along the time axis by the convolution operation.

In pharmacokinetics, an intravenous bolus injection is the nearest approximation to the delivery of an impulse to the circulating fluids. A subcutaneous or intramuscular injection or the administration of an enema may be considered as extravascular impulse release functions for which the full dose becomes instantaneously available at the site of administration if the subsequent absorption step is nonsaturable and time-invariant. On the other hand, an aqueous solution ingested orally over a short time may be a poor approximation to an impulse delivered peripherally because the time course of absorption is likely to be perturbed by physiological factors such as the kinetics of gastric emptying. For oral administration, a gelatin capsule filled with a water-miscible solution of the drug may be a closer approximation to impulse input.

II. MASS BALANCE METHODS

The oldest methods used to reconstruct the time course of drug absorption from pharmacokinetic data were based on mass balance considerations in compartmental models. Because they are relatively simple and transparent, they are still frequently used. The Wagner–Nelson method (2) will be summarized in somewhat different terms than originally proposed by the authors.

A. Wagner–Nelson Method

For the one-compartment model, with its monoexponential impulse response function, the amount of drug remaining at the site of administration at time t after administration at t_{adm} is equal to the dose administered (D) minus the amount absorbed, minus the amount eliminated presystemically. If only the plasma level profile (or the time course of urinary excretion) of the parent compound is assayed, there is no way to track the extent and kinetics of presystemic elimination. Therefore, the method is referenced only to the three components of the bioavailable fraction of the dose (F), which are still at the site of administration, presently in the body, and already eliminated. The extent of absorption is equal to the total area under the plasma level curve AUC_0^∞ times the subject's total body clearance CL_{tot}.

$$FD = \mathrm{AUC}_0^{\infty}\mathrm{CL}_{\mathrm{tot}} \tag{6}$$

The amount of drug in the body $m_B(t)$ is equal to the concentration observed in the circulating fluids c_B times the volume of distribution,

$$m_B = c_B V \tag{7}$$

and the amount eliminated $m_E(t)$ is equal to the area under the concentration–time curve up to t times the total body clearance:

$$m_E = \mathrm{CL}_{\mathrm{tot}}\mathrm{AUC}_0^t \tag{8}$$

For the one-compartment open-body model, the clearance is simply the product of the volume of distribution and the elimination rate constant k_E:

$$\mathrm{CL}_{\mathrm{tot}} = Vk_E \tag{9}$$

The bioavailable fraction of the dose administered is equal to the total amount eliminated from the system:

$$\mathrm{AUC}_0^{\infty}\mathrm{CL}_{\mathrm{tot}} = m_{E,\infty} = FD \tag{10}$$

The fraction of the dose that will be absorbed but is still at the site of administration ($m_A(t)$) is then given by

$$\frac{m_A(t)}{FD} = 1 - \frac{c_B(t)V + k_E V\mathrm{AUC}_0^t}{k_E V\mathrm{AUC}_0^{\infty}} = 1 - \frac{c_B(t) + k_E\mathrm{AUC}_0^t}{k_E\mathrm{AUC}_0^{\infty}} \tag{11}$$

Note that the volume of distribution, which can be determined only by a reference experiment in which the drug is given intravenously, cancels out. The convenience of not having to administer an intravenous reference contributes to the popularity of this method, but it comes at a price: the results are valid only if the one-compartment model adequately represents the disposition kinetics, and if the elimination rate constant can be determined reliably from the terminal part of the plasma level curve.

The expression on the left of Eq. (9) can be viewed as the complement of the distribution function of an empirical residence time distribution, from which the input rate function $f(t)$ is readily obtained.

B. Loo–Riegelman Method

We shall consider only the simplest case of a mammillary two-compartment model, because it can be readily generalized. An intravenous reference experiment is required to find the number of kinetically distinguishable compartments and their microscopic apparent rate constants. Wagner (3) has shown

that assumptions concerning the internal structure of the mammillary disposition system, particularly about the absence or presence of elimination pathways originating from peripheral compartments, are of no consequence for the input profiles obtained.

When there is more than one body compartment, it is convenient to number them. Customarily, the central compartment is given the index 1 and peripheral compartments indexes 2, . . . , M, where M is the number of distinguishable compartments in the mammillary system. Internal (microscopic) transfer rate constants are denominated k_{ij}, where i is the index of the source and j that of the target compartment (as distinguished from hybrid rate constants λ_ℓ, $\ell = 1, \ldots, M$). The microscopic elimination rate constant from the central compartment will be called k_{1E}.

Although irrelevant for the present derivation, the formal order of precedence of peripheral compartments can imply factual content in the sense that the ranks correspond to relative rates of equilibration with the central compartment. Peripheral compartments are distinguishable only if they differ in this property, which is characterized numerically by the values of apparent return rate constants. One way of expressing this relation is that shallow compartments are given low index numbers and deep compartments high ones.

In the mammillary two-compartment model, fractions of drug absorbed are either in the central compartment, in the peripheral compartment, or eliminated, so that

$$m_A(t) = FD - \frac{V_1 c_1(t) + k_{1E} V_1 \int_0^t c_1 dt + m_2(t)}{k_{1E} V_1 \int_0^\infty c_1 dt} \tag{12}$$

where the amount in the peripheral compartment is computed stepwise

$$m_2(t_i) = m_2(t_{i-1}) e^{-k_{21}\Delta t_i} + \frac{k_{12} m_1(t_{i-1})}{k_{21}} (1 - e^{-k_{21}\Delta t_i}) + \frac{k_{12} \Delta m_{1\cdot i} \Delta t_i}{2} \tag{13}$$

and $\Delta t_i = t_i - t_{i-1}$ and $\Delta m_{1\cdot i} = m_1(t_i) - m_1(t_{i-1})$. For details of the derivation see also Gibaldi and Perrier (5). The procedure is readily extended to mammillary systems with three and more compartments. Similar to the Wagner–Nelson method, it does not imply any assumptions concerning the kinetics of drug input. An advantage is that absolute amounts can be computed because of the intravenous reference experiment required.

One interesting point concerns the robustness of the method for potentially erroneous assumptions on intercompartmental transfers and routes of elimination. The disposition model is taken as a representative of a set of alternatives, of which it is in a sense the simplest member. Note that this kind of model independence would not hold for problems related to correlations between the time course of observable drug concentrations in body fluids and the intensity and duration of pharmacological effects.

III. DIRECT NUMERICAL METHODS

A. Impulse Train

The simplest direct numerical deconvolution method was introduced by Chiou (6). Samples are taken as before at times t_i, $i = 0, 1, \ldots, N$, and the amount of drug (expressed as a fraction of the dose administered) that enters the system within the interval $[t_{i-1}, t_i]$ is called f_iD. The algorithm is based on the assumption that the input kinetics of f_iD is an impulse located at $(t_{i-1} + t_i)/2$ (i.e., at the midpoint of the sampling interval). The input rate function is depicted as an impulse train similar to the one in Fig. 1a, and the cumulative input function is a multistep function. The underlying assumption is not particularly plausible, but the computations are simple and the cumulative input profile is reasonable.

Although it is not customary to consider the dose fractions f_i, $i = 1, \ldots, N$ as parameters of an input model, that, in effect, is what they are. For more elaborate deconvolution methods, the problem can also be stated as, ''how can a smooth cumulative input profile be best described by not more than one rate parameter for each observation?''

B. Pulse Sequence

The next logical step is to represent the input rate profile by a succession of pulses, where the input rate f_i during the ith sampling interval is constant, and the input rate profile is a close succession of rectangular pulses. In general, numerical deconvolution algorithms assume a particularly simple form if the time intervals are of equal length. An example that is amenable to a manual computation scheme was given by Stepanek (7). If g_0, the initial value of the impulse response function, is greater than zero, and the time interval is Δt, then f_0, the input rate within the first interval is

$$f_0 = \frac{h_0}{\Delta t g_0} \tag{14a}$$

for the second interval we have

$$f_1 = \frac{1}{\Delta t g_0} - \frac{1}{g_0} f_0 g_1 \tag{14b}$$

for the third

$$f_2 = \frac{h_2}{\Delta t g_0} - \frac{1}{g_0} (f_0 g_2 + f_1 g_1) \tag{14c}$$

while the full recursive formula is given by

$$f_n = \frac{h_n}{\Delta t g_0} - \frac{1}{g_0} \sum_{i=0}^{n-1} f_i g_{n-1} \tag{14d}$$

This method is, in principle, also suited to deconvolve pharmacokinetic absorption rate profiles after extravascular administration if $g(t)$ is taken to be the impulse response function observed after an intravenous bolus administration, but the requirement of observations spaced at equal intervals limits its suitability for this purpose.

A related problem is the deconvolution of in vivo release kinetics if the impulse response function observed after peripheral administration is known. In the simplest case $g(t)$ is then a Bateman-type function corresponding to a one compartment model with first order absorption. Here, $g(0) = 0$. If objections concerning the influence of gastric emptying on absorption kinetics and questions as to whether the permeability of the intestinal wall is constant and how dilution of the volume of intestinal contents from which drug is absorbed as it passes along the gastrointestinal tract might affect the rate of its appearance in the circulating fluids are disregarded, the following alternative deconvolution formula for the pulse sequence input model (7) can be applied:

$$f_0 = \frac{h_1}{\Delta t g_1} \tag{15a}$$

$$f_1 = \frac{h_2}{\Delta t g_2} - \frac{1}{g_1} f_0 g_2 \tag{15b}$$

$$f_2 = \frac{h_3}{\Delta t g_3} - \frac{1}{g_1} (f_0 g_3 - f_1 g_2) \tag{15c}$$

$$\vdots$$

$$f_n = \frac{h_{n+1}}{\Delta t g_1} - \frac{1}{g_1} \sum_{i=0}^{n-1} f_i g_{n+1-i} \tag{15d}$$

The difficulty here, as before, is that equally spaced samples are uncommon in pharmacokinetics—and for a good reason: the information content of plasma concentrations toward the end of the terminal exponential disposition phase is fairly low. A similar algorithm was published by Vaughan and Dennis (8), who also addressed the more complex case of unequal sampling intervals illustrated in Fig. 2 without elaborating the details. A first-order (exponentially decreasing or constant fractional rate) input profile is displayed in Fig. 2a as both the rate function and the cumulative input function, along with an approximation by a sequence of five pulses of unequal length. In Fig. 2b, the corresponding plasma level profiles are shown: a Bateman function and its approximation by a superimposition of four response functions to a sequence of (infusion-like) constant rate input processes.

C. Trapezoidal Formula

A better approximation is obtained if the input rate is assumed to change linearly between the time points at which it is computed from observations (i.e., if the input rate function is approximated by a sequence of trapezes, rather than rectangles). For an impulse response function with $g_0 > 0$ the corresponding deconvolution formula is

$$f_0 = \frac{2h_1 - \dfrac{h_2}{2}}{\Delta t g_0} \tag{16a}$$

$$f_1 = \frac{2h_1}{\Delta t g_0} - \frac{f_0 g_1}{g_0} \tag{16b}$$

$$f_2 = \frac{2h_2}{\Delta t g_0} - \frac{1}{g_0}(f_0 g_2 + 2 f_1 g_1) \tag{16c}$$

$$\vdots$$

$$f_n = \frac{2h_n}{\Delta t g_0} - \frac{1}{g_0}\left(f_0 g_n + 2\sum_{i=1}^{n-1} f_i g_{n-i}\right) \tag{16d}$$

FIG. 2 Approximation of a first-order input function by a pulse sequence: (a) solid line, pulse sequence input rate and cumulative input function; dashed line, first-order input rate and cumulative input function; (b) plasma concentration response functions.

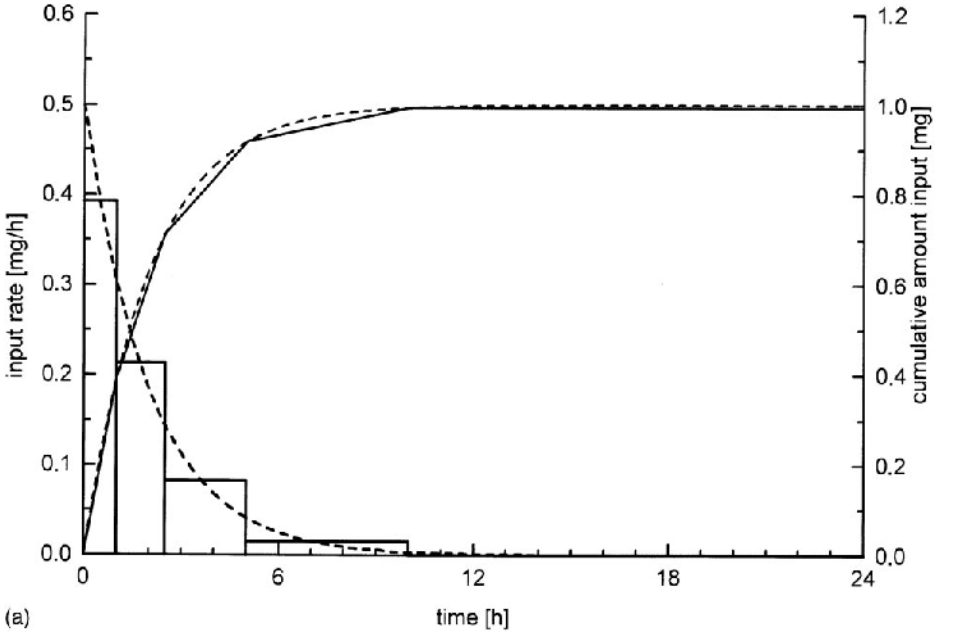
0.6
0.5
0.4
0.3
0.2
0.1
0.0
input rate [mg/h]
1.2
1.0
0.8
0.6
0.4
0.2
0.0
cumulative amount input [mg]
0
6
12
18
24
time [h]

(a)

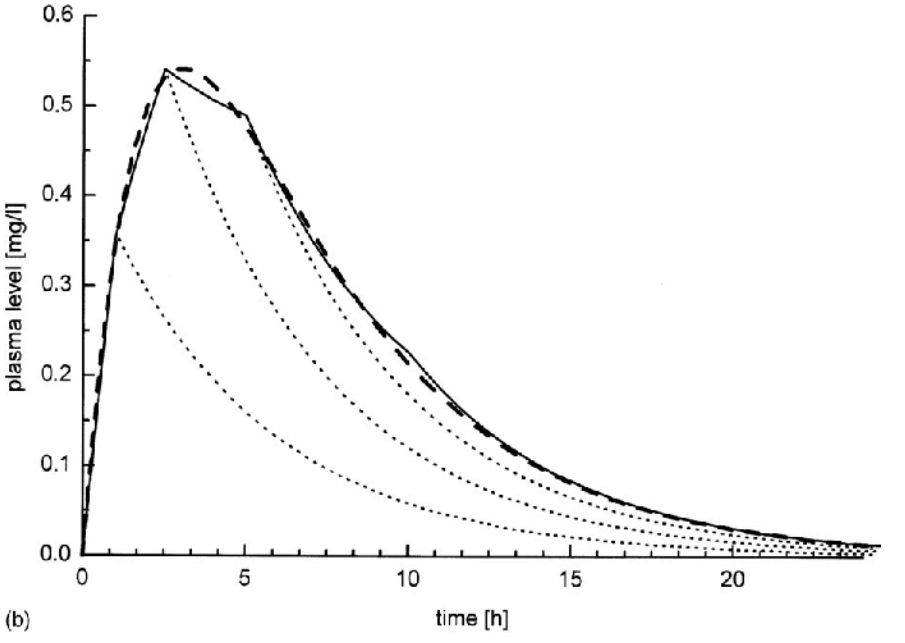
0.6
0.5
0.4
0.3
0.2
0.1
0.0
plasma level [mg/l]
0
5
10
15
20
time [h]

(b)

Direct deconvolution methods are unstable in the presence of experimental error in the data. A simple but illustrative example is given in Fig. 3. A monoexponential impulse response function (squares) was convolved with a constant rate input function (closed triangles, background) to yield the familiar time course of plasma levels after infusion for the one-compartment model as the output function (circles). At about 90% of the steady-state level, a negative error of about 10% of the function value is added to just one data point and the deconvolved input rate profile is plotted as open triangles in the foreground. The magnitude of the resulting error in the input rate is initially about 50% of the true function value and increases temporarily to 100% before declining exponentially. From this example, it is obvious that the results become unpredictable when the error structure is more complex.

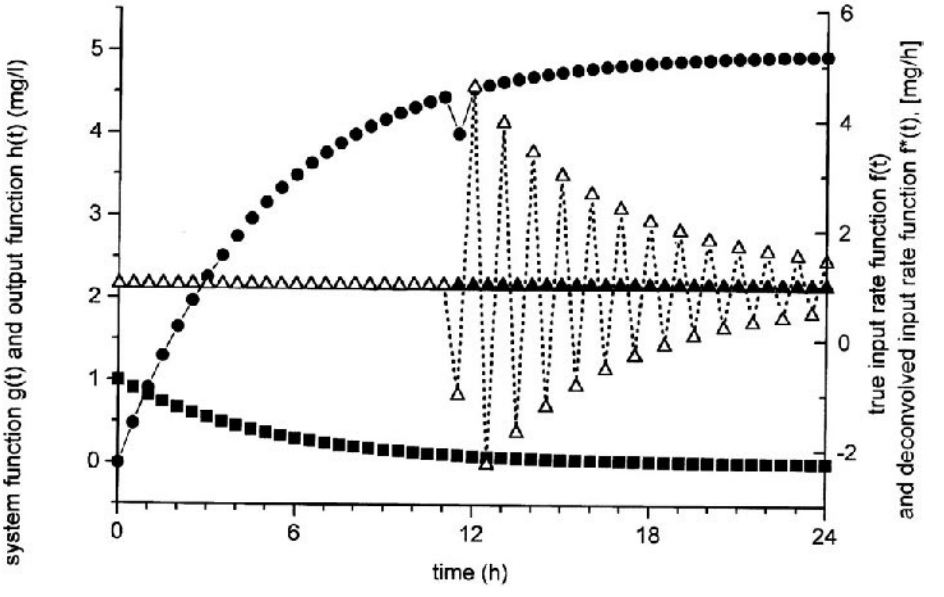

FIG. 3 Error propagation on convolution using the trapezoidal formula [see Eq. (16a) to (16d)]: squares, impulse response function (monoexponential); closed triangles, true input rate function (constant, first half not visible behind deconvoluted input rate profile); circles, output function, only one negative error added at 90% of steady-state level; open triangles, deconvoluted input function.

Equivalent formulas for the case of $g_0 = 0$ are available, but because more stable alternatives are presented later, they are only mentioned here and not discussed in detail.

Verrotta (1) considered the problem of instability in terms of a system of linear equations and proposed a discrete convolution scheme where the input function is a sequence of pulses and the impulse response function is analytically or numerically integrable (some of his symbols are replaced by equivalents used above).

$$h(t_i) = \sum_{j=1}^{i} f(t_j) \int_{t_{j-1}}^{t_j} K(t_i - \tau) d\tau \tag{17}$$

Defining $G_{ij} = \int_{t_{j-1}}^{t_j} K(t_i - \tau) d\tau$ and the matrix

$$\boldsymbol{G} = \begin{pmatrix} G_{11} & 0 & \cdots & 0 \\ G_{21} & G_{22} & \cdots & \cdot \\ \cdot & \cdot & \cdots & \cdot \\ G_{n1} & G_{n2} & \cdots & G_{nn} \end{pmatrix} \tag{18}$$

then the problem of obtaining the column vector $\boldsymbol{f}$, given the column vector of observations $\boldsymbol{y}$, each of which is the sum of a function value and an error $y_i = \boldsymbol{h}_i + \varepsilon_i$, amounts to solving the system of linear equations

$$\boldsymbol{y} = \boldsymbol{G}\boldsymbol{f} \tag{19}$$

The errors are assumed to be independently distributed with mean zero. The solution is

$$\boldsymbol{f} = \boldsymbol{G}^{-1}\mathbf{y} \tag{20}$$

where $\boldsymbol{G}^{-1}$ is the matrix inverse of $\boldsymbol{G}$. The elements of $\boldsymbol{G}$ right of the diagonal are zero, this suggests a recursive formula for the computation of $\boldsymbol{f}$.

$$f_i = \frac{y_i - \sum_{j=1}^{i-1} f_j}{G_{ii}} \tag{21}$$

The problem with this deceptively simple approach has already been discussed: it is the propagation of the errors. With noisy data, the deconvolved input profile begins to oscillate unpredictably after a few computation steps,

particularly if the kernel does not decrease rapidly. Problems in which the relative error of the estimate increases drastically, even if the errors in the observations is small, are called ill-conditioned. There are several methods to deal with this situation, some of which will be discussed later.

IV. TRANSFORMATION METHODS

Functions that are linearly related to measurable quantities by the convolution integral occur frequently in technical contexts. Examples are particle size distributions, which are analyzed by the diffraction of laser beams, or relaxation time spectra of macromolecules in solution obtained from the strains caused by oscillating external forces. More complex two-dimensional varieties arise in image processing, for example, in astronomy when optical or radio signals of point-stars are spread over several detector elements and the best approximation of the true image is reconstructed by deconvolution using the instrument's ''point-spread function'' (i.e., the two-dimensional analog of the impulse response function).

A. Fourier Transform

For signals sampled at constant intervals Δt, the discrete Fourier transform is a powerful numerical tool for both convolution and deconvolution, particularly in the form of the fast Fourier transform (FFT). The discrete Fourier transform of N points h_k evenly spaced in time into the frequency domain is denoted $H_n(f)$:

$$H_n(f) \equiv \sum_{k=0}^{N-1} h_k(t) e^{2\pi i k n/N} \tag{22}$$

and the inverse transformation is

$$h_k(t) = \frac{1}{N} \sum_{n=0}^{N-1} H_n(f) e^{-2\pi i k n/N} \tag{23}$$

and the convolution theorem

$$g(t) * h(t) \leftrightarrow G(f)H(f) \tag{24}$$

states that the Fourier transform of the convolution is just the product of the Fourier transforms of the two functions. Although the problem of high-frequency random error in the data can, in principle, be handled by filtering using the same method, this approach has not caught on in pharmacokinetics and biopharmaceutics. As in the foregoing simple direct deconvolution schemes, the requirement of constant sampling intervals makes it poorly suited to this field of applications.

B. Laplace Transform

The Laplace transform is a powerful tool for the solution of systems of ordinary differential equations, which are the base of linear pharmacokinetic models. It can also be used to convolve and deconvolve impulse response functions and input functions analytically (7,10–14).

Let $\mathcal{L}\{f(t)\} = F(s)$ be the Laplace transform of $f(t)$ with suitably chosen transform variable s, so that

$$F(s) = \int_0^\infty f(t)e^{-st}dt \tag{25}$$

then the convolution in the time domain corresponds to an arithmetic multiplication in the transformation domain:

$$f(t) * g(t) \leftrightarrow F(s)G(s) \tag{26}$$

Notice that the convolution operation is commutative, that is,

$$f(t) * g(t) = g(t) * f(t) \tag{27}$$

This property is of interest if the input rate function $f(t)$ is to be decomposed into the underlying processes of in vivo release and absorption, which are described by corresponding functions $d(t)$ and $a(t)$,

$$f(t) = a(t) * d(t) \tag{28}$$

In principle this is possible if either process or both are linear. Because neither can be observed directly, salient features of the input rate function, such as near-instantaneous changes, have to be rationalized by physicochemical interpretation, rather than by mathematical methods.

V. LEAST-SQUARES METHODS

A. Analytical Input Functions (Parametric Least Squares)

If $f(t)$ is assumed to be a function with p parameters Θ_k, $k = 1, \ldots, p$, the deconvolution problem can be restated as a regression problem, in which the parameters are estimated by curve-fitting. In the simplest case, the objective function to be minimized is just the sum of squares:

$$\sum_{i=1}^{N} (y(t_i) - g(\theta, t_i))^2 \tag{29}$$

If the number of parameters is small, and if they are not correlated, this is the obvious way to proceed.

Cutler (15) proposed use of the exponential input rate function with rate constant k_{in}

$$f(t) = k_{in} F D^{-ek_{in}t} \tag{30}$$

Its convolution with the monoexponential disposition function

$$g(t) = \frac{1}{V} e^{k_{el}t} \tag{31}$$

is simply the popular Bateman function

$$h(t) = c_p(t) = \frac{FDk_{in}}{V(k_{el} - k_{in})} (e^{-k_{in}t} - e^{-k_{el}t}) \tag{32}$$

but the method is also applicable to polyexponential disposition functions. Veng Pedersen (16) suggested a polyexponential input rate function of the form

$$f(t) = \sum_{i=1}^{q} k_{in \cdot i} D_i e^{-k_{in \cdot i}t} \tag{33}$$

as a further generalization. The convolution integral of this type of input functions with polyexponential disposition functions has a simple analytical form: if the number of input exponentials is q and that of disposition exponentials is m, the output function is a sum of $q + m$ exponential terms, provided that all the exponential rate constants are distinct.

Mono- and poly-(or rather oligo-)exponential input functions are popular, and the early grand master of pharmacokinetics, F. H. Dost, even considered the Bateman function the most fundamental of all pharmacokinetic mod-

els (17). Because there is a tendency for input rates to decline over time, they frequently correspond fairly well to observations, particularly if there are not too many observations during the input phase. Sometimes, the notion of a (first-order) ''input rate constant'' (i.e., a constant fractional input rate) is used uncritically as a canonical representation of the rate aspect of biovailability. On closer inspection, the picture usually becomes more complex.

Cutler (15) also proposed to use a rate equation describing the dissolution of monodisperse powders, known in pharmaceutics as ''cube-root-law,'' as an input function, where t_{dis} is the time at which dissolution is complete. It characterizes the overall rate of the process:

$$f(t) = \begin{cases} \dfrac{3D}{t_{dis}}\left(1 - \dfrac{t}{t_{dis}}\right)^2 & \text{for} \quad t \leq t_{dis} \\ 0 & \text{for} \quad t > t_{dis} \end{cases} \tag{34}$$

In this instance, the convolution with the impulse response function characterizing the biological system is computed numerically. The approach is valid if the kinetics of the subsequent absorption step are known (e.g., in terms of a constant first-order absorption rate constant) or if they can be neglected because absorption is much faster than the dissolution or release kinetics described by the cube-root model (see also Chapter 13).

B. Polynomials

Polynomials are a particularly flexible type of approximating functions, they can be evaluated using only the operations of addition and multiplication, and they are easily integrated and differentiated. It has been suggested by Cutler (18) that input functions can be represented by polynomials, and this approach appears to work well with smooth functions and low-order polynomials. Its drawback seems to be that it fails if the input function is not well-behaved anywhere in the interval of approximation. In this instance the approximation is poor everywhere (19).

C. Splines

Two piecewise approximations to the input rate function have been discussed in the foregoing, which can be viewed as special cases of polynomials: the sequence of rectangles or zero-order rate processes, which is also called a

''staircase function'' is a zero-order polynomial, where the only rate parameter in each interval is a constant coefficient,

$$f(t) = b_{0\cdot i} = r_{in\cdot i} \qquad \text{for} \qquad t_{i-1} < t < t_i \tag{35}$$

the first derivative is zero in the interior of the intervals and not defined at the abscissas t_i. For the trapezoidal formula used in the numerical deconvolution scheme [see Eqs. (16a)–(16d)], the input rate is assumed to change linearly between observations, so that the first derivative is constant and the second is zero in the interior of the intervals, and at the boundaries both have no finite values.

$$f(t) = f_{i-1} + \frac{f_i - f_{i-1}}{t_i - t_{i-1}}(t - t_{i-1}) \qquad \text{for} \qquad t_{i-1} < t < t_i \tag{36}$$

As a matter of convenience, the smooth pieces of the latter two input rate functions have been assumed to coincide with sampling intervals, but that is not a necessity.

Piecewise fourth-order polynomials defined over a nondecreasing sequence of breakpoints or knots where the first derivatives are smooth and the second derivatives are continuous at the breakpoints are called cubic splines. In the current context, the independent variable is time, so that the breakpoints may be denominated t_j., $j = 1, 2, \ldots, m$. Natural splines satisfy the end condition that the function value and its derivatives are zero at both end points. Splines are computationally efficient and can be used for both interpolation and smoothing. In the latter instance they are called regression splines, where the degree of smoothing can be chosen by attributing a suitable value in the range [0,1] to a control parameter (19). In spline representation, the input function can be written

$$f(t, \rho) = \sum_{j=1}^{m} \alpha_j N_k(t) \tag{37}$$

where the $N_j(t)$ are spline basis functions and the ρ_j characterize both the input rate and its change (The symbol ρ [rho] is used here to indicate a close relation to the pharmacokinetic notation, where the zero-order input rate in the jth sampling interval is denoted $r_{in\cdot j}$.) The output function is linear with respect to ρ:

$$h(t, \rho) = \int_0^t \sum_{j=1}^{m} \rho_j N_j(\tau) K(t - \tau) d\tau \tag{38}$$

and when G_{ij} is redefined as

$$G_{ij} = \int_0^{t_i} N(\tau)K(t - \tau)d\tau \tag{39}$$

the deconvolution problem is again reduced to a linear regression problem (20), where G may be better conditioned by smoothing. Verrotta suggests (21) that the robustness of the method can be further improved by introducing constraints on the input rate function (e.g., by requiring it to be nonnegative, which is natural in view of its alternative interpretation as the density function of a residence time distribution), or nonnegative and nonincreasing, which appears, however, to be problematic, particularly for the enteral route of administration.

D. Regularization Methods

We have seen that the matrix $\boldsymbol{G}$ is usually ill-conditioned so that small errors in the data have large effects on the least-square estimates of $f(t_i)$. It is the many ''input rate parameters'' that cause the problem, and it becomes worse if the number of observations increases. In addition, the least-squares solution is not unique, and several sets of input rate parameters may be consistent with the data. It is, however, possible to choose a particular function $f(t)$, by adding the requirement that

$$J(f) = \int_I (f''(t))^2 dt \tag{40}$$

be minimal over the interval I in which f is to be determined under the constraint

$$S = \sum_{i=1}^{N} \left(\frac{y_i - \int f(t)K(t, \tau)d\tau}{\sigma_i} \right) \tag{41}$$

where S is a number that is at first set equal to N. After introducing a Lagrange multiplier λ we now seek the minimum of

$$J(f, \lambda) = \int_I [f''(t)]^2 dt + \lambda \left[\sum_{i=1}^{N} \left(\frac{y_i - \int f(\tau)K(t, \tau)d\tau}{\sigma_i} \right)^2 - S \right] \tag{42}$$

For a given λ, the minimum of $J(f, \lambda)$ is the same as the minimum of

$$\begin{aligned} \tilde{J}(f, \lambda) &= \lambda J\left(f, \frac{1}{\lambda}\right) + S \\ &\equiv \sum_{i=1}^{N} \left(\frac{y_i - \int f(\tau) K(t, \tau) d\tau}{\sigma_i} \right)^2 + \lambda \int_I f''(\tau) d\tau \end{aligned} \tag{43}$$

In this case, the objective function has two terms: the discrepancy, which is the only one minimized in the linear regression, and an expression ensuring the smoothness, which restricts the class of acceptable functions (22,23).

Several regularization methods are available that differ in the function added to assure smoothness and in the way by which the regularization parameter λ is computed.

VI. MAXIMUM ENTROPY METHODS

It has already been mentioned that any time course of drug input can be expressed in terms of a residence time distribution, where the input rate function $f(t)$ corresponds to the probability density of the transition from the site of administration into the system. For a continuous input function, the entropy of the residence time is

$$S(f) = \int [-\ln f(t)] f(t) dt \tag{44}$$

where $f(t)$ is made dimensionless by expressing it in terms of fractions of dose absorbed. The entropy of a distribution can be viewed as a measure of the amount of information it contains: the information content is high if it is concentrated, and low if it is spread out nearly uniformly over a wide range.

Maximum entropy methods have been developed and are widely used in the field of image analysis to deblur pictures (9). A typical application is the problem of obtaining the sharpest possible picture of a stellar object in astronomy, given the diffraction pattern of the instrument and atmospheric interferences. The distortion of the signal caused by instrumental and other factors is characterized by a point-spread function, the two-dimensional analog of the impulse response function discussed in the foregoing.

In the present context it is noteworthy that humans are used in an instrumental mode to observe in vivo release characteristics of drug preparations, usually in conjunction with the transition kinetics of drug molecules dissolved

at the site of administration across some biological barrier into the general circulation. Instruments have to be calibrated, and this is achieved in biopharmaceutical studies by a reference experiment, which serves primarily to determine the system functions (i.e., the disposition kinetics) of individual subjects. Apart from legal and regulatory aspects, this perspective has interesting scientific consequences for the choice of reference preparations, which will now be discussed briefly.

Maximum entropy methods also have a strong philosophical flavor because they are founded on bayesian probability theory. Bayes' theorem can be expressed as follows:

Let y be the data, f the input function sought, and H the background information including the impulse response function and the error structure, then the following conditional probabilities, which are functions with values in the range [0, 1], are considered:

$\Pr(f\|H)$	is the *prior*: the knowledge of or assumptions about f before the data are available.
$\Pr(y\|fH)$	is the *likelihood* of the data if a specific f were true.
$\Pr(f\|yH)$	is the *posterior* or ''*inference*'': the knowledge of f on account of the data.
$\Pr(y\|H)$	is the ''*evidence*.''

Bayes' theorem concerning the best input function in view of the data and prior information is

$$\Pr(f|yH) = \frac{\Pr(y|fH)}{\Pr(y|H)} \Pr(f|H)$$

or (45)

$$Posterior = \frac{likelihood}{evidence}\, prior$$

The method has been applied by Charter and Gull to the analysis of drug absorption profiles (23,24). In a rheological context, Honerkamp demonstrated that the results of regularization and maximum entropy methods can be very similar (22).

VII. CONSTRAINED DIRECT SEQUENTIAL ESTIMATION WITH ITERATIVE IMPROVEMENT

If a linear pharmacokinetic system has a polyexponential impulse response function

$$g(t) = \sum_{j=1}^{M} A_j e^{-\lambda_j(t)} \tag{46}$$

then its response function to a constant-rate (zero-order, infusion) input beginning at $t_{in\cdot 0}$ is

$$h_0(t) = \begin{cases} 0 & \text{for} \quad t < t_{in\cdot 0} \\ r_{in}\left(B_0 - \sum_{j=1}^{M} B_j e^{-\lambda_j(t-t_{in\cdot 0})}\right) & \text{for} \quad t \geq t_{in\cdot 0} \end{cases} \tag{47}$$

where B_0 is the reciprocal of the total body clearance if $g(t)$ is the plasma level function. The obvious relations between the coefficients A_j in the impulse response function and B_j in the constant input rate response function need not be discussed here.

If the input is stopped at $t_{in\cdot 1}$, a truncation correction function is added, which has the same form as the constant input rate response function, but opposite sign, and is shifted along the time axis (25)

$$h_0(t) = \begin{cases} 0 & \text{for} \quad t \leq t_{in\cdot 0} \\ r_{in}\left(B_0 - \sum_{j=1}^{M} B_j e^{-\lambda_j(t-t_{in\cdot 0})}\right) & \\ \left[r_{in}\left(B_0 - \sum_{j=1}^{M} B_j e^{-\lambda_j(t-t_{in\cdot 0})}\right) \right. & \text{for} \quad t_{in\cdot 0} < t \leq t \\ \left. -r_{in}\left(B_0 - \sum_{j=1}^{M} B_j e^{-\lambda_j(t-t_{in\cdot 1})}\right)\right] & \text{for} \quad t > t_{in\cdot 1} \end{cases} \tag{48}$$

This approach can be generalized for multiphasic constant rate processes, where

$$f(t) = \begin{cases} 0 & \text{for} \quad t \leq t_{in\cdot 0} \\ r_{in\cdot 1} & \text{for} \quad t_{in\cdot 0} < t \leq t_{in\cdot i} \\ \vdots & \vdots \\ r_{in\cdot N} & \text{for} \quad t_{in\cdot N-1} < t \leq t_{in\cdot N} \\ 0 & \text{for} \quad t > t_{in\cdot N} \end{cases} \tag{49}$$

This provides the starting point for a numerically stable deconvolution procedure, where the breakpoints of the input function are taken to be the sampling

times, and the index *in* with respect to times will therefore be omitted. The underlying notion that the input rate should change its value instantaneously whenever the output function is observed, is somewhat strange, but is implicit in the staircase function approach. The parameters of the disposition model are determined in a separate reference experiment.

Proceeding from left to right, linear estimates of the input rates inside the sampling intervals are obtained sequentially. Let $\hat{c}_{z\cdot i}$ be the expected concentration if the input rate in the time interval $[t_{i-1}, t_i]$ had been zero, $\hat{c}_{u\cdot i}$ the expected concentration if it had been unity, and $c_{obs\cdot i}$ the concentration actually observed at t_i. The estimate of $r_{in\cdot i}$ is then

$$\hat{r}_{in\cdot i} = \frac{c_{obs\cdot i} - \hat{c}_{z\cdot i}}{\hat{c}_{u\cdot i} - \hat{c}_{z\cdot i}} r_{in\cdot u} \tag{50}$$

where $r_{in\cdot u}$ can be conveniently chosen (Fig. 4). The stability of the method is assured by the constraint that acceptable values for $\hat{r}_{in\cdot i}$ are positive or zero, and if a negative value is obtained, it is substituted by zero for the subsequent calculations. A negative value indicates that an observation is inconsistent with the disposition kinetics. There may be several reasons for this, and the discrepancy should be interpreted wherever possible. Initial estimates of the $\hat{r}_{in\cdot i}$ are biased, they can be refined by a subsequent iterative nonlinear least-squares method in which local deviations are distributed over neighboring observations. The method has been found to be numerically stable and efficient (26,27).

VIII. DISCUSSION

In view of the mathematical problems discussed, it may seem that the main difficulties in biopharmaceutical convolution and deconvolution operations are caused by the ill-conditioning of matrices arising in inverse problems, but that would be a misleading impression. Handling the intra- and interindividual variability of humans, both relative to their disposition kinetics, as with in vivo drug release and absorption, is at least as problematic. Also, the interpretation of data in terms of underlying processes such as secondary peaks arising (e.g., from enterohepatic recirculation) is important and should not be discarded in order to apply a particularly elegant black-box method.

Regularization methods, splines, and maximum entropy methods rely on assumptions concerning the smoothness of the underlying functions. This may be adequate for many applications, but the saying *natura non facit saltus*

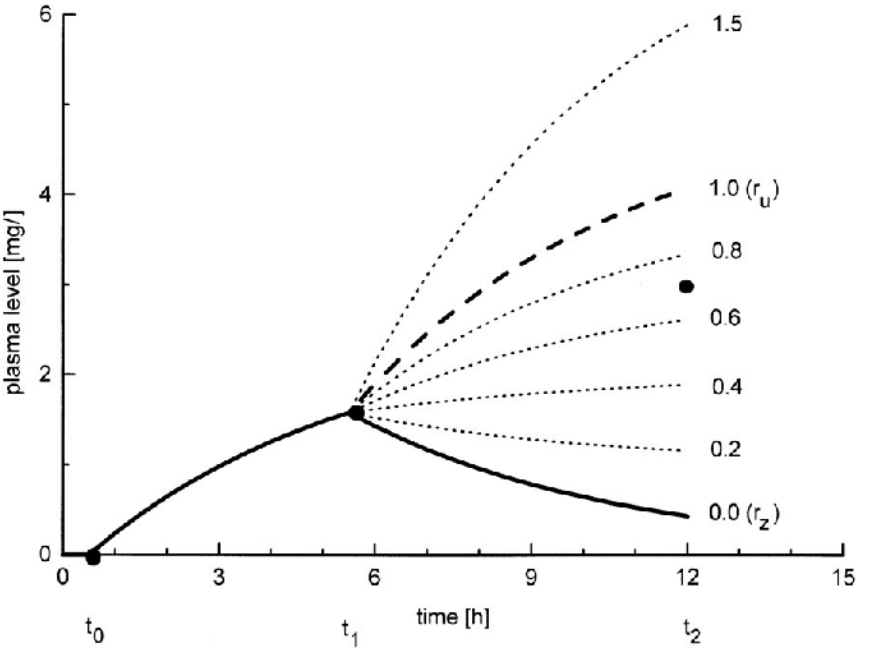

FIG. 4 Constrained direct sequential estimation (monoexponential disposition function): r_u, expected response to unit input rate; r_z, expected response to zero input rate.

does not apply to peristaltic intestinal transport. In the analysis of absorption profiles, the times at which the input rate increases is indicative of the kinetics of gastric emptying or the dissolution behavior of an enteric coat and a rapid terminal decline can signal an absorption window. In these instances, the times at which the input rate function jumps are important parameters.

In the present context, the distinction between parametric and nonparametric models appears to vanish: a staircase function with, say, 24 steps, each of which can be viewed as a zero-order process is certainly not an input model in the classic sense, and estimating an input rate parameter for each sampling interval brings us to the very limit of pharmacokinetic modeling.

The real problem comes after deconvolution: to summarize salient features of the input kinetics in a few meaningful parameters that can be compared between individuals and used to characterize populations and drug products. Descriptive statistical models, characterized by mean residence times, percen-

tiles, or moments of residence time distributions are useful, but more specific models are still more attractive, if available.

The problem of suitable reference formulations has been addressed in the foregoing, and it seems to be a good point for closing the discussion. From a practical and regulatory point of view, it is convenient to use the marketed product of a prime manufacturer as a common reference for all comparable preparations. In the context considered here, reproducibility and robustness relative to physiological perturbations seem to be the most desirable properties, because the response to the reference is reflected in the convolution kernel. The consistency of performance has so far not been given due recognition as an important aspect of biopharmaceutical quality.

REFERENCES

1. Verrotta D. Deconvolution. Anaesth Pharmacol Rev 1994; 2:250.
2. Wagner JG, Nelson E. Kinetic analysis of blood levels and urinary excretion in the absorptive phase after single doses of drug. J Pharm Sci 1964; 53:1392.
3. Wagner JG. Application of the Loo–Riegelman absorption method. J Pharmacokinet Biopharm 1975; 3:257.
4. Loo JCK, Riegelman S. New method for calculating the intrinsic absorption rate of drugs. J Pharm Sci 1968; 57:918.
5. Gibaldi M, Perrier D. Pharmacokinetics, 2nd ed. New York: Dekker, 1982, p. 155.
6. Chiou WJ. New compartment- and model-independent method for rapid calculation of drug absorption rates. J Pharm Sci 1980; 69:57–62.
7. Stepanek E. Praktische Analyse linearer Systeme durch Faltungsoperationen. Leipzig: 1976.
8. Vaughan DP, Dennis MJ. Mathematical basis of point-area deconvolution method for determining in vivo input functions. J Pharm Sci 1978; 67:663–665.
9. Press WH, Teukolsky SA, Vetterling WT, Flannery BP. Numerical Recipes in C, 2nd ed. Cambridge: Cambridge University Press, 1992:538 ff.
10. Ameling W. Laplace–Transformation. Dusseldorf: Bertelsmann Universitäts Verlag 1975.
11. Doetsch G. Anleitung zum praktischen Gebrauch der Laplace–Transformation und der Z-Transformation, 5th ed. Munich: Oldenbourg 1985.
12. Benet LZ. General treatment of linear mammillary models with elimination from any compartment as used in pharmacokinetics. J Pharm Sci 1972; 61:536.
13. Wolf M. Modellentwicklung in der Pharmazie II. Verallgemeinerte theoretische Darstellung linearer Kompartimentmodelle beliebiger Struktur. Arzneimittelforschung 1977; 27:900–904.

14. Veng Pedersen P. General treatment of linear pharmacokinetics. J Pharm Sci 1978; 67:187–191.
15. Cutler DJ. Numerical deconvolution by least squares: use of prescribed input functions. J Pharmacokinet Biopharm 1978; 6:227–241.
16. Veng Pedersen P. A novel deconvolution method for linear pharmacokinetic systems with polyexponential impulse response. J Pharm Sci 1980; 69:312–318.
17. Dost FH. Grundlagen der Pharmakokinetik. 2nd ed. Stuttgart: Thieme 1968.
18. Cutler DJ. Numerical deconvolution by least squares: use of polynomials to represent the input function. J Pharmacokinet Biopharm 1978; 6:243–263.
19. de Boor C. A Practical Guide to Splines. New York: Springer 1978.
20. Verrotta D. Estimation and model selection using splines in constrained deconvolution. Ann Bioeng 1993; 21:605–620, quoted from (1).
21. Verrotta D. An inequality-constrained least-squares deconvolution method. J Pharmacokinet Biopharm 1989; 17:269–289.
22. Honerkamp J. Stochastic dyamical systems. New York: VCH 1994.
23. Charter MK, Gull SF. Maximum entropy and its application to the calculation of drug absorption rates. J Pharmacokinet Biopharm 1987; 15:645–655.
24. Charter MK, Gull SF. Maximum entropy and drug absorption. J Pharmacokinet Biopharm 1991; 19:497–520.
25. Süverkrüp R. Discontinuous input functions in linear pharmacokinetic models. J Pharm Sci 1979; 68:1395–1400.
26. Süverkrüp R, Bonnacker I, Raubach HJ. Numerical stability of pharmacokinetic deconvolution algorithms. J Pharm Sci 1989; 78:1395–1400.
27. Bagli M, Süverkrüp R, Rao ML, Bode H. Mean input times of three oral chlorprothixene formulations assessed by an enhanced least-squares deconvolution method. J Pharm Sci 1996; 86:434–439.

15
The Correlation of In Vitro and In Vivo Drug Dissolution

Dierk Brockmeier
Justus Liebig University, Giessen, Germany

I. INTRODUCTION

Because the oral route is the most convenient and popular way of applying a drug, oral formulations dominate drug therapy. Frequently, the systemic availability of orally administered formulations is determined during drug development. The pharmacokinetic fate of a drug in the body after intravenous administration may explain or even predict reduced systemic availability of some oral formulations.

However, the impaired systemic availability of many drugs following oral administration is not always fully understood. Not infrequently, impaired availability is attributed to poor permeability or incomplete dissolution. Because oral formulations play such a dominant role in drug therapy, qualitative explanations of this kind are unsatisfactory. Research should show and quantify the reasons for reduced availability. Special attention should be focused on extended-release (ER) formulations and drug substances with low solubility or slow dissolution rates. For these, it becomes a crucial factor whether the drug is absorbed along the intestinal tract at the same rate and extent or whether either the rate or the extent differs for the various segments of the intestinal tract. The period during which a formulation or drug substance resides in a particular segment of the gastrointestinal tract (GIT) will become a decisive factor for drugs with a limited rate of absorption or that are absorbed from only a particular segment of the GIT.

In an analogous manner, the rate of drug release from a solid oral dosage form, and particularly from extended-release formulations, may affect the extent of absorption, depending on the total time the formulation resides in the gastrointestinal segment with favorable absorption properties for the drug, or even the entire gastrointestinal residence time. In vitro studies, consideration of the physiology of the gastrointestinal tract, and experimental results led to the assumption that drug absorption takes place preferentially in the upper part of the gastrointestinal tract. In the concept of Biopharmaceutical Classification System (BCS) for intestinal absorption (1) this conservative assumption is considered in permeability and solubility evaluations, but is not an inherent feature. Hirtz has questioned the existence of absorption windows because of the ''absence of convincing experimental proof for its existence'' (2,3) and his own results with metoprolol (4).

Meanwhile, various tools and experimental procedures have been developed (5–11) to facilitate the experimental investigation of the absorption properties of particular segments of the gastrointestinal tract. The application of these techniques for various drugs have shown that the rate constant of absorption often varies along the GIT and that the differences may be moderate or pronounced, but a uniform rate constant of absorption, as in the case of metoprolol, seems to be the exception and not the rule.

In this chapter, a mathematically based approach is presented that creates a causal relation between in vitro and in vivo results for dissolution, either in terms of the statistical moments of dissolution and residence times, or in terms of a point-by-point comparison between the in vitro results of drug dissolution and the hypothetical in vivo dissolution profile obtained by deconvolution. The results of this approach can provide insight into the absorption properties of the intestinal tract (12,13).

II. IN VITRO–IN VIVO CORRELATION OF DRUG DISSOLUTION BY GLOBAL CHARACTERISTICS (LEVEL B CORRELATION)

The fate of drug molecules administered orally is determined by the sequence of the subsequent events of dissolution, absorption, distribution, and elimination. Consequently, the time an individual molecule spends in these sequential states is strictly additive:

$$t_{i\cdot\text{total}} = t_{i\cdot\text{diss}\cdot\text{vivo}} + t_{i\cdot\text{abs}} + t_{i\cdot\text{vss}} \tag{1}$$

where $t_{i\cdot\text{total}}$ represents the total time of an individual molecule between its administration until its elimination from the body; $t_{i\cdot\text{diss}\cdot\text{vivo}}$ is the time elapsed until the molecule is dissolved in the fluid of the gastrointestinal tract; and $t_{i\cdot\text{abs}}$ is the time between being dissolved and appearing in the central circulation; $t_{i\cdot\text{vss}}$ represents the time the molecule spends in the steady-state volume of distribution before being eliminated from the body, either by metabolism or excretion (14).

Summing all individual times as $t_{i\cdot\text{total}}$ and dividing this sum by the total number of molecules (N) gives the mean of all times according to the definition in descriptive statistics:

$$\begin{aligned}\frac{1}{N}\sum t_{i\cdot\text{total}} &= \frac{1}{N}\sum\left(t_{i\cdot\text{diss}\cdot\text{vivo}} + t_{i\cdot\text{abs}} + t_{i\cdot\text{vss}}\right)\\ &= \frac{1}{N}\sum t_{i\cdot\text{diss}\cdot\text{vivo}} + \frac{1}{N}\sum t_{i\cdot\text{abs}} + \frac{1}{N}\sum t_{i\cdot\text{vss}} \qquad (2)\\ \text{MT}_{\text{total}\cdot\text{vivo}} &= \text{MT}_{\text{diss}\cdot\text{vivo}} + \text{MT}_{\text{abs}} + \text{MT}_{\text{vss}}\end{aligned}$$

Thus the total mean time ($\text{MT}_{\text{total}\cdot\text{vivo}}$) is the sum of the mean dissolution time in vivo ($\text{MT}_{\text{diss}\cdot\text{vivo}}$), the mean absorption time (MT_{abs}), and the mean time in the steady-state volume of distribution (MT_{vss}) (15), the latter of which is frequently referred to as the mean residence time ($\text{MRT} = \text{MT}_{\text{vss}}$).

A basic assumption for in vitro–in vivo correlation (IVIVC) of drug dissolution is that the mean in vivo dissolution time is linearly related to the mean in vitro dissolution time:

$$\text{MT}_{\text{diss}\cdot\text{vivo}} = a + b\,\text{MT}_{\text{diss}\cdot\text{vitro}} \qquad (3)$$

where $\text{MT}_{\text{diss}\cdot\text{vivo}}$ and $\text{MT}_{\text{diss}\cdot\text{vitro}}$ are the mean in vivo and in vitro dissolution times respectively; a is a constant additive term that accounts for a time delay in vivo as compared with in vitro and the slope b is a transformation factor for the mean times. This slope, b, indicates whether the in vivo dissolution runs—in general—ahead or behind the in vitro dissolution. For example, if a is zero and b is 2, this indicates that the mean in vivo dissolution time is twice as large as the mean time when the dissolution is determined in an in vitro dissolution apparatus. In other words, the release under in vitro and in vivo conditions do not run at the same speed, and a rescaling of the time is necessary. Only when the slope parameter is 1 are the mean in vitro and in vivo dissolution times the same. Reasons for assuming that the relation is linear will be given in the following.

If we rearrange Eq. (2) using the assumption stated in Eq. (3) it yields the following relation:

$$\begin{aligned} MT_{total\cdot vivo} &= a + b\ MT_{diss\cdot vitro} + MT_{abs} + MT_{vss} \\ MT_{total\cdot vivo} &= a + b\ MT_{diss\cdot vitro} + MT_{body} \end{aligned} \tag{4}$$

where $MT_{total\cdot vivo}$ and $MT_{diss\cdot vitro}$ have the same meaning as previously and MT_{body} is the mean of all times a molecule remains in the body after being dissolved (i.e., the sum of MT_{abs} and MT_{vss}).

When several different formulations are considered, Eq. (4) states that a linear relation between the total mean times observed in the in vivo experiments ($MT_{total\cdot vivo}$) and the mean in vitro dissolution times ($MT_{diss\cdot vitro}$) for the respective formulations will be observed (16,17).

Clearly, to validate such a linear relation, at least three formulations that differ clearly in their mean in vitro dissolution times have to be tested in vitro and in vivo. If the mean dissolution times for the formulations considered differ only slightly, the set of formulations is not suitable to scrutinize the correlation (4). Furthermore, it is assumed that the mean time in the body system (MT_{body}) (i.e., the mean of times after the molecules have been dissolved) is independent of the formulation. In other words, it is assumed that MT_{body} is a constant across all formulations tested. By using this assumption, Eq. (4) can be simplified:

$$MT_{total\cdot vivo} = A + b\ MT_{diss\cdot vitro} \tag{5}$$

where A is the sum of MT_{body} and a possible lag time a for dissolution under in vivo conditions.

For different carbochromene formulations a linear relation between $MT_{total\cdot vivo}$ and $MT_{diss\cdot vitro}$ exists (17,18). Figure 1 shows the data for this relation. Because the time delay a was practically zero for these formulations, the intercept represents the mean time in the body system (MT_{body}).

Such a linear relation has also been demonstrated for other drugs and formulations (19–25), indicating that the aforementioned assumptions are, at least in some cases, reasonable.

This methodology (i.e., the correlation of the mean in vitro dissolution time and the total mean time in the in vivo system) has been termed the global approach to IVIVC of drug dissolution (26).

Two further techniques that do not differ in their principal ideas from that just outlined, but do in the way they are carried out have been used. The first is the use of deconvolution techniques to estimate the hypothetical in vivo dissolution profiles; from these profiles the mean in vivo dissolution times

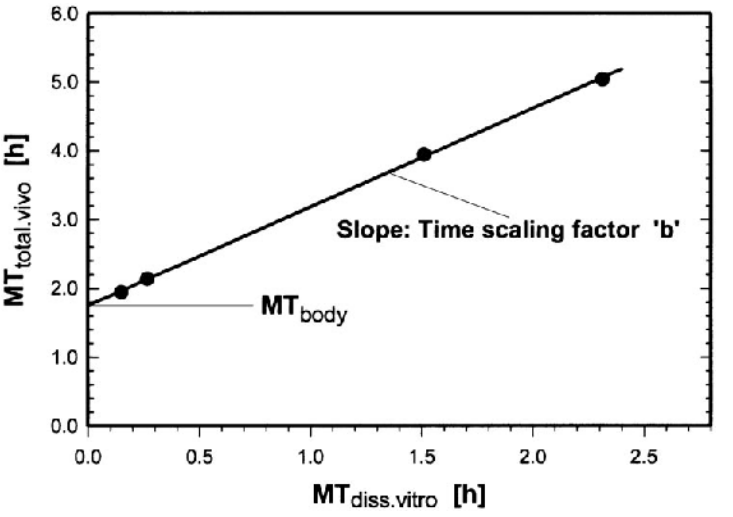

FIG. 1 In vitro–in vivo correlation of global dissolution time characteristics: The total mean time ($MT_{total.vivo}$) of four different formulations of carbochromene-HCl studied in healthy volunteers is plotted against the respective mean in vitro dissolution time ($MT_{diss.vitro}$) of these formulations. The solid line is the result of linear regression. (From Ref. 17.)

are computed and thereby correlated with the corresponding mean in vitro dissolution times (20).

The second uses the additivity of mean times and calculates the mean in vivo dissolution times as the difference between the total mean time in the system after administration of the extended-release formulation and the total mean time after administration of the reference formulation. For these purposes the reference formulation is in general an oral solution, but might also be a fast-dissolving solid formulation or an intravenous application. The use of either of the latter two reference formulations, however, requires thorough justification. After computation of the mean in vivo dissolution time as a difference, these values are correlated with the mean in vitro dissolution times as described earlier (21).

In any case when correlation of global dissolution time characteristics is attempted, it is necessary to test at least three formulations in vitro and in vivo. When alternative techniques are used, this requires the in vivo study of a further fourth formulation, in general a solution. It is inherently assumed that the transformation parameters *a* and *b* are the same for all four different

formulations—at least relative to the global dissolution time characteristics. Only under these conditions will the approach result in a linear relation.

III. CONTINUOUS IN VITRO–IN VIVO CORRELATION OF DRUG DISSOLUTION (POINT-BY-POINT CORRELATION)

With IVIVC of global dissolution time characteristics we are faced with a situation in which each of several different formulations must be tested, not only in an in vitro dissolution system, but also—and even more importantly in terms of effort and expense—in humans. A correlation according to Eq. (5) should be carried out with a minimum of three different formulations. This means that even if only one formulation is finally selected for development as a therapeutic system, several different formulations with clearly different mean dissolution times have to be developed and tested in humans to demonstrate a (not always satisfactory) mathematical correlation. Occasionally, it may be difficult to justify the time and effort required. Therefore, it would be desirable to develop a method in which a single formulation is tested in vitro and in vivo and which is able to quantify the degree to which the in vitro dissolution results reflect the in vivo dissolution process. Continuous IVIVC (CIVIVIC) opens one possibility.

The theoretical basis for CIVIVIC is exactly the same as for the correlation of global dissolution time characteristics. Proceeding from Eq. (3) it follows:

$$\begin{aligned} \frac{1}{N}\sum t_{i\cdot\text{diss}\cdot\text{vivo}} &= a + b\,\frac{1}{N}\sum t_{i\cdot\text{diss}\cdot\text{vitro}} \\ &= \frac{1}{N}\sum a + \frac{1}{N}\sum (b\; t_{i\cdot\text{diss}\cdot\text{vitro}}) \\ &= \frac{1}{N}\sum [a + b\; t_{i\cdot\text{dis}\ni\text{vitro}}] \\ t_{i\cdot\text{diss}\cdot\text{vivo}} &= a + b\; t_{i\cdot\text{diss}\cdot\text{vitro}} \end{aligned} \tag{6}$$

Equation (6) states that the in vitro dissolution profile might run ahead or behind the in vivo (i.e., they might not be superimposable per se). Cumulative dissolution curves are samples of the statistical distribution function of the random variable $Z_{i\cdot\text{diss}}$, where the random variable $Z_{i\cdot\text{diss}}$ can be interpreted as

the residence time of drug molecules in the pharmaceutical formulation under in vitro and in vivo dissolution conditions, respectively (27).

$$Z_{i\cdot\text{diss}\cdot\text{vivo}} = a + b\, Z_{i\cdot\text{diss}\cdot\text{vitro}} \tag{7}$$

a and b have the same meaning as in Eq. (3), the only difference is that in Eq. (3), it is sufficient that the relation is valid for the global dissolution time characteristics of several formulations whereas in Eq. (7) it is stated that this relation is valid for a complete single dissolution profile in a point-by-point manner. Equation (7) also instructs how this point-by-point comparison has to be carried out; this will be described in the next section.

The proof that cumulative dissolution curves are samples of the statistical distribution function of residence times of molecules in the formulation has been given in detail elsewhere (14,27). It is this property of dissolution curves (i.e., that they are samples of a statistical distribution function) that dictates the method by which they are compared.

IV. RESULTS FOR THEOPHYLLINE

A rescaling of the time axis when progressing from in vitro to in vivo is often necessary, as clearly shown by the following example. Figure 2 shows the in vitro release of theophylline from Solosin Retard under five different dissolution conditions that clearly differ in the duration of release: 90% release is achieved after about 4 h with the leftmost test (*USP* Paddle 500 mL water, 200 rpm, 37°C), whereas under an alternative condition, the release of 90% is not achieved until about 10 h for the rightmost curve (*USP* Paddle 500 mL water, 100 rpm, 37°C). There is no unique dissolution profile and only one—if any—could be identical with the in vivo dissolution profile. It should be kept in mind that if there is no unique in vitro dissolution profile, then it is even less likely that there is one, single in vivo release profile.

Clearly, dissolution profiles are the product of a chance, the chance that a molecule is released from the formulation before a certain time. This chance is affected by the prevailing dissolution conditions.

The proof that none of the dissolution profiles depicted in Fig. 2 is identical with the in vivo dissolution profile can be shown by convolution. The in vivo concentration–time profile based on any of the in vitro dissolution profiles can be predicted by convolution and, thereafter, this prediction can be compared with the real observations. For this prediction one needs the characteristic impulse response or transfer function of the body; this impulse response was taken from the concentration–time profile observed for healthy

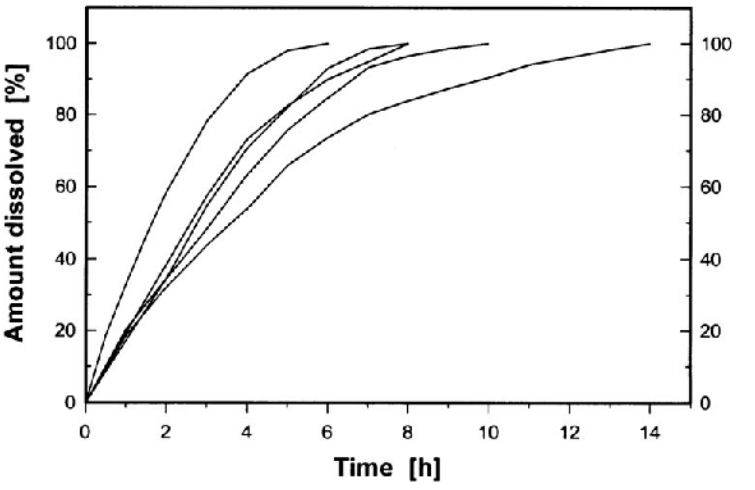

FIG. 2 In vitro dissolution profiles for an extended-release formulation of theophylline: The solid lines show the results of dissolution of the same formulation under different in vitro dissolution conditions. From left to right: A, *USP* Paddle 500 mL water, 200 rpm, 37°C; B, Sartorius, 100 mL water with beats, 1.2 rpm, 37°C; C, Sartorius, 100 mL water, 1.2 rpm, 37°C; D, Sartorius, 170 mL water, 1.2 rpm, 37°C; E, *USP* Paddle 500 mL water, 100 rpm, 37°C. (From Ref. 13.)

volunteers after oral administration of a solution and after normalizing for the dose. Convolution gave the results depicted in Fig. 3.

None of the predictions fit the observations—not even broadly. Therefore none of the in vitro dissolution profiles is identical with the true in vivo dissolution characteristics. All in vitro dissolution profiles appear to run ahead of the in vivo after the first few hours. The gastrointestinal tract simply does not ''paddle'' in the same way or at the same rate as the in vitro dissolution apparatus. As a logical consequence, Levy et al. (28) suggested calibrating the in vitro dissolution test procedure using the results of an in vivo study. However, this procedure is time-consuming, and it is not clear if the calibration, once carried out, would also be valid for other formulations, or if the study were to be repeated in a new test group. The calibration problem may be overcome by the mathematical considerations considered next.

The comparison of predicted concentration–time profiles and the actually observed concentrations in volunteers shown in Fig. 3 is one type of continuous in vitro–in vivo correlation. One might now compare the values of prediction and observation for the same times as proposed by the guidance

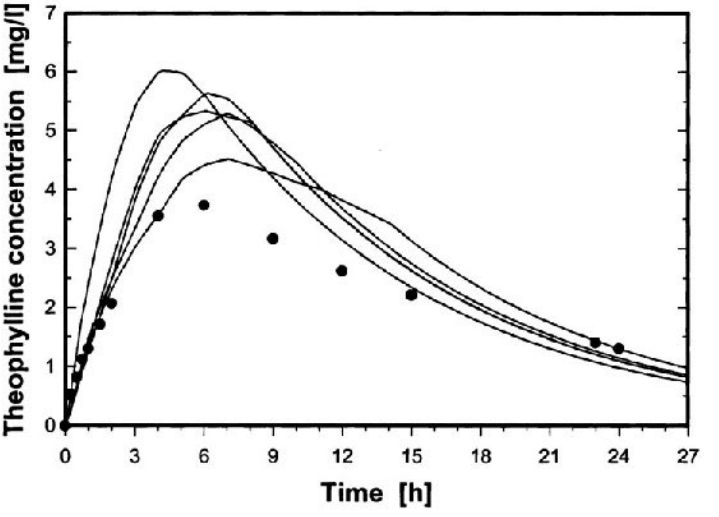

FIG. 3 Predicted concentration–time profiles of theophylline: The filled circles represent mean values of concentration–time data when the extended-release formulation of theophylline was administered to volunteers. The solid lines show the results of prediction by convolution based on the assumption that the in vivo drug release from the formulation would be the same as determined in the various in vitro tests and that the impulse response function is valid for the time period of prediction. None of the predictions fit the observations. (From Ref. 13.)

(29); although not shown, it can be anticipated that such a correlation for the data in Fig. 3 will not result in a linear relation between observed and predicted values. There is, however, an alternative approach to CIVIVIC that allows a more critical analysis of this correlation and that might provide a better insight into the relation between in vitro and in vivo dissolution.

The basic equation for CIVIVIC [Eq. (7) and also, implicitly, Eq. (3)] states that two dissolution profiles may be made superimposable by a uniform linear transformation of the time axis, but that this is only possible if the times at which the same amounts have been dissolved are linearly related to one another. There are two ways to obtain the parameters a and b for the uniform linear transformation of the times:

1. The parameters for the time transformation can be calculated using the statistical moments of the dissolution times (15,30). However, because this method can be subject to pronounced error, it will not be described in further detail here.

2. A much better method is described by Fig. 4, which uses three of the in vitro dissolution profiles already shown to illustrate the computational steps. To keep the figure clear, only three of the five in vitro dissolution profiles for the extended-release formulation of theophylline (i.e., the fastest, the middle one, and the slowest of those shown) have been selected.

The times at which the same amounts have been dissolved are determined either graphically or numerically; interpolation of one of the two profiles may be necessary to arrive at the necessary values.

One starts with a measurement at time $t_{i\cdot A}$ under condition A, and searches for the same amount dissolved under condition B, which gives the time $t_{i\cdot B}$. The pairs of times determined in this way are plotted against one

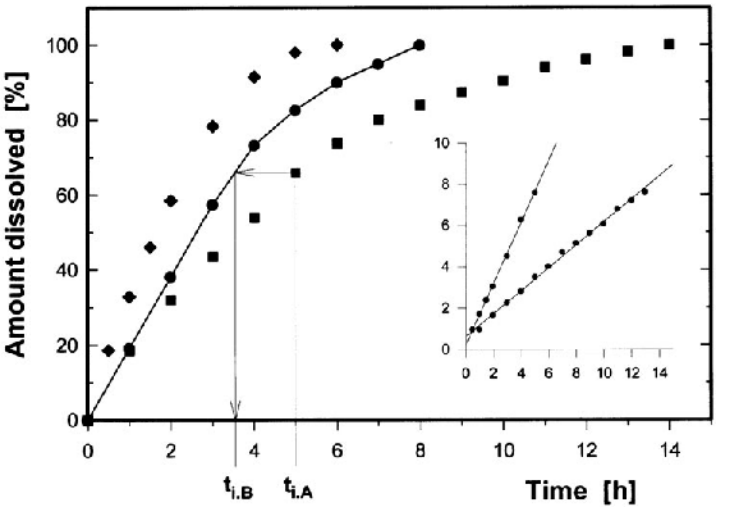

FIG. 4 Comparison of times corresponding to identical amounts dissolved: Three dissolution profiles from Fig. 2 have been selected to illustrate the method of continuous in vitro–in vivo correlation (CIVIVIC). For a given amount dissolved under condition A, the time $t_{i\cdot A}$ is noted and the time $t_{i\cdot B}$ is determined at which the identical amount is dissolved under condition B. The time $t_{i\cdot B}$ is determined by interpolation for the case illustrated. The data pairs for times $t_{i\cdot A}$ and $t_{i\cdot B}$ that correspond to the same amount dissolved are shown in the inset (Levy plot) for both comparisons. They are almost perfectly and linearly related to one another indicating homomorphism of all three dissolution profiles.

another. If there is a linear relation, then the dissolution profiles compared are superimposable and the parameters for the transformation of times a and b can be read from the regression. The time pairs that belong to the same amount dissolved are shown for both comparisons in the inset of Fig. 4. They are almost perfectly and linearly related to one another. This type of graphic analysis has been titled by the author as the Levy plot (13,31).

The time values for each dissolution data pair related to the fast-paddle dissolution profile (see leftmost in Fig. 4) have been transformed by the same, uniform, linear equation as read from the regression in the inset and replotted as open diamonds in Fig. 5. The same procedure was followed for the rightmost (slow) paddle dissolution profile—the filled (original data) and open (transformed data) squares: the transformed curves are both superimposable with the middle curve (filled circles) that was obtained with the Sartorius apparatus.

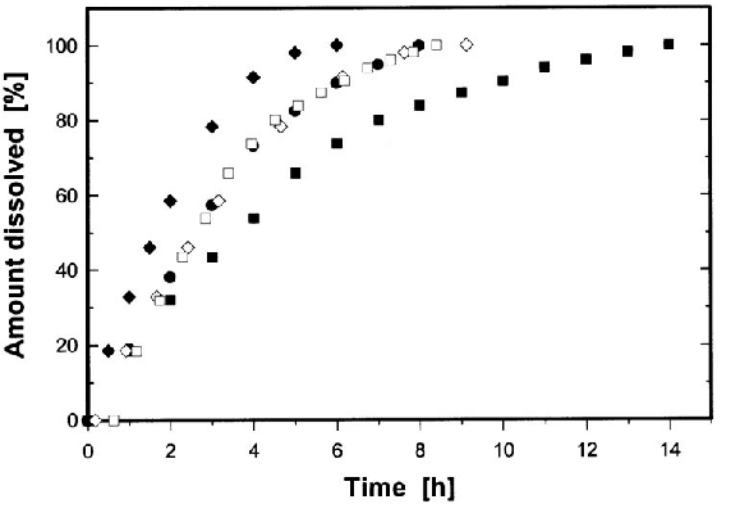

FIG. 5 Rescaling of the time axis: Three dissolution profiles from Fig. 2 have been selected to illustrate the consequences of CIVIVIC. The time axes for the leftmost and rightmost dissolution curves have been rescaled. The parameters for the transformations according to Eq. (6) have been read from the regression depicted in the inset of Fig. 4. After transformation the data originating from the USP Paddle dissolution test (open symbols) become both almost perfectly superimposable with the middle curve, which originates from the Sartorius apparatus.

This means first, that it is the pharmaceutical formulation that defines the type of the dissolution profile and not the conditions and, second, that the information gained from these three dissolution curves is identical. The only difference is that this information is obtained within about 6 h, 8 h, or within about 14 h.

In early publications (31) this feature was unfortunately denoted as being equivalent, because an equivalent information can be gained from these dissolution curves; the term ''homomorphic'' would be more accurate. If the profiles are homomorphic, the statistical distribution function of dissolution times is of the same type, irrespective of whether the distribution function can be described by a single model (equation) or not. The only difference lies in the scaling of the time axis.

The linearity of time transformation is important: Only if it is present do the distribution functions remain of the same type. For example, a dissolution curve, according to the cube-root law, remains a dissolution curve according to the cube-root law, even after transformation of the time axis. The same applies to other types of profiles; if, for example, the residence times of molecules in the pharmaceutical formulation follow a log-normal Gaussian distribution, the distribution will be Gaussian after transformation. The profile might be stretched or compressed under the various dissolution conditions, but the type is the same.

This comparison in the horizontal direction follows directly from the fact that two different statistical distribution functions for the random variable, *dissolution time* ($Z_{i\cdot\mathrm{diss}}$), have to be compared. The oft practiced comparison of amounts dissolved at the same time—the vertical direction—has no statistical justification and will result in a straight line only if the dissolution profiles are superimposable per se.

When all the in vitro dissolution profiles for the extended-release formulation of theophylline were compared, it followed that they were all superimposable (results not shown; see Ref. 13). Although the correlation of in vitro and in vivo dissolution profiles is the aim, the digression to the correlation of in vitro dissolution profiles with another is necessary to show that IVIVC should really be attempted only if in vitro testing has demonstrated that homomorphic dissolution profiles are obtained under varying dissolution conditions.

The comparison with the in vivo dissolution profile is enormously complicated because—unlike in vitro dissolution—it is impossible to measure directly; indirect methods of determination, for example, deconvolution must be employed. Deconvolution requires linear and time-invariant pharmacokinetics and, for the study protocol, a sufficient sampling of the concentration–time profile during the phase of in vivo dissolution and absorption. Even when this

is fulfilled, the overall result of deconvolution is highly sensitive to the accuracy of the early readings, because they influence the calculation of the subsequent hypothetical dissolution values.

It cannot be assumed that the in vitro and the hypothetical in vivo dissolution profiles will be superimposable, because a variety of in vitro dissolution curves can be generated, as in the theophylline example. There is no possibility of deciding in advance which of the in vitro profiles might be valid for the in vivo situation.

Equation (6) proceeds from the less restrictive assumption that, although the in vitro and in vivo dissolution profiles might not be superimposable per se, they are homomorphic (30,31). This concept of homomorphism is the essential step in the CIVIVIC: It means that the in vitro and in vivo dissolution profiles do not differ in their general shape (morphology). They might be stretched or shortened relative to each other, but they can be superimposed by linear rescaling of the time axis. Homomorphism in vitro–in vivo can be interpreted as indicating that the physicochemical principles of drug release from the formulation are the same for both the in vitro and the in vivo conditions.

To estimate the in vivo dissolution profile, the dose-normalized response following the administration of an oral solution or a fast-dissolving tablet is used as a weighting function $w(t)$. The observed concentrations are considered as response $r(t_i) = C(t_i)$, and the hypothetical input of drug ΔD_k can be calculated using the following general deconvolution formula (30):

$$\Delta D_k = \frac{C_{\text{obs}}(t_{k+1}) - C_{\text{predict}}(t_{k+1})}{w(t_{k+1} - t_{\text{k}})} \tag{8}$$

where $C_{\text{obs}}(t_{k+1})$ represents the $(k + 1)$th measured concentration when the extended release formulation is administered, and $C_{\text{predict}}(t_{k+1})$ is the predicted concentration after k individual doses ΔD_i considered as already accounted for as inputs into the system up to time t_k. The denominator, $w(t_{k+1} - t_k)$, represents the value of the dose-normalized weighting function at time $(t_{k+1} - t_k)$ and can be any sum of exponential functions.

If $w(t)$ is composed of a sum of pure exponentials [i.e., $w(t) = {}_j\sum h_j e^{-\lambda_j t}$] the input ΔD_k is interpreted as a bolus input. If $w(t)$ consists of a sum of infusion functions (i.e., $w(t) = {}_j\sum h_j/[(t_{k+1} - t_k)\lambda_j](1 - e^{-\lambda_j t})$, then ΔD_k is considered to be a dose that is administered by a constant input during the period t_k to t_{k+1}. The value of $C_{\text{predict}}(t_{k+1})$ is then calculated according to the appropriate interpretation of administration of the drug.

By analogy to the in vitro dissolution profiles, the hypothetical in vivo dissolution profile is obtained in cumulative terms by summing the individual doses:

$$M_k = M(t_k) = {}_{i=1}\sum^{i=k} \Delta D_i \tag{9}$$

The deconvolution formula [Eq. (8)] has been applied to the data for theophylline using the dose-normalized concentration–time profile observed after oral administration of a theophylline solution as the impulse response. The hypothetical in vivo dissolution profile is shown as a cumulative plot in Fig. 6. In addition, the graph shows one of the in vitro dissolution profiles for the theophylline formulation considered. A single curve is sufficient because all the in vitro profiles are homomorphic. It is immediately obvious that the in vitro dissolution profile is ahead of the hypothetical in vivo dissolution curve, except for the first hour.

The test for homomorphism was applied by graphing the time to dissolve and absorb certain amounts under in vivo conditions versus the corresponding

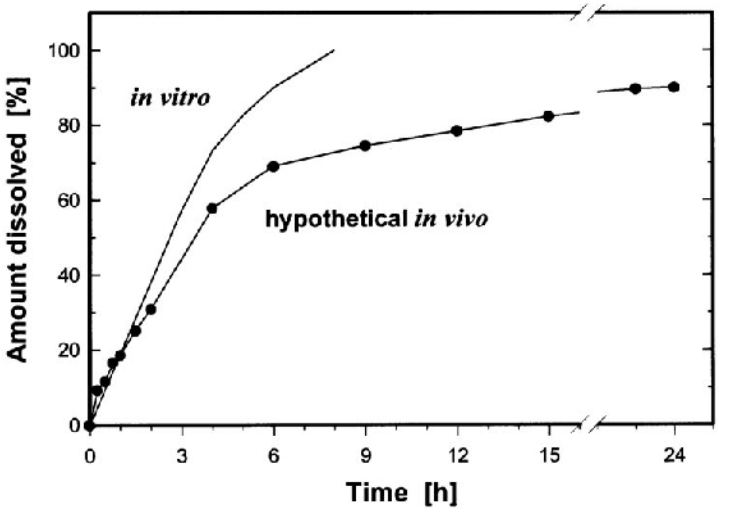

FIG. 6 In vitro and hypothetical (deconvoluted) in vivo dissolution profiles for theophylline: The graph shows one of the homomorphic in vitro dissolution profiles for the extended-release formulation of theophylline and, in addition, the hypothetical in vivo dissolution profile estimated by deconvolution. The in vitro dissolution profile is ahead of the hypothetical in vivo dissolution curve except for the first hour. (From Ref. 30.)

times needed to dissolve the same amount under in vitro conditions using the Levy plot. Times related to identical amounts dissolved might be taken directly from a graph, as in Fig. 6, or determined numerically (31). The correlation of times at which the same amounts were dissolved is shown in Fig. 7 where the *x*-axis gives those times related to the in vitro dissolution, and the *y*-axis is related to the hypothetical in vivo dissolution. The results for mean values are shown.

Comparison of the times related to the same amount dissolved does not show a simple linear relation, rather, it is biphasic. Both phases are, however, linear. Thus, the in vitro and the hypothetical in vivo dissolution profiles are not homomorphic over the entire dissolution profile. Similar results were found for all other subjects in the study and also in other studies with different theophylline formulations (12), and Krämer reports further findings for theophylline in this volume (see Chapter 16).

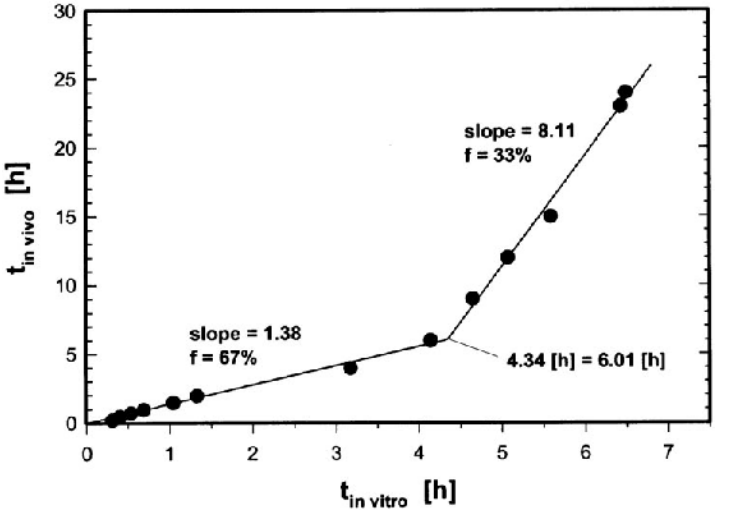

FIG. 7 Continuous in vitro–in vivo correlation (CIVIVIC) for theophylline: The times required for certain amounts to be dissolved and absorbed from the extended-release formulation of theophylline administered to healthy volunteers are plotted against the corresponding times needed to dissolve the identical amounts under in vitro conditions (Levy plot). Values for the mean profiles are shown. The same pattern of a biphasic Levy plot was determined for each individual in the study. (From Ref. 30.)

A biphasic in vitro–in vivo correlation of this type may have many causes. The possible interpretations for a biphasic relation of this sort have been discussed in detail for theophylline (30). It was concluded that, for theophylline, the most likely interpretation for a biphasic Levy plot is that the rate constant of absorption changes as the drug moves down the gastrointestinal tract. Furthermore, because the time of transition from the first linear section to the second occurs after about 5 h, it is highly likely that this change occurs when the formulation enters the colon. This purely heuristic conclusion was later confirmed by another group of scientists using an alternative experimental approach with the HF capsule (5). It must be emphasized that the preceding conclusions require a thorough consideration of all physicochemical and pharmacokinetic properties of the drug and the formulation, accompanied by extensive in vitro testing of the formulation considered. It might not be sufficient to test the formulation under only one condition: homomorphism should be challenged using several apparatuses and modes.

The lower linear portion in Fig. 7 indicates that the in vitro and in vivo release profile is superimposable, but only up to a certain time. After this, a different time transformation would have to be used to make the profiles superimposable. However, CIVIVIC indicates more than the likelihood of a change in the rate constant of absorption as the formulation passes through the gastrointestinal tract. It shows that an average of 64% of the drug is absorbed from the small intestine—with a range of 32–84%—while 25% was absorbed from the colon (range 14–47%). It seems that the greater the fraction of the dose remaining on passage into the colon, the more was absorbed from the colon. In other words: the colon offers an adequate surface and sufficient residence time for absorption, even when the formulation passes very quickly into it. The bioavailability of this formulation was almost always close to 100%.

The biphasic course (the kink) in Fig. 7 is the result of an inappropriate use of deconvolution; inappropriate, because the impulse response is assumed to be invariant. Over a period of 24 h (see Fig. 6), the formulation passes from the stomach through the duodenum, jejunum, and ileum, into the colon, where it, presumably, spends the most time. Along its way, it comes into contact with different pH, different degrees of agitation, different volumes, different enzymes, and different solubilizers. The importance of all of these different influences can, at least partially, be established in vitro. A further key point is that the absorption characteristics are not the same at the different sites in the gastrointestinal tract. If the drug were to be injected as a solution into the lumen at these different sites and could be held in place, one would likely obtain different concentration–time profiles in plasma. These individual con-

centration–time profiles would then represent the true impulse response or transfer function of the system for the respective regions in the GI tract.

Deconvolution is based on a principle of systems theory; namely, that one can determine an unknown input signal to the system if the response to this input and the impulse response are known: the latter information is obtained by analyzing the response of the system to a known input. In pharmacokinetics this response is frequently deduced from the observations after oral administration of a solution; for this application it is assumed for most drugs that absorption takes place in the upper part of the intestine. Special considerations are, however, necessary for drugs that are poorly soluble or absorbed slowly. In the context of extended-release formulations and deconvolution an important assumption is made for the impulse response: that it does not vary with time and that it is independent of the extent of the input function.

The impulse response of the system is, however, dependent on local absorption conditions in the gastrointestinal tract. Because the extended-release formulation requires a certain time to reach these sites, the impulse response is time-dependent because the absorption rate is region-dependent. The assumption that absorption in the upper intestine is representative of absorption throughout the intestinal tract is unlikely to be true for many drugs. However, the break in the Levy plot that results from an ''inappropriate'' use of deconvolution can be used to advantage in investigating whether the drug or dosage form behaves at different locations in the GI tract.

V. RESULTS FOR PIRETANIDE

For theophylline, it was concluded from the biphasic Levy plot that the rate constant of absorption changes along the intestinal tract and that this most likely occurs between the small intestine and the colon or within the colon; this was later confirmed by direct measurements.

The best way to test this interpretation of the Levy plot is to apply the method to a drug for which a change in the rate constant of absorption has already been shown and for which an extended-release formulation has been studied both in vitro and in vivo. Piretanide, a loop diuretic, fulfills all these criteria.

Figure 8 shows the concentration–time profile following endoscopic instillation of 3 mg piretanide solution into the stomach, the duodenum, and the ascending colon (32). The absorption of piretanide was delayed after administration into the stomach. After duodenal instillation, the concentration–time course resembles that after intravenous administration, indicating an extremely

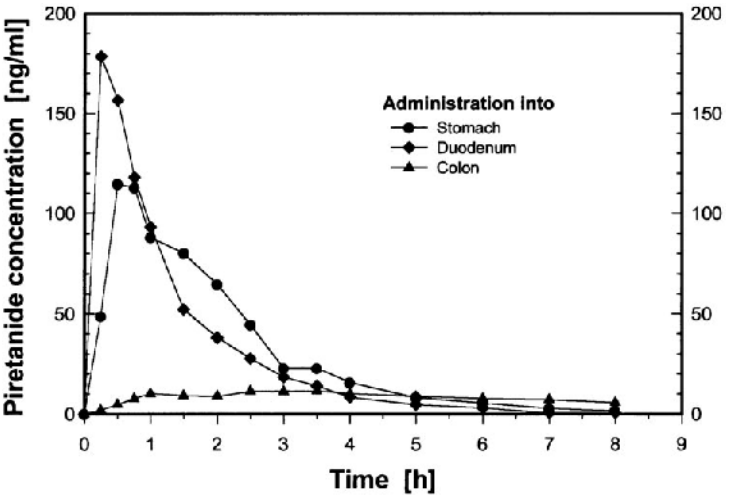

FIG. 8 Concentration–time profiles after instillation of piretanide into different segments of the gastrointestinal tract: The instillation of piretanide was performed through an endoscope under visual control. Although the absorption after gastric placement of the dose was delayed compared with duodenal administration, practically the same amount was absorbed. However, when piretanide was instilled into the ascending colon, a clearly smaller fraction of the dose was absorbed at a striking smaller rate. (From Ref. 32.)

rapid absorption of the instilled dose from the duodenum. A remarkably low concentration–time profile after instillation into the colon was observed, demonstrating a very low absorption rate for this site. In some subjects, the concentration never or only sporadically exceeded the limit of detection. In others, the concentration–time curves resembled very much those seen after constant infusion (i.e., zero-order input).

According to these absorption profiles of the intestinal tract (32,33), CIVIVIC should be able to show changes in the rate constant of absorption very clearly by a biphasic Levy plot. This is indeed so.

A study was conducted to compare concentration profiles after administration of an oral extended-release formulation of piretanide, a conventional tablet, and an intravenous administration in a randomized crossover design (12). The dose for all routes was 6 mg. Deconvolution for the extended-release formulation was carried out using the dose-normalized profile for intravenous administration as the impulse response. This is not a serious drawback; it only

implies that the result of deconvolution cannot be considered as the pure in vivo dissolution profile, but encompasses the absorption as well. Because the concentration–time response after intraduodenal instillation is almost the same as after intravenous administration, the use of the response after such administration in deconvolution equates, in this example, to the impulse response after intraduodenal administration.

The deconvoluted in vivo dissolution profile differed clearly from that determined in the in vitro test. Application of CIVIVIC resulted in the biphasic Levy plot depicted in Fig. 9. The graph shows the two subjects with the largest and smallest ratio between the slopes for the first and second segment of the biphasic linear regression. The same pattern was observed in 26 of 27 subjects enrolled in the study. In one individual, no biphasic correlation was found because nothing was absorbed in the second phase.

In general, the Levy plots differed both in the slopes for the two linear segments and the time of transition from the first to the second segment. This

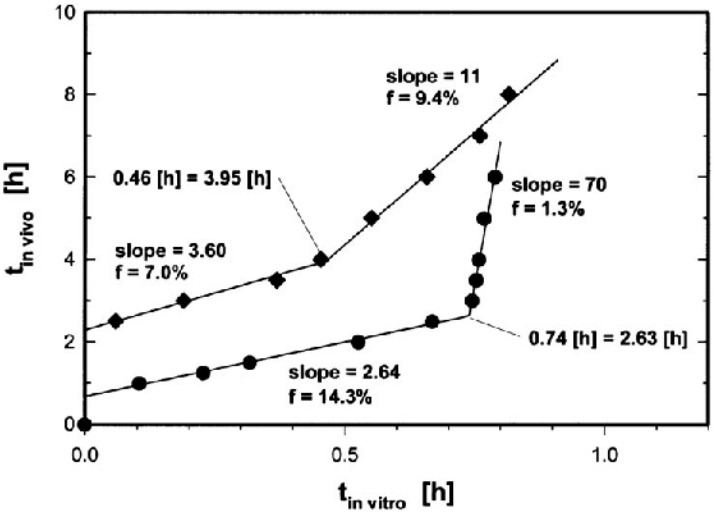

FIG. 9 Continuous in vitro–in vivo correlation for piretanide: The times required for certain amounts to be dissolved and absorbed from the extended-release formulation of piretanide is plotted against the corresponding times needed to dissolve the identical amounts under in vitro conditions (Levy plot). The graph shows the two subjects with the largest and smallest ratio between the slopes for the first and second segment of the biphasic linear regression. The same pattern was observed in 26 of 27 subjects. (From Ref. 13.)

time of transition varied from 2.1 to 5 h, with a mean of 3.6 h (12). During the first phase 18.6% (7–37%) of the administered dose was absorbed, whereas only 4.4% (1.2–9.4%) was absorbed during the second phase. It is noteworthy that the ratio of the slopes for the two phases of the Levy plot was, for most subjects, much greater than those determined for theophylline.

CIVIVIC indicates that piretanide is absorbed mainly in the upper small intestine and only to a very small extent in the distal small intestine and the colon. The fraction of the dose that leaves the well-absorbing segment of the upper small intestine is effectively lost for systemic availability. The systemic availability, therefore, is predominantly determined by the time the formulation resides in the part of the gastrointestinal tract that has good permeability for piretanide.

Figure 10 confirms this conclusion; it shows the relation between the time the piretanide formulation resided in the well-absorbing window and the systemic availability. The intercept of the regression line indicates that, on

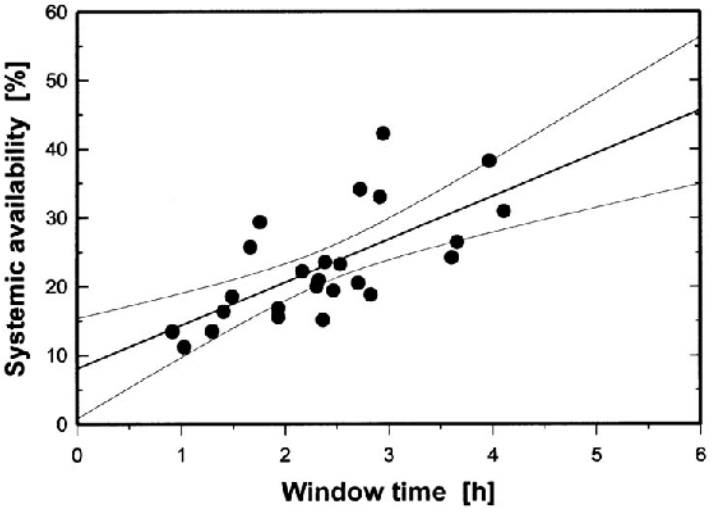

FIG. 10 Bioavailability of piretanide from the extended-release formulation: The bioavailability from the extended-release formulation depends on the time the formulation resides in the segment of the intestinal tract where piretanide is well absorbed. The fraction of the dose that leaves the permeable segment of the upper small intestine is effectively lost for systemic availability. The time the formulation resided in the permeable window can be read from the CIVIVIC. The longer the formulation resides in the segment where it is well absorbed, the higher is the bioavailability. (From Ref. 13).

average, only 8% of the drug is absorbed outside this section. The longer the formulation resided in the section of the gastrointestinal tract in which it was well absorbed, the higher was the bioavailability. The time the formulation resided in the window can be read from the CIVIVIC. This formulation was not further developed.

Based on the data compiled for gastrointestinal transit times, it can be deduced that for piretanide the permeable region ends already in the distal part of the small intestine. CIVIVIC is suitable for revealing the length of such absorption windows in terms of time available for absorption.

VI. DISCUSSION AND CONCLUSION

The theoretical and methodological basis for continuous in vitro–in vivo correlation of drug dissolution (CIVIVIC) has been described by elaborating the concept of global IVIVC using the mean in vitro dissolution and mean time in the body system. The method compares times at which identical amounts have been dissolved under in vitro and in vivo conditions. This comparison of dissolution curves differs from that in the guidance (29) in which amounts dissolved after a given time are compared.

The method of CIVIVIC has been illustrated by the results of a study with an extended-release theophylline formulation. The analysis resulted in a biphasic Levy plot. It was interpreted that this is caused by a change in the absorption rate constant for theophylline with the site of the intestinal tract. This interpretation has been confirmed by Staib and co-workers (5) who demonstrated that the rate constant of absorption was smaller in the distal segments of the intestinal tract (particularly in the colon) than in the proximal part of the small intestine.

Qualitatively similar results were recorded in other studies with different theophylline formulations (12,13; see also Chapter 16). The slopes for the two segments of the Levy plot were different from those reported in the foregoing, even when the same in vitro dissolution apparatus was used for comparison. However, on average, the time for transition from the first linear segment to the second was very similar for all these studies.

For drugs such as piretanide, for which an extensive change in the rate constant of absorption (permeability) has been revealed experimentally (32,33), it can be anticipated that CIVIVIC will most likely not result in a single linear correlation, but with an at least biphasic Levy plot; this has been exactly demonstrated for piretanide. Moreover, CIVIVIC revealed that the time the formulation resides in the well-absorbing part of the gastrointestinal tract predominantly determined the systemic availability of piretanide from

the formulation studied. CIVIVIC can therefore be used to determine the ''length'' of the absorption window in terms of time. This time is decisive for further formulation development, because any drug released after this time is effectively lost for systemic availability; window residence time in relation to release/dissolution becomes the crucial factor for bioavailability for any formulation developed. Equally as helpful, CIVIVIC provides an estimate of how this in vivo absorption window residence time can be transformed into the in vitro experimental time.

CIVIVIC can only be predictive—as with any IVIVC—when the release properties of an extended release formulation determined in vitro are reflected in the release profiles determined in vivo. The in vivo relevance of the in vitro dissolution properties of an extended-release formulation can be assessed by a series of in vitro studies. Such experiments can partly challenge the hypothesis that the release profile will be reflected in the concentration–time profile, without having to perform a study in humans. An important requirement for in vivo relevance of an in vitro dissolution profile is that the profile of in vitro dissolution is broadly independent of environmental conditions, such as pH, physical agitation, enzymes, solubilizer, etc., used in the in vitro experimental series.

Clearly, if different environmental conditions in vitro result in nonhomomorphic dissolution profiles, one does not know which of the different profiles should be considered as the input to the body system. If the morphology of the dissolution profile is highly sensitive to environmental conditions, this will be reflected by high intraindividual and interindividual variability of the in vivo release profile and thus homomorphism of in vitro and in vivo dissolution profiles cannot be expected.

On the other hand, if variation of the test conditions results in homomorphic in vitro dissolution profiles, any representative of this class can be used to link in vitro and in vivo dissolution. In the ideal case, the profile is independent of environmental factors. In such a case, one could assume, with confidence, that the dissolution profile in vivo will be the same as in the in vitro experiments.

The latter independence has been partly demonstrated for formulations based on the osmotic pump as an oral delivery system; the osmotic pump is considered to be a system that usually releases the drug independently of the environmental dissolution conditions. Results for such an osmotic pump, the oral delivery system GITS with nifedipine, have been presented by Bode (34). He applied the methods as described in this paper and revealed that the in vitro dissolution profiles were nearly superimposable with the deconvoluted in vivo dissolution profiles for the first 3–4 h, after which they ran ahead. In other words, a one-to-one correlation was valid only for 3–4 h, and thereafter,

the correlation clearly deviated from the line of identity, resulting in a biphasic Levy plot. These findings were independent of the type of in vitro dissolution conditions applied. Not surprisingly, Bode and co-workers (35) have also shown that the rate of nifedipine absorption for the same dose administered is clearly slower from the colon than from the upper intestine.

With CIVIVIC it is assumed that the total in vitro dissolution profile can be projected isomorphically to yield the in vivo dissolution profile: this means that the in vitro and in vivo dissolution profiles must not differ in their morphology, but need only be stretched or shortened relative to each other. Otherwise, neither the prediction of the concentration by convolution (including time base rescaling) nor the correlation of the hypothetical in vivo dissolution obtained by deconvolution with the in vitro test will produce a meaningful correlation.

In contrast to continuous correlation, the assumptions for the global approach of in vitro–in vivo correlation are less restrictive, similarity ''on average'' may be sufficient.

In summary, with a suitable extended-release formulation it is possible to study the absorption features of the gastrointestinal tract relative to the drug considered by combining the technique of deconvolution and CIVIVIC. The procedure turns extended-release formulations into probes that can be used to determine differences in the rate and extent of absorption from different parts of the gastrointestinal tract. The information gained from this analysis can be used to direct strategies for the further development of extended-release dosage forms.

REFERENCES

1. Amidon GL, Lennernäs H, Shah VP, Crison JR. A theoretical basis for a biopharmaceutical drug classification: the correlation of in vitro drug product dissolution and in vivo bioavailability. Pharm Res 1995; 12:413–420.
2. Hirtz J. The gastrointestinal absorption of drugs in man: a review of current concepts and methods of investigation. Br J Clin Pharmacol 1985; 19:77S–83S.
3. Hirtz J. The absorption window: fact or fiction? Pharm Int 1987; 5:175–178.
4. Godbillon J, Evard D, Vidon N, Duval M, Schoeller JP, Bernier JJ, Hirtz J. Investigation of drug absorption from the gastrointestinal tract in man. III. Metoprolol in the colon. Br J Clin Pharmacol 1985; 19:113S–118S.
5. Staib AH, Loew D, Harder S, Kollath J, Graul EH, Schuster O, Hugemann EH. Theophyllin. Absorption in verschiedenen Darmabschnitten. In: Rietbrock N, Woodcock BG, Staib AH, Loew D, eds. Drug Absorption at Different Regions of the Human Gastro-Intestinal Tract: Methods of Investigation and Results. Wiesbaden: Friedr. Vieweg & Sohn, 1987:53–62.

6. Staib AH, Fuhr U. Drug absorption differences along the gastrointestinal tract in man: detection and relevance for the development of new drug formulations. In: Kuhlmann J, Weihrauch TR, eds. Food–Drug Interactions. New York: W Zuckschwerdt Verlag, 1995:34–56.
7. Gramatté T, El Desoky E, Klotz U. Site-dependent small intestinal absorption of ranitidine. Eur J Clin Pharmacol 1994; 46:253–259.
8. Gramatté T. Die Lokalisationsabhängigkeit der Arzneistoffresorption im Dünndarm des Menschen. Dissertation Habilitation, Universität, Dresden, Germany, 1995.
9. Lennernäs H, Ahrenstedt O, Hallgren R, Knutson L, Ryde M, Paalzow LK. Regional jejunal perfusion, a new in vivo approach to study oral drug absorption in man. Pharm Res 1992; 9:1243–1251.
10. Lennernäs H, Fagerholm U, Raab Y, Gerdin B, Hallgren R. Regional rectal perfusion: a new in vivo approach to study rectal drug absorption in man. Pharm Res 1995; 12:426–432.
11. Lennernäs H. Does fluid flow across the intestinal mucosa affect quantitative oral drug absorption? Is it time for a reevaluation? Pharm Res 1995; 12:1573–1582.
12. Brockmeier D. Analyse der Zeitabhängigkeit der Resorption von Arzneistoffen aus dem Gastrointestinaltrakt durch in vitro in vivo Korrelation der Arzneistofffreisetzung. Habilitation Dissertation, Justus-Liebig-Universität, Giessen, Germany, 1990.
13. Brockmeier D. Comparison of in vitro and in vivo dissolution for the study of colonic drug absorption. In: Bieck PR, ed. Colonic Drug Absorption and Metabolism. New York: Marcel Dekker, 1993:109–135.
14. Brockmeier D, von Hattingberg HM. Mean residence time. Methods Find Exp Clin Pharmacol 1986; 8:309–312.
15. Brockmeier D. In vitro/in vivo correlation of dissolution using moments of dissolution and transit times. Acta Pharm Technol 1986; 32:164–174.
16. von Hattingberg HM, Brockmeier D. A concept for the assessment of bioavailability in complex systems in terms of amounts and rates. In: Bozler G, van Rossum JM, eds. Pharmacokinetics During Drug Development: Data Analysis and Evaluation Techniques. New York: Gustav Fischer Verlag, 1982:315–323.
17. von Hattingberg HM, Brockmeier D, Voegele D. A method for in vivo–in vitro correlation using the additivity of mean times in biopharmaceutical models. In: Rietbrock N, Woodcock BG, Neuhaus G, eds. Methods in Clinical Pharmacology. Wiesbaden: Friedr. Vieweg & Sohn, 1980:85–93.
18. Voegele D, von Hattingberg HM, Brockmeier D. Ein einfaches Verfahren zur Ermittlung von in vitro in vivo Zusammenhängen in der Galenik. Acta Pharm Technol 1981; 27:115–120.
19. Tanigawara Y, Yamaoka K, Nakagawa T, Uno T. Correlation between in vivo mean dissolution time and in vitro mean dissolution time of ampicillin products. J Pharmacodyn 1982; 5:370–372.

20. Möller H, Langenbucher F. In vitro and in vivo dissolution of some sustained release tablets of theophylline. Pharm Ind 1982; 44:3–8.
21. Nicklasson M, Ellstrom K, Sjoqvist R, Sjovall J. Linear system analysis and moment analysis in the evaluation of bacampicillin bioavailability from microcapsule suspensions. J Pharmacokinet Biopharm 1984; 12:467–478.
22. Graffner C, Nicklasson M, Lindgren JE. Correlation between in vitro dissolution rate and bioavailability of alaproclate tablets. J Pharmacokinet Biopharm 1984; 12:367–380.
23. Zerbe H, Luckow V, Cawello W, Cordes G. Isosorbide-5-nitrate sustained-release pellets—an example of computer-supported drug development. Pharm Res 1985; 1:30–36.
24. Huhuenin RN, Zullinger HW, Niederer R. In vitro in vivo correlation exemplified by sustained release formulations of suprofen. Arzneimittelforsch 1988; 38:305–308.
25. Drewe J, Guitard P. In vitro in vivo correlation for modified release formulations. J Pharm Sci 1993; 82:132–137.
26. von Hattingberg HM, Brockmeier D, Voegele D. Moment–Analyse und in vitro–in vivo-Korrelation. Acta Pharm Technol 1984; 30:93–101.
27. Brockmeier D, von Hattingberg HM. In vitro–in vivo correlation, a time scaling problem? Basic considerations on in vitro dissolution testing. Arzneimittelforsch 1982; 32:248–251.
28. Levy G. Effect of dosage form on drug absorption. A frequent variable in clinical pharmacology. Arch Int Pharmacodyn 1964; 152:59–68.
29. FDA Guidance for Industry. Extended Release Oral Dosage Forms: Development, Evaluation, and Application of In Vitro/In Vivo Correlations. 1997.
30. Brockmeier D, Dengler HJ, Voegele D. In vitro–in vivo correlation of dissolution, a time scaling problem? Transformation of in vitro results to the in vivo situation, using theophylline as a practical example. Eur J Clin Pharmacol 1985; 28:291–300.
31. Brockmeier D, Voegele D, von Hattingberg HM. In vitro–in vivo correlation, a time scaling problem? Basic techniques for testing equivalence. Arzneimittelforsch 1983; 33:598–601.
32. Brockmeier D, Grigoleit HG, Leonhardt H. The absorption of piretanide from the gastro-intestinal tract is site-dependent. Eur J Clin Pharmacol 1986; 30:79–82.
33. Brockmeier D, Grigoleit HG, Heptner H, Meyer BH. Kinetics of piretanide absorption from the gastro-intestinal tract. Methods Find Exp Clin Pharmacol 1986; 8:731–739.
34. Bode H. Biopharmazeutische Charakterisierung von Nifedipin Retardformulierungen. Dissertation, Friedrich-Wilhelm-Universität, Bonn, Germany, 1996.
35. Bode H, Brendel E, Ahr G, Fuhr U, Harder S, Staib AH. Investigation of nifedipine absorption in different regions of the human gastrointestinal (GI) tract after simultaneous administration of ^{13}C- and ^{12}C-nifedipine. Eur J Clin Pharmacol 1996; 50:195–201.

16
IVIVC: A Perspective from the Workbench

Johannes Krämer
LQS Eschborn, Germany

I. IVIVC: AN INTEGRAL PART OF DISSOLUTION METHODOLOGY

Identity, purity, assay, and uniformity of dose are the classic parameters for the quality of pharmaceuticals. Beside these, biopharmaceutical tests are required to evaluate the rate of drug release from oral dosage forms. Fast and complete release is the prerequisite for bioavailability of immediate-release (IR) oral drug products, whereas a constant rate of release that is robust to the local conditions is preferred for controlled-release (CR) formulations.

Drug release can be tested either in vivo or in vitro. If in vitro methods are ''verified'' by in vivo data, they may be used as surrogates for clinical trials. This so-called in vivo verification of in vitro specifications is necessary to interpret dissolution profiles obtained from investigations in any stage of a drug product's lifecycle. From the early phase of technological development through scaling-up procedures to the pharmaceutical quality control of marketed batches at the time of release and the end of shelf life, meaningful in vitro data are mandatory to evaluate possible changes or differences in drug release in the context of drug product safety and efficacy.

Dissolution testing is a powerful tool to estimate the in vivo performance of a drug product. The ''reliability'' of dissolution profiles should be verified by qualification and calibration of the equipment and by validation of methods. Additionally, the biopharmaceutical verification of methods includes the proof

of a correlation of in vitro and in vivo performance as well as their discriminatory power to detect the absence of nonbioequivalent units within one lot and between lots of a given product. In general, dissolution-testing methods have to be developed for each formulation individually on the basis of an in vitro–in vivo correlation (IVIVC).

II. QUALIFICATION OF EQUIPMENT AND VALIDATION OF METHODS IS ESSENTIAL BEFORE STARTING AN IVIVC

For the in vitro characterization of most drug products, the compendial dissolution apparatuses are well suited. It is commonly accepted that alternatives are recommended only in cases when the pharmacopoeial apparatus (e.g., as described in *Ph. Eur.*, *PJ*, and *USP* cannot be used) (1).

Qualification of dissolution equipment should be performed in the same manner as for any other equipment used in pharmaceutical analysis. Qualification concerns itself with the general proof of suitability of the dissolution apparatus. In addition, individual qualification of modifications to the methodology, for instance, devices for automated sampling, sinkers, and filters, may be necessary. Some qualification work can be performed by checking physical parameters (e.g., centering shafts, measuring wobble), others require ''chemical'' calibration tests with calibration standards. The commonly used pharmacopoeial test procedure is described in the *U.S. Pharmacopeia* (*USP*) as the ''apparatus suitability test'' (2).

Great progress has been achieved in harmonization of methodological specifications. Only small differences in dissolution equipment generated by differences in pharmacopoeial specifications and industrial standards (e.g., between European and U.S. equipment) still exist. Moreover, most of these differences do not affect the results of dissolution experiments (3). Finally, it should be noted that validation is both product- and method-related. It should consider the formulation properties, the properties of the drug substance, the stability of the analyte throughout the pharmaceutical analysis, as well as dissolution media, sampling, sample transfer, and the method for chemical analysis. The qualification and validation of all technical instruments and analytical methods is prerequisite to verification with in vivo-data.

III. IN VITRO DISSOLUTION METHODOLOGY IN LIGHT OF PHYSIOLOGICAL FACTORS

Good technical operating conditions are mandatory, but a fine-tuning of methods relative to the ''dissolution conditions'' in the human gastrointestinal tract

is also highly desirable. The chance of achieving an IVIVC increases if biorelevant parameters are included in dissolution method development. The choice of an appropriate method should be based primarily on the drug product's properties. Multiparticulate dosage forms may require methods different from those of monoparticulate formulations (4). The drug substance's properties also have to be considered. Appropriate conditions for the in vitro characterization of IR-dosage forms can be chosen within the framework of the Biopharmaceutical Drug Classification system (BCS), which is a categorization of drug substances according to their solubility and permeability (5; see also Chapter 9). The applicability of this system to the conception of in vitro methods is, however, limited because dissolution remains unaffected by solubility as long as in vitro dissolution experiments are performed under ''*sink conditions*.'' According to the definition in the FIP-dissolution guideline, sink conditions means that under the conditions of the chosen dissolution method, complete release of the drug from an individual dosage form results in a concentration not exceeding 30% of its maximum solubility (1).

In vitro dissolution does not necessarily reflect in vivo dissolution. To reach better concordance with physiology, further research has to be undertaken to define the relevant physiological conditions. Composition of a dissolution medium should simulate the physicochemical properties of body fluids (6). For routine dissolution testing, physiological substances could be replaced stepwise by synthetic reagents showing the same physicochemical effects but which are available in analytical quality (7). Little is yet known about the hydrodynamics of the gastrointestinal tract in relation to how they affect release from dosage forms before and at the site of absorption. Meanwhile, further investigations are being undertaken to improve established dissolution apparatus (8).

For oral dosage forms, no one dissolution apparatus is known to be optimal. The performance depends rather on the combination of dosage form, apparatus, and operating conditions. Also, the pharmacopoeias do not stipulate how data are to be presented (e.g., as fractional or cumulative curves release). A fit to mathematical functions describing release mechanisms is not usually desirable because the fitting procedure introduces a loss of precision.

IV. WELL-HIDDEN IN VIVO PARAMETERS

The concept of IVIVC requires a clear definition of the kinetic step that has to be determined. For the case of solid oral dosage forms, the in vivo dissolution is to be correlated with the respective in vitro process. The dissolution

behavior of a certain dosage form in the GI tract is experimentally inaccessible. But as long as absorption occurs much faster than dissolution, the in vivo dissolution may be extracted from the plasma concentration versus time profile after oral application of the drug. The concentration versus time profiles represent a combination of overlapping kinetic processes, including drug input, distribution, and elimination. Parameters useful for describing plasma profiles in bioavailability studies, such as time to peak, maximum concentration, and area under the curve (AUC) provide precise information about the extent of drug absorption, but cannot be used for IVIVC purposes because a clear parameter for the rate of absorption is missing. Therefore, the input kinetics have to be extracted form the profiles by comparative ''peeling off'' of the other processes. If such a comparison is undertaken with a parenteral solution, a direct separation of dissolution and absorption kinetics will not be possible. If an oral solution should be given as the reference medication, the absorption process may be clearly identifiable. In a simplified description, any differences observed after application of the same dose of drug in a solid oral dosage form should be due to the dissolution process having to take place before absorption. This forms the basis of the concept of peeling off the in vivo parameters to be correlated or compared with the in vitro profiles (see also Chapters 14 and 15).

It should be noted that the results of this extraction provide only an apparent or hypothetical dissolution profile because it combines the contributions of in vivo dissolution and absorption, from which dissolution can be accurately estimated only if it is the rate-limiting step. Consequently, an IVIVC can be achieved only when all of the drug being dissolved in vivo is quickly and quantitatively absorbed. In general, the BCS provides important information on how to estimate which of the two kinetic processes could be the rate-limiting step. But the BCS does not assess dissolution and absorption directly, but rather, solubility and permeability parameters, which are difficult to interpret in terms of kinetic parameters. The most useful way to determine the relation of absorption and dissolution rates is from absorption studies of aqueous drug solutions applied at different sites of the GI tract, for instance, as published by Staib and co-workers for theophylline (9). A comparison of absorption kinetics at different regions of the GI tract with the deconvoluted profiles obtained from studies with solid oral dosage forms is easy to perform and provides the information on which is the rate-limiting step. An example, for a graphic comparison, is given in Fig. 1.

Once it is proved that the absorption process is not the rate-limiting step, the results from deconvolution can be assumed to represent in vivo dissolution and used further for IVIVC purposes.

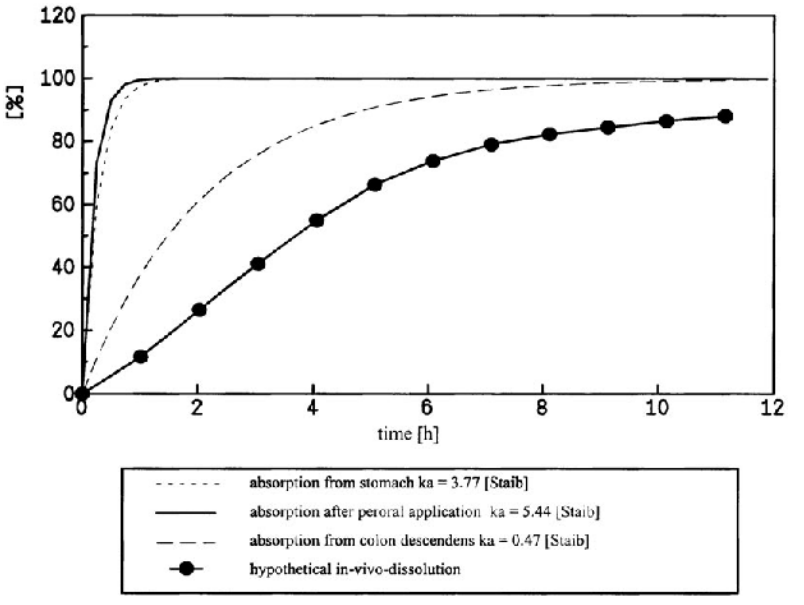

FIG. 1 Comparison of the hypothetical mean in vivo dissolution profile obtained from numerical deconvolution of response function after application of a monoparticulate theophylline extended-release dosage form with absorption profiles generated from rate constants, k_a (From Ref. 9.)

V. VERIFICATION OF DISSOLUTION METHODS: THE CORRELATION ITSELF

Depending on the amount of information to be used in the correlation, the *USP* introduces a rank order to follow. This rank order of correlation procedures (listed in *USP*'s chapter ⟨1088⟩; 10) is also the background for regulatory recommendations in Europe (11) and is generally accepted for the establishment of in vitro–in vivo correlation. At level A, entire profiles are correlated point by point. At the next level B, a data reduction is performed using statistical moment theory to calculate the correlation parameters. At level B, the shapes of the profiles are described by their skewness and curtosis. The parameters calculated for a level B correlation are called the moments. The first moment is the so-called mean time, which is calculated for both the in vitro and in vivo profiles. For a correlation in a strict sense, more than one set of in vivo data are required. The same is true for level C, in which the data

reduction procedures do not necessarily lead to analogous parameters for the characterization of the in vitro and in vivo profiles.

A. Level A Correlation

Level A correlations provide a way of verifying dissolution methods, by showing similarity of the entire (hypothetical) in vivo dissolution profile with the entire in vitro dissolution profile. The in vivo concentration profiles can be analyzed by a model-independent procedure called deconvolution, or by fit to compartmental models. The term ''deconvolution'' is often used to describe both procedures, which is in a way misleading. However, the performance of deconvolution may require prior fitting of experimental data, to a suitable model.

Deconvolution is a simple method requiring results from the application of the solid oral dosage form under concern and an oral aqueous solution of the drug substance, given in two separate phases of a clinical study to the same group of volunteers. The general design of the study is that of a bioavailability study (i.e., a two-phase–crossover design). The subjects being studied must fulfill all inclusion and exclusion criteria for bioavailability studies. The number of volunteers depends on the estimated variability and desired statistical power. The sampling schedule should be based on the pharmacokinetic properties of the drug substance and the expected behavior of the dosage form, making sure that the dosage–form-related segments of the concentration curve can be clearly described by a satisfactory number of data points. The subjects' kinetic responses are interpreted and compared on an individual basis. For deconvolution purposes, the drug is usually given in one phase as the oral solution and in the other phase as the formulation of interest. There are also more sophisticated designs, including more than two variations of one formulation, but no solution (12). The application of the oral solution characterizes the human body as a system which transforms the administered drug in a characteristic way. The signal response to the oral solution is called the system function, and the signal response to the solid oral dosage form is called the response function. By deconvolution, which can either be performed algebraically or numerically, the input function, which is the in vivo transition process from solid to dissolved drug (i.e., the dissolution process), may be determined. The scheme is depicted in Fig. 2.

Besides being reversible, one major advantage of deconvolution is that it requires no fit to a model and, if performed correctly, the resulting mean in vivo curve yields asymptotically to the point estimate of oral bioavailability gained from the intraindividual comparisons of the amounts absorbed from

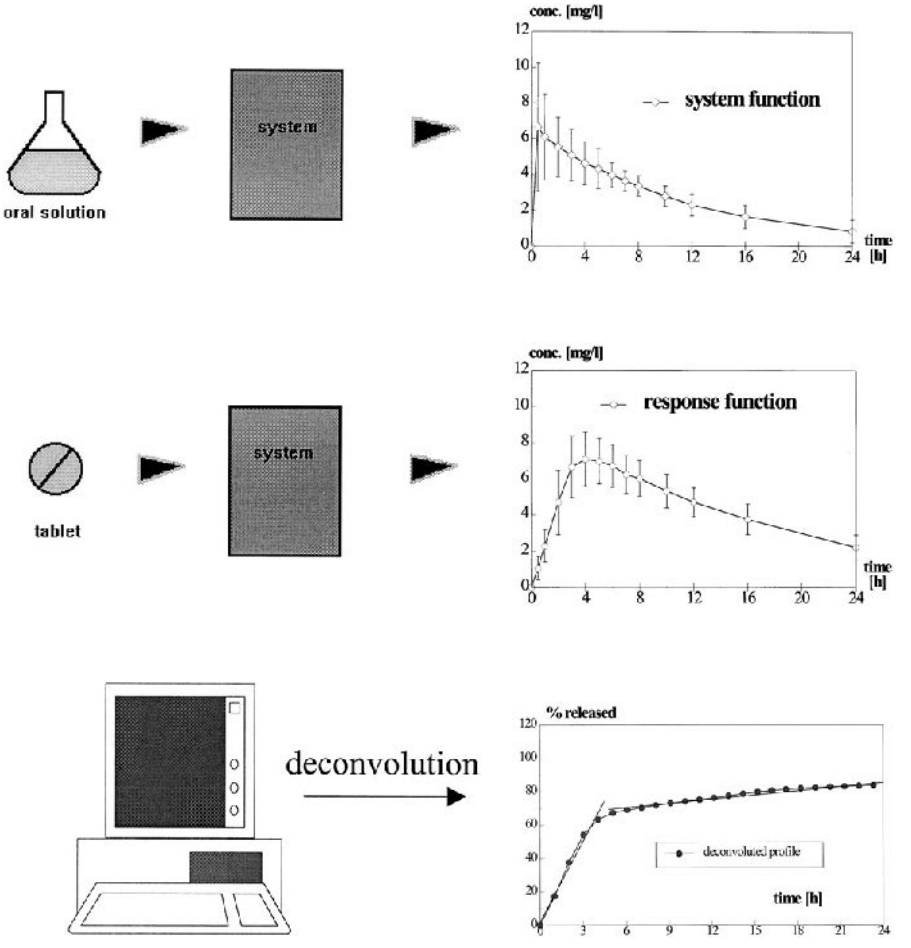

FIG. 2 Principle of numerical deconvolution displayed for a monoparticulate oral dosage form containing 540 mg theophylline. System function obtained from application of an aqueous oral solution containing 270 mg (n = 18).

the oral solution and the solid oral dosage form. The prerequisites to perform deconvolution are linearity of the system (i.e., that the drug exhibits a linear pharmacokinetics) and its invariance over time. This limits its use to drugs with linear pharmacokinetics, at least in the therapeutic range. A further limitation is that the response function and system function are obtained from a finite set of data points that usually contain errors. These errors are then propagated by the deconvolution, which is particularly problematic in the case of numerical deconvolution because of the algorithm's remarkable numerical instability (13).

Whereas deconvolution needs no model fitting to obtain hypothetical in vivo dissolution profiles, but rather uses the data of an alternative application

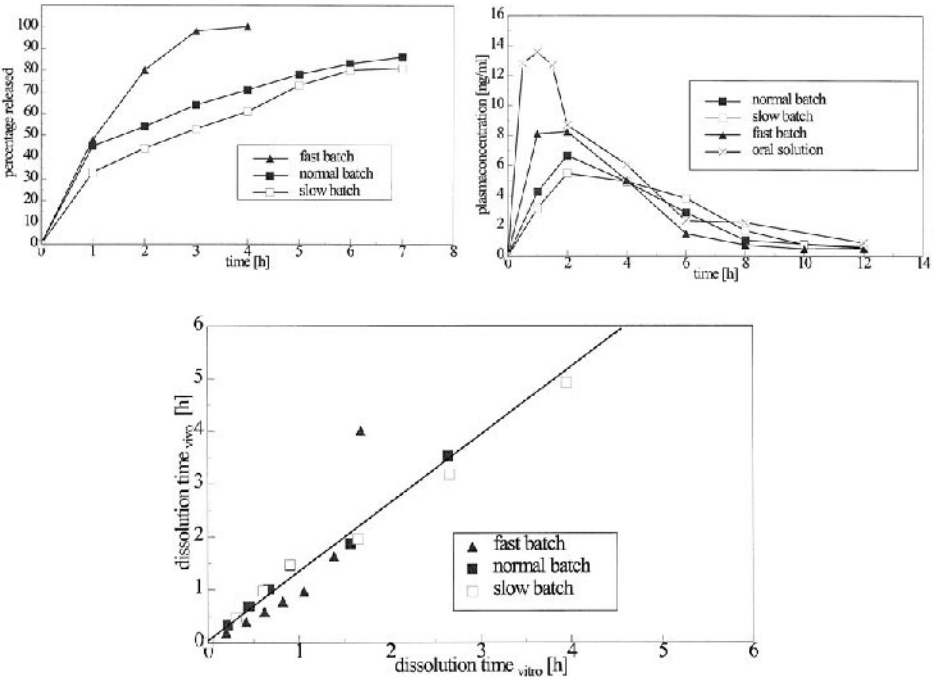

FIG. 3 (Left) In vitro dissolution of three batches of a 10-mg monoparticulate extended-release formulation. *USP* apparatus ⟨2⟩, 100 rpm, 1000 mL purified water, 37°C, mean (n = 6). (Right) Corresponding plasma 'concentration vs. time profiles, mean (n = 6), dose correction for 20-mg oral solution and 20-mg fast batch. (Bottom) Level A IVIVC for the three batches after performance of Wagner–Nelson method.

of the drug as an oral solution, level A correlation may also be performed after fitting to pharmacokinetic compartmental models. In addition to multicompartmental models, the fit to a one-compartment model using the so-called Wagner–Nelson method (14) may be suitable to characterize the pharmacokinetic behavior of many drugs. It is a mass balance procedure and provides no information about the relative bioavailability if used solely for the application of the formulation under concern. Furthermore, it has no built-in control, as described in the foregoing, for the numerical deconvolution. However, if the relative bioavailability is known, the resulting curve may be standardized. Beside its use for the verification of the similarity of in vivo and in vitro dissolution profiles, the Wagner–Nelson method may also be applied to proof the discriminatory power of a dissolution method, as exemplified in Fig. 3.

The advantage of this method is its simple application using standard in vivo plasma concentration versus time profiles. However, the algorithm requires an absolutely precise estimation of the elimination rate constant. The method may be used for both single-dose applications and multiple-dose applications, as long as the design of the study allows an exact description of the terminal phase and, hence, enough data for a precise estimation of the elimination rate constant.

Both numerical deconvolution and the Wagner–Nelson method use entire profiles, thereby maximizing the use of the information provided. These continuous methods make it easy to set specifications on the basis of biofindings, thus ensuring that all batches that meet the specifications are bioequivalent.

1. *Level A Correlation May Provide Information on the Transit of Solid Dosage Forms*

The IVIVC is usually displayed as Levy plots as a display of time intervals needed to dissolve equal masses on the in vivo and the in vitro side (15). But the Levy plot can provide additional information. With the transit of the dosage form through the gastrointestinal tract, the hypothetical deconvoluted in vivo dissolution profile may change. This can be due to changes in the dissolution pattern of the dosage form when the environmental conditions affect drug release (i.e., full control of the drug release is not provided by the technology of the dosage form). It can also be due to changes in the relation of dissolution versus absorption rate as the rate-controlling step to appearance in the blood. As the absorption rate may change with region in the gut, changes in the hypothetical dissolution profiles may, in fact, represent the phenomenon of

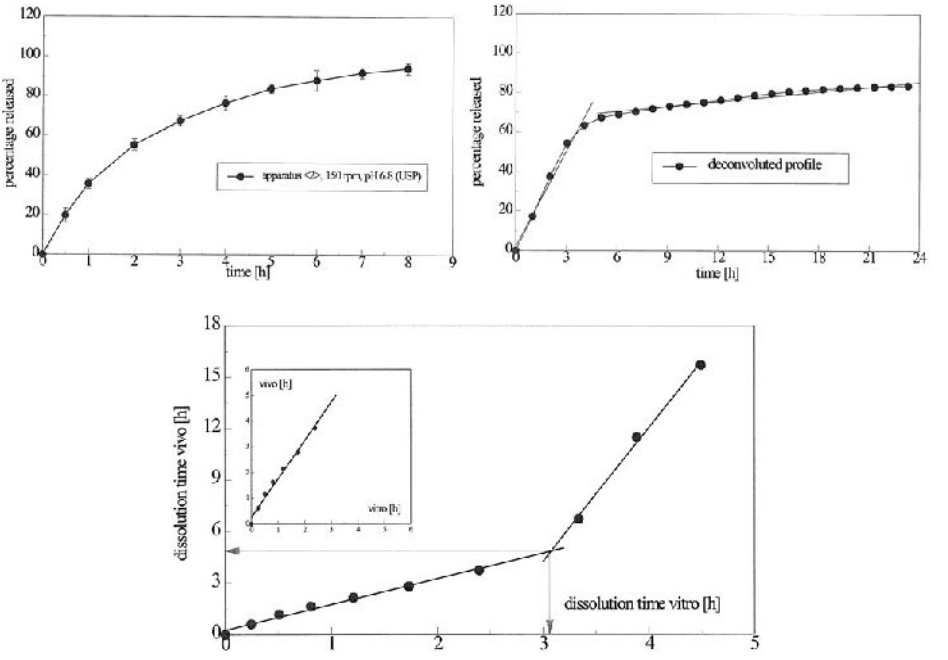

FIG. 4 (Left) In vitro dissolution of a 540-mg monoparticulate extended-release theophylline formulation in *USP* apparatus ⟨2⟩, 150 rpm, 900 mL phosphate buffer, pH 6.8 *USP*, 37°C, mean (n = 6). (Right) Hypothetical in vivo dissolution profile after numerical deconvolution, mean (n = 18). (Bottom) Level A IVIVC. Biphasic regression plot. Inset with identical scales for initial phase.

absorption becoming the rate-limiting step. This happens typically with extended-release dosage forms after the dosage form's transition from the small to the large bowel (see Chapter 15). By using the more stable in vitro dissolution kinetics as a measure to determine changes in the in vivo pattern, the Levy plot depicts discontinuities that may be interpreted as the time of entry into the colon. Depending on whether the dosage form is administered with food, the residence time in the proximal part of the GI tract will vary and the occurrence of the discontinuity may be delayed. An example is depicted for a monoparticulate extended release dosage form containing theophylline (16), as shown in Fig. 4. Comparable results were found for a multiparticulate dosage form after analysis of in vivo data taken from the literature (17,18) and in vitro data from inhouse studies, as depicted in Fig. 5.

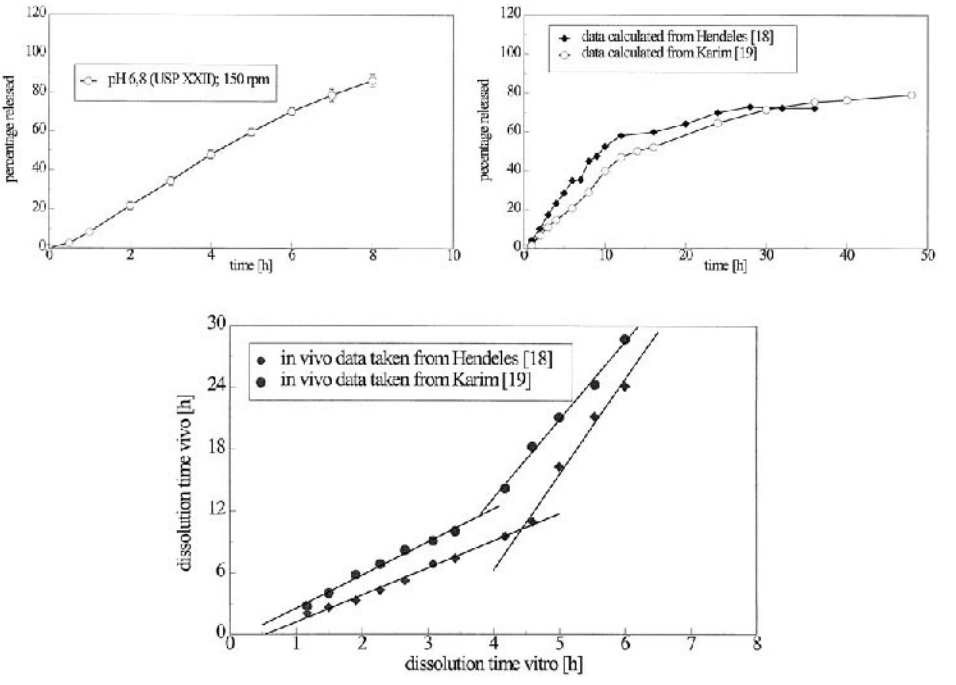
pH 6.8 (USP XXII); 150 rpm
percentage released
time [h]
data calculated from Hendeles [18]
data calculated from Karim [19]
percentage released
time [h]
in vivo data taken from Hendeles [18]
in vivo data taken from Karim [19]
dissolution time vivo [h]
dissolution time vitro [h]

FIG. 5 (Left) In vitro dissolution of a 200-mg multiparticulate extended-release theophylline formulation. *USP* apparatus ⟨2⟩, 150 rpm, 900 mL phosphate buffer pH 6.8 *USP*, 37°C, mean (n = 6). (Right) Hypothetical in vivo dissolution profile after performance of Wagner–Nelson method. (Bottom) Level A IVIVC: biphasic regression plot.

B. Level B Correlation: The Statistical Moment Theory

If the entire profile cannot be used for correlation, data reduction that leads to comparable and preferably analogous parameters on the in vivo and the in vitro side is required. The statistical moment theory uses empirical distribution functions, and it is a model-independent method. But as in the Wagner–Nelson method, a precise estimation of the elimination rate constant is a must. For the experimental in vitro data, dissolution experiments should be performed until drug release is complete. This restricts the method to experiments in which the volume and composition of the medium do not limit the final amount dissolved (i.e., dissolution under sink conditions). The results on the level of the first moment are composite results of mean times. By simple arithmetic

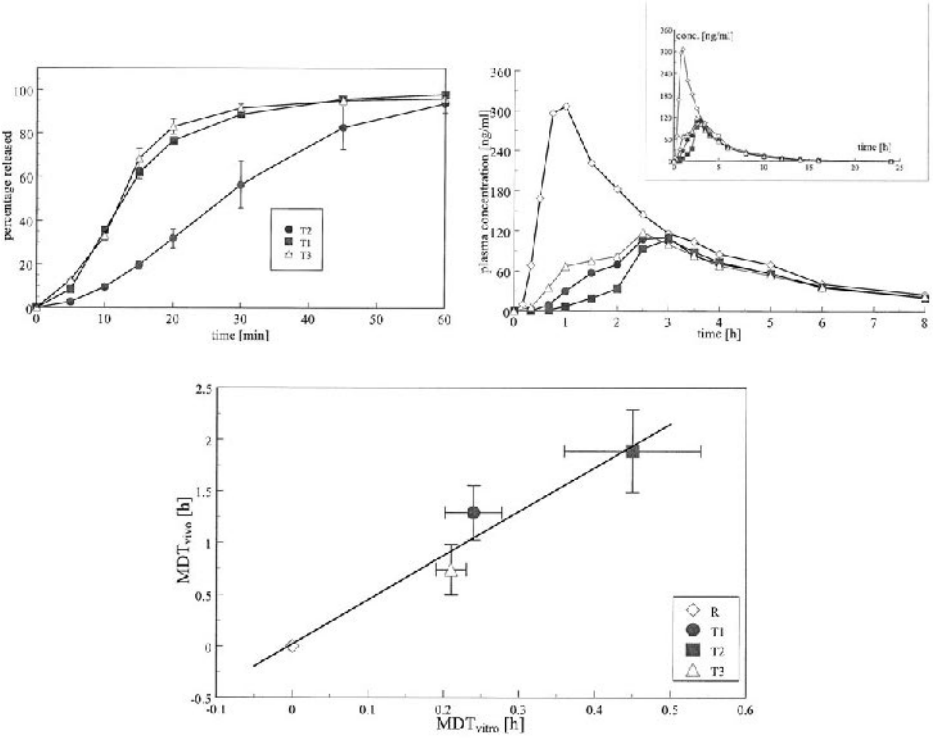

FIG. 6 (Left) In vitro dissolution of three manufacturing variables of a 50-mg immediate-release propafenone formulation. *USP* apparatus ⟨2⟩, 75 rpm, 1000 mL artificial gastric fluid *USP*, 37°C, mean (n = 6). (Right) Corresponding plasma from concentration vs. time profiles from 0 to 8 h, mean (n = 19). Inset 0–24 h. (Bottom) Level B IVIVC: regression plot of mean dissolution times, means and CVs.

operations, such as subtraction, mean dissolution times in vivo may be computed from mean residence times and correlated with mean dissolution times in vitro.

Figure 6 shows an example of a successful level B correlation (19). The drug propafenone, given as a film-coated tablet, was found to undergo extensive first-pass metabolism. Linear pharmacokinetics, a prerequisite to performing deconvolution, did not apply. The total amount absorbed—one third of the oral solution—was too low to obtain a meaningful correlation at level

A in terms of providing enough safety for the patients. By using the statistical moment theory, a correlation was established, which showed that the in vitro method was suitable for characterizing formulation variables in the dosage form under investigation. Moreover, in vitro dissolution occurred approximately four times faster than in vivo dissolution, which was very important for setting in vitro dissolution specifications.

The major disadvantage of the statistical moment theory is that it is nonreversible. This means that profiles with different shapes may have identical mean times and that from mean times, no backtracking to the in vivo profile is possible. But when the correlation is established for the dissolution of one product, profiles of variations of that one product do not usually differ that much in shape. If only the slope and not the shape is different, profiles are homomorphic. Methods have been published on how to set specifications for homomorphic profiles (20).

C. Level C Correlation

Level C correlation also implies data reduction. The use of correlated parameters needs to be justified (21). An example in which the in vivo pharmacokinetic parameters are verified by results from concomitantly recorded pharmacodynamic parameters is described for the oral antidiabetic drug glibenclamide (22).

VI. THE SETTING OF SPECIFICATIONS

The setting of specifications should be based on biological (pharmacokinetic) findings and not on mechanistic approaches (23). General pharmacopoeial standards (i.e., those applicable to more than one product) are difficult to define. The *European Pharmacopeia* does not describe any individual monograph on formulations. A general requirement such as 70% of total drug dissolved within 45 min is of no great use to discriminate the biopharmaceutical quality of products. Specifications at earlier time points are most desirable (e.g., after 15 or 20 min), but are limited to certain drugs belonging to class I of the BCS. For ''nonbioproblem'' drugs, it was discussed whether Q 80% in 30 min would be physiologically relevant, because the t_{max} in vivo of many of these drugs in the fasted state bioavailability studies is about 30 min (24). However, a comparison of in vitro and in vivo time axes is most desirable, because a time-scaling factor as great as 4 or more may be required (19).

If absorption, rather than in vivo dissolution, is the rate-limiting step,

dissolution specifications cannot be based on bioavailability findings. Inasmuch as dissolution is not necessarily a predictor of absorption, tests are limited to their use as a quality control tool on a routine or periodical basis in these cases. If input is absorption-controlled, the predictive power should be assessed taking into account the physical behavior and the specifications of the drug substance.

The CR or MR dosage forms are best candidates for establishing in vitro–in vivo correlation, because the product is inherently designed to make the release significantly slower than absorption. Although correlation in the mathematical sense does not necessarily imply discriminatory power, in the biopharmaceutical sense it implies both, and the setting of specifications should be based on bioavailability data (e.g., using side batches at the upper and lower level of the bioequivalence range). Side batches may be produced by variations of critical manufacturing steps within the limits tolerated by Good Manufacturing Practices (GMP). They should represent realistic modifications of one product, rather than different but similar products.

Nevertheless, if IVIVC is successfully established for one product, there may be a chance to extend the IVIVC to a series of homologous formulations or even to other products containing the same drug substance. There are a few examples, such as glibenclamide, for which a substance-related correlation was established for more than one IR product. In a second step, comparative (bioavailability) studies may be performed to extend those specifications verified by IVIVC to other (generic) products of different origin, demonstrating that these products are interchangeable. If nonanalogous parameters are correlated—and this often occurs in so-called single-point correlation—statistical reasons do not warrant interpolation on the basis of in vitro data. Relative to the requirement that in vitro dissolution must discriminate between different qualities in the preparation, specifications must first be set for each product individually.

REFERENCES

1. Siewert M, et al. FIP Guidelines for Dissolution Testing of Solid Oral Products. Pharm Ind 1997; 59:760–766.
2. The United States Pharmacopeia. Chapter ⟨711⟩. Rockville, MD: USPC 1995.
3. Krämer J. European perspective—American and European equipment calibration issues. AAPS/USP Workshop on Dissolution, Calibration, and Testing, Arlington, 1995.
4. Krämer J, Blume H. Biopharmaceutical aspects of multiparticulates. In: Ghebre-

Selassie I, ed. Multiparticulate Oral Drug Delivery. New York: Marcel Dekker, 1994:307–332.
5. Amidon GL, Lennernäs H, Shah VP, Crison JR. A theoretical basis for a biopharmaceutic drug classification: the correlation of in vitro drug product dissolution and in vivo bioavailability. Pharm Res 1995; 12:413–420.
6. Dressman JB, Bass P, Ritschel WA, Friend DR, Rubinstein A, Ziv E. Gastrointestinal parameters that influence oral medications. J Pharm Sci 1993; 82:857–872.
7. Stippler E, Krämer J, Dressman JB. Comparison of synthetic with natural surfactant systems for in vitro dissolution testing. Proceedings 2nd World Meeting on Pharmaceutics, Biopharmaceutics, and Pharmaceutical Technology. Paris, 1998: 345.
8. Borst I, Beckett AH, Quach T, Gray V, Dressman JB, Qureshi SA. Roundtable conference report: the importance of hydrodynamics in dissolution testing. Dissol Technol 1998; 5:19–21.
9. Staib AH, Loew D, Harder S, Graul EH, Pfab R. Measurement of theophylline absorption from different sections of the gastro-intestinal tract using a remote controlled drug delivery device. Eur J Clin Pharmacol 1986; 30:691–697.
10. The United States Pharmacopeia. Chapter ⟨1088⟩. Rockville, MD: USPC 1995.
11. EC Guideline on Prolonged Release Dosage Form Commission of the European Communities, CPCMP Working Party on Quality of Medicinal Products: Quality of Prolonged Release Oral Solid Dosage Forms. In: III/3172/91-EN.
12. Gillespie WR. Convolution-based approaches for in vivo–in vitro correlation modeling. In: Young D, Devane JG, Butler J, eds. In Vitro–In Vivo Correlations. New York: Plenum Press, 1997:53–65.
13. Süverkrüp R, Bonnacker I, Raubach HJ. Numerical stability of pharmacokinetic deconvolution. J Pharm Sci 1989; 78:948–954.
14. Wagner JG, Nelson E. Per cent absorbed time plots derived from blood level and/or urinary excretion data. J Pharm Sci 1963; 52:610–611.
15. Levy G. Effect of dosage form on drug absorption—a frequent variable in clinical pharmacology. Arch Int Pharmacodyn 1964; 152:59–68.
16. Krämer J, Voegele D, Blume H. Einfluß von fettem Essen auf die Liberation und Resorption von Theophyllin am Beispiel einer verlängert freisetzenden oralen Zubereitung. Düsseldorf Universität/APV Colon Resorption und Targeting. Düsseldorf, 1996.
17. Hendeles L, Weinberger M, Milavetz G, Hill M, Vaughan L. Food-induced ''dose dumping'' from a once-a day theophylline product as a cause of theophylline toxicity. Chest 1985; 87:758–765.
18. Karim A, Burns T, Wearly L, Sreicher J, Palmer M. Food induced changes in theophylline absorption from controlled-release formulations. Part II. Importance of meal composition and dosing time relative to meal intake in assessing changes in absorption. Clin Pharmacol Ther 1985; 38:642–647.
19. Krämer J, Elze MJ, Fieger-Büschges H, Potthast H, Blume H. Level B correlation to detect biorelevant manufacturing changes of a propafenone immediate release

dosage form by in vitro dissolution [abstr]. Pharm Res 1997; 14(suppl):S-121.
20. Krämer J. Role of in vitro dissolution test. In: Midha KK, Nagai T, eds. Bioavailability, Bioequivalence and Pharmacokinetic Studies. Tokyo: Business Centre for Academic Societies, 1996:303–311.
21. Stricker H. Die Korrelation analoger zu nicht analoger In Vitro/In Vivo-Verfügbarkeitsdaten. Pharm Ind 1979; 41:279–284.
22. Blume H, Stenzhorn G, Ali SL. Zur Bioverfügbarkeit und pharmakodynamischen Aktivität handelsüblicher Glibenclamid-Fertigarzneimittel. Pharm Ztg 1985; 130:1062–1069.
23. Siewert M. In vitro dissolution testing of oral controlled release products. In: Gundert-Remy U, Möller H, eds. Oral Controlled Release Products Therapeutic and Biopharmaceutic Assessment. Stuttgart: Wissenschaftliche Verlagsgesellschaft, 1989:139–154.
24. Blume H, Cartwright AC, Möller H. Setting specifications for drug substances and products. Drugs Made Ger 1996; 39:45–50.

Index

Absorption number, 139
Animal models for absorption (*see* Dogs, Intestinal permeability, Perfusion studies, Rabbits, Rats)

Bile acids:
  disorders of secretion, 20, 22
  enhancement of drug dissolution, 147, 213
  fasted state levels in humans, 112
  and maldigestion, 24
Bioavailability:
  effect of formulation, 199
  factors influencing, 32
  relation to lipophilicity, 44
Biopharmaceutics classification system, 38, 137, 157, 191, 282, 310
  application to extended-release products, 192
[Biopharmaceutics classification system]
  permeability determinations, 105
  properties of Class 1 drugs, 157
  properties of Class 2 drugs, 159
Biowaivers, 198
Brush border membrane vesicles, 52, 53
  comparison with % intestinal absorption, 54

Caco-II monolayers, 40 (*see also* Intestinal permeability, Cell cultures)
  assessment of efflux mechanisms, 75
  assessment of metabolism during transport, 75
  correlation to colon permeabilities, 66
  correlation to human data, 82

[Caco-II monolayers]
correlation to log D, 41,42
expression of transporters, 66, 82
role in high throughput screening, 66
transepithelial electrical resistance, 64
Capsules (*see* Dosage forms)
Carbohydrates:
fermentation in colon, 21
malabsorption, 21
Cell cultures, 52, 64 (*see also* Caco-II monolayers, HT29-18-CI cell lines)
Colitis (*see* Inflammatory disorders of the GI tract)
Colon:
colonic gas, 5
expression of transporters, 85
fermentation of carbohydrates, 21
mixing efficiency, 5
permeability, 84
transit times, 5
Convolution methods (*see* Deconvolution and convolution methods)
Crohn's disease (*see also* Inflammatory disorders of the GI tract), 12, 15, 22, 25
bile acid loss, 24

Deconvolution and convolution methods (*see also* In vitro–in vivo correlations), 255–280
assumption of linearity, 256
concerns with methodologies available, 277, 314
convolution, 287
[Deconvolution and convolution methods]
deconvolution, 311
deconvolution of in vivo dissolution, 292
direct numerical methods, 262, 314
impulse input, 256, 257, 259
input rate function, 256
instability due to experimental error in data, 266
least-squares methods, 270
Loo-Riegelman method, 260
maximum entropy methods, 274
regularization methods, 273
response function, 256
transformation methods, 268
Wagner-Nelson method, 259, 314
Diarrhea and malabsorption, 24, 27
Diffusion chambers (*see also* Caco-II monolayers), 52
to detect metabolism during transport, 75
using intestinal tissue, 60, 126
Dissolution:
aims of dissolution testing, 183, 197
agitation rate, 175, 203
biopharmaceutically relevant tests, 156, 198, 308
biowaivers, 198, 201, 215
Class 1 drugs, 158, 159
Class 2 drugs, 161, 167, 168, 169, 212
Class 3 drugs, 173
Class 4 drugs, 174, 212
considerations for extended-release dosage forms, 185, 209

[Dissolution]
decision tree for dissolution testing, 179
deconvolution of in vivo dissolution, 292
direct measurement in humans, 110
dissolution number, 139
in emulsions, 148
enhancement by surfactants, 145, 171
equipment, 174, 209
food effects, 164, 220
immediate release products, 155–181
importance of hydrodynamics, 175, 203, 205
in vivo–in vitro comparison, 113
rate, 212, 233
peak vessels, 175, 205, 177, 207
robustness to GI conditions, 199, 200, 214
role in product development, pre- and postapproval, 184, 193, 197, 198, 201, 215
specifications for extended-release products, 187
study design, 230
test conditions for extended-release products, 186, 205, 207
test duration, 171, 186
Dissolution data:
analysis, 229–254
changes in boundary layer thickness during dissolution, 236
changes in surface area during dissolution, 234
[Dissolution data]
characterization of the dissolution profile, 231
dissolution efficiency, 233
mean dissolution time, 232
prediction of in vivo performance, 245
profile comparison, 238 (*see also* Dissolution profiles, comparison)
semi-empirical models, 236
single vs. multipoint assessment, 229
Dissolution media:
biorelevant media, 164
Class 1 drugs, 158
Class 2 drugs, 161, 212
Class 3 drugs, 173
Class 4 drugs, 174, 212
Ensure, 164
extended-release products, 185
FaSSIF and FeSSIF, 164
food effect studies, 164, 220
hydroalcoholic media, 171
milk, 164
poorly soluble drugs, 161, 174, 212
sink conditions, 212, 213
use of surfactants, 171, 172, 213, 215
Dissolution profiles, comparison, 238
difference factor, f_1, 241
index approaches, 240
model-dependent methods, 244
model-independent methods, 239
multivariate approaches, 245
Rescigno index, 243
similarity factor, f_2, 190, 241

[Dissolution profiles, comparison]
statistical approaches, 239
Weibull function, 244
Dogs, as an absorption model, 86 (*see also* Perfusion studies)
Dosage forms:
colonic transit, 5
design of formulation-specific dissolution tests, 205, 207
esophageal transit, 2
formulation and robustness of absorption profile, 199, 214
gastric emptying, 3
robustness of release to GI conditions, 199, 200, 214
small intestine transit, 5
transit times via IVIVC data, 315
Dose number, 139
Dose:solubility ratio, 161
Drug properties relevant to absorption, 33
hydrogen bonding, 38, 39, 106
lipophilicity, 35, 36, 37, 44, 84, 104, 106
molecular charge, 38
molecular size, 38, 39, 43
Rule of Five, 33
solubility, 34, 137–153

Efflux mechanisms (*see* P-Glycoproteins)
Esophagus, transit time, 2
Everted intestinal rings, 55
correlation with bioavailability, 58
Everted intestinal sacs, 52, 57
Extended-release dosage forms, 183–195
[Extended-release dosage forms]
in vitro–in vivo correlations, 200
robustness to GI conditions, 199, 200, 214
Extent of drug absorption, 73, 99

Fats:
malabsorption, 19
maldigestion, 24
Fluid volumes in the GI tract, 145
Food effects on drug absorption:
extended-release formulations, 193
mechanisms, 220
prediction of food effects, 220, 221
Formulation-specific dissolution tests (*see* Dosage forms, Dissolution)
Fourier transforms, use in convolution and deconvolution, 268
Fraction absorbed:
correlation with human permeability data, 141
equations, 140, 260, 261
f_2 (*see* Similarity Factor [f_2])

Gastric emptying (*see also* Transit times):
influence on absorption pattern, 151
use in prediction of plasma profiles, 248

High throughput screening, 66, 120
HT29-18-CI cell line (*see also* Intestinal permeability), 40

Hydrodynamics:
artifacts in in vitro testing, 207
in dissolution testing, 175, 203
and formulation density, 203
special needs for erodible matrices, 209
variability in vivo, 204
Hydrogen bonding and drug absorption (*see* Drug properties relevant to absorption)

Ileocecal junction, transit, 7
Inflammatory disorders of the GI tract, 25
AIDS enteropathy, 26
celiac disease, 26
and colonic transit, 6
Crohn's disease, 25
and permeability, 12
Intestinal cell suspensions, 52, 54
Intestinal malabsorption, 18
after small bowel resection, 28
carbohydrates, 21
and diarrhea, 24, 29
drug-induced, 23, 27
in the elderly, 28
fats, 19
proteins, 22
radiation induced, 27
role of systemic diseases, 26
tables, 19, 20, 22
Intestinal maldigestion, 20, 22
Intestinal perfusions (*see also* Perfusion studies), 76
Intestinal permeability, 40 (*see also* Perfusion studies)
age-dependency, 76
analysis from Levy plots, 295
animal models, 43
apparent permeability, P_{app}, 61
[Intestinal permeability]
comparison of in vitro methods, 68
comparison of methods with human bioavailability, 103, 126
correlation with fraction absorbed, 141
correction for tissue binding, 56, 75
Crohn's disease, 12
in effective permeability, P_e, 73, 102,140
equations based on physical properties, 42
human, 43
measurement with Loc-I-Gut, 13
mechanisms of absorption (*see* Uptake mechanisms)
pathogenic alterations, 12
pharmacological alterations, 12
prediction using cell lines, 40
reference compounds for validating permeability methods, 78
regional dependency, 84, 281–305, 307–322
variability in data, 68
viability of tissue/monolayers, 78, 128
wall permeability
P_o, 56
P_w, 138
In vitro–in vivo correlations (IVIVC), 149, 281–305, 307–322
assumption of linearity, 256, 283, 292
biowaivers, 198
biphasic Levy plots, 295, 195, 297

[In vitro–in vivo correlations]
case examples (extended-release products), 200, 205, 207
case examples (immediate-release products), 248, 249, 250
causality in IVIVC, 282
Class 2 drugs, 246
continuous IVIVC, 286, 287, 312
dissolution tests, 198, 203
expectations based on the BCS, 149, 192
extended-release products, 188
food effects, 220
global approach, 282, 285, 316
homomorphism of dissolution profiles, 292, 294
level A, B, and C correlations, 282, 286, 312, 316
Levy plots, 291, 295, 299, 315, 318
mean dissolution time correlations, 283
point-by-point correlation, 286
preparation of in vitro data, 245
side batches, 188

Laplace transforms, use in convolution and deconvolution, 269
Least-squares methods, use in convolution and deconvolution, 270
Levy plots, 291, 315
Limitations to drug absorption, 31, 51, 156
first pass metabolism, 81, 90, 107

[Limitations to drug absorption]
importance to drug development, 120
instability, chemical, 75, 156
P-Glycoprotein mediated efflux, 45, 86
poor permeability, 31, 129, 139
poor solubility, 34, 137–153, 160
Lipophilicity and drug absorption, 36, 35, 36, 37, 44, 84
correlation to human permeability data, 104, 106
Loc-I-Gut methodology, 11–17, 77, 101
antipyrine as reference, 105
correlation to human bioavailability, 103
correlation to log D, 104
drugs studied, 105
Loo-Riegelman method, 260 (*see also* Deconvolution and convolution methods)

Malabsorption (*see* Intestinal malabsorption)
Maldigestion (*see* Intestinal maldigestion)
Mechanisms of absorption (*see* Uptake mechanisms)
Metabolism in the intestinal wall, 90, 107
Molecular charge and drug absorption, 38
Molecular size and drug absorption, 38, 39, 43

Oesophagus (*see* Esophagus)
Osmolality of gastric and jejunal fluids, 112

Pancreatic secretions:
and malabsorption, 19, 21, 27
and maldigestion, 22
Peak vessels, 175, 177, 205
Pellets (*see* Dosage forms)
Perfusion studies (*see also* Loc-I-Gut)
comparison of rat with human data, 79
data analysis, 78, 102
single pass perfusions in dogs, 77
single pass perfusions in humans, 12, 99
single pass perfusions in rats, 76
viability of tissue, 78
Permeability, intestinal (*see* Intestinal permeability)
P-Glycoproteins:
in Caco-II cells, 66
inducers, 89
mediated efflux, 45, 86
physiological role, 87
relation to metabolism, 107
substrate specificity, 87, 107
pH in stomach, 163
Poorly soluble drugs:
dissolution testing, 161, 174, 212
dose:solubility ratio, 161
limitation to absorption, 34, 137–153, 160
relationship to fraction absorbed, 142
sink conditions for dissolution tests, 212
Postapproval changes:
extended-release dosage forms, 201, 215
food effects, 193
Proteins, malabsorption, 22
Pulsincap, 5, 6

Rabbits, as an absorption model, correlation to human bioavailability, 126, 127
Rats, as an absorption model (*see* Brush border membrane vesicles, Everted intestinal rings, Everted intestinal sacs, Perfusion studies)
Reference compounds for permeability studies, 78, 105
Regional dependency of drug absorption, 84, 295
Rule of Five for drug absorption, 33

Similarity factor (f_2):
comparison of dissolution profiles, 241
dissolution profiles of extended-release products, 190
Small intestine:
factors affecting mucosal homeostasis, 14
malabsorption (*see* Intestinal malabsorption)
maldigestion (*see* Intestinal maldigestion)
metabolism in the small intestine, 90
mucosal inflammation, 14
transit times, 5
Solubility and drug absorption, 34, 137–153
dose:solubility ratio, 161
relationship to fraction absorbed, 142

Solubility and drug dissolution, 212
Stomach:
  fed/fasted differences, 3
  pH, 163
  surface tension, 163
  transit time, 2
Surface tension, gastric, 163
Surfactants and drug dissolution, 145, 171, 213
  choice of surfactant, 215, 217, 218
  purity of surfactant, 214

Tablets (*see* Dosage forms)
Transit times:
  colon, 5
  and duration of dissolution test, 172
  during sleep, 7
  esophageal, 2
  ileocecal junction, 7
  influence of motility phase, 150
[Transit times]
  from IVIVC, 313
  small intestine, 5
  stomach, 3, 150
  timing of dose, 7

Uptake mechanisms, 31, 32, 124, 125
  carrier-mediated absorption, 125
  efflux mechanisms (*see* P-Glycoproteins)
  paracellular pathway, 43, 124
  passive transcellular diffusion, 31, 124
Uptake vs. transport-based in vitro methods, 52, 53
Ussing chambers (*see* Diffusion chambers)

Wagner-Nelson method (*see also* Deconvolution and convolution methods), 259